

**Design and synthesis of novel cytochrome *bc*₁ inhibitors for
the treatment of toxoplasmosis**

James Alexander Gordon

Submitted in accordance with the requirements for the degree of
Doctor of Philosophy (PhD)

The University of Leeds
School of Chemistry

June 2018

The candidate confirms that the work submitted is his own, except where work which has formed part of jointly-authored publications has been included. The contribution of the candidate and the other authors to this work has been explicitly indicated below. The candidate confirms that appropriate credit has been given within the thesis where reference has been made to the work of others.

Work from the below publication features throughout Chapters 2-3:

Publication 1: M. McPhillie, Y. Zhou, K. El Bissati, J. Dubey, H. Lorenzi, M. Capper, A. K. Lukens, M. Hickman, S. Muench, S. K. Verma, C. R. Weber, K. Wheeler, J. Gordon, J. Sanders, H. Moulton, K. Wang, T.-K. Kim, Y. He, T. Santos, S. Woods, P. Lee, D. Donkin, E. Kim, L. Fraczek, J. Lykins, F. Esaa, F. Alibana-Clouser, S. Dovgin, L. Weiss, G. Brasseur, D. Wirth, M. Kent, L. Hood, B. Meunieur, C. W. Roberts, S. S. Hasnain, S. V Antonyuk, C. Fishwick and R. McLeod, New paradigms for understanding and step changes in treating active and chronic, persistent apicomplexan infections., *Sci. Rep.*, 2016, **6**, 29179.

This copy has been supplied on the understanding that it is copyright material and that no quotation from the thesis may be published without proper acknowledgement.

The right of James Alexander Gordon to be identified as Author of this work has been asserted by him in accordance with the Copyright, Designs and Patents Act 1988.

© 2018 The University of Leeds and James Alexander Gordon

Acknowledgements

There are a number of people I would like to thank for their support throughout the duration of my project and during the writing of this thesis.

This project would not have been possible without the large collaboration of researchers brought together by Dr Rima McLeod, and her tireless enthusiasm. My thanks to her team at the University of Chicago especially; Ying Zhou for the invaluable biological assays performed; to Craig Roberts at the University of Strathclyde for his work on the *in vivo* mouse assays; Sylvia N. Moreno and Zhu-Hong at the University of Georgia for their work on the mitochondrial inhibition assays, Mark Hickman and his team at the Walter Reed Army Institute of Research for their work on the malaria assays both *in vivo* and *in vitro*; Samar Hasnain, Svetlana Antonyuk, Michael Capper & at the University of Liverpool for their work on generating the X-ray crystal structures; Giancarlo Biagini & Richard Priestley at the Liverpool School of Tropical Medicine for their work on the comparative metabolic toxicity assays.

I'd like to thank my supervisor Prof Colin Fishwick for his advice and guidance throughout the project and thesis writing, similarly Dr Martin McPhillie who has been invaluable as a source of ideas and experience, and for his assistance in offering corrections and direction in the writing of this thesis.

I'd like to thank all the members of the Fishwick research group that I had the pleasure of working alongside during my time, with special thanks to Lewis Turner and Ryan Gonciarz who helped make the entire three years not only bearable but immensely enjoyable.

My thanks to my friends and family who have supported me throughout my studies, in particular my parents who have always supported and encouraged me throughout.

My thanks to the contributions made by Abigail Spedding and Nisha Pokar who I had the pleasure of supervising throughout their master's projects.

My thanks to all of the technical staff at the University of Leeds and the University itself for my funding.

A number of compounds were synthesised by master's students Abigail Spedding and Nisha Pokar under the candidate's supervision and are annotated within the text by the symbols ⁺ & [^] respectively.

Abbreviations

- 2,2,2-TFE- 2,2,2-Trifluoroethanol.
- ADMET- Absorption, distribution, metabolism, excretion and toxicity.
- AIDS - Acquired immune deficiency syndrome.
- ATP- Adenosine triphosphate
- BBB- Blood brain barrier.
- BPP- Blood plasma proteins.
- Caco-2- Colorectal adenocarcinoma-2
- CDPK1- Calcium dependent kinase.
- CNS- Central nervous system.
- D/RNA- Deoxy/ribonucleic acid.
- DHFR- Dihydrofolate reductase.
- DHPS- Dihydropteroate synthetase.
- DMF- N,N-dimethylformamide.
- Dppf- Diphenylphosphineferrocene
- EGS-
- ELQ- Endochin like quinolone.
- EM- Electron microscopy.
- ENR- Enoyl acyl carrier protein reductase.
- ERAD- Endoplasmic reticulum-associated degradation.
- FAS- Fatty acid synthesis.
- Fmoc- Fluorenylmethyloxycarbonyl
- Fsp3- fraction of sp³ hybridised carbons.
- GSK- GlaxoSmithKline
- HAT- Histone acetyl transferases.
- HDAC- Histone deacetylase.
- hERG- human ether-a-go-go related gene.
- HIV- Human immunodeficiency virus.
- (v)HTS- (virtual) High throughput screening.
- LCMS- Liquid chromatography mass spectroscopy.
- MDCK- Madin-Darby Canine Kidney
- NADH- Nicotinamide adenine dinucleotide
- NIS- N-iodosuccinimide.

NMR- Nuclear magnetic resonance.

P.falciparum- Plasmodium falciparum

PK- Pharmacokinetics.

ROCS- Rapid overlay of chemical structure.

ROCS- Rapid overlay of chemical structures.

SAR- Structure activity relationship.

SBDD- Structure-based drug design.

SOT- Solid organ transplant.

STAB- Sodium triacetoxy borohydride

T.gondii- *Toxoplasma gondii*.

TE – Toxoplasmic encephalitis.

TFE- Trifluoroethanol

THQ- Tetrahydroquinolone.

TPSA- Topological polar surface area.

Abstract

Toxoplasmosis is a highly prolific and neglected disease, and current treatments fail to adequately address the challenges it presents. As such development of new more efficacious treatments, tailored to the complex nature of the infection, is required. The causative parasite *Toxoplasma gondii* is a resilient and resourceful organism, adept at invasion, avoidance and survival within its host. The cytochrome *bc*₁ complex has been proven to be a validated target for the treatment of a number of apicomplexan parasitic diseases, including both malaria and toxoplasmosis. Recent work has also identified overexpression of this complex within a strain expressing the difficult to treat bradyzoite phenotype, which supported by findings that treatment with known *bc*₁ inhibitor atovaquone shows reduction in cyst burden, suggests this may be a particularly promising target for an effective systemic parasite treatment.

Within discusses the design, synthesis and analysis of a number of cytochrome *bc*₁ inhibitors across several novel scaffolds. Designs focused on improving deficiencies identified in previous inhibitors. Successful synthesis of a number of these designs and biological evaluation identified several sub-micromolar examples. After preliminary ADMET evaluation of the synthesised scaffolds the tetrahydroquinolone scaffold was selected for further development. Optimisation of the synthesis to the tetrahydroquinolones (THQ's) resulted in access to a library of analogues. From these analogues compound **169** was selected for further analysis, characterisation and ultimately progressed to early stage *in vivo* assays, in which it demonstrated exceptional potency and efficacy.

Table of Contents

Chapter 1 Introduction	1
1.1 <i>Toxoplasma gondii</i>	1
1.1.1 Life cycle	1
1.1.2 Structure and morphology of the <i>T.gondii</i> parasite.....	3
1.1.3 Environmental stage.....	4
1.1.4 Primary host	4
1.1.5 Prevalence	5
1.1.6 Strains	6
1.2 Pathology of Toxoplasmosis	6
1.2.1 Transmission/acquisition	6
1.2.2 Pathogenesis of Toxoplasmosis.....	7
1.2.3 Pathology within Immuno-Competent Patients.....	8
1.2.4 Pathology within Immuno-compromised Patients.....	8
1.2.5 Pathology of Congenital and Antenatal Infections.....	9
1.2.6 Ocular Toxoplasmosis.....	9
1.2.7 Behavioural and Neurological Effects of Toxoplasmosis.	10
1.3 Treatments and Molecular Targets	11
1.3.1 Past and Current treatments.	11
1.3.2 Deficiencies of current treatments.....	15
1.4 Drug Design and Development; Anti-Parasitics.	16
1.4.1 Hit identification.....	16
1.4.1.1 Phenotypic based screening	16
1.4.1.2 Target based screening.....	17
1.4.1.3 High Throughput screening	18
1.4.1.4 Structure based drug design and vHTS	18
1.4.2 Hit to lead.....	20
1.4.2.1 From Ligand to Drug; Multi-parameter Optimisation	20
1.4.3 Opportunities and Challenges of Parasitic Diseases.....	21
1.4.4 The Apicomplexa Phylum: <i>T.gondii</i> and other related parasitic diseases.....	22
1.5 Developing New Anti-Parasitic Agents.....	24

1.5.1 Current Work on Future Drugs and Targets for Toxoplasmosis	24
1.5.1.1 Improving upon existing targets	24
1.5.1.2 Targets from other infectious diseases.....	25
1.5.1.3 New targets	27
1.5.1.4 Epigenetic approaches.....	28
1.5.1.5 Drugs with unknown biological targets	30
1.5.2 The Cytochrome <i>bc</i> ₁ complex, and its potential as a drug target.....	31
1.5.2.1 The <i>bc</i> ₁ complexes role in the electron transport chain.	32
1.5.2.2 The Q cycle	33
1.5.2.3 Q _i vs Q ₀ site.....	35
1.5.3 Selectivity at the Q _i site	36
1.5.4 Quinolones and Pyridones as Cytochrome <i>bc</i> ₁ Inhibitors.	37
1.6 Summary.....	41
1.7 Project Goals and Summary	42
1.7.1 Overall aims	42
1.7.1.1 Design, synthesis and evaluation of novel scaffolds.....	42
1.7.1.2 Hit to lead development of Tetrahydroquinolones	42
1.7.1.3 Evaluation and further development of Tetrahydroquinolone lead.	42
Chapter 2 Design and Synthesis of Cytochrome <i>bc</i>₁ Inhibitors; Exploring novel scaffolds for improved properties.	43
2.1 Design of new cores.....	43
2.1.1 Metrics in Medicinal Chemistry.....	45
2.1.2 Assessment of designs	46
2.1.3 Design and Synthesis of Tetrahydroquinolones based inhibitors.....	47
2.1.4 Design and Synthesis of Cyclo-penta/hepta-[b]pyrid-4-one based inhibitors	49
2.1.5 Design and Synthesis of the Triazolo/pyrazolo[1,5-a]pyrimidin-(4H)-ones based inhibitors.....	51
2.1.6 Design and Synthesis of Tetrahydroquinazolinediones based inhibitors.....	54

2.1.7 Design and Synthesis of Naphthyridin-(4H)-ones based inhibitors.....	56
2.2 Cellular Activity and Physiochemical Evaluation of novel inhibitors.....	64
2.2.1 Preliminary ADMET and Physiochemical Properties.....	66
2.2.1.1 Aqueous solubility	66
2.2.1.2 Metabolic stability	67
2.2.2 Computational modelling.....	69
2.3 Summary and future work	73
Chapter 3 Design, Synthesis and Optimisation of Tetrahydroquinolones	75
3.1 Validation of target site.....	75
3.1.1 Yeast mutagenic studies	75
3.1.2 Plasmodium assays	76
3.1.3 Synergistic studies	77
3.1.4 Co-crystallisation: crystal structure of 57 within bovine Q _i site.	78
3.2 Series development	79
3.2.1 Design of Tetrahydroquinolones Series	80
3.3 Synthesis of Tetrahydroquinolone series	81
3.3.1 Retrosynthesis of tetrahydroquinolones	81
3.3.2 Synthesis of Tetrahydroquinolone fragment.....	82
3.3.3 Diaryl ether synthesis.....	83
3.4 Route development/optimisation	90
3.4.1 Forming the tetrahydroquinolone boronic ester.....	90
3.4.2 Stepwise synthesis.....	91
3.4.3 Eliminating the alkylation/dealkylation steps.	96
3.4.4 Other synthesis	99
3.5 Summary of synthesis.....	101
3.6 Biological, ADMET and physiochemical evaluation.....	102
3.6.1 Cellular assay results	102
3.6.2 Structure Activity Relationships	105
3.6.2.1 Acid moieties.....	105
3.6.2.2 Heterocycles	105
3.6.2.3 Terminal ring substitution pattern.....	106
3.6.2.4 <i>m</i> - vs <i>p</i> - vs extended diaryl linkage	106
3.6.3 Mitochondrial assay.....	106

3.6.4 Cytotoxicity assays.....	109
3.6.5 Preliminary ADMET and physiochemical properties	109
3.6.6 Metabolic stability	109
3.6.7 Aqueous solubility	111
3.7 Summary.....	113
Chapter 4 Progression of Compound 169 and Further Development of the Tetrahydroquinolone series	115
4.1 Further evaluation of tetrahydroquinolone-based leads as potential antiparasitics.....	115
4.1.1 Efficacy vs Bradyzoites <i>in vitro</i>	115
4.1.2 Permeability studies	115
4.1.3 Protein Binding.....	118
4.1.4 CYP450, HERG, and HepG2 studies	119
4.1.5 <i>In Vivo</i> efficacy studies.....	120
4.1.6 Mitochondrial toxicity: comparative metabolic assays	121
4.2 Further development of Tetrahydroquinolones.....	122
4.2.1 Increasing selectivity	122
4.2.2 Design of more selective THQ inhibitors	123
4.2.3 Synthesis of six- and seven-substituted Tetrahydroquinolones	124
4.2.4 Synthesis of 2-position methyl hydroxy and carboxylate derivatives.....	132
4.2.5 Prodrugs.....	138
4.2.6 Cocrystallisation studies of compound 169 in the cytochrome <i>bc₁</i> complex	141
4.3 Summary and future work	142
4.4 Summary & Achievements	144
4.4.1 Future work.	147
Chapter 5 Experimental	150
5.1 General procedures	150
5.2 Experimental: Chapter 2	152
5.2.1 General method A (Cyclisation of pyrazoles/triazoles)	152
5.2.2 General method B (Deprotection)	152
5.2.3 General method C (Naphthyridone formation)	152
5.2.4 General method D (iodination)	152
5.2.5 General method E (O-alkylation).....	153
5.3 Experimental: Chapter 3	171

5.3.1	General method F (Chan Lam)	171
5.3.2	General method G (Copper coupling)	171
5.3.3	General method H (One Pot Suzuki alkylated).....	171
5.3.4	General method I (One Pot Suzuki)	172
5.4	Experimental: Chapter 4.....	211
5.4.1	General procedure J (Quinolone formation)	211
5.4.2	General method K (Hydrogenation)	211
5.4.3	General method L (Iodination).....	211
5.4.4	General method M (One Pot Suzuki)	211
5.4.5	General method N (Suzuki).....	212
5.4.6	General method O (Conjugate addition).....	212
5.4.7	General method P (Thermal cyclisation)	212
5.4.8	General method Q (N-Oxide formation)	213
5.4.9	General method R (Boekelheide rearrangement)	213
	Molecular Modelling/Chemogenomics.	253
	<i>In Vitro</i> Challenge Assay for Toxoplasma Tachyzoites	270
	In vitro Challenge Assay for Bradyzoites.....	271
	X-ray crystallography studies	272
	Solubility assay	273
	Microsomal stability assays.....	273
	Protein Binding assay	274
	MDCK MDR1 Permeability.....	275
	CYP inhibition assay	275
	hERG inhibition assay.....	277
	<i>T.gondii</i> <i>In Vivo</i> mouse assay	278
	<i>P.berghei</i> causal prophylaxis <i>in vivo</i> model	278
	Hep G2 toxicity studies	280

Chapter 1 Introduction

Classified as a neglected tropical disease toxoplasmosis is in fact found worldwide, and while not as frequently lethal as better-known infectious diseases, its widespread prevalence makes it a substantial burden on human health.

In order to better understand, treat and eliminate toxoplasmosis, it is first necessary to understand the disease and its causative agent; the parasitic organism *Toxoplasma gondii* (*T.gondii*).

1.1 *Toxoplasma gondii*

The parasite was first isolated in 1908 from a gerbil like mammal, identified incorrectly as *Ctenodactylus gondii* (correctly *Ctenodactylus gundi*), and the tissue of rabbits by Nicolle and Manceaux, and Splendore respectively.¹ *Toxoplasma gondii* is an obligate, intracellular, protozoan parasite, it is prevalent globally and infects all species of mammals, and in addition it has been isolated from every tissue in experimentally infected rodents. Altogether this makes a compelling argument to consider *Toxoplasma gondii* one of the most successful parasites on the planet even in relation to prokaryotic and viral diseases.²

Classification:

Phylum: Apicomplexan

Class: Sporozoasida

Subclass: Coccidiasina

Order: Eimeriorina

Family: Toxoplasmatidae

Genus: Toxoplasma

Figure 1.1:

Taxonomical classification of *Toxoplasma gondii*

1.1.1 Life cycle

The life cycle of the parasite *Toxoplasma gondii* is complex, with multiple stages, and the possibility of both vertical and horizontal transmission at several stages between hosts. Vertical transmission occurs when an infection

is acquired congenitally, horizontal transmission can occur through several routes involving environmental exposure, primarily ingestion.

The parasite can survive in three behaviourally distinct environments; in an external environmental stage, within its intermediate hosts, such as mammals and birds, and within its definitive hosts; Felids. *T. gondii* exists in several distinct life stages dependent on these environments. As an intermediate host, the most relevant stages to human infection are known as the bradyzoite and tachyzoite. Both stages can be seen in the green section of **Figure 1.2**.

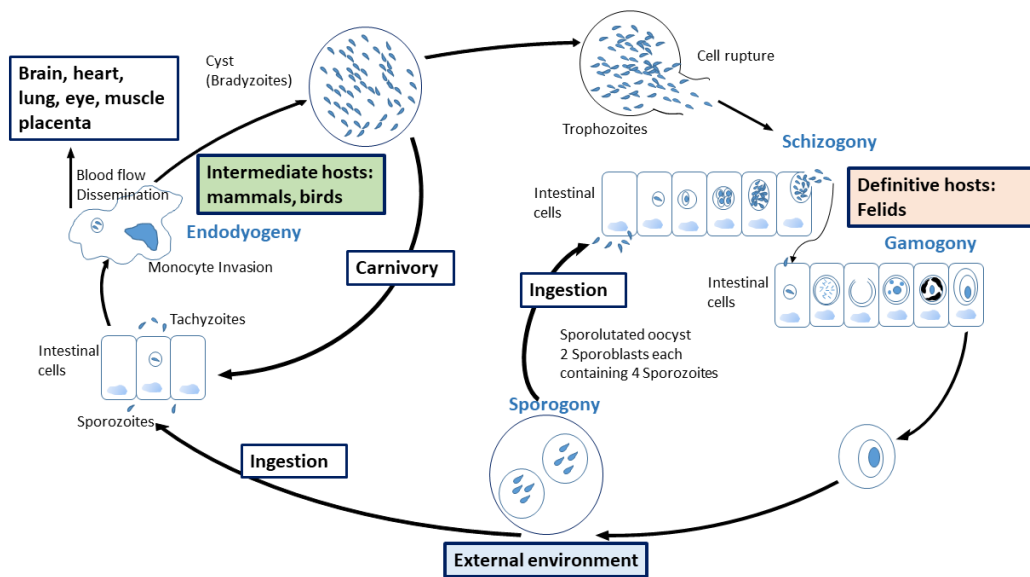


Figure 1.2:

The life cycle of *Toxoplasma gondii* parasite. Adapted from clinical microbiology review 2012.³

The bradyzoite stage is the latent or dormant form of the parasite and replicates slowly. Bradyzoites form cysts preferentially within brain and muscle tissue, varying in size depending on maturity with small 10 μm cysts containing only two bradyzoites and larger 100 μm cysts containing several hundred parasites.³ These cysts remain intracellular throughout their growth.⁴ The protective cyst wall in combination with slow metabolism enables the bradyzoites to survive for extensive periods of time. The cyst wall itself is made of a limiting membrane and a granular inner-layer, but this can be disrupted by host cell death, triggering the release of the bradyzoites within.

During the tachyzoite stage the parasite proliferates and disseminates rapidly, through asexual reproduction. Specifically, tachyzoites reproduce via endogeny, a specific form of reproduction in which two progeny form within the parent parasite, eventually consuming it. Impressively the tachyzoite

organism is able to invade almost all vertebrate cell types,³ aiding the parasites impressive proliferative abilities.

Transition between infective stages is believed to be triggered by environmental factors. An example being particular forms of stress which induces tachyzoite to bradyzoite transformation. Stresses may be in the form of heat, chemical, nutrient deprivation or changes in pH. *In vivo* this allows the parasite to move from the rapidly growing tachyzoite to the more resilient bradyzoite stage when its environment becomes hostile. Typically, such situations being during the immune response of the host. The full extent of the mechanisms and signalling involved in this transition are not fully elucidated, but there is a clear transition in biological behaviour including a move to a glycolysis dependent metabolic pathway over an oxidative phosphorylation based one.²

1.1.2 Structure and morphology of the *T.gondii* parasite

In both the tachyzoite and bradyzoite infective stages the parasite has very similar morphology and structure (shown in Figure 1.3), like many single cell eukaryotes, *T.gondii* possess a single mitochondrion. Morphologically the parasite is crescent shaped with a rounded posterior end and the apical frontal end containing the organelles that form the phylum's name sake apical complex.⁵ This organelle structure is conical and situated at one end of the parasite giving it its apical shape and plays a role in allowing the parasite to enter a host cell.⁵ The organelles that form the apical complex are the conoid, rhoptries, dense granules and micronemes all of which are suspected to function in aiding the parasite during host cell invasion.

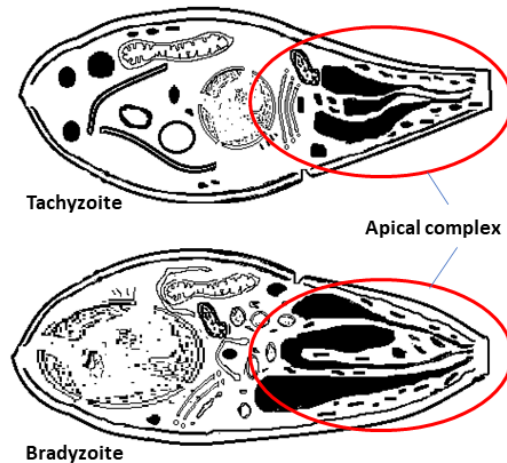


Figure 1.3: Bradyzoite and tachyzoite cell structures; Illustrating the many organelles involved and the complexity of the apical complex. Recreated based on image from Structures of *Toxoplasma gondii* Tachyzoites, Bradyzoites, and Sporozoites and Biology and Development of Tissue Cysts⁶

1.1.3 Environmental stage

In addition to the bradyzoites and tachyzoites, there is also a third infective stage of *T.gondii*; known as sporozoites. Sporozoites exist outside of a host protected within a protective structure known as an oocyst. As with all coccidian members of the *Eimeria* order, *T.gondii*'s oocysts each hold a total of eight sporozoites split between two sporocysts.⁷ Oocysts are a multi-layered structures, 12-13 μm in length with an ovoid shape, designed to protect the sporozoites from environmental damage both mechanical and chemical. These oocysts function exceptionally well in protecting their cargo with the organism known to survive viably for over a year outside a host.⁷

1.1.4 Primary host

Toxoplasma gondii is able to reproduce both sexually and asexually depending on its host, with sexual reproduction only occurring in the definitive hosts; felids (cats).⁸ This cycle begins with ingestion of prey tissue infected with bradyzoite cysts, the cysts wall is ruptured during digestion to release the bradyzoites, which then settle within enterocytes. Bradyzoites have been shown to be resistant to pepsin, a primary enzyme released in the stomach to degrade proteins, allowing them to survive during ingestion.⁹ Having embedded themselves, the bradyzoites go through a number of self-limiting replications, characterised by the development of merozoites within schizonts;

this is followed by sexual development to form the male and female gametes.^{10,11} After fertilisation these gametes then form oocysts which will be released upon disruption of the host cell, to be excreted with the felids faeces. Only after exposure to the environment will sporogony occur, to form the two sporocysts, each containing four haploid sporozoites, within the oocyst (blue section of **Figure 1.2**).

Once matured oocysts can then infect almost all warm-blooded organisms to some degree. Transmission to these intermediate hosts usually occurs through ingestion of contaminated food sources. During infection of an intermediate host the parasite is capable of asexual reproduction only. This begins with ingestion and the release of sporozoites into the intestinal epithelium. After penetrating the hosts' epithelium, sporozoites differentiate into the rapidly disseminating tachyzoites to spread throughout the host, replicating through endodyogeny (the process of asexual development in which no separate nuclear division occurs) in any host cell. After dissemination throughout the host the tachyzoites transform into bradyzoites forming cysts within the hosts' tissue. These cysts and the contained parasites can then survive the life time of the host, remaining infectious if cyst contaminated tissue is consumed. In addition to these horizontal routes of transmission, vertical (or congenital) transmission may occur if the acute stage (tachyzoite dissemination) of the infection occurs during host pregnancy. This due to the tachyzoite organism being capable of traversing the placenta, and thereby entering the foetal blood stream.

1.1.5 Prevalence

The multiple stages of *Toxoplasma gondii* coupled with its various route of transmission result in an extremely complex life cycle, which is well adapted to make it one of the most successfully distributed parasites. Its ability to be transmitted effectively has led to an estimated third of the human population being infected.¹²

The first report of *T.gondii* appeared in 1908 and the presence of tachyzoites in North African rodents.¹³ Since then the parasite has been found around the world across a broad range of geographic and economic environments. In human populations, seropositive individuals are found across the globe, with some suggested correlation between warmer moister climates and more rural

developing economies. However, these are not exclusive determinants for levels of seropositive population. Other more cultural factors, such as consumption of raw meat, have effects due to the nature of the parasite's life cycle.

In addition to its flexible lifecycle and numerous methods of transmission *T.gondii* has another method to maximise its potential for dissemination which involves affecting host behaviour. These behavioural changes have been mostly observed in its definitive host; cats, and their natural prey/food-source; rodents. The two best examples of this are the ability of the parasite to reverse the innate fear response that rodents associate with feline urine to one of attraction, and additionally to increase the sexual appeal of male felids to females.¹⁴ Both of these examples can clearly be seen as highly beneficial to parasite proliferation. The combination of versatile routes of transmission and adaptive behaviour has made *T.gondii* an impressively prevalent parasite.

1.1.6 Strains

The species *T.gondii* consists of three known strains; known as type I, II & III.¹⁵ These strains differ in virulence and pattern of epidemiology. Notably type II is the strain most commonly identified in AIDS patients. Type I & II have been noted in congenitally infected patients while type III is the most common strain identified in animal hosts.¹⁶ Understanding the genetic difference between strains and the corresponding pathogenic discrepancies may help in the management and treatment of the disease caused by *T.gondii* infection in human toxoplasmosis.

1.2 Pathology of Toxoplasmosis

T.gondii is the causative agent of the human disease known as toxoplasmosis. In general, the known symptomatic activity is caused by the tachyzoite stage of the parasite which is capable of proliferating rapidly. If this proliferation is left unchecked by either the immune system or treatment, death can result.

1.2.1 Transmission/acquisition

In humans, toxoplasmosis can be acquired through a number of routes; environmental, congenital and via organ transplant.¹⁷

Most commonly infection is a result of ingestion. This may come about in a number of ways, primarily the main sources are either; environmentally contaminated water or food (oocysts), or undercooked meat from infected livestock (tissue cysts). This environmental transmission appears to be a substantial contributor to parasite proliferation; demonstrated by the strong correlation between seroprevalence and eating and hygiene habits of a population.

The risks of congenital infection are greatest if acquisition occurs during gestation, with the parasite gaining access to the foetal circulation via infection of the placenta, in these cases congenital transmission rates range from 1-10 in 10000 live births.¹⁸ Infections occurring previous to gestation are of low to no risk, with the exception of mothers who acquired the disease within at most 3 months of conception. Infection acquired within the first 2 weeks of gestation does not result in vertical transmission in women taking Spiramycin. In contrast, transmission rates may be greater than 60% during the final trimester. Importantly, and fortunately, there is an inverse relationship between transmission frequency and disease severity.

The Final route of transmission; via organ transplantation, can occur when a seropositive donor's organ is transplanted into a seronegative recipient for most solid organ donations. It is also possible for transplantation to cause reactivation of latent infection in bone marrow and haematopoietic stem cell, and liver transplant patients. In addition there have been rare incidence of infection via blood from immunocompetent to immunocompromised individuals known, in this case it is the usually environmentally sensitive tachyzoite that is transmitted.¹⁹ Needle stick transmission has also been documented.³

1.2.2 Pathogenesis of Toxoplasmosis

After transmission, usually via ingestion, the oocyst will be broken down by digestive enzymes releasing the sporozoites. The sporozoites will then penetrate the intestinal wall and are taken up by macrophages. At this point the organism is considered a tachyzoite. The tachyzoite resides within a membrane bound parasitophorous vacuole, and the host cell is unable to destroy the parasite as it inhibits the fusion with the lysosomal vessels. Cell invasion is a complex process, and toxoplasmosis is not limited in respect to

cell type of its host and therefore does not require tissue specific receptor molecules. It does however, require sequential coordination of a number of organelles including; the micronemes, rhoptries, and dense granules all located in the apical end of the parasite.¹⁸

The macrophages play host to replication of the parasite and act to distribute the parasite around the body. Each macrophage will have 10-20 tachyzoites produced within until eventually succumbing to the infection and releasing the parasite to the surrounding tissue.¹⁸ Further replication continues until an induced immune response is triggered. The results of this rapid proliferation can be extensive tissue damage. When the immune response is initiated the tachyzoites are forced to differentiate in to the bradyzoite stage. The bradyzoite divides by both endodyogeny and endopogony and then organise into cysts.

1.2.3 Pathology within Immuno-Competent Patients

In healthy humans, the pathology of the disease is relatively mild and often initial infection is asymptomatic. When symptoms are noted infection is characterized by fever, malaise and lymphadenopathy (swelling of lymph nodes). Very rarely more severe symptoms may present in otherwise healthy individuals, these include; myocarditis, polymyositis, pneumonitis, hepatitis or encephalitis.³ Despite its usually mild symptoms, toxoplasmosis is nevertheless the most common food-borne parasitic infection requiring hospitalisation, and the third most common cause of hospitalisation due to food-borne infection overall.²⁰ As a result toxoplasmosis is a leading cause of loss of disability adjusted life years.^{17,20,21} it is important to note that, even in asymptomatic presentations, it is believed the parasite persists within the host for the duration of the host's life, allowing for recrudescence and or further transmission should opportunity allow.²²

In addition, significant association between infection and meningioma (tumours arising in the meninges, the membranous layers surrounding the CNS) has been demonstrated.²³

1.2.4 Pathology within Immuno-compromised Patients

Those most vulnerable and at risk to toxoplasmosis are those with a compromised immune system. The most common reasons for

immunocompromised status are; AIDS as a result of HIV infection; as a result of medication for cancer or as a result of immune suppressant medication for the prevention of rejection during transplanted organs. The danger for these patient groups is significantly higher in proportion to many other infectious diseases due to the persistent nature of the parasite within its host. This is due to the afore-mentioned cysts formed within patient tissue (bradyzoites), allowing the evasion of short-term treatment. In these cases, reactivation of toxoplasmosis occurs as a result of the infection taking advantage of the compromised immune systems. In the worst cases, infection results in toxoplasmic encephalitis as a result of tissue damage caused by replication of the parasites and the release process compounded by inflammation triggered in response. Before the advent of highly active antiretroviral therapy toxoplasmic encephalitis (encephalitis is the potentially fatal inflammation of the brain) (TE), caused by toxoplasmosis, was a leading cause of death amongst HIV patients.

1.2.5 Pathology of Congenital and Antenatal Infections.

Toxoplasmosis also poses a number of dangers if contracted during pregnancy due to the ability of the parasite to cross the placenta and infect the foetus. This danger can be exceptionally severe commonly causing miscarriage, still birth or severe developmental damage in new-borns, including blindness and epilepsy. The severity of the developmental damage is highly dependent on the timing of infection with regards to the stage of pregnancy. Infection during the first trimester will most likely result in severe foetal damage, as a result of rapid tachyzoite growth.²⁴ However, infection in later stages may still cause extensive damage to the foetus, up to and including miscarriage. Fortunately, the risk of transmission correlates inversely with the potential for harm, minimising the frequency of worst-case outcomes.

1.2.6 Ocular Toxoplasmosis

In infants asymptomatic at birth, the possibility of illness in later life still exists, commonly including ocular lesions, as a result of retinochoroiditis, that can result in blindness. Retinochoroiditis is the inflammation of the retina and choroid. It was previously thought that retinochoroiditis was purely a result of

congenital infection. However more recently it has been suggested that this can occur as a result of acute infection. The likelihood of acute infection causing retinochoroiditis is largely dependent on the strain of *T.gondii*, as shown by large variation in incidence rates between areas with different parasite strains.^{25,26}

1.2.7 Behavioural and Neurological Effects of Toxoplasmosis.

Since its original discovery, research into the dangers of toxoplasmosis has largely concentrated on the acute stage in immunocompromised individuals and the congenital effects that can occur from acute infection during pregnancy, as these are the most obviously dangerous and harmful. Given the affinity of the parasite for brain tissue and the central nervous system (CNS), it is not entirely surprising that infection can have neurological and behavioural effects.

Acute infections have been described presenting psychiatric complications such as disorientation, psychoses with schizophreniform features, anxiety and depression.^{27,28} Case studies have demonstrated that seropositive patients expressing depression and exhibiting poor response to antidepressants, can have an improved response after treatment for *Toxoplasma gondii*.²⁹

In addition, since the 1990's, investigations have been conducted on the long term effects of the chronic form of infection, especially on neurological functions, which were previously regarded as clinically unimportant.³⁰ It has since been suggested that chronic or latent infection may also cause neurological changes such as those described in acute conditions. In China, surveys have also positively correlated sero-positivity with decreased capacity for learning and memory and increased simple reaction time. The infected subjects had lower IQ and lower probability of achieving a higher education.³¹ The behavioural effects of the latent parasite have been demonstrated to be sex and age dependent. In young males, seropositive subjects were found to be more prone to higher impulse sensation seeking, while women experience increased reactive aggression.^{32,33}

It has been suggested that these neurological alterations are a result of changes in dopamine levels in brain tissue, brought on by the presence of *Toxoplasma gondii* cysts.³² It is possible that these behavioural effects are a

by-product of the effects seen in the primary host and their prey, designed to increase transmission.

A large amount of research into the parasite and its neurological pathology remains ongoing, but is largely beyond the scope of this project, other than emphasising the potential that toxoplasmosis has an even greater impact on global health than currently understood.

1.3 Treatments and Molecular Targets

Toxoplasmosis as a disease presents a number of challenges to developing an effective treatment. This combined with several non-scientific factors that contribute to its status as a neglected tropical disease (although given its widespread prevalence tropical is debatable), have led to a lack of development of suitable drugs.

1.3.1 Past and Current treatments.

There are a number of anti-infective agents to treat toxoplasmosis used across the globe, depending on the context of infection and individual nation's policies. The main circumstances for treatment of toxoplasmosis are; in seropositive AIDS patients, solid organ transplant (SOT) patients, ocular toxoplasmosis and to prevent congenital infections.³

In the case of prevention of congenital toxoplasmosis, treatment is highly dependent on the stage of pregnancy at which the infection was detected. Spiramycin (1) is usually given in the first trimester of pregnancy after which treatment may change to a combination therapy consisting of sulfadiazine (2) and Pyrimethamine (3) (**Figure 1.4**).³⁴

In cases of toxoplasmosis in immunocompromised individuals the normal approach is prophylactic treatment. In toxoplasma-seropositive AIDS patients, prophylactic application of trimethoprim (4) and sulfamethoxazole (5) (co-trimoxazole) is often used to prevent recurrence leading to fatal TE.³⁵ Alternatively, in cases where this treatment is not tolerated, patients are given combination treatments of dapsone (6), pyrimethamine (7) or sulfadoxine (8) and pyrimethamine (3).³ Atovaquone (9) with or without Pyrimethamine (3) (with folinic acid 10) can also be used, provided adequate absorption is achieved.³⁶

In general, immunocompetent adults will not require treatment, however in the case of severe symptoms; treatment with a combination of pyrimethamine (**3**), sulfadiazine (**2**), and folinic acid (**10**) for two to four weeks is typical.

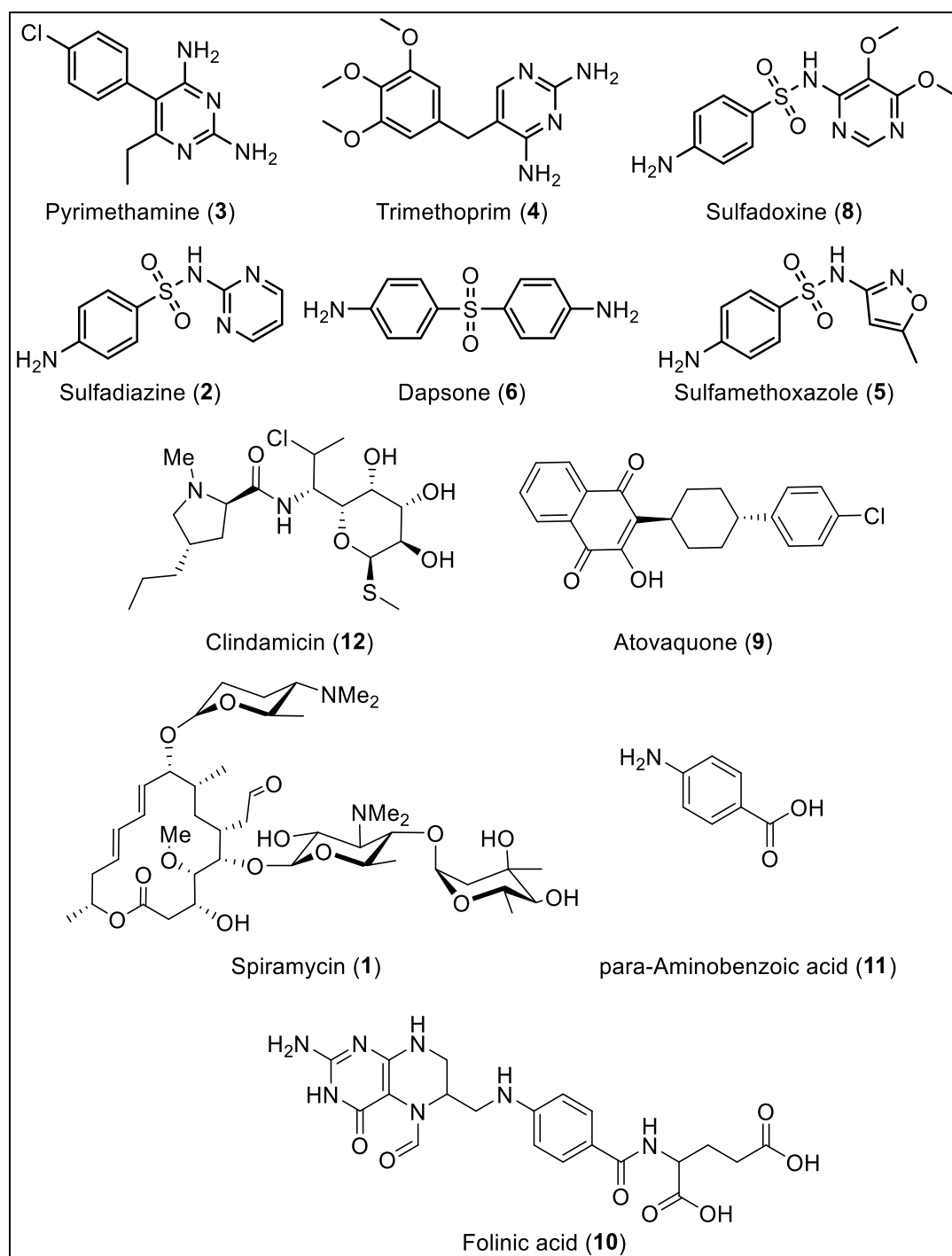


Figure 1.4: Current treatments (**1-9**) and examples of competing natural substrates (**10-11**)
The treatments above target a variety of pathways within the parasite including dihydropteroate synthetase, dihydrofolate reductase, microbial ribosome and the cytochrome *bc*₁ complex

The first group of these the sulphonamides were the first class of antimicrobials and include sulfadiazine (**2**), sulfamethoxazole (**5**) and sulfadoxine (**8**), and achieve their therapeutic effect through the competitive

inhibition of the enzyme dihydropteroate synthetase (DHPS), an enzyme involved in folate synthesis, Dapsone (**6**), while not a sulphonamide, also acts through this mechanism.³⁵ These compounds act as competitive antagonistic inhibitors competing with *para*-aminobenzoate (**11**) to prevent synthesis of dihydrofolic acid. The downstream effect of this inhibition is to eliminate the parasites ability to synthesis amino acids, purine and thymidine.

The second group of compounds including; pyrimethamine (**3**) and trimethoprim (**4**), are commonly given in conjunction with sulphonamide-based drugs. This is because like the sulphonamides these compounds interfere with the parasite's folate synthesis cascade. In this case they specifically interfere with tetrahydrofolic acid synthesis from folic acid by inhibiting the enzyme dihydrofolate reductase (DHFR). DHFR is the next enzyme in the folate synthesis process following DHPS to produce tetrahydrofolic acid. Pyrimethamine (**3**) and trimethoprim (**4**) both act through competitive inhibition binding in place of dihydrofolate. Tetrahydrofolic acid synthesis is needed for DNA and RNA synthesis in many species, including protozoa.³⁷

By using a combination of these two types of compounds, a synergistic effect is observed. It has been shown that sulphonamides strongly potentiate the effect of pyrimethamine (**3**).^{37,38} The precise mechanism of this synergism has been disputed as, while potentiating effects as a result of inhibiting consecutive enzymes in a given pathway have been proven (illustrated in **Figure 1.5**), there is also evidence of sulphonamides modestly inhibiting DHFR and that single enzyme synergism has been observed.^{39,40}

Synergism is naturally a highly desirable effect, with the potential to increase therapeutic index and confer protection against the development of resistance. This certainly contributes to the successful usage of combination treatments, especially in the case of pyrimethamine (**3**) which otherwise has relatively poor selectivity.

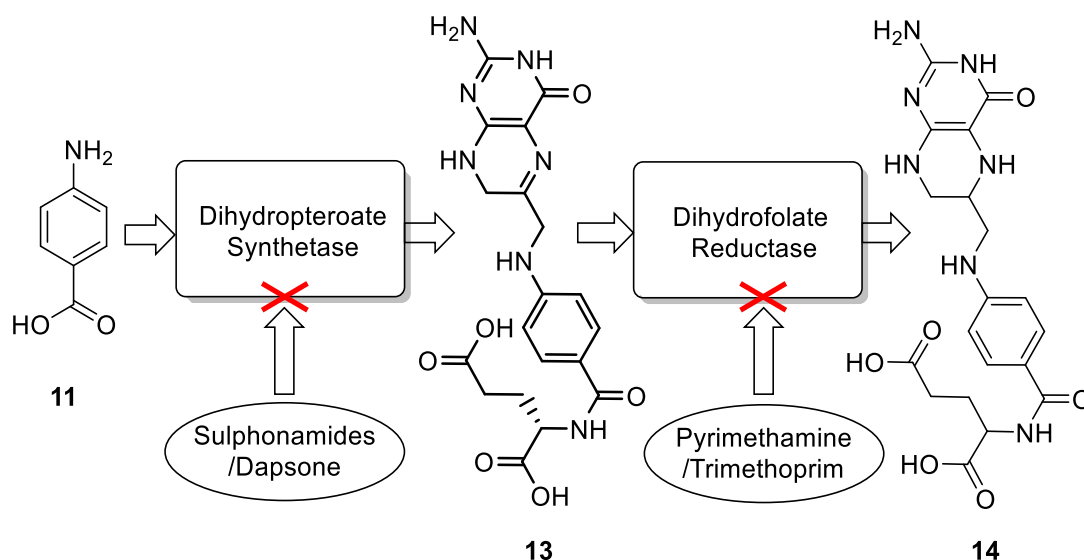


Figure 1.5:

Folic acid synthesis pathway, illustrating the respective points of inhibition for sulphonamides and pyrimethamine/trimethoprim.

A second important advantage to inhibition of the folate synthesis pathway is the ability of vertebrates to make use of pre-synthesized folic acid. This means that folinic acid can be administered as part of the treatment without adverse effect, while reducing the potential side effects.

As a macrolide, Spiramycin (**1**) has a different mechanism of action to the folic acid synthesis inhibitors. Like other macrolides, Spiramycin acts via binding to the large ribosomal subunit and interfering with protein synthesis, thereby killing the parasite. Despite lower efficacy than treatments such as pyrimethamine or the sulphonamides, Spiramycin has the advantage of being well tolerated, as a result Spiramycin (**1**) has been used for the primary prevention of congenital toxoplasmosis.⁴¹ The rationale behind the use of Spiramycin (**1**) being to reduce the parasite burden in the mother, specifically tachyzoites, and thereby lower the risk of transmission. Since this molecule is largely impermeable to the placental barrier there is little risk of adverse drug effects on the fetus.^{34,42}

Clindamycin (**12**) works in a similar way to macrolides like Spiramycin (**1**), and also interferes with protein synthesis. Specifically, it inhibits ribosomal translocation binding to the 50S rRNA of the large bacterial ribosome subunit. Clindamycin is primarily used in cases of ocular toxoplasmosis as it has the advantage of being injectable directly into the eye.

Atovaquone (**9**) targets a different mechanism to those mentioned previously. Designed as an anti-malarial it acts by inhibiting electron transport in the bc₁

complex, which leads to the collapse of mitochondrial membrane potential.^{43–}
⁴⁵ Notably atovaquone has been shown to have some effect on cyst burden.
⁴⁶ Identifying targets with potential to reduce cyst burden is a step towards developing treatments capable of eliminating the risk of recrudescence. As such the cytochrome *bc*₁ complex discussed further, below.

1.3.2 Deficiencies of current treatments

The majority of current treatments for toxoplasmosis are either old or repurposed antimalarial drugs and as such have several deficiencies.

The combination of sulphonamides and pyrimethamine (**3**), while effective on the acute stage of infection, is not able to eradicate the parasite. In addition to this the high rate of elimination of sulpha-compounds requires daily doses over several weeks or months and toxicity of Pyrimethamine (**3**) also makes it undesirable for sustained use. Side effects from treatment include; thrombocytopenia and/or leukopenia. They are also of limited efficacy against ocular infection.¹⁸

As mentioned above, Spiramycin (**1**), is well tolerated but its efficacy against *T.gondii* is limited and therefore its use is limited to during pregnancy where low risk of adverse effects are highly desirable, especially in comparison to Pyrimethamine (**3**) which is classified as a teratogen and so not desirable to use during pregnancy.

Additionally, none of these compounds are able to eliminate the latent infection, given that toxoplasmosis' primary danger is in combination with other chronic diseases such as HIV infection, the inability to eradicate the parasite and prevent recrudescence is highly limiting.

While Atovaquone (**9**) has been shown to reduce cyst burden to some extent, it falls short of eliminating the parasite. Another problem associated with Atovaquone (**9**) is the known risk of resistance development, which is well reported in the case of malaria and one of the main reasons it is usually administered in combination with an additional anti-infective.⁴⁶ This risk of developing resistance is exasperated when a treatment is used long term such as in prophylaxis and chronic infections.

Overall relatively little progress has been made over the last 50 years in developing new anti-toxoplasma agents and there is a strong need for the development of new drugs, better suited to the demands of the disease.

1.4 Drug Design and Development; Anti-Parasitics.

The development of a new drug is an extremely intensive process with respect to resources and time and as a result invariably expensive. The result of this is a prioritisation of research focus which has left many “unprofitable or high risk” diseases under resourced. Infectious diseases have suffered particularly as a result and, part of this is due to the challenges that they present as drug targets in addition to economic reasons. This can be seen in the lack of progress in toxoplasmosis treatments. Efforts to optimise and increase the efficiency of the drug discovery process are constantly ongoing with the methods evolving rapidly with increasing understanding, knowledge and technological advances.

1.4.1 Hit identification

The first step in drug discovery is identifying an initial starting point. The methods used for this have evolved with increasing understanding and technology, however they can essentially be split into phenotypic and target-based approaches.

1.4.1.1 Phenotypic based screening

Phenotypic screening is the screening of compounds based on them inducing a desirable observable phenotype. Within infectious diseases this phenotype is typically death of the infectious organism but could quite simply be survival of the host.

As such, phenotypic screening is the earliest form of drug discovery. These medicines were derived from natural sources, effectively screened on a phenotypic basis. As technology has advanced, it is now possible to identify individual natural products responsible for the observed biological effect. In the context of parasitic diseases, the desired phenotypical outcome is usually simply parasite death, screened on cell-based assays.

Phenotypic screening has a number of advantages; firstly, a known biomolecular target is not required. While it may be desirable for optimisation and development, it is not necessary to have a specific target identified when carrying out phenotypic screening. Secondly; hits from a phenotypic screen have demonstrated efficacy beyond simple ligand activity (after accounting for

potential assay artefacts) lowering the risk of failure in later stages for reasons such as inability to reach the target site, often a problem in antimicrobials.^{47,48} Phenotypic screening remains the basis of many successful drug discovery programmes, with recent examples including the discovery of teixobactin, a novel antibiotic natural product produced by soil bacteria.^{49,50} However, phenotypic screening does have a number of limitations; most notably that optimisation of the desired compound can be challenging as without target information there is little rationale to guide drug development. This means development must be conducted essentially blind. This also limits the ability of a project to anticipate likely potential pitfalls or opportunities. Alternatively, efforts could be made to determine the mechanism of action and thereby the target, to move towards a more structure-based development. Phenotypic screening, along with genomic analysis, is an important method in identification of novel targets, feeding into target-based design.

1.4.1.2 Target based screening

The advances in understanding disease mechanisms and the use of genomics in the identification of targets, along with improved protein production methods have all contribute to rapid development in the ability to identify promising molecular targets and develop appropriate assays for a wide range of proteins.⁵¹ While genomics has perhaps not delivered as richly as prophesised, it has still provided a rich basis for target based screening, through the mapping, and elucidation of the structure and function of genomes.^{47,51,52} The advantages of target based screening are that more rational approaches to screening and design may be made, potentially eliminating wasted resources. Specifically, a targeted approach opens up other possibilities, such as; substrate inspired design, structure-based design and fragment-based approaches.

The difficulty of target-based screening program is the intensive biological work required to identify a 'druggable' protein, or other biological target, involved in the disease pathway. This is frequently a bottle neck in developing new treatments, and results in many drug programmes focusing on existing better understood targets. In the case of antimicrobials desirable biological pathways to target are usually those crucial to the survival of the pathogen.

1.4.1.3 High Throughput screening

High throughput screening can be carried out both phenotypically and against a specific target, provided a robust assay exists. As both the technology and techniques to perform assays rapidly, reproducibly and in large numbers, typically >1 million compounds, has become available, alongside the emergence of an increasing number of commercially available small molecules libraries, High throughput screening became an increasingly popular method of hit identification, and many companies invested significant resources in developing and synthesising their own sizable compound libraries, as an alternative to screening natural products, which pose a number of difficulties in isolating due to the requirement of extracting and purifying. These libraries can then be screened against either specific identified molecular targets or more phenotypic style assays, while this approach has perhaps not delivered the huge number of leads envisioned at its conception (like most drug discovery innovations) it is still a prominent method of hit identification. Limitations of HTS are that although the number of compounds tested may be vastly more than via traditional methods, the quality and diversity of commercial libraries remains below ideal, with a tendency to cluster around flat synthetically amenable points in chemical space. While this problem has been identified and attempts are being made to mitigate this,⁵³ the feasibility of certain chemistry will naturally bias the composition of any commercial library. In addition, the need for robust assays amenable to HTS can be technically challenging and expensive to develop.

1.4.1.4 Structure-based drug design and vHTS

Structure-based drug design (SBDD) is an extension of target-based screening. The first SBDD based projects began yielding success within a decade of initiation, in the mid 80's.^{54,55} Having identified a target protein, the structure of the protein and binding site must then be characterised or modelled. There are a number of methods to characterise and model a target site including X-ray crystallography, NMR, cryogenic electron microscopy and sequence-based modelling.⁵⁶⁻⁵⁸ Obtaining a high-resolution crystal structure of the target protein from the target species is the ideal starting point as this is likely to carry the lowest degree of error. This is most beneficial if the structure

has a bound molecule, such as the protein's substrate bound in the targeted site as this can account for conformational changes that may occur on binding. Although significantly different ligands may, induce different conformations further complicating matters. NMR spectroscopy may also be used to gain further information, as this is done in solution, it can give useful insights into the protein's dynamics. An alternative approach where a crystal structure is not attainable, either for the species or the protein, is the use of a homology model based on analysis of the protein's sequence compared to existing characterised structures. The reliability of structures acquired through this method varies depending on the similarity of the template and target amino acid sequence.

From this point, there are a number of possible computational methods to discover an initial virtual hit. The primary techniques are; substrate-inspired design, virtual high throughput screening (vHTS) and *de novo* or fragment-based design. In each case, specialised software can be used. The main software used within the research group for *de novo design* is SPROUT, which uses a stepwise approach to progressively build a molecule from a selection of fragments, optimising for steric and electronic interactions.⁵⁹ The use of software such as rapid overlay of chemical structure (ROCS) can be used in substrate inspired design approach.⁶⁰ Lastly vHTS can be accomplished using software such as eHiTS which is able to dock and score large virtual libraries of compound.⁶¹ *In silico* approaches to ligand design have several advantages over a traditional approaches. Firstly, it is capable of accessing a far broader swathe of chemical space than small molecule compound libraries, including compounds not yet synthesised which might require significant resource investment to reach. The second advantage is that by screening compounds in *in silico* many unsuitable compounds can be eliminated resulting in fewer compounds needing to be screened, physically drastically reducing cost. The disadvantage remains the reliability of the output, which is heavily based on understanding the important factors during input, these range from correct confirmation of target site, to the appropriate tautomer and charge state of the ligand.

1.4.2 Hit to lead

Having identified a hit compound via one or a combination of approaches listed above, there is then usually the need to optimise this towards a more lead-like properties. Typically, a hit is simply a compound that exhibits activity against the selected biological target. The transition to a lead requires further evaluation, both to validate the activity and the potential for further development.

To do this a library of related compounds is synthesised and tested. Structure Based Drug Discovery (SBDD) is a powerful tool in designing compounds to optimise their binding affinity for a target site, however in addition to obtaining high *in vitro* activity it is also crucial in drug development to ensure that any compounds developed will be successful *in vivo*. The SAR elucidated from these results can then be fed back into the design of progressively improved molecules, this iterative process is important in optimising a lead compound.

1.4.2.1 From Ligand to Drug; Multi-parameter Optimisation

A consistent problem in drug development is the high attrition rate throughout the process. Minimising this is a complex challenge, part of which means ensuring that the compound has acceptable absorption, distribution, metabolism, excretion and toxicity (ADMET) properties. The nature of drug discovery and the inevitable demand on resources requires most drug discovery ventures to develop a screening cascade. This cascade acts to minimise the required resources, while maximising the amount of useful SAR data obtained. Typically, alongside measuring efficacy of a compound the other early stage assays within a project will include a measure of metabolic stability and a counter screen of some form to ensure observed activity is at least moderately specificity of mode of action. Another important measure is that of aqueous solubility (potentially in a variety of physiological conditions). Later stages in the cascade may only assess candidate compounds which have performed sufficiently in early stage assays.

These might include testing for inhibition against human homologues and other common important targets such as hERG (human ether-a-go-go related gene) and key CYP450 isoforms. Favourable results in these *in vitro* studies give increased confidence for a leads suitability in progression into *in vivo*

models. Ideally these properties will be measured alongside the inhibitory efficacy in the iterative process of lead optimization to prevent the development of a superb ligand at the cost of being an unusable drug.

1.4.3 Opportunities and Challenges of Parasitic Diseases

Each disease type brings its own set of challenges and opportunities to drug discovery and infectious diseases are no different. Even within the area of infectious diseases there are large differences. For example, protozoan diseases will differ from bacterial infections due to the huge differences between prokaryotic and eukaryotic biology. Infectious diseases, as a whole, do offer several advantages, namely; the potential for large differences between host and target biology and clear understandable phenotypes. In the case of differing biology, while these may be more dramatic between the entirely different kingdoms that separate bacterial diseases there are none the less large differences between parasite and host. These differences vary in level from entirely different organelles down to more subtle sequence differentiation in homologous enzymes however all can be exploited to achieve selectivity. Some of the most apparent differences in the apicomplexan phylum include the collection of organelles that make up the invasive apical complex, and notable difference in energy metabolism. With regards to phenotype, there is at least a clear biological outcome, inhibition of the infectious organism, while it may be substantially more complicated in some cases, it is unlikely to present the same difficulties in many other human diseases such as Alzheimer's were the causative mechanisms and therefore sensible approaches to treatment remain fiendishly difficult to elucidate.

One of the consistently most challenging down sides of infectious diseases is delivering drugs in sufficient intracellular concentrations to be effective. This is largely due to the increasing number of membranes and barriers necessary to cross. Toxoplasmosis further enhances this challenge forming both protective cysts and preferentially locating itself within CNS tissue and therefore further protected from small molecules by the blood brain barrier. In addition to this the multiple life stages of the parasite must also be considered, while morphologically the bradyzoite and tachyzoite stages may be very similar there are demonstrable differences between their metabolic activity, a pathway required in one life stage may not necessarily remain so for the other.

As with all infectious diseases the development of resistance is also an ever-present concern. This is shown particularly well in malaria which has demonstrated rapid development of resistance to Atovaquone (.09) for example.

1.4.4 The Apicomplexa Phylum: *T.gondii* and other related parasitic diseases.

When considering toxoplasmosis, it's also worth considering the related disease and their causative organisms, as previously mentioned these have been the original target of several current toxoplasmosis treatments. The parasite *T.gondii* belongs to the phylum Apicomplexa notably one of the least explored taxonomical groups relative to their degree of biodiversity.⁶² This could be considered surprising, given it is the largest group of entirely parasitic organisms, and therefore of great importance in parasitology and medicine.⁶² In addition to *Toxoplasma gondii*, this phylum contains the *Plasmodium* family and the *Cryptosporidium* family, the parasites responsible for the human diseases malaria and cryptosporidiosis respectively. The characterisation of the phylum is based on the presence of an organelle called the apicoplast which is present for at least one stage of the organism's life cycle. The apicoplast itself is a non-photosynthetic plastid but its function is still very poorly understood despite investigation into its origin and structure, generally considered to be involved in cell invasion.⁶³

Successfully developing treatments that are effective for the treatment of *Toxoplasma gondii* has, in addition to the direct impact against a prevalent and dangerous parasite, the potential to lead to a greater understanding and ability to treat other taxonomically-related human parasites.

The Apicomplexa are an interesting phylum from an evolutionary perspective regarding the electron transport chain, as they demonstrate a clear move towards a reduced mitochondrial presence and dependence. This move towards a relatively degenerate mitochondrion has been inferred by the large reduction of mitochondrial DNA (mtDNA) found in several species. Examples include *Plasmodium falciparum* with only 6 kb DNA sequences, arrayed in tandem, of mtDNA while the *Cryptosporidium* species appear to have eliminated all of the mitochondrial genome, while retaining a vestigial mitochondrion-like organelle.

In *Toxoplasma gondii* it is hard to determine precisely the extent of mitochondrial degradation due to the difficulty of identifying the complete mitochondrial genome. This is due to the apparent retro-transposition of mitochondrial sequences into the nuclear genome.

However other apicomplexans have been identified as lacking the large energy conserving complex I.⁶⁴ It has been suggested that instead it is possible for reducing equivalents from NADH to be donated directly to ubiquinone in the mitochondrial membrane by a single-subunit NADH dehydrogenase.⁶⁴

Studies have shown that essentially all ATP in some Apicomplexa was obtained through glycolysis with virtually all of the glucose consumed converted to fermentative end products.⁶⁵ Given the apparent loss of certain subunits used for oxidative phosphorylation in addition to these findings it has been suggested that members of the apicomplexan phylum have lost the ability to carry out mitochondrial oxidative phosphorylation.⁶⁵

Despite the apparent absence of oxidative phosphorylation, apicomplexan species maintain an active mitochondrial electron transport chain, suggesting that it is required for other functions critical to parasite survival.⁶⁴ These have been suggested to include: providing an electron sink for the ubiquinone-dependent dehydrogenases required for cellular metabolism, such as dihydroorotate dehydrogenase, to energize the transmembrane proton gradient required for the transport of metabolites and proteins across the mitochondrial membranes, and to reduce the formation of reactive oxygen species by eliminating oxygen.⁶⁶

This highly degenerated nature of Apicomplexa mitochondria is of interest from a therapeutic perspective as it supports the idea that the remaining conserved features are essential for the organisms' survival, but also that there is high probability of significant differences in these essential structures to those of non-degenerate systems. Those difference might represent a significant opportunity for ensuring high selectivity.⁶⁴

These biological differences to host eukaryotics, among others, are important considerations in respect to choosing the most promising targets when designing new drugs. And several examples of current drug development programmes demonstrate this.

1.5 Developing New Anti-Parasitic Agents

As previously mentioned there are several problems associated with current treatments, and as such there is a need for improved drugs capable of treating toxoplasmosis effectively. Currently there are several new antimalarial agents being developed to treat protozoan infection, some of which inhibit *T.gondii*. A number of these are designed as anti-malarials which, due to the similarity between *Plasmodium falciparum* and *Toxoplasma gondii*, may be effective against both parasites. However, it has become increasingly clear with analysis of parasite genomics and variation in life cycle, invasion techniques and disease pathology that there are large differences in individual parasite species underlying biology, and that specific targeted efforts to optimize drugs towards improving treatment of toxoplasmosis are required.

For successful treatment of toxoplasmosis, new drugs would ideally be able to eliminate the latent bradyzoite cysts in addition to the tachyzoites present during the acute phase of the infection. This would eliminate the risk of reactivation of the parasite and reduce need for prophylactic treatment. Additionally, a clean side effects profile, while always desirable, is crucial if a treatment is required chronically.

1.5.1 Current Work on Future Drugs and Targets for Toxoplasmosis

Currently there a large number of compounds that have been screened or designed for anti-toxoplasmic activity across a range of compound classes and biological targets. These targets include; the calcium dependent kinase (CDPK1), dihydrofolate reductase (DHFR), endoplasmic reticulum-associated degradation pathway (ERADs), fatty acid synthesis pathway, DNA gyrase/topoisomerases, Histone deacetylases/acetyltransferases, ribosome/protein synthesis, pantothenate synthetase and the cytochrome *bc₁* complex, in addition there are a number of compounds screened that show activity without a currently well-defined/suspected target.⁶⁷⁻⁷⁰

1.5.1.1 Improving upon existing targets

A number of these compounds target the same sites as existing treatments, for example; DHFR and the *bc₁* complex along with macrolides targeting

protein synthesis via ribosome inhibition. These are all targets of existing therapies, aiming to improve upon their efficacy and reduce their liabilities. New DHFR inhibitors such as JPC-2067-B (**15**) and JPC-2056 (**16**) are focused on reducing the toxicity associated with existing compounds such as Pyrimethamine (**3**) by improving selectivity for the parasite over host which is currently poor.⁶⁷ The dihydrotriazine (**15 & 16**) based compounds are another example of a series originally designed for malarial efficacy.⁷¹ The macrolide Azithromycin works similar to clindamycin (**12**), inhibiting the 50S ribosomal subunit, and has been used for bacterial infections. The derivative (**17**) below was created in an effort to achieve greater anti-parasitic activity, of particular interest is the ‘delayed death’ phenotype exhibited by both azithromycin and its derivative.^{72,73} This ‘delayed death’ is characterised by modest inhibition of the first round of parasite replication followed by much more severe inhibition in the daughter cells.

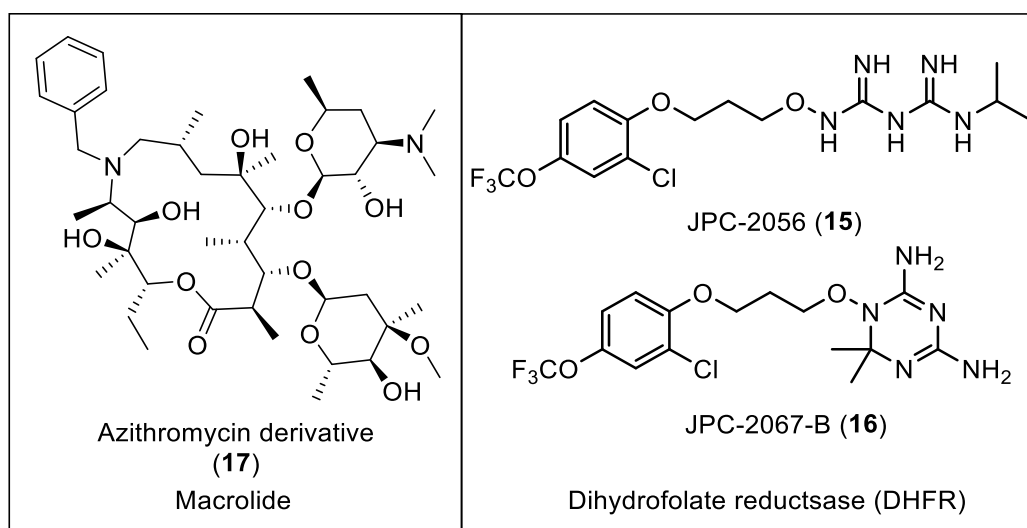


Figure 1.6: Novel compounds based on improving existing therapeutics. Examples DHFR inhibitors **15 & 16** and macrolide **17**.

1.5.1.2 Targets from other infectious diseases.

Other compounds have been derived from compounds used against targets in alternative diseases, such as anti-microbials. The enoyl acyl carrier protein reductase (ENR) is such an example, with a range of compounds previously designed to target it in other organisms.⁶⁹ ENR is an example of an enzyme harboured in the apicoplast of the parasite, and is part of their fatty acid synthesis pathway, FASII, this pathway offers a promising target in parasitic diseases as it is far more prokaryotic-like than the FASI pathway (typically carried out by a single polypeptide complex) used by most other eukaryotic

organisms.⁶³ One of the major challenges for this target is delivery of compounds to within the apicoplast.⁷⁴ The antimicrobial triclosan (**18**) is an example of an existing ENR inhibitor, and several triclosan derived compounds (**19** & **20**) have been produced in an attempt to improve their anti-parasitic activity by improving delivery.

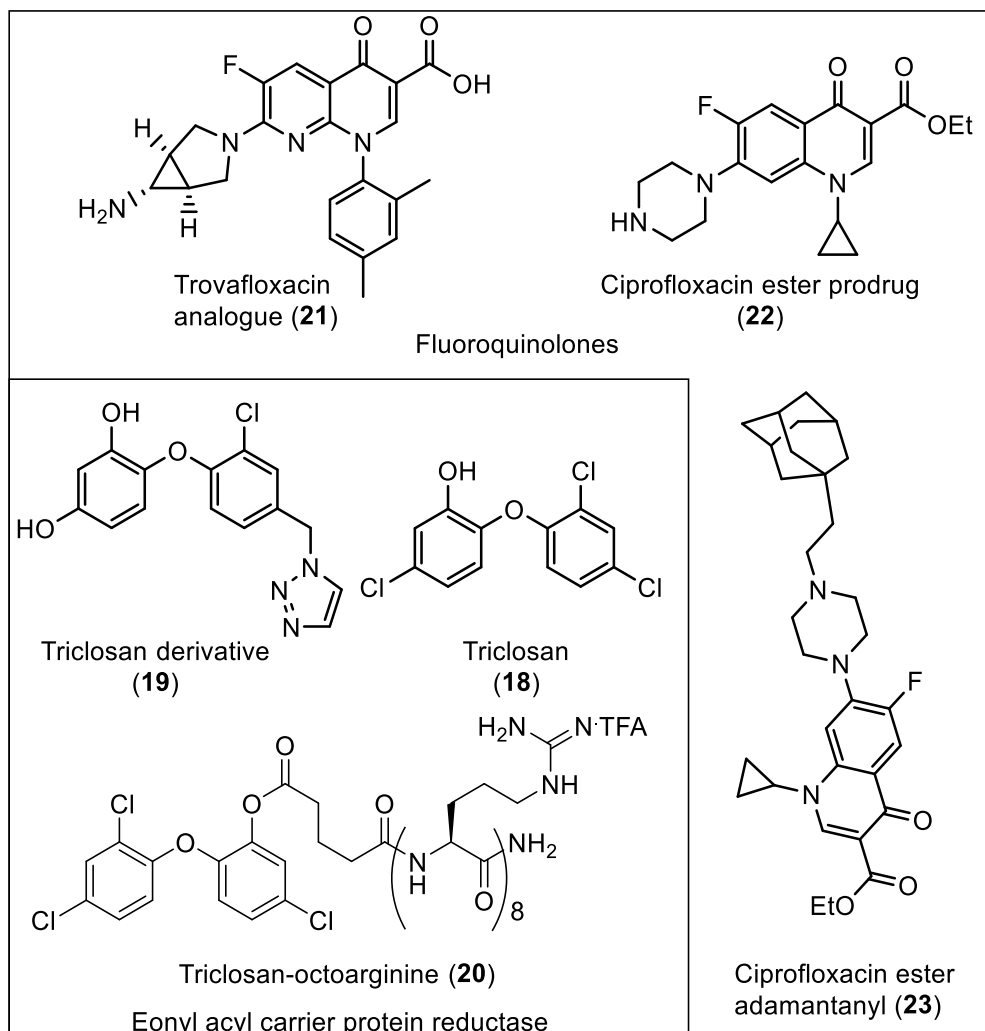


Figure 1.7: Therapeutics being repurposed from other infectious diseases.
Examples: ENR inhibitors (**18-20**) and DNA gyrase/topoisomerase inhibitors (**21-23**)

Another example would be the fluoroquinolone DNA gyrase/topoisomerase inhibitors which have been of interest as antibiotics, trovafloxacin (**21**) was found to be of use against *T.gondii* however toxicity has led to its withdrawal from use.⁷⁵ The mechanism of action of fluoroquinolones against *T.gondii* remains unclear but it is suspected to act through inhibition of DNA synthesis in the apicoplast. A number of trovafloxacin analogues were prepared by Khan *et al*,⁷⁶ while Dubar *et al*⁷⁷ synthesised ciprofloxacin variants (**22** & **23**) and tested for their anti-parasitic activity showing improved activity, and no host cell toxicity.

1.5.1.3 New targets

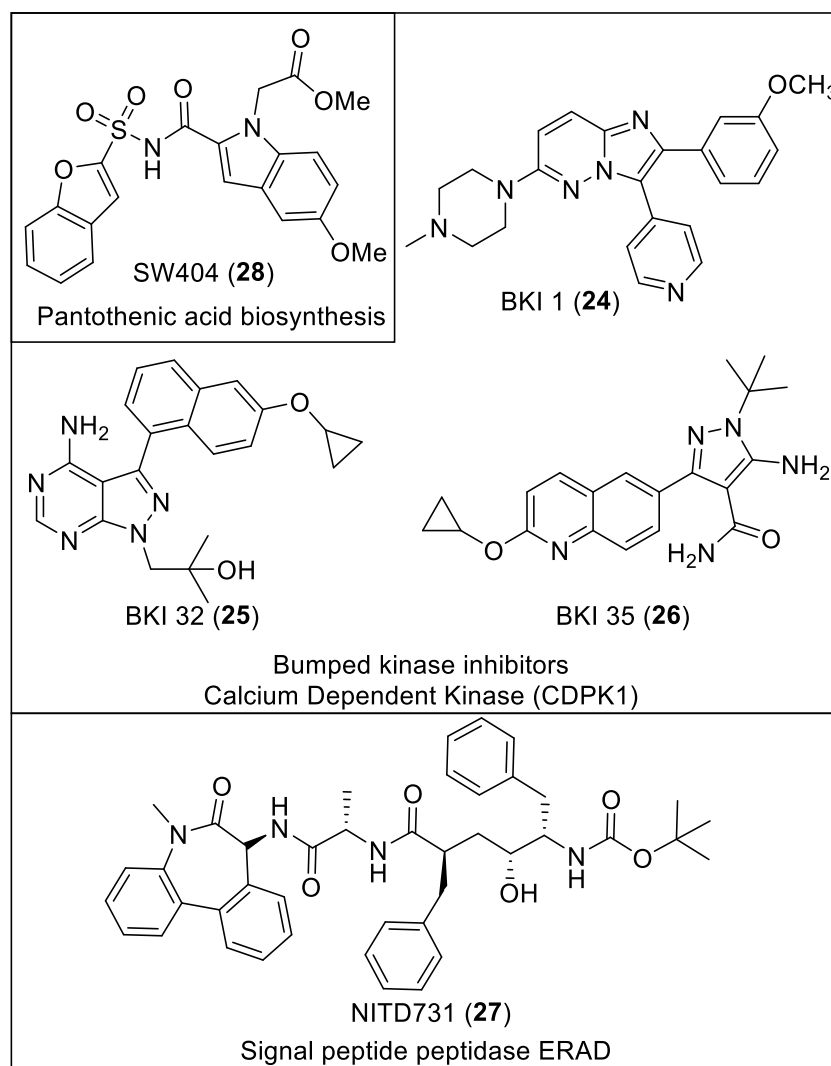


Figure 1.8: Compounds targeting novel targets.

Examples Pantothenate synthase inhibitor (**28**), CDPK1 inhibitors (**24-26**) and ERAD inhibitors (**27**)

Recent publications have described the calcium dependent kinase (CDPK1), as a potential new target for treating *T.gondii* infections. TgCDPK1 is responsible for the regulation of microneme secretion, which is required for gliding, host cell invasion and egress.⁷⁸ The bumped kinase inhibitors (**24-26**) are good examples of using structure based design to take advantage of key difference between the parasite and human homologues.⁷⁹ In this case the smaller glycine residue, at the 'gatekeeper' position, in the parasite were used to engineer selectivity.

The endoplasmic reticulum associated degradation (ERAD) system has also been identified as a particularly vulnerable pathway in protozoan parasites. This pathway is responsible for the recycling of misfolded proteins, the

majority of eukaryotic organisms have comprehensive systems in place to manage this, however protozoan parasites appear to have evolved with a much more limited system.⁸⁰ Harbour *et al*⁸⁰ screened compounds known to inhibit this pathway in an effort to identify compounds efficacious against *T.gondii* this lead to the identification of a series of signal peptide peptidase inhibitors (**27**), with nano-molar activity and no host cell toxicity, validating the potential of the ERAD system as an anti-protozoan target.

Pantothenate synthetase inhibitors arose after work identified that like plants, fungi and bacteria, *Toxoplasma gondii* obtains pantothenate (vitamin B) via a de novo synthesis from pyruvate.⁸¹ This pathway is not present in animals that acquire pantothenate through environmental sources (diet), as a result this presents a selective pathway for inhibition. A series of inhibitors designed for Mycobacterium tuberculosis was tested and two compounds identified with promising activity (one example **28**).⁸¹

1.5.1.4 Epigenetic approaches

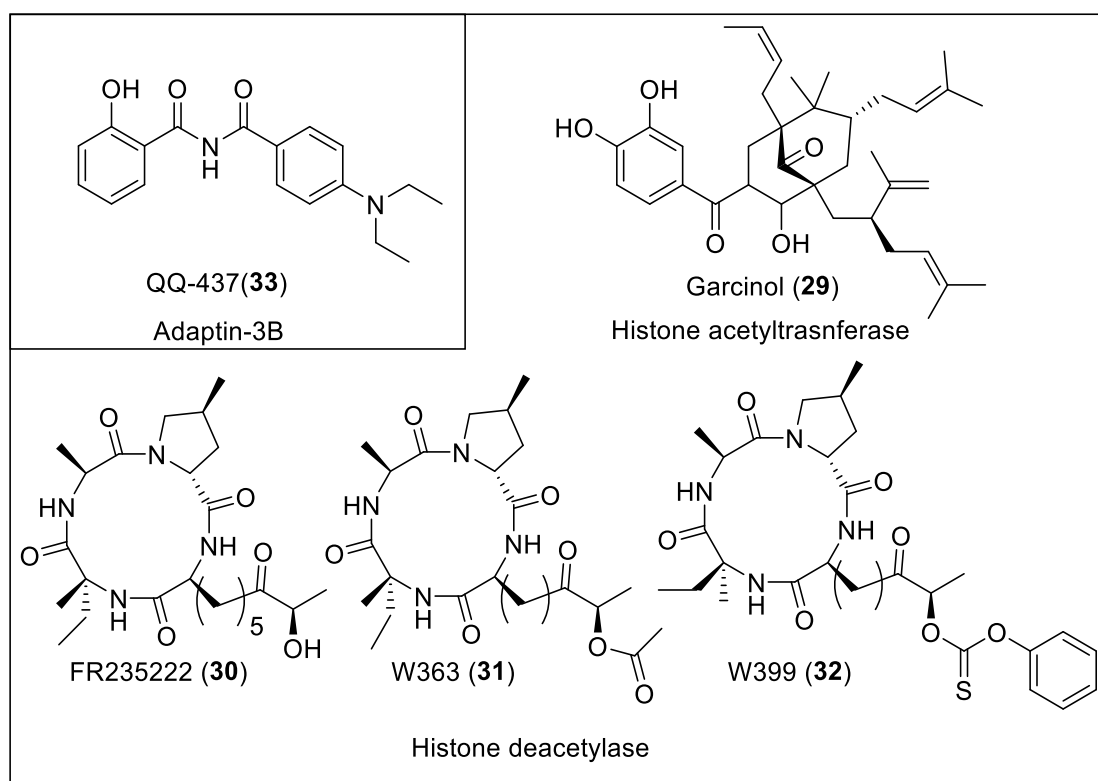


Figure 1.9: Compounds targeting posttranslational modification pathways.
HAT inhibitor (**29**), HDAC inhibitors (**30-32**) and Adaptin inhibitor (**33**)

Epigenetic approaches to treatment have also been explored with inhibitors of both histone acetyl transferases (HAT) (compound **29**) and histone deacetylase (HDAC) (compounds **30-32**) investigated.⁸² These upregulate

and down regulate gene transcription respectively, given the many changes in gene expression between life stages it is unsurprising that effective regulation is critical to *T.gondii*, and therefore that inhibitors such as the cyclic tetrapeptides have been shown to be highly effective at inhibiting parasite growth. This has been supported with EM work indicating distorted morphology and multiple nuclei phenotypes observed on their administration. The N-benzoyl-2hydroxybenzamides are a result of a phenotypic screening approach, a library of synthetic compounds were tested for tachyzoite activity and compound QQ-437 (**33**) identified, further work using an insertional mutation library suggests that adaptin-3 β is the target protein. The role of adaptin-3 β is poorly elucidated, however related adaptin-1 function is understood to be linked to sorting proteins from Golgi complex to rhoptries. Electron microscopy (EM) studies support a role in interference with the parasites secretory process.

1.5.1.5 Drugs with unknown biological targets

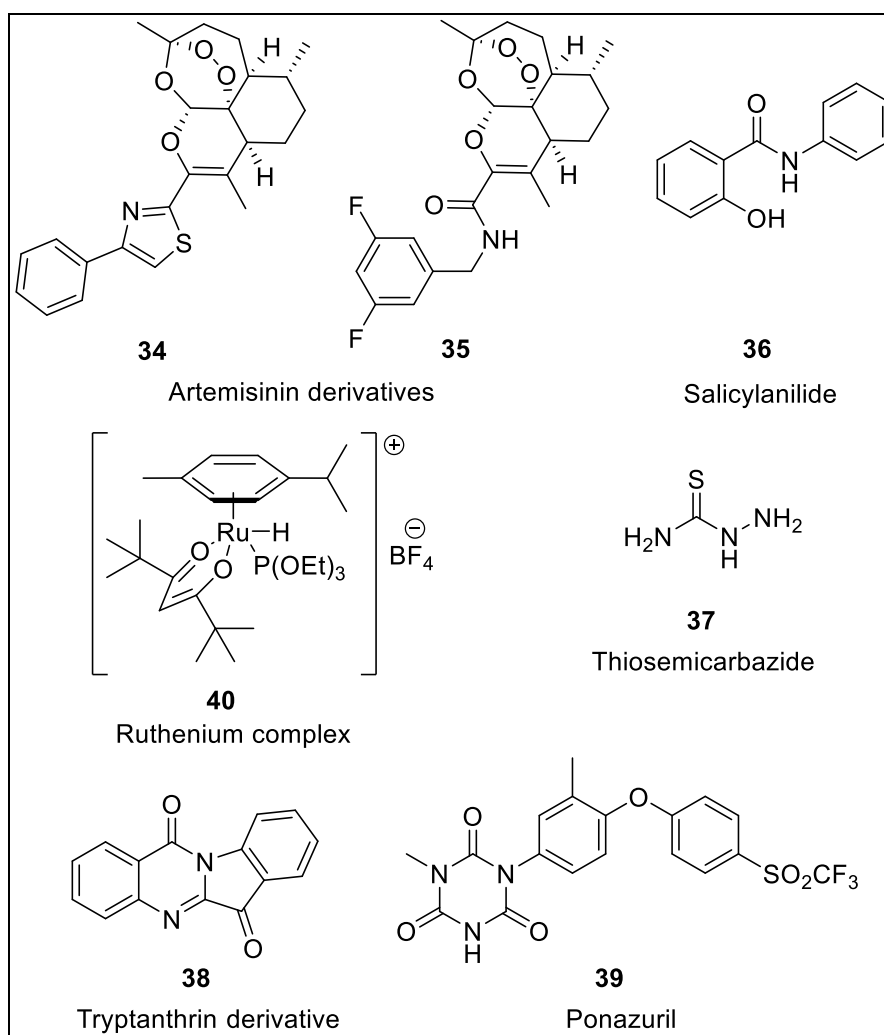


Figure 1.10: *T.gondii* inhibitors with unknown mechanisms of action.

artemisinin derivatives (**32** & **33**), salicylanilide (**34**), thiosemicarbazide (**35**) and tryptanthrin derivatives (**36**) as well as ruthenium-based complexes (**37**), and the toltrazuril metabolite; ponazuril (**38**).

Other compounds identified as having anti-*T.gondii* activity with unknown mechanism of action include; artemisinin derivatives (**34** & **35**), salicylanilide (**36**), thiosemicarbazide (**37**) and tryptanthrin derivatives (**38**) as well as ruthenium based complexes (**39**), and the toltrazuril metabolite; ponazuril (**40**).^{83–87} A number of these are either derivatives of existing drugs, which have shown activity, or their metabolites.

Over all there are a number of drug discovery efforts currently being made against toxoplasmosis at various stages with varying methodology and focus.⁶⁹ While many remain by-products of malarial programmes, or have been limited to validation of a target using drugs designed for other organisms,

there are still a number that take advantage of *Toxoplasma gondii*'s unique biology.

1.5.2 The Cytochrome bc_1 complex, and its potential as a drug target.

As previously mentioned, Atovaquone is an example of an anti-malarial that has found use in treatment against toxoplasmosis, with relatively few side effects. Its mechanism of action is now well established as inhibiting the cytochrome bc_1 complex. As a known valid target, and the only one to have indicated any noticeable effect on cysts, it is an attractive prospect for further improved anti-toxoplasmic agents,

In addition; recent work by a number of groups (GSK, Riscoe *et al*, O'Neill *et al*) has focused on developing inhibitors that target cytochrome bc_1 complex III.^{88,89} These compounds are based upon similar structures using scaffolds based upon pyridone and quinolone core fragments and will be discussed further. Endochin (**41**) is an example of an unsuccessful quinolone that is currently being re-examined to overcome its limiting nondrug-like properties.

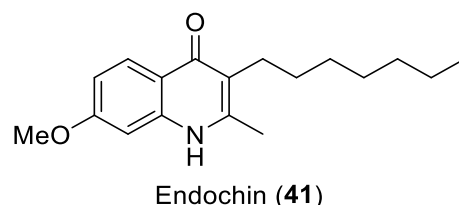


Figure 1.11: Structure of Endochin (**41**)

One of the most promising indicators for cytochrome bc_1 as an effective treatment for both tachyzoite and bradyzoite life stages and therefore potential as a more complete toxoplasmosis therapy is found in observations in the EGS strain. The EGS strain is a form of toxoplasmosis which forms cysts *in vitro*, this makes it exceptionally useful for studying bradyzoite behaviour.⁹⁰ It has been discovered through study of this EGS strain that bradyzoites show increased expression of the cytochrome b complex this suggests that is critical to the life cycle stage in addition to that of the tachyzoite. This is supported by reports of Atovaquone (**9**), an existing cytochrome bc_1 inhibitor, having an effect on cyst burden.⁹¹

The bc_1 complex is part of the electron transport chain. Understanding its role and structure can bring deeper insight into why it has potential as a promising therapeutic target.

1.5.2.1 The *bc*₁ complexes role in the electron transport chain.

In most eukaryotes the electron transport chain is composed of four integral enzyme complexes in the mitochondrial inner membrane; NADH-ubiquinone oxidoreductase (complex I), succinate: ubiquinone oxidoreductase (complex II), ubiquinol-cytochrome *c* oxidoreductase (complex III or cytochrome *bc*₁), and cytochrome *c* oxidase (complex IV or cytochrome *aa*3), with ubiquinone (Coenzyme Q) and cytochrome *c* functioning as electron carriers between the complexes Figure 1.12. ⁹²

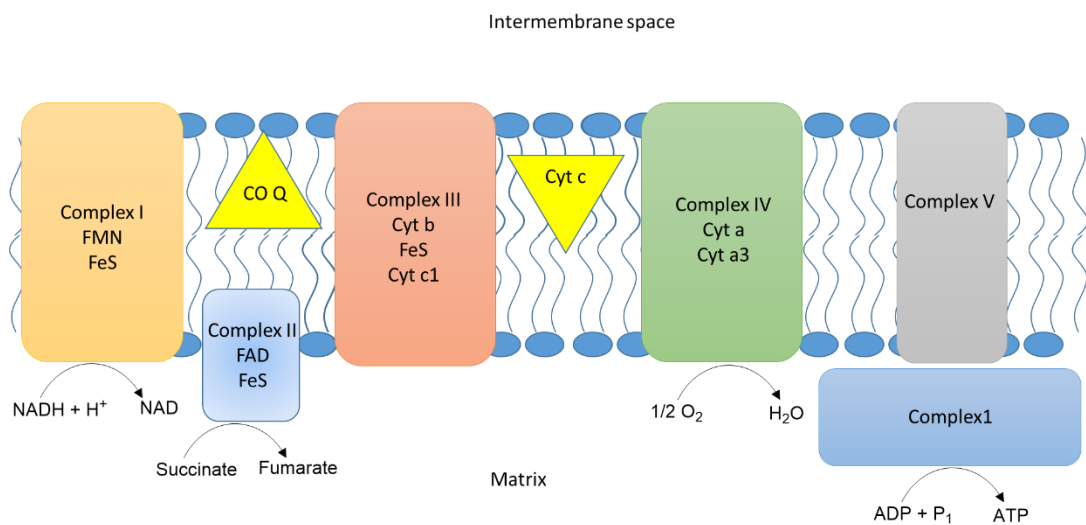


Figure 1.12: Schematic of electron transport chain in higher order Eukaryotic organisms. ⁹²

Crystallographic structures of the *bc*₁ complex have been obtained for chicken, yeast and bovine species, including examples with bound inhibitors.^{93,94} The *bc*₁ complex is homo-dimeric in structure, with multiple subunits (**Figure 1.13**). Each monomer of the complex consists of three catalytic subunits.⁹² Each of these subunits contains prosthetic groups, namely cytochrome *b* carries two *b*-type hemes, cytochrome *c*₁ carries a *c*-type heme, and the Rieske protein contains a [2Fe-2S] cluster. The central domain of the complex is formed by eight transmembrane helices of cytochrome *b* per monomer. Cytochrome *c*₁ and the Rieske protein are anchored to this core via single transmembrane helices; their catalytic domains are located in the intermembrane space.

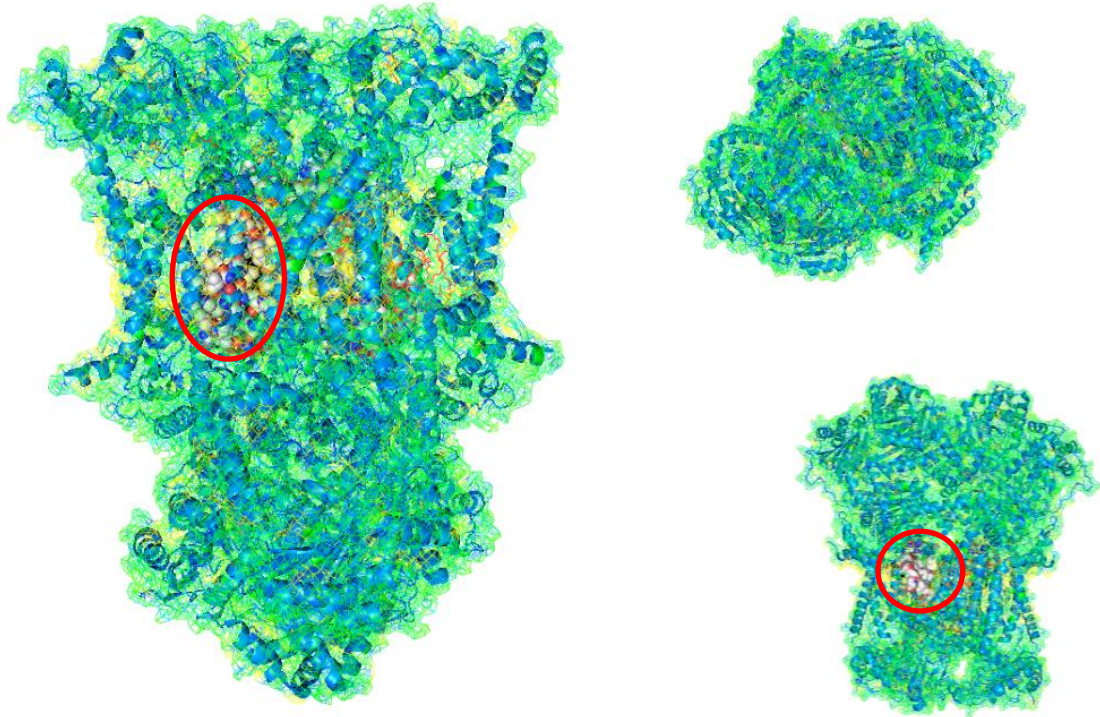
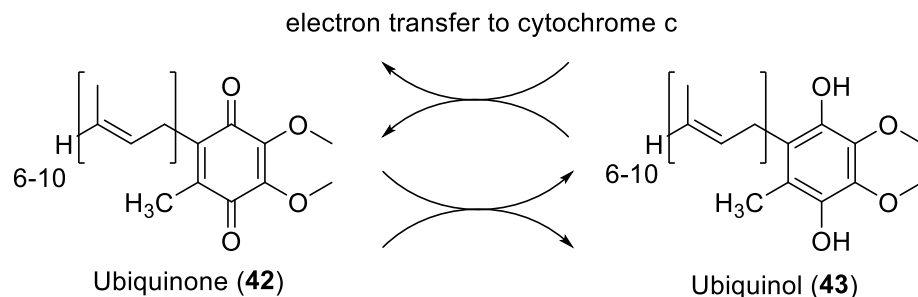


Figure 1.13: Crystal structure of the bovine cytochrome bc_1 complex
Composition of secondary structures with the surfaces of the two substrate binding sites, Q_i and Q_o shown, and their location circled in red.

1.5.2.2 The Q cycle

Both substrate binding sites are located at the border of the hydrophobic core of the enzyme, therefore only short proton transfer pathways are required for proton uptake and release upon ubiquinone/ubiquinol (**42/43**) redox reactions. The complex carries out energy transducing electron transfer through the reduction and oxidation of ubiquinone (**42**) and ubiquinol (**43**). The overall process is called the Q-cycle which takes place over the two active sites of the complex; Q_o and Q_i , (**Scheme 1.1**).



Scheme 1.1: Simplified illustration of the Q cycle.

Showing interconversion between ubiquinone and ubiquinol through reduction and oxidation reactions.

Starting with ubiquinol (**43**) in the Q_o site oxidation of ubiquinol (**43**) at centre Q_o consists of ubiquinol (**43**) delivering two electrons divergently to the Rieske cluster and the b_L heme, followed by the resulting ubiquinone (**42**) leaving the

Q_0 site. This process occurs through ubiquinol replacing a proton of the imidazole nitrogen of His181 on the Rieske iron-sulphur protein (RISP) to form a transient quinol-imidazolite complex, this complex then forms a hydrogen bond to the Glu272 residue of cytochrome b to form the electron donor complex. Electrons are transferred simultaneously from the electron donor complex to the Rieske cluster and the b_L heme, resulting in dissociation of the complex and release of ubiquinone.⁹²

After the dissociation of the complex and release of ubiquinone (**42**), the Rieske cluster moves to within electron transfer distance of cytochrome c_1 heme. Of the two protons released, one is released to the aqueous phase from the Q_0 site when the Rieske cluster is oxidized by cytochrome c_1 while the other is transferred in parallel with the electron to heme b_L .

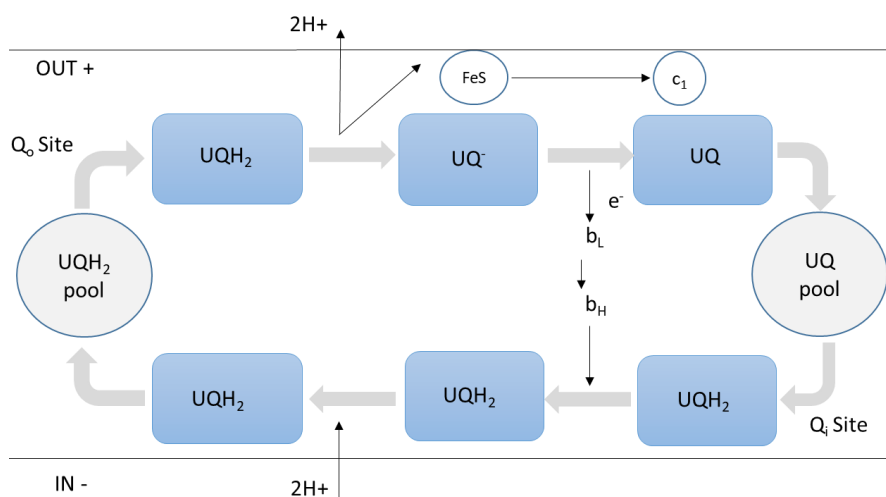


Figure 1.14: Illustration of the key stages of the Q cycle

The cycles net result is the pumping protons across the mitochondrial membrane.

The protonated residue of cytochrome b dissociates from the electron donor complex and the proton then moves toward the heme propionate of heme b_L , to be conducted to the aqueous phase via another residue of cytochrome bc_1 . Lastly, the electron is transferred from the b_L to b_H heme, which in turn reduces ubiquinone to ubisemiquinone. Following the oxidation of a second ubiquinol at the Q_0 site and reduction of the b cytochromes, the b_H heme reduces ubisemiquinone to ubiquinol, this is accompanied by uptake of two protons at the Q_i site. The net result of this entire process, occurring at opposite sides of this trans-membrane protein, is the transportation of protons across the membrane.

It is the Q_0 site which Atovaquone (**9**) targets. It binds within the site competing with ubiquinol (**43**), but also acts at this stage in the Q-cycle to lock the RISP

into its Q_o proximal position preventing the cycle from progressing. Unfortunately it appears that the Q_o site is prone to mutations in parasitic species causing the rapid development of resistance, which may be a problem for any drugs targeting this site, an example being the Y302C point mutation in *Plasmodium*.^{43,95} It is also of note that the Q_o site is relatively large, capable of binding two molecules of ubiquinol (**43**) at once, perhaps indicating lower specificity.⁹⁶ Work done on atovaquone has identified a number of key differences in the Q_o site of parasitic and mammalian complex, that explain its selectivity for protozoa.⁹⁷

1.5.2.3 Q_i vs Q_o site

Recent crystallographic studies (by M. Capper *et al*) of inhibitors bound in the Q_i site of the bc₁ complex have aided understanding of the relative position and orientation of the compounds, when bound. Specifically compound GSK932121 (**44**) bound in bovine bc₁ complex (**Figure 1.15**).⁹⁸

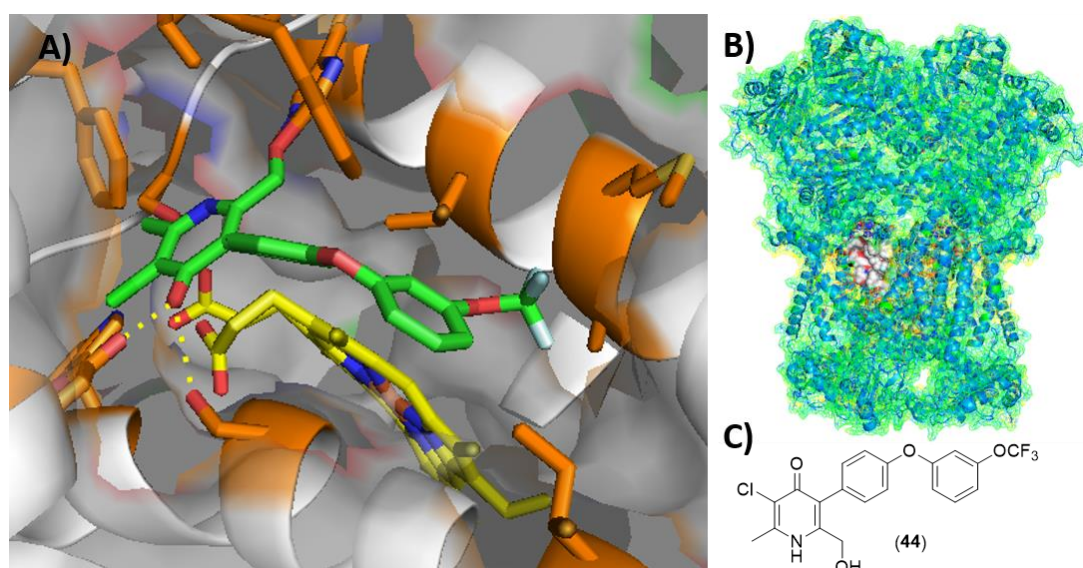


Figure 1.15:

A) Q_i site of cytochrome b containing GSK932121 (**44**), residues within 4 Å shown in orange, Heme b_L shown in yellow, yellow dotted lines indicate possible hydrogen bonding interactions. B) Surface model of bc₁ complex, red indicates position of the Q_i site. C) The structure of GSK932121 (**44**).

An important aspect of the Q_i and Q_o sites reported recently is that there is a very fine balance between a compound's preference in binding site between the two. This is perhaps unsurprising given their very similar natural substrates (ubiquinol/ubiquinone). Site specificity of compounds in malaria has been evaluated using mutagenic studies. The lack of resistance from Atovaquone

resistant strain, Tm90.C2B, is also used as an indicator of Q_i selectivity. The study on what determined this selectivity also produced a Q_i site mutant through incubation with a Q_i inhibitor. Interestingly this produced a relatively specific resistance profile and was only produced at substantial inhibitor concentration (>10 x IC₅₀). Overall this suggests that mutation within the Q_i site carries a substantial cost to the organism fitness, this would hopefully retard clinical development of resistance, a significant advantage in a treatment.⁹⁹

1.5.3 Selectivity at the Q_i site

Like DHFR, the downside of the cytochrome *bc*₁ complex as an anti-infective target is the existence of a mammalian homologue and, given the essential nature of the complex it is vital to achieve selectivity between the two to prevent potentially devastating toxicity. To reduce this risk understanding the difference between the structures of the active site is crucial

The residues involved in forming the Q_i site primarily reside in the positions 1 to 60 and 180 to 240 of the bovine cytochrome b sequence (**Figure 1.17**). The heme b_H structure also lies in close proximity to this pocket. The key residues involved in binding pyridone type structures appear to be the Histidine (H201) and Aspartic acid (D228) residues (**Figure 1.16**). Residue D228 can be seen interacting with the oxygen of the pyridone while residue H201 lies close to the nitrogen of the pyridine ring.

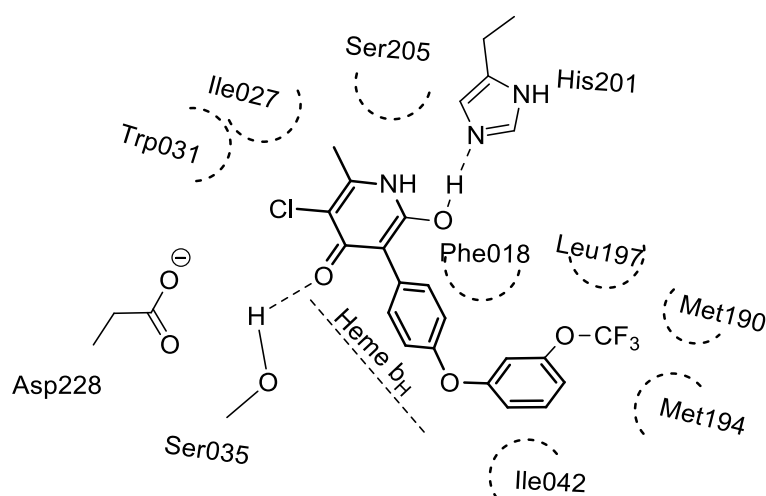


Figure 1.16:
GSK932121 (**44**) interaction diagram with the bovine Q_i site.

Both of these residues are conserved between bovine, human and *T.gondii* organisms. However, the Serine (S035) residue also shown interacting with

carbonyl head group is not conserved in the *T.gondii* sequence and appears to be replaced with a phenylalanine residue (F034), this might be expected to have a large effect on the positioning of compounds within this site. The difference can be seen most notably in the sequence alignment of the proteins, by focusing on the residues in closest proximity to the active site.

P00157	BOVIN	MTNIRKSHPLMKIVNNAFIDLPAPSNISSWVNFSGLLGICLILQILTGLFLAMHYTSDTT	60
P00156	HUMAN	MTPMRKTNPLMKLINHSFIDLPTPSNISAWVNFSGLLGACLIHQITTTGLFLAMHYSPPAS	60
Q02768	PLAFA	-----MNFYSINLVKAHLINYPCLNINFLWNYGFLGIIFFIQIITGVFLASRYTPDVS	55
O20672	TOXGO	-MVSRTLSSLMSLFRHLVVFYRCALNLNSSYNFGFLVAMTFVLQIITGITLAFRYTSEAS	59
P00157	BOVIN	AFHFILPFFIIMAIAMVHLLFLHETGSNNPTGISSDVKIPFHPYYTIKDI LGALLLILAL	239
P00156	HUMAN	TFHFILPFFIIAALATLHLLFLHETGSNNPLGITSHSDKITFHPYYTIKDALG LLLFLLSL	239
Q02768	PLAFA	VLHFILPFFIGLCIVFIHIFFLHLHGSTNPLGYDTA-LKIPFYPNLLSLDVKGFNNVILF	229
O20672	TOXGO	VLHFILPFFIGCIIIVLHIFYLHLNGSSNPAGIDTA-LKVAFYPHMLMTDAKCLSYLIGLI	234

Figure 1.17:

Sequence alignment of Human, Bovine, Toxoplasma and Malaria. Residues within 4 Å of ligands are highlighted in blue, those within 12 Å highlighted in grey.¹⁰⁰

Currently a limiting factor in the accuracy of structure-guided approaches to targeting the cytochrome *bc*₁ complex is the lack of parasite X-ray crystal structure, while structures exist for mammalian homologues as shown, the reliance on homology models increases the uncertainty involved and may not account for subtle but important structural effects.

1.5.4 Quinolones and Pyridones as Cytochrome *bc*₁ Inhibitors.

Several inhibitors of the *bc*₁ complex, in addition to Atovaquone (**9**), have been explored. As previously discussed Atovaquone (**9**), among others, has been shown to inhibit the Q_o site of the *bc*₁ complex. Several other compounds have been developed with a similar frame-work, based upon a quinolone structure. The quinolone structure originates from the compound endochin (**41**) which showed potential against avian parasites but did not significantly affect mammalian infection. Recently this has been explained as a result of it being very metabolically unstable, the heptyl side chain and methoxy group are particularly susceptible to degradation.¹⁰¹ As a result work has gone into developing a range of endochin-like-quinolones (ELQ's), with improved metabolically stable compounds based on the endochin core. The Riscoe group has explored a substantial library of these ELQ's and identified a preclinical candidate. These molecules are based on the endochin core with a more metabolically stable substituent at the 3-position which has been used

successfully in a previous compound series.⁵⁰⁻⁵ GSK has progressed a similar compound based on a smaller clopidol core, until it was found to be toxic in rats, this was attributed to a low selectivity between the mammalian and parasite *bc*₁ complex.¹⁰⁵

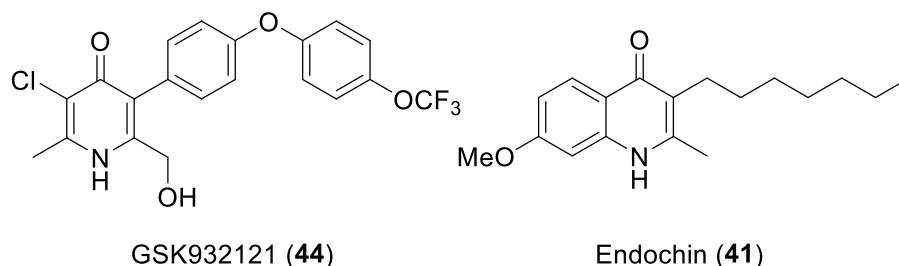


Figure 1.18:
Structures of GSK932121 (**44**) and Endochin (**41**)

Because of the structural similarity between pyridines and quinolones and therefore the likely hood that they will have similar biological targets, the ELQ's were tested against the human structure *bc*₁ complex. This revealed that the larger quinolone core itself showed some selectivity for the parasitic target, and that this selectivity is enhanced extensively with substitutions in the six and/or seven positions of the quinolone.^{88,101} This was demonstrated in the difference in inhibition values observed for human Cytochrome *bc*₁ of ELQ's 271 and 316, at 1.9 μ M and > 10 μ M respectively.

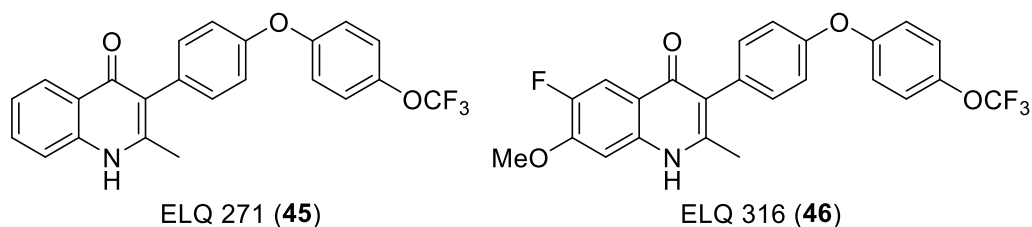


Figure 1.19:
Structures of lead ELQ compounds 271 (**45**) and 316 (**46**)

It is important to consider that a large amount of the SAR elucidated to date has been derived via focus on *Plasmodium falciparum* *bc*₁ complex and while the two parasites have similarly structured Q_i sites there are significant differences. Not only that but although both parasites have multiple life stages the localisation and physiology of these vary, and therefore a successful *T.gondii* treatment may require different PK profile to that of an antimalarial. A second important factor in understanding the SAR of pyridone and quinolone-based inhibitors is the precise site of inhibition. As mentioned previously the cytochrome *bc*₁ complex has two 'active sites' (**Figure 1.13**). Therefore, confirming which site is involved in compound binding is essential

to avoid misleading SAR. It would be advantageous for a new drug to target the Q_i site as this would reduce the risk of cross resistance with existing Q_o site inhibitors such as Atovaquone (**9**), which has been demonstrated to be vulnerable to site mutations.

Work on ELQ's, conducted by Riscoe *et al*, has suggested that the balance in site selectivity of the quinolone-based systems is finely tuned.⁹⁹ They report that substitution of the ELQ nucleus at the 3, 5, 6 & 7 positions all have effects on selectivity between Q_i and Q_o sites. However, the rationalisation provided requires the compounds to dock in a 'flipped' orientation relative to that described by the recent crystal structures of the pyridone compound GSK932121 (**44**) bound in the active site, shown in **Figure 1.15**

There are several important features and structure activity relationships that can be deduced from the current extensive region of chemical space that has been explored by a number of groups (**Figure 1.20**).

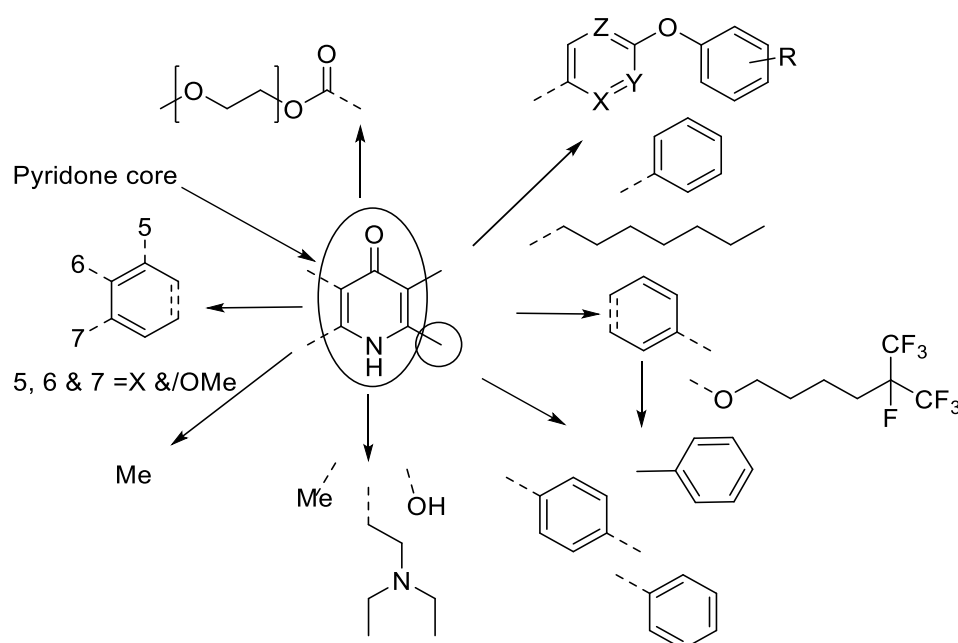


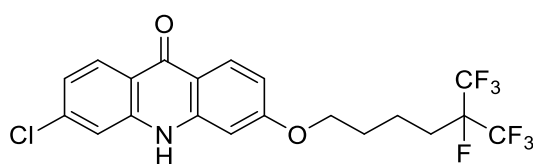
Figure 1.20: Scope of pyridone based inhibitors explored in literature.

Examples of the structural diversity and the size of chemical space explored around pyridone based inhibitors ($X, Y, Z = C/N$, 3 & 4 $R = CF_3, OCF_3, Hal$, 5, 6 & 7 = H, F, Cl, OMe).

It appears that increased steric bulk on the benzoid fused side of the molecule increases species selectivity, seen in the trend from pyridone \rightarrow quinolone \rightarrow substituted quinolone. A range of substitution patterns in this area have also been explored and it appears 6-chloro, 7-methoxy motifs are especially active for unsaturated cores. It can also be seen that both pyridine and quinolone cores contain a central ring able to tautomerize between the with ketone-enol

tautomers.¹⁰⁶ The balance of this tautomerism has been shown to be affected strongly by the nature of the substituent in the two position. Recent work has identified a methyl substituent at the two position as also beneficial in regard to stabilising the pyridone tautomer, whereas electro-withdrawing substituents are detrimental to this. This is likely to be a result of the pyridol-stabilising effect that electron withdrawing groups have in this position opposed to the methyl group favouring the pyridone tautomer. This may be relevant to the expected binding method revealed in the crystal structure of analogous compounds. Substituents at the two position, such as the methyl group, are also likely to have a large effect on the dihedral angle between the core and the diphenyl side chain, rotating it from its otherwise favourable near-planar conformation. This will affect its positioning within the binding site. A range of substituents have been trialled in the three position, in addition to the diarylethers, including the carboxyquinolones, these have been designed with carboxyl groups at the three position as these have the potential to affect the balance between tautomer's within the compounds, stabilising the alcohol tautomer through internal hydrogen bonding.¹⁰⁷

The acridone class of compounds are tricyclic analogues of the pyridones and quinolones, these have been demonstrated to have exceptionally high potency and selectivity indices, the example below exhibits an antimalarial IC_{50} of 1 pM and selectivity for parasitic vs human activity in the range of 100,000 although the precise target is unknown it is assumed to inhibit cytochrome *bc*₁.¹⁰⁸



Acridone derivative (**47**)

Figure 1.21:
Structure of lead Acridone compound (**47**).¹⁰⁸

While achieving good potency, the major drawback of these compounds in terms of their use as drugs has been their insolubility, metabolic stability and toxicity.

1.6 Summary

Toxoplasmosis is a highly prevalent and potentially dangerous disease and a significant health burden across the globe especially to those most vulnerable, despite this treatment had not advanced significantly in the last 50 years and there is a clear need for drugs that are both more tolerable and better capable of eliminating infection. There are a number of ongoing efforts to design new drugs against a broad range of therapeutic targets. The cytochrome *bc₁* complex shows promise as a drug target candidate being both a validated target in tachyzoites as well as mounting evidence of potential to eliminate bradyzoites. The possibility of a novel site of action reduces the risk of resistance associated with atovaquone (**9**) and presents the opportunity of a synergistic therapy partner. While experimental structural information for the parasite organism remains unavailable, homology modelling provides a viable alternative to enable a structure guided drug design effort. A successful lead will build upon the efficacy demonstrate by previous quinolone/pyridone based compounds while improving upon undesirable physiochemical properties and demonstrating potent bradyzoite inhibition.

1.7 Project Goals and Summary

1.7.1 Overall aims

The overall aim of this project was to design and develop a novel compound towards the improved treatment of toxoplasmosis.

The project could be broadly split into three areas of work, based on the progression towards these goals starting from; identifying novel scaffolds, followed by development of the hit tetrahydroquinolone candidate to a viable lead compound (THQ's), and finally; further evaluation of the lead candidate and continued optimization and characterisation of the series.

1.7.1.1 Design, synthesis and evaluation of novel scaffolds

Discusses; the design and synthesis of a number of bicyclic pyrid-(4H)-one containing scaffolds; the preliminary evaluation of these scaffolds, and comparison with computational docking results to assess the value of computational guidance to series development and generation of novel cores, and finally the selection of the tetrahydroquinolone (THQ) scaffold to progress to hit to lead development is discussed.

1.7.1.2 Hit to lead development of Tetrahydroquinolones

Discusses; the use of THQ candidate to probe the mechanism of action and target site of the series; the design and synthesis, including route optimisation, of further tetrahydroquinolones based compounds; the evaluation of their anti-toxoplasmitic activity and the selection of the lead candidate for further studies and development.

1.7.1.3 Evaluation and further development of Tetrahydroquinolone lead.

Discusses; the evaluation of the lead compound in more advanced biological assays; including hERG, CYP450, permeability and finally in vivo efficacy. In addition; the continued to development of the series to address existing deficiencies such as solubility and selectivity/on target toxicity.

Chapter 2 Design and Synthesis of Cytochrome *bc*₁ Inhibitors; Exploring novel scaffolds for improved properties.

As previously discussed, there has been a large amount of work performed on developing existing endochin/quinolone base scaffolds in the treatment of apicomplexan infections.¹⁰⁹ Many of these molecules have demonstrated promising potency both in enzymatic and cellular assays, with some also demonstrating favourable activity in rodent models, in many cases against malarial infections but also in *T.gondii* models. However despite this, there have been no candidates, from any of these series, progressed beyond the preclinical stage of development. This is due to each series demonstrating key liabilities that have not been overcome, preventing further progression. The most prominent of these having been physicochemical properties; namely poor aqueous solubility, although maintain selectivity and avoiding toxicity, has also presented a challenge.^{101,105,110}

2.1 Design of new cores

With the large number of compounds explored, it is somewhat surprising how little variation exists around the core ring systems. Currently this is limited to addition of fused benzene rings to the pyridone core, leading to the quinolone and acridone series respectively.^{106–108} As might be expected both of these contribute detrimentally to physicochemical properties, through increased log P and high planarity.

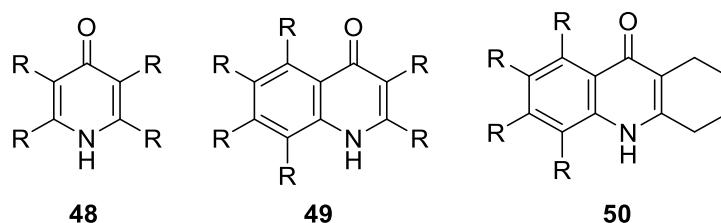


Figure 2.1: Pyridone (**48**), quinolone (**49**) and tetrahydroacridone (**50**) structures.

It was thought that by exploring a wider area of chemical space, around the pyridone core, that there was potential to address some of the innate deficiencies of the quinolones/acridones, while retaining their demonstrated potent biological activity.

To help understand the differences in selectivity between the ELQ and pyridone series and the enhancement in biological activity caused by substituents on the six and seven position, the Q_i binding sites of mammalian and parasite species were compared.¹⁰¹

This was visualised by overlaying a homology model of the parasite protein with existing crystal structures of the pyridone GW844520 (**44**) (PDB code: 4D6U)⁹⁸, **Figure 2.2**. The differences in pocket size appear to support the hypothesis; that this steric factor is responsible for the observed selectivity achieved by bicyclic inhibitors. It can be seen that there is a larger pocket on the side of the cavity in which the second ring points into, in the parasite homology model than observed in the mammalian crystal structure.

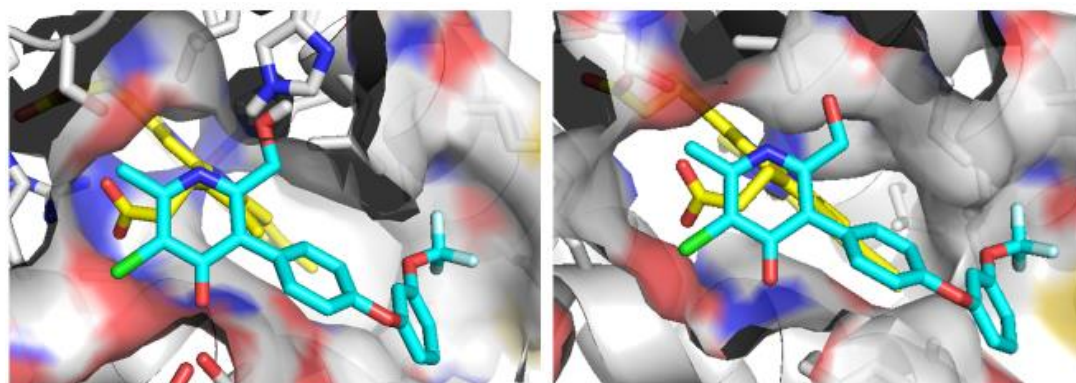


Figure 2.2: Comparison of Q_i binding sites.

Crystal structure of **44** bound within the bovine Q_0 site (PDB: 4D6U)⁹⁸ (left) compared with the ligand positioned within the homology model of the *T.gondii* site (right)¹¹¹, illustrating the increased space within the *T.gondii* site.

On the basis of this steric-based selectivity hypothesis, a number of novel alternative scaffolds were designed. These designs focused primarily on addressing those concerns known to have impeded quinolone/pyridone based cytochrome *bc_1* inhibitors development; namely solubility and selectivity. With the apparent success of bicyclic compounds at reducing selectivity concerns in the quinolone systems,¹⁰¹ it was felt that design focus should be directed towards other bicyclic compounds. Other key considerations were then to focus on properties most likely to increase aqueous solubility such as; introduction of polarity via heteroatoms, increasing sp^3 ratio and reducing planarity.

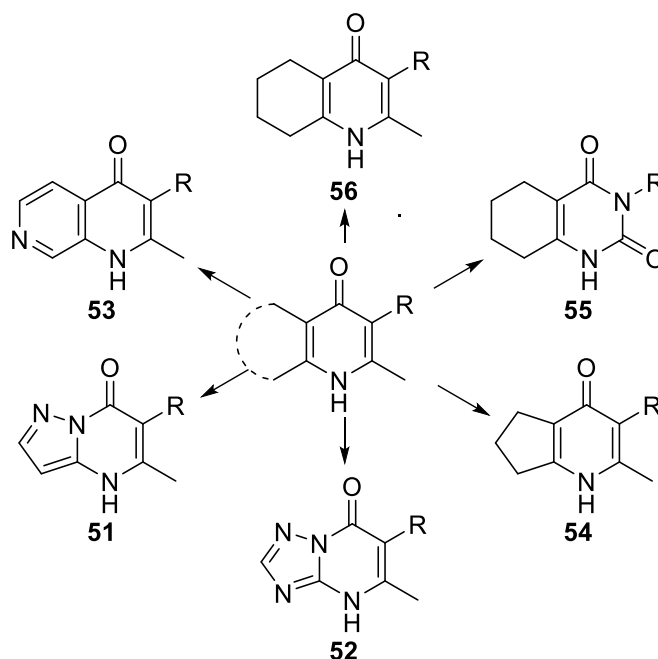


Figure 2.3: Novel scaffold ideas

Proposed scaffold structures designed for increased aqueous solubility while maintaining the advantages of a bicyclic system: the triazolo/pyrazo.631,5-a]pyrimidin-(4H)-ones (**51/52**), the naphthyridones (**53**), the cyclopenta[b]pyrid-4-ones (**54**), the tetrahydroquinazolinones (**55**) and the tetrahydroquinolones (**56**)

The designed molecular scaffolds envisaged could be broadly exemplified by the six scaffolds shown in **Figure 2.3**; the triazolo/pyrazo.631,5-a]pyrimidin-(4H)-ones (**51/52**), the naphthyrid-4(1H)-ones (**53**), the cyclopenta[b]pyrid-4(1H)-ones (**54**), the tetrahydroquinazolinones (**55**) and the tetrahydroquinol-4(1H)-ones (**56**). It is also possible to imagine combinations or further variation of these approaches; for example addition of heteroatoms into the saturated systems or increasing ring size to cycloheptanes, or movement of heteroatoms around the ring.

2.1.1 Metrics in Medicinal Chemistry

As a result of increasing efforts for diminishing returns within drug discovery, and the vastness of chemical space, the need to optimise the process of drug development has led to an increasing use of metrics. These metrics aim to weed out less promising designs earlier and allow medicinal chemists to focus on areas of chemical space with better potential for success. Beginning with Lipinski's rule of 5,¹¹² and progressing with ideas such as 'escape from flatland',¹¹³ an ever expanding list of parameters to better characterise the key dimensions and boundaries of 'Drug like' space has been developed. These parameters are further complicated by the nature of individual diseases. A

leading contributor to this difference between diseases, is the desired localisation of the drug. In the case of toxoplasmosis due its microbial nature and predilection for brain tissue penetration into both the parasite and the CNS are required of treatment, presenting additional challenges. A number of multiparameter optimisation scoring systems exist for CNS penetration, typically including; limiting H-Bond donors to < 2 , and a desirability for topological polar surface area (TPSA) below 90 \AA^2 . Other successful drugs have a tendency towards low molecular weight, higher lipophilicity and basic centres, however it is important to account for bias within existing CNS drugs which have a propensity for aminergic targets, and does not necessarily well describe the limits of BBB penetrate chemical space, this is highlighted well in Zoran Rankovic's recent review of CNS property space.¹¹⁴ Penetration into microbials is also highly challenging, and can be dependent on the specific organism.

Overall this highlights many of the challenges within drug discovery, importantly while large data can produce helpful trends, individual cases remain largely empirical.

2.1.2 Assessment of designs

At this stage our molecular designs were primarily assessed against parameters most strongly related to physiochemical properties namely; computational log P (cLogP), fraction of sp^3 hybridised carbons (F_{sp^3}) and total polar surface area (TPSA). Together these give a preliminary indicator of comparative aqueous solubility of the designs. With their Log P and TPSA giving an indication of lipo/hydrophilicity and F_{sp^3} a degree of insight into the flexibility and potential crystallinity. Which strongly contributes a compounds solubility. Rotatable bond count is also another metric commonly used for this purpose however the fragment and fixed bicyclic nature of these cores results in equivalency across scaffolds. This does not account for the increased flexibility offered by the saturated systems.

As can be seen in **Table 2.1** each of these bicyclic systems has a calculated Log P significantly lower than that of the quinolone analogue, in addition they either poses significantly higher F_{sp^3} or a greater TPSA than the quinolone core. The cyclopenta[b]pyridone suggests a particularly promising combination of a low predicted log P and high F_{sp^3} .

Table 2.1:

Calculated log P's, fraction of sp³ carbons (Fsp³) and topological polar surface area (TPSA) of quinolone analogues (R=H)

Compound	cLog P*	Fsp ³	TPSA*
Quinolone	0.62	0.10	29.1
Triazolo[1,5-a]pyrimidin-(4H)-one	-0.70	0.17	57.1
Pyrazolo[1,5-a]pyrimidin-(4H)-one	-	0.14	44.7
1,7-Naphthyridone	-0.71	0.11	41.5
Tetrahydroquinazolinediones	0.05	0.50	58.2
Cyclopenta[b]pyrid-4(1H)-one	-0.55	0.44	29.1
Tetrahydroquinolones	-0.13	0.50	29.1

* calculated using Chemdraw Prime 16

While it is important to consider that several other factors contribute to aqueous solubility and prediction is notoriously difficult, as a provisional guide, this supports the hypothesis that these scaffolds could offer improvement over the quinolone core.

2.1.3 Design and Synthesis of Tetrahydroquinolones based inhibitors

The rationale behind the design of a tetrahydroquinolinone core was to retain similar steric and nonpolar functionality as the aromatic quinolone systems while increasing sp³ character and thereby decreasing planarity, it also introduces potential for substituents at novel vectors. These factors combined should offer the opportunity for a compound series with inherently improved solubility and subtly different binding potential. Compound (**57**) was designed to demonstrate proof-of-concept with replacement of the alkyl chain of endochin with a diaryl ether having been shown to be greatly beneficial to compounds metabolic stability; the 4-phenoxyphenyl diaryl ether was chosen for the commercial availability of the corresponding boronic acid (**58**).

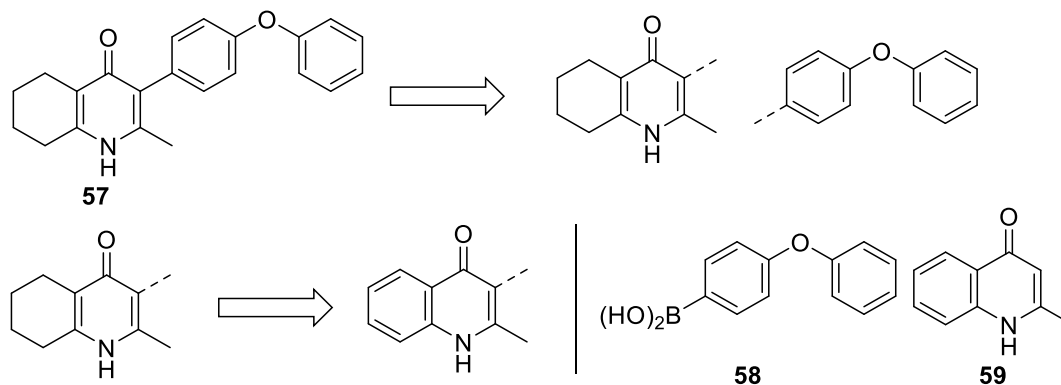
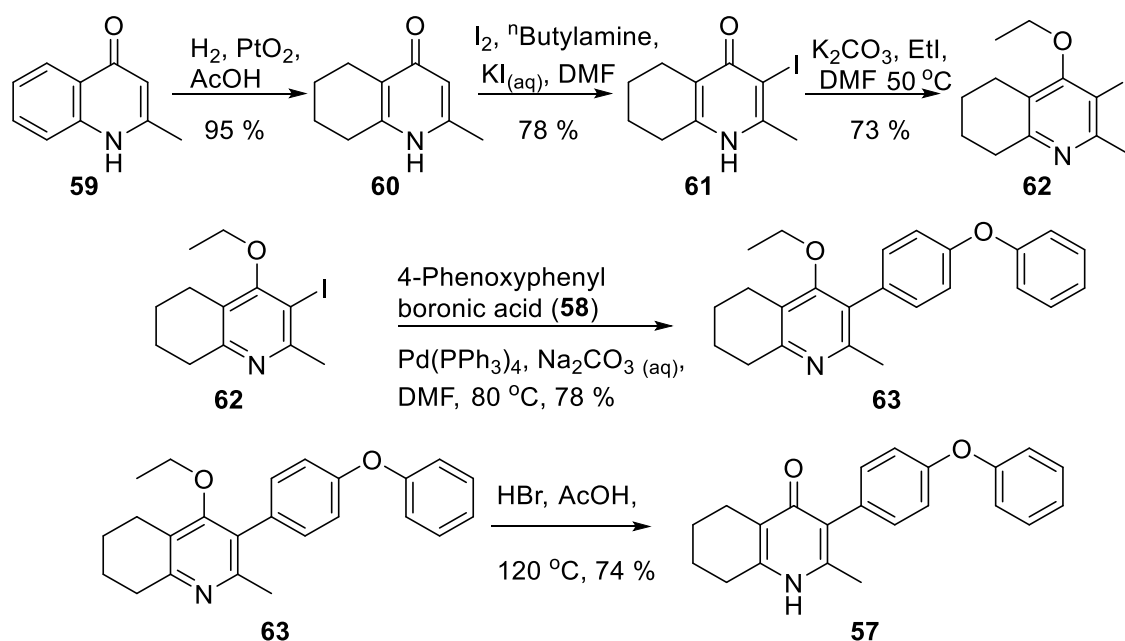


Figure 2.4 Retrosynthetic analysis of tetrahydroquinolone design **57**, with commercially available starting materials **58** & **59**.

The selective hydrogenation of 2-methylquinolone (**53**) to reach the tetrahydroquinolone core (**59**) was achieved using a method identified, from Bradbury *et al*,¹¹⁵ and the remaining steps, through intermediates **59-64**, were adapted from a route used by Riscoe *et al*,⁹⁸ in the synthesis of the ELQ series (synthesis shown in **Scheme 2.1**).^{101,116}



Scheme 2.1: Five step reaction scheme for synthesis of compound **57** Starting from **59** via a hydrogenation (**54**), iodination (**60**), alkylation (**61**), Suzuki coupling with **58** (**63**) and finally deprotection to give **57**.

This five-step route produced compound **57**. The synthetic route and its optimisation will be discussed in detail later in **Chapter 3**.

2.1.4 Design and Synthesis of Cyclo-penta/hepta-[b]pyrid-4-one based inhibitors

The cyclopenta[b]pyrid-4-one (**64**) was designed to investigate the combined effects of ring size and saturation on solubility. They also offered potential to explore different areas of the binding pocket with different vectors for substituents to that of 6,6 systems. In addition, dependent on a viable synthetic route, there is potentially to adapted this to access the 7,6-analogue; the hepta[b]pyridine-4-ones, or as an alternative method to deliver tetrahydroquinolone. The planned synthetic route was analogous to that of the tetrahydroquinolone example (**57**), however unlike the 6,6-systems there is no equivalent system aromatic bicyclic system to be reduced, and relatively limited synthetic precedent. Therefore a new synthetic approach was required to reach intermediate **65**.

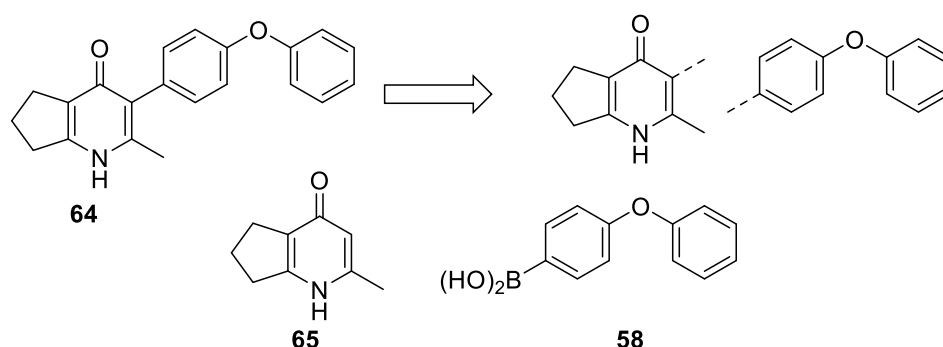
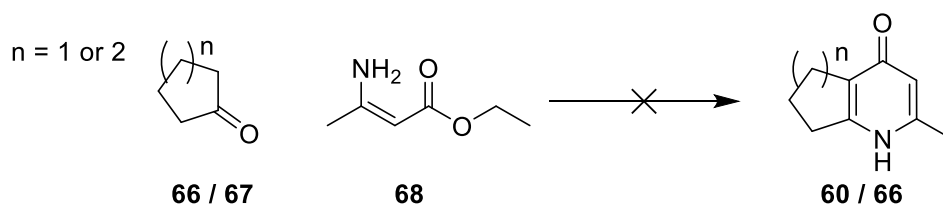


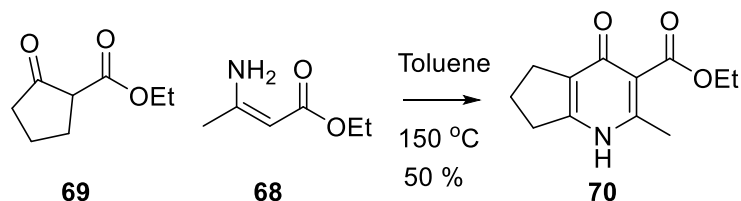
Figure 2.5:
Retrosynthesis of Cyclo-penta[b]pyrid-4-one design **64**.

Initially it was hoped that it may be possible to force cyclisation directly from the cyclic ketone and 3-amino-crotonate ester (**Scheme 2.2**). However this was not successful in forming either the six or five cycloalkyl-pyridone system.



Scheme 2.2:
Failed cyclisation of 3-amino-crotonate and cyclo-pent/hexan-one.

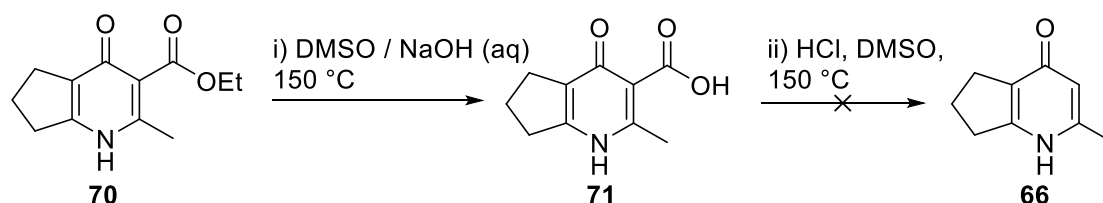
There exists some precedent for using 1,3-estercarbonyls to form the 3-carboxyl pyridones and it was hoped this could be extended to the readily available ethyl-2-carboxycyclopentanone.¹¹⁷



Scheme 2.3:

Formation of ethyl-3-carboxylatecyclopenta[b]pyrid-4-one (**70**) from 3-aminocrotonate (**68**) and 2-(ethoxycarbonyl)-1-cyclopentanone (**69**).

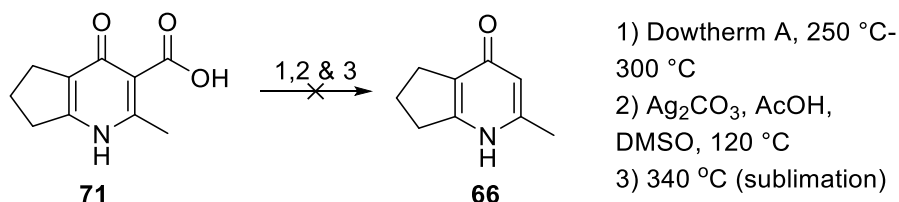
The cyclisation proceeded in moderate yield on a reasonable scale providing **70** in good quantities. Unfortunately, the decarboxylation of the cyclopenta[b]pyrid-4-ones proved to be challenging. Hydrolysis of **70** to the acid **71** proceeded efficiently under high temperature basic conditions, however when neutralised and heating continued no decarboxylation was observed.



Scheme 2.4:

Failed decarboxylation of **70** via acid **71**.

A range of alternative conditions were used; high temperature, in both solvent and direct heating, as well as catalysis with silver carbonate. A small amount of product (<1%) was isolated after direct heating at very high temperatures (~340 °C) where sublimation was achieved. However this was insufficient for the continuation of the synthesis. This would suggest that further development of the conditions, either by identifying a suitable catalyst or accessing higher temperature methodology, could provide access to **66**.



Scheme 2.5:

Failed decarboxylation reaction conditions.

As a result of the synthetic intractability this series was not progressed.

Routes to the cyclopentyl and heptyl systems have been established by Bradbury *et al*,¹¹⁵ however these are multistep and generally low yielding, and deemed unsuitable to rapid library synthesis and therefore limit the potential for further development.

2.1.5 Design and Synthesis of the Triazolo/pyrazolo[1,5-a]pyrimidin-(4H)-ones based inhibitors

The 5,6-heterocyclic systems were designed to investigate the combined effect of changes to ring size and addition of heteroatoms into the ring system. Importantly in these systems the bridging position between the pyrazolo/triazolo ring and the ketone of the pyridone moiety is occupied by a nitrogen atom. This could be expected to have substantial effect on the pyridone systems preference in tautomeric states, and to determine the effects on binding.

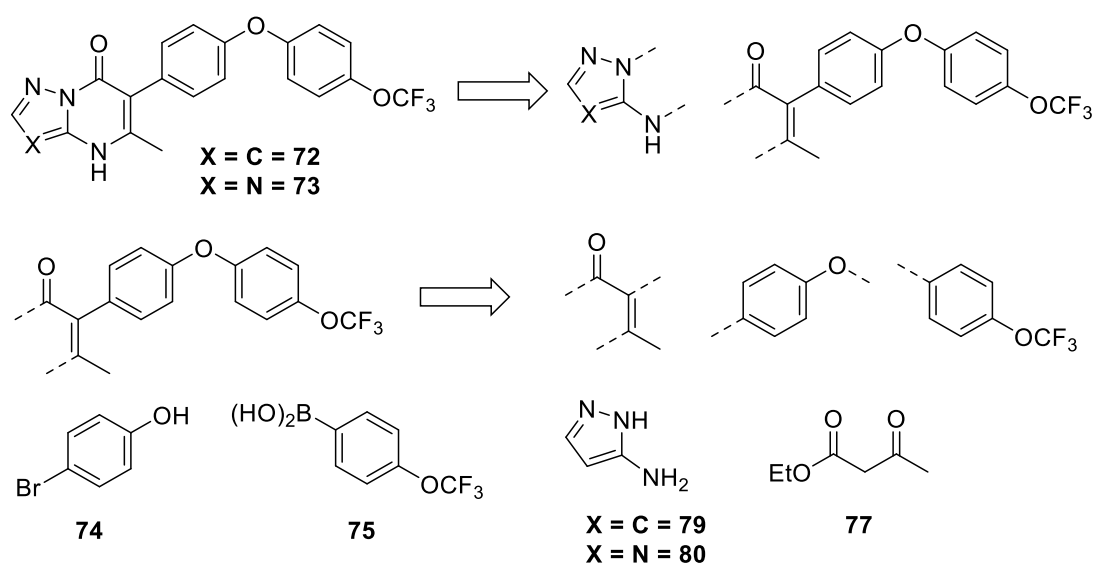
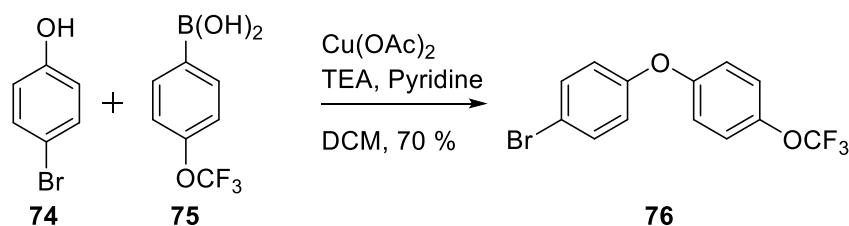


Figure 2.6: Retrosynthesis of pyrazolo/triazolo-pyridone designs (**72 / 73**).

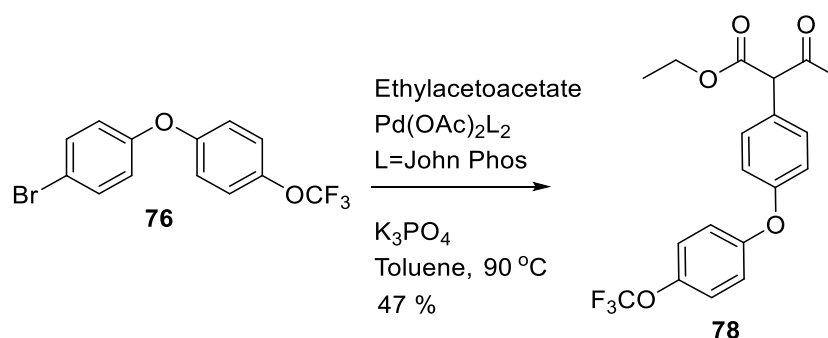
Synthesis of the triazolo/pyrazolo[1,5-a]pyrimidin-(4H)-ones was achieved in three steps. This started with synthesis of the diaryl system by coupling 4-bromophenol (**74**) and 4-(trifluoromethoxy)phenyl boronic acid (**75**) using Chan Lam conditions (**Scheme 2.6**).¹¹⁸ This particular diaryl ether system; formed from 1-bromo-4-(4-trifluoromethoxy)phenol)phenyl (**76**), was chosen as it had been reported in work by Yeates and co-workers¹⁰⁶ and explored by Riscoe¹⁰¹ as a metabolically stable alternative to the use of an alkyl chain, such as in endochin, while maintaining a degree of flexibility in the side chain.



Scheme 2.6:

Chan-Lam coupling of 4-bromophenol (**74**) and 4-(trifluoromethoxy)phenyl boronic acid (**75**) to form diaryl ether 1-bromo-4-(4-(trifluoromethoxy)phenyl)phenol (**76**).

This is followed by palladium catalysed coupling of **76** to ethyl acetoacetate, which proceeded in reasonable yield (**Scheme 2.7**), although purifying the product proved difficult via column chromatography with persistent impurities remaining difficult to separate without extensive reduction in yield. The Proton NMR of **78** in particular appeared far more complex than predicted, suggesting a mixture of tautomer states present in solution, although this was not confirmed.

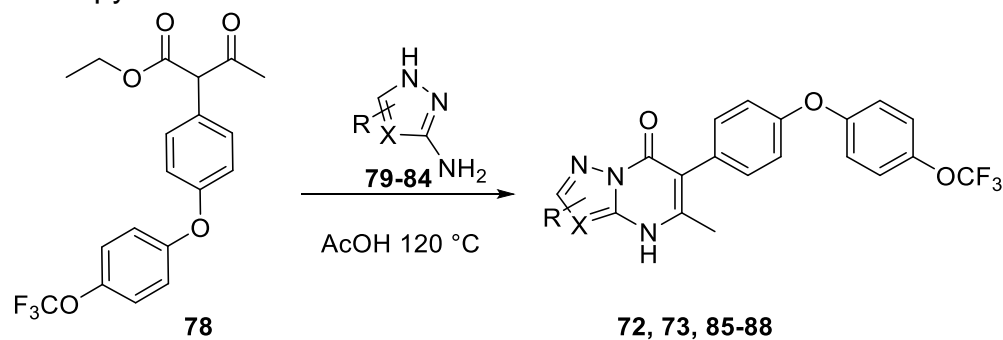


Scheme 2.7:

Palladium catalysed coupling of ethyl acetoacetate (**77**) and 1-bromo(4-(4-(trifluoromethoxy)phenyl)phenyl) (**76**) to give Ethyl 3-oxo-2-(4-(4-(trifluoromethoxy)phenoxy)phenyl)butanoate (**78**).

Finally, cyclisation of **78** with the amino-triazole/pyrazole in acetic acid resulted in the desired triazolo/pyrazolo-pyridone in moderate yield (**Table 2.2**). Initially only the unsubstituted triazolo and pyrazolo compounds where synthesised, however given the concise nature of the route a further four compounds were synthesised from commercially available pyrazoles/triazoles (**81-84**).

Table 2.2: Cyclisation of 3-amino pyra/tria-zoles to generate pyra/tria-zolopyridones.



Product	3-Amino Triazole/Pyrazole	Yield
72		48%
73		23%
85		36%
86		74%
87		23%
88		39%

The yields across substrates was relatively consistent, with the exception of the phenyl pyrazole. The phenyl substituted pyrazole substrate proved to be substantially higher yielding, this may have been a result of the product precipitating out of solution on formation and thereby assist driving the reaction forwards.

While the synthesis of this series was relative rapid in principle, the size of the library was limited with respects to the availability of desirable amino pyrazoles/triazoles, and therefore enlarging the series to investigate a more targeted of chemical space would require more extensive synthetic efforts. Future compounds could investigate fluoro, chloro, ethyl and cyclopropyl

substituents, at varied positions, as a priority. This would better determine how large and which position substituents can be tolerated.

2.1.6 Design and Synthesis of Tetrahydroquinazolinediones based inhibitors

The tetrahydroquinazolinediones were designed after shape similarities between the pyridone based systems (e.g. **44**) and the coccidiostat Toltrazuril (**39**) were identified.

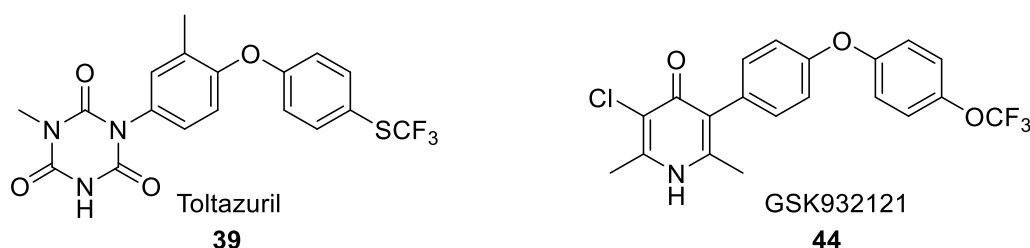


Figure 2.7:
Comparison of Toltrazuril **39** and pyridone GSK932121 **44** structures.

There is some evidence to suggest that Toltrazuril acts through inhibition of the electron transport chain,^{119,120} and as such, could potentially function via inhibition of cytochrome *bc*₁. As a result, the hybrid design combining aspects of the two systems with a saturated ring system was generated. A simplified design (**89**) was decided on for ease of synthesis and to establish proof of concept, shown in **Figure 2.8**.

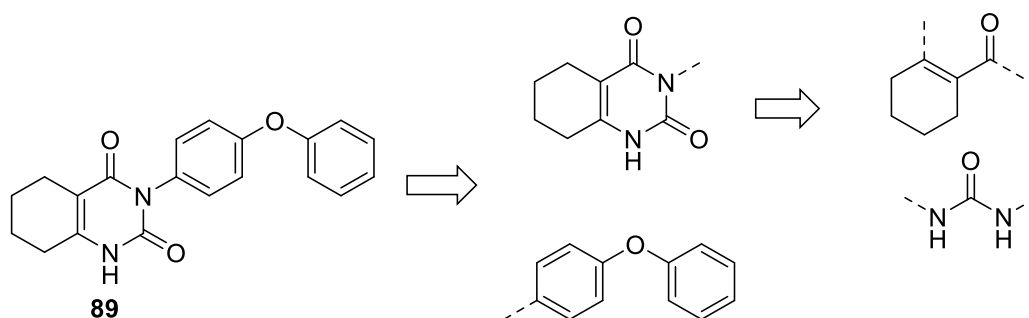
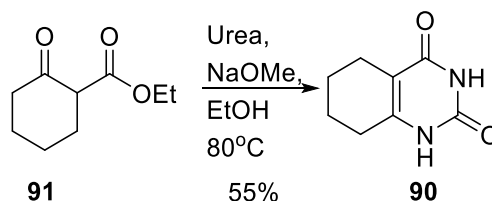


Figure 2.8:
Retrosynthesis of Toltrazuril-like tetrahydroquinazolinedione (**89**).

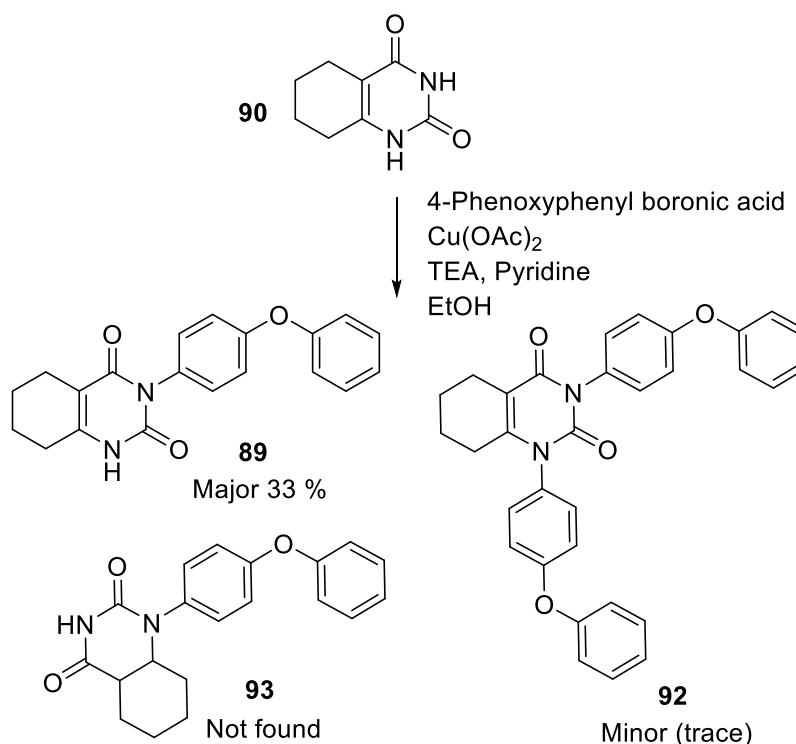
Retrosynthesis of the designed compound produced a two-step synthesis; the formation of the tetrahydroquinazolinedione core **90** followed by the coupling of the diaryl ether, using **58**. The formation of the tetrahydroquinazolinedione core (**90**) was achieved by cyclising the ethyl-2-oxocyclohexanecarboxylate (**91**) with urea under basic conditions to give **90** in 55% yield (**Scheme 2.8**).



Scheme 2.8:

Cyclisation of ethyl-2-oxocyclohexanecarboxylate (**91**) and urea to form tetrahydroquinazolidinedione (**90**).

The Chan-Lam coupling was initially trialled with the same conditions as used previously in the formation of the diaryl-ether **76**. Although the solubility characteristics of the substrates necessitated the change in solvent from DCM to ethanol. The only major concern for the forward synthesis was the regioselectivity of the Chan Lam coupling. However, while some double addition of 4-phenoxyphenyl boronic acid to **90** was observed in the LCMS trace (~10%) (to give compound **92**), the majority of compound formed was of a single mono-substituted regioisomer and purification was achieved via basic workup.



Scheme 2.9:

Chan Lam coupling reaction; notably although some double addition was observed only one regioisomer was formed.

Confirmation of the synthesised regioisomer was determined via NOESY NMR, this showed coupling between the NH and the aliphatic protons (blue)

while no coupling was observed between the aliphatic and aromatic protons (red).

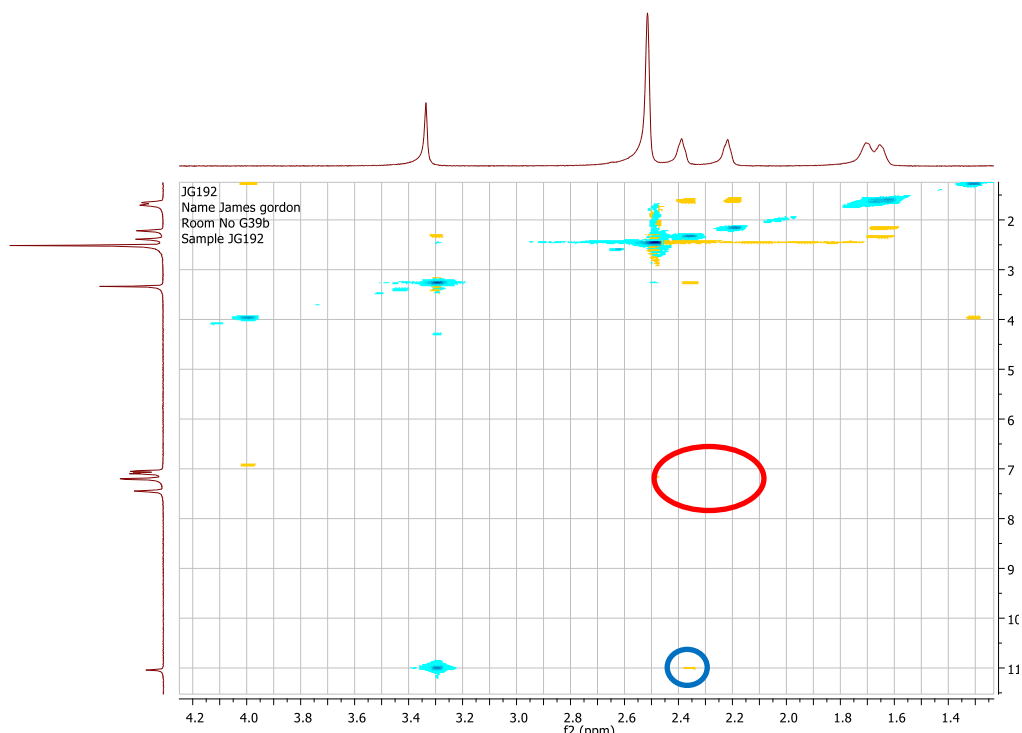


Figure 2.9: NOESY NMR to confirm regioisomer

Observed coupling between the NH and the aliphatic protons (blue) while no coupling was observed between the aliphatic and aromatic protons (red).

This synthesis should also be applicable to forming the 5,6 system from the corresponding ethyl-2-oxocyclopentanecarboxylate, if the 6,6-system demonstrated potential in the *T.gondii* inhibition assays.

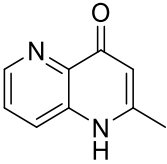
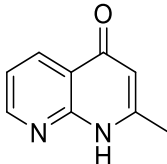
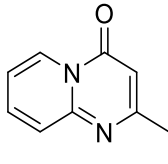
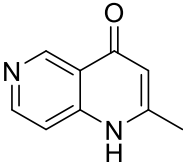
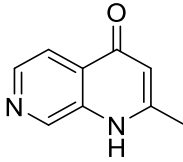
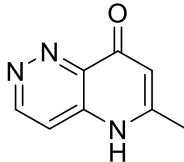
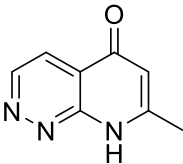
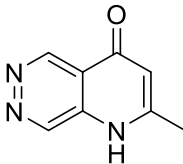
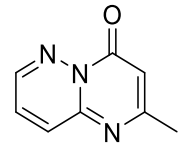
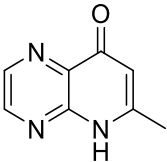
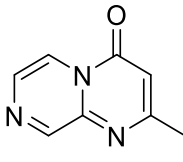
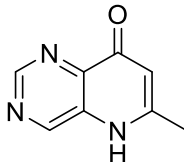
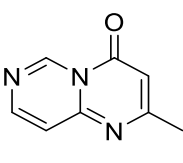
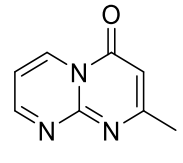
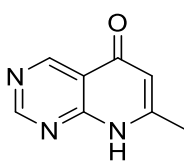
2.1.7 Design and Synthesis of Naphthyridin-(4H)-ones based inhibitors

The naphthyridones mimic the quinolone core very closely in shape, with the addition of a heteroatom predicted to markedly reduce the lipophilicity, and therefore improve aqueous solubility. There are also a large number of naphthyridone isomers that could be explored, and the potential to expand to investigate further addition of nitrogen into the ring system, for example looking into the effects of pyridopyrimidine examples.

The large effect on Log P and how it varies between regioisomers and further addition of heteroatoms into the ring is illustrated in

Table 2.3. It also illustrates the large number of distinct compounds possible to enumerate from a relatively minor and simple change.

Table 2.3: Examples of naphthyridone cores and their calculated log P. Extended to include pyrimidine/pyrazidine/pyrazine-pyridones (**94-108**).

Isomer	cLog P	Isomer	cLog P	Isomer	cLog P
	-0.29		0.00		0.13
94		95		96	
	-0.71		-0.71		-0.68
97		98		99	
	-0.39		-1.11		-0.45
100		101		102	
	-0.91		-0.16		-0.89
103		104		105	
	-0.33		-0.15		-0.60
106		107		108	

The potential draw back to nitrogen enhanced ring systems is the reduction in points of diversification, with the addition of each nitrogen into the ring, a point of substitution is lost. Naphthyridones are also clearly an entirely aromatic system, and therefore highly planar and may suffer from high crystallinity, limiting potential improvements in solubility.

Retrosynthesis presented two potential synthetic approaches; firstly to form the naphthyridone initially and then to attach the diaryl-ether ring (**Figure 2.10: A**) analogous to THQ series. The second option was to form the naphthyridone ring system in the final step in a manner analogous to the pyrazolopyridones (**Figure 2.10: B**).

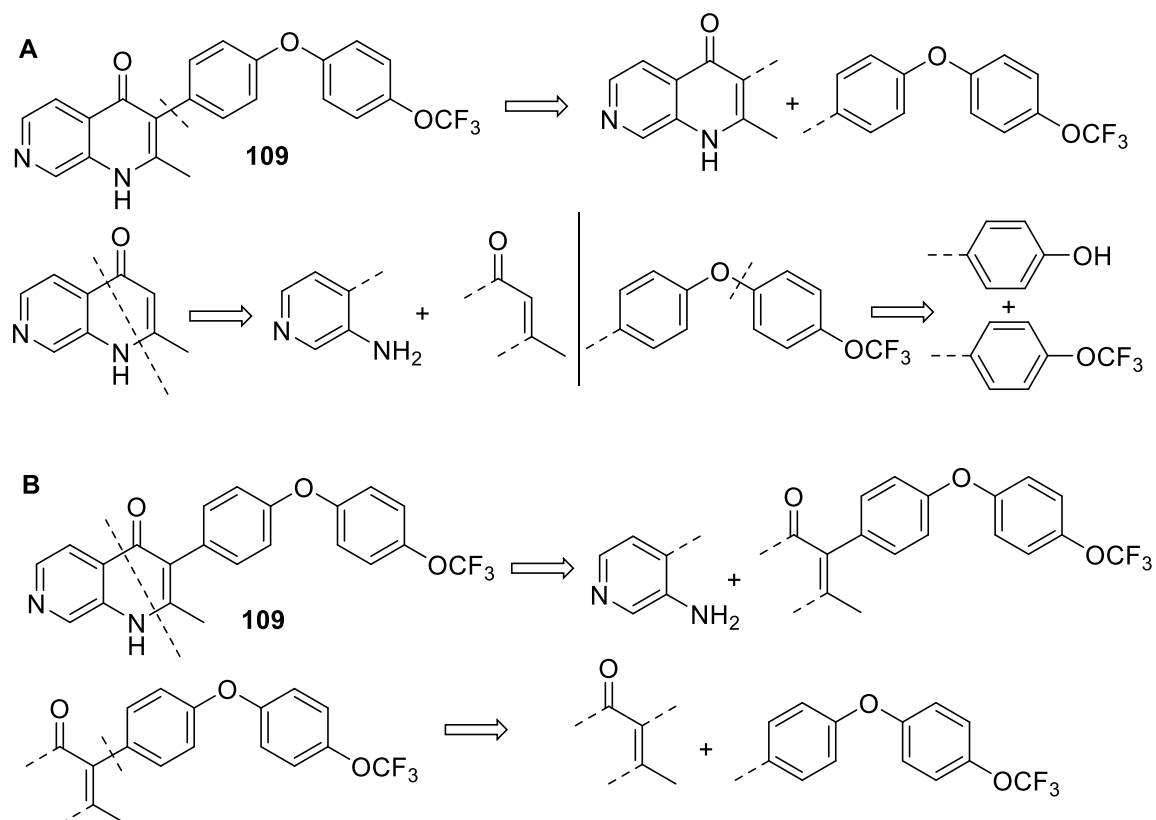
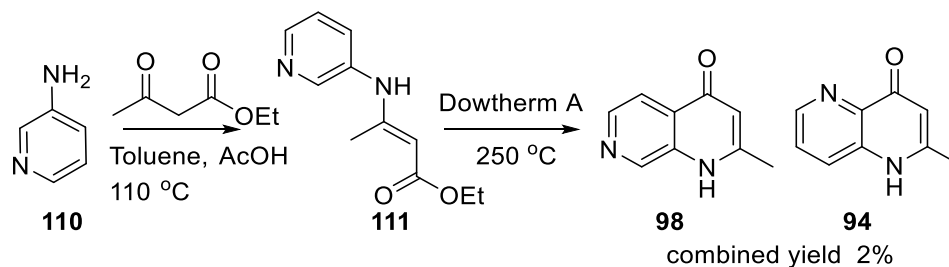


Figure 2.10: Retrosynthesis to Naphthyridone scaffolds.

Two possible retrosynthetic approaches to naphthyridone based compounds, example shown for 1,7-naphthyridone.

The first step was to synthesise the naphthyridone core, Conrad-Limpach conditions¹²¹ were trialled first however these proved to be very poor yielding, and therefore unsuitable for providing sufficient material to continue synthesis.



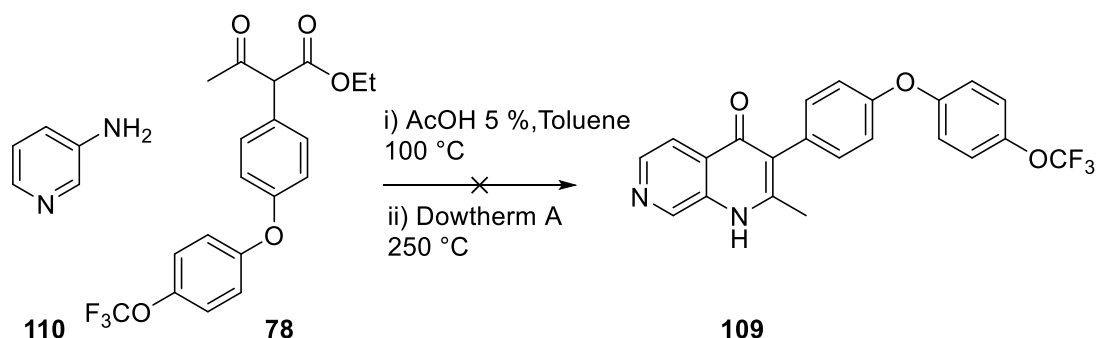
Scheme 2.10:

Conrad Limpach based synthesis of naphthyridones.

As a result, it was decided to explore the second approach, similar to that of the triazolo/pyrazolo-compounds. Replacing the 3-amino pyrazole with an amino-pyridine/pyrazine/pyridazine/pyrimidine to form the desired 6,6-bicyclic system.

To compensate for the far more electron deficient nature of pyridine and therefore less nucleophilic behaviour it was expected that harsher conditions

would be required to achieve cyclisation of **78**. However, even under higher temperature conditions the cyclisation could not be made to proceed.



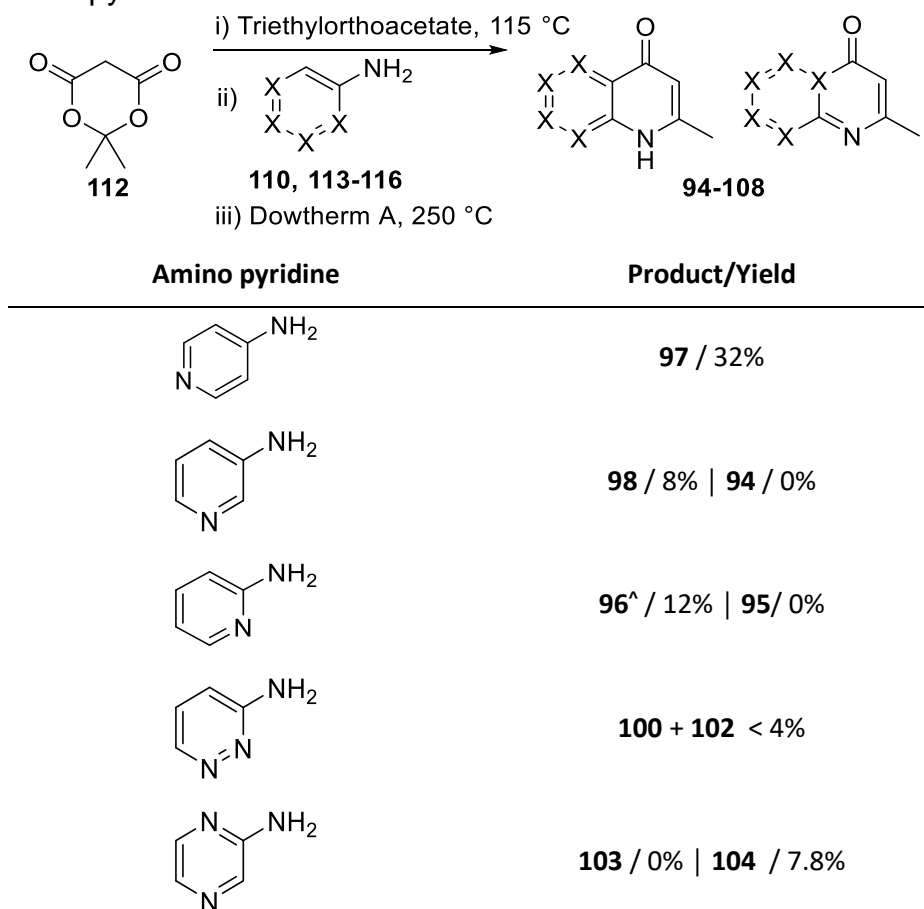
Scheme 2.11:

Cyclisation attempt from substituted ethyl acetoacetate and aminopyridine.

Analysis of the crude imine intermediate formed suggested that the ethylacetoester had been hydrolysed during imine formation and this may have caused the cyclisation step to be less favourable. It is also possible that the more electron deficient pyridine ring was not nucleophilic enough to cyclise under these conditions.

Approach A was then revisited, moving to alternative cyclisation conditions within quinolone literature suggested that using Meldrums acid (**112**) and triethyl orthoacetate, followed by the amino pyridine to form the ketene via thermal decomposition on the acid and finally cyclisation to the naphthyridone.

Table 2.4: Formation of naphthyridones from meldrums acid and aminopyridine.

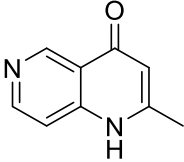
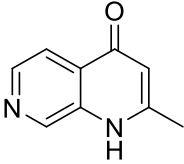
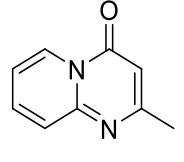
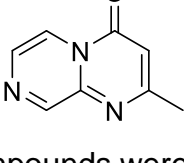


While this was successful, as can be seen in Table 2.4; one of the key problems with the cyclisation reaction was formation of both regioisomers, providing additional challenges in both separating and identifying the components, achieved through NMR. This was particularly troublesome with regards to the pyridazine/pyrazines as they also cyclised at the nitrogen position giving compounds **96**, **102** & **104**.

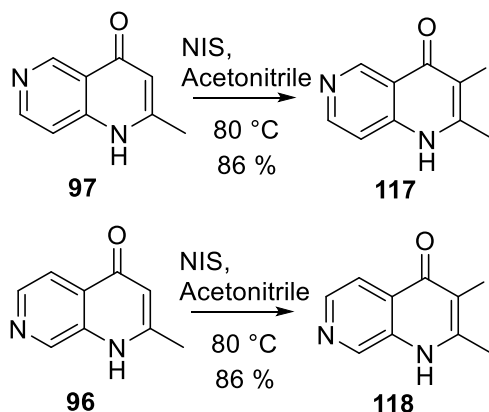
The resulting mixtures of regioisomers were then difficult to separate and, given the poor yields, unsuitable for progression. The *N*-cyclised compounds were also of less interest as they would be unable to tautomerize between the pyrid-(4H)-ol and pyrid-(1H)-one which is hypothesised to be important for binding.¹¹⁰ It was also interesting to observe the dramatic difference in melting points between the *N*-bridged compounds and the *C*-bridged compounds (**Table 2.5**). This is a strong indicator of how large an effect the hydrogen bonding, between NH and the naphthyridone carbonyl, is having on crystal

lattice energy and therefore suggests this has an influential effect on overall solubility of the series.

Table 2.5: Naphthyridone melting points

Compound No.	Naphthyridone	Melting Point
97		>250 °C
98		>250 °C
96		126.9-130.4 °C
104		116.0-117.2 °C

The 6 and 7 naphthyridone compounds were both iodinated using NIS as with the THQ example, proceeding in good yields (86%) as seen in **Scheme 2.12**.

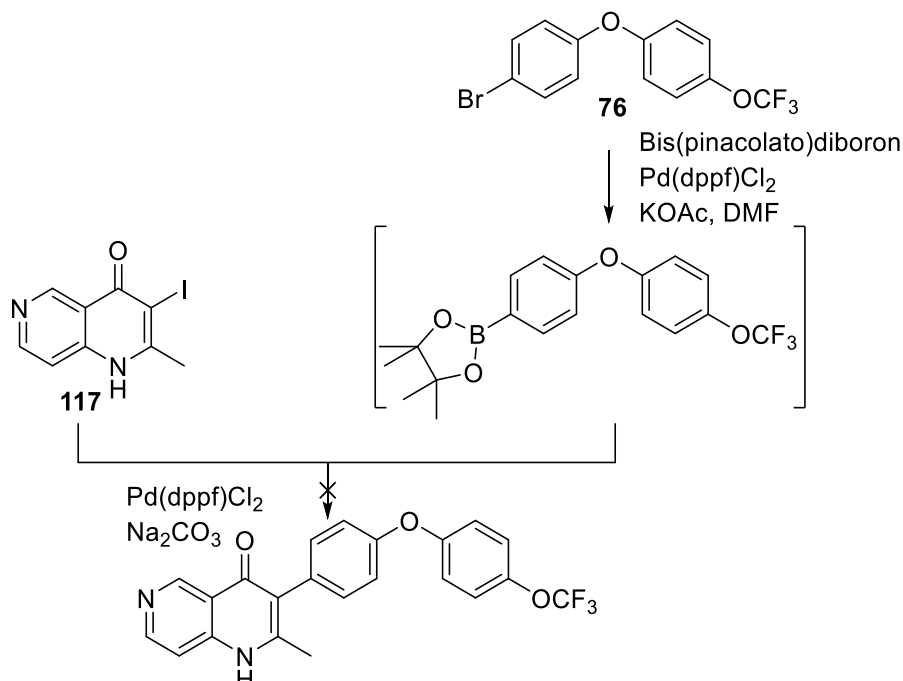


Scheme 2.12: Iodination of naphthyridones

The decision was made to advance only one of the regioisomers initially, to optimise the synthesis and demonstrate proof-of-principle, before committing to further synthetic endeavours.

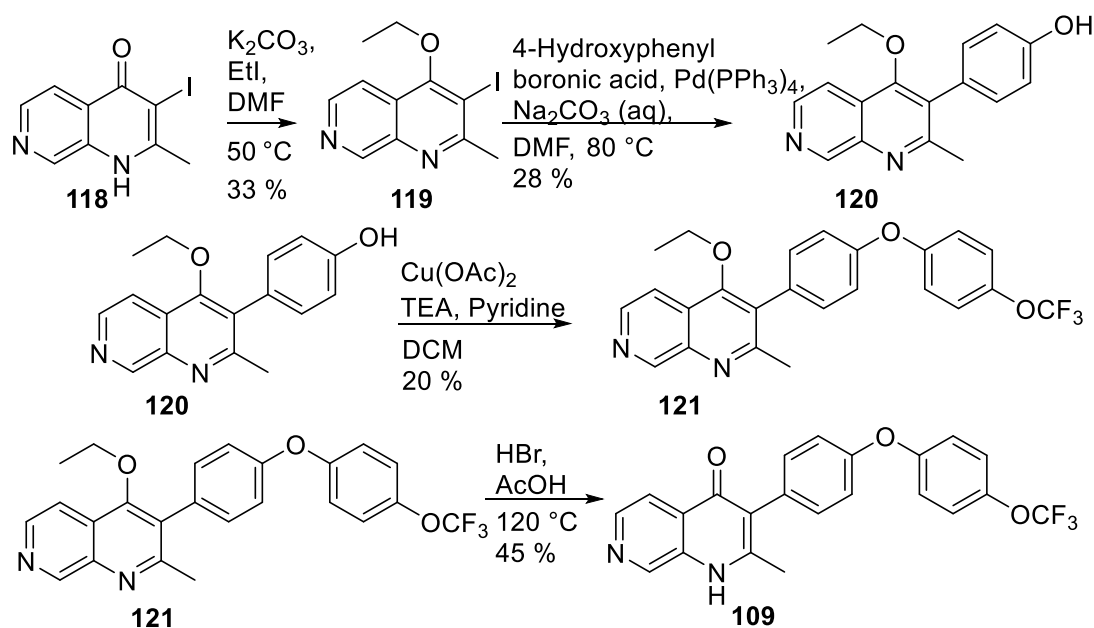
Proceeding via one-pot Suzuki coupling methodology¹²² was then attempted to directly reach the final compound (**Scheme 2.13**), however while the mass

off desired product **119** was detected using LCMS, no product was isolated following work up and purification, via column chromatography.



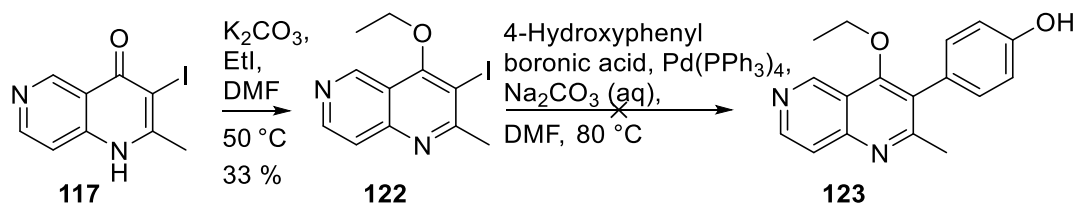
Scheme 2.13: Unsuccessful one-pot Suzuki reaction.

Finally, a longer synthetic route similar to the route developed for the THQ series was attempted. While this proved successful, yields across both the alkylation and coupling steps was greatly diminished relative to that of the tetrahydroquinolinone analogues.



Scheme 2.14: Synthetic route to naphthyridone **109**.

After this route to successfully synthesise the 1,7-naphthyridone derivative was developed, it was hoped it could be directly applied to the alternative regioisomeric naphthyridones, primarily the 1,6 and 1,5 regioisomers. However while the initial steps of the synthesis proceeded in similar yields the Suzuki coupling reaction could not be made to proceed with 1,6 naphthyridone.



Scheme 2.15:

Unsuccessful attempt to synthesise 6-naphthyridone analogue via **123**.

Attempts to circumvent this were unsuccessful, as a result only the 1,7-naphthyridone derivative was successfully synthesised and tested.

2.2 Cellular Activity and Physicochemical Evaluation of novel inhibitors.

Having synthesised nine compounds across five different core designs, the compounds were then evaluated for their activity against *Toxoplasma gondii*. In the first instance this was done by assessing their efficacy in inhibiting the tachyzoite stage, in a cellular assay. These tachyzoite assays were conducted by collaborators at the University of Chicago. The assay was based on fluorescently labelled parasites, grown on human fibroblast foreskin cultures. Infected cultures are then treated with the test compound at varying concentrations.⁹⁰ Reduction in fluorescence is then observed and from this an IC₅₀ curve can be created (see appendix for full experimental detail). An example of data from the cellular assay for a single compound is shown below (Figure 2.11).

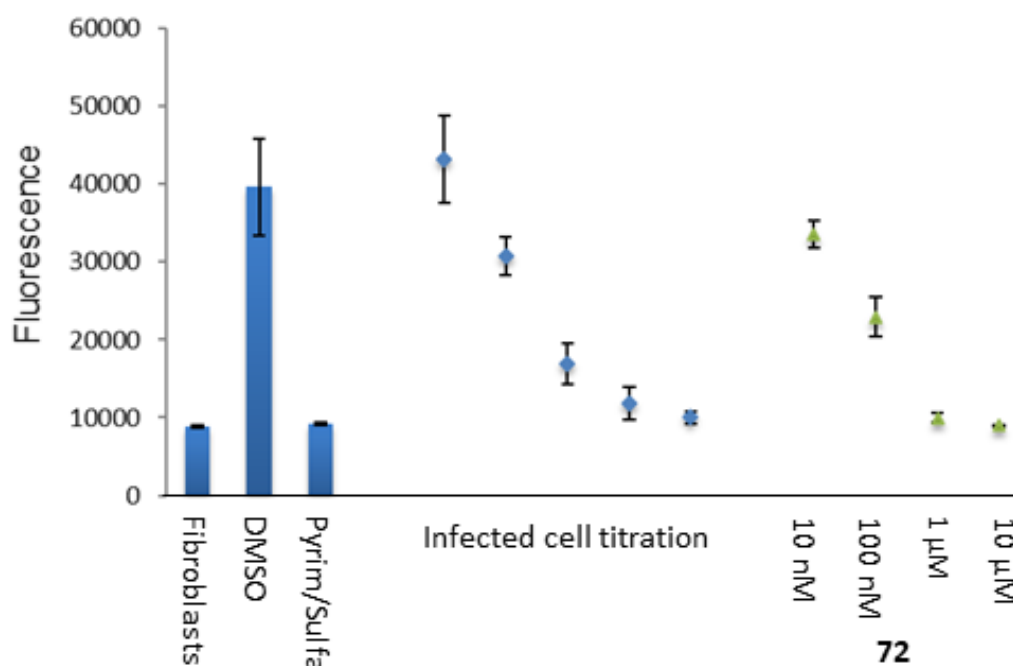


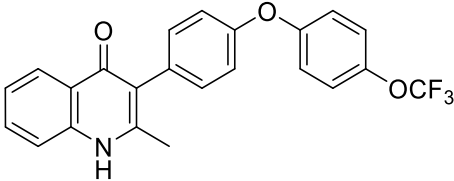
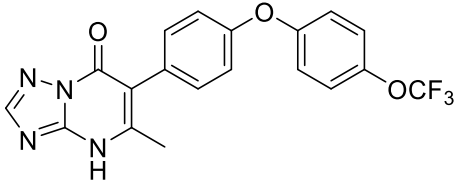
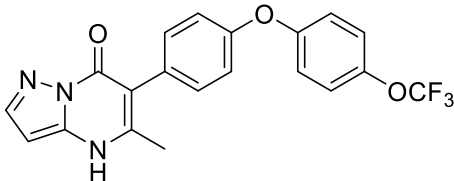
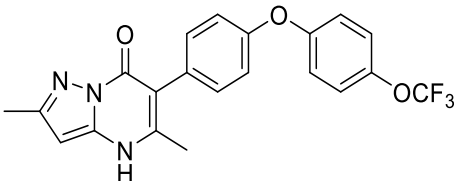
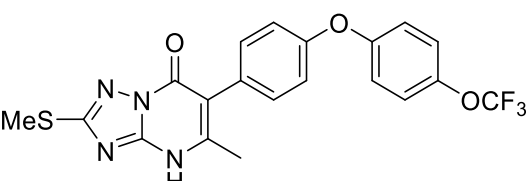
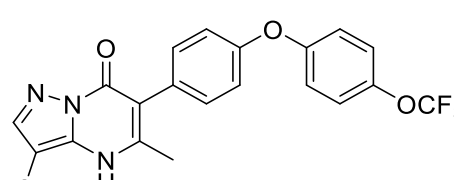
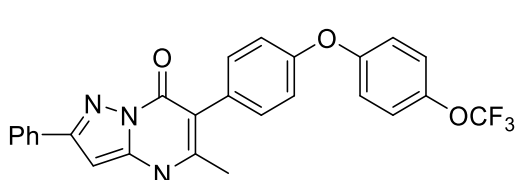
Figure 2.11: Tachyzoite IC₅₀ plots.

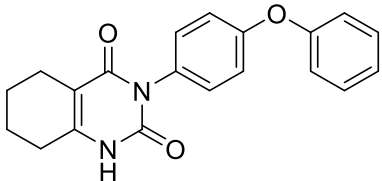
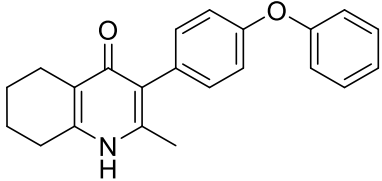
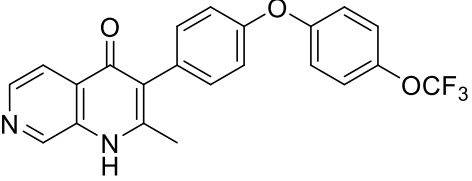
Example of data from cellular tachyzoite assay: control bars shown in blue (left to right); untreated fibroblasts, DMSO & pyrimethamine/sulfadoxine, and titrated infected cell curve. An example compound dosage curve is shown in green.

The assay is run with both positive and negative controls. A combination of pyrimethamine/sulfadiazine (current standard treatment) was used as the positive control, indicating fluorescence comparable to uninfected fibroblast

cultures. A negative control of DMSO was also used to account for any effects from formulation. The results are summarised for all compounds in **Table 2.6**. In addition a number of compounds were assessed for their activity against EGS strain of *T.gondii* as an assessment of efficacy vs the bradyzoite stage, however difficulties with the assay resulted in overall low-throughput.

Table 2.6: Summary of antiparasitic activity for compounds; **45, 57, 72, 73, 85-89 & 109**.

No.	Compound	Tachy IC ₅₀	Brady IC ₅₀
45		30 nM	1.0 μM
73		1.0-10 μM	>10 μM
72		1.0-10 μM	1.0-10 μM
85		0.1-1 μM	N.D
88		>10 μM	N.D
87		>10 μM	N.D
86		1.0-10 μM	N.D

89		>10	N.D
57		0.03 μ M	4.0
109		0.1 μ M	N.D

2.2.1 Preliminary ADMET and Physicochemical Properties

After initial screening in the cellular assay compounds with sufficient tachyzoite activity were then evaluated for their metabolic stability and their aqueous solubility. These two criteria are both crucial early stage parameters in drug discovery and both have been identified as liabilities in previous pyridone/endochin based *bc1* inhibitors.

2.2.1.1 Aqueous solubility

Aqueous solubility is important for a number of reasons including; ease of administration, absorption and distribution.¹²³ Poorly soluble compounds can prove difficult to administer effectively, creating difficult, if not insurmountable challenges for formulation. In addition, if the limited solubility is a result of high lipophilicity then it is likely that the compound may have poor availability *in vivo* due to high plasma protein binding. Finally and perhaps most importantly since most assays are conducted in an aqueous system, poorly soluble compounds may not be assessed accurately within these assays. In best case scenario compounds may be underperforming, however in the worse cases this may be hiding serious deficiencies such as toxicity. As such gauging a compounds kinetic solubility is an important early stage assessment in almost all drug discovery programs. Conversely if solubility is too high, especially as a result of a large number of highly polar functionalities, there is a high risk of rapid excretion in addition to presenting challenges to membrane permeability,

in the absence of transporters. Generally it is desirable to achieve a solubility of $>100 \mu\text{M}$, however this may be dependent on route of administration and other factors.

Aqueous solubility of a molecule is usually a result of two distinct factors namely; the lipo/hydro-philicity of the compound and the crystal lattice energy. Highly lipophilic compounds with strong crystallinity are very poorly water soluble while hydrophilic compounds and those less able to form strong crystal lattices are more soluble. Lipophilicity is intrinsic to the molecule itself and requires modification of the compound itself, such as formation of a prodrug, to alter. Crystallinity is more complicated and raises an important caveat regarding solubility measurements; the importance of a compounds polymorph when measured.¹²⁴ This factor can have a substantial effect on solubility and determining the most polymorph can be crucial in preventing future problems in formulation. Unfortunately the more stable forms also tend towards being the least soluble, with the most soluble generally being that of the amorphous non-crystalline forms. While it is possible to produce and stabilise desirable polymorphs through production and formulation techniques, there will always be a risk of conversion to the more stable forms.¹²⁴ Solubility was measured externally by ChemPartner, including comparative standards representing high, moderate and low solubility; Propranolol ($>100 \mu\text{M}$), Ketoconazole ($\sim 30 \mu\text{M}$) and Tamoxifen ($0.16 \mu\text{M}$) respectively (see appendix/experimental for full details).

2.2.1.2 Metabolic stability

A robust metabolic stability profile is important for a drug candidate as it will have a substantial effect on the drugs impact and dosing regimen. If the stability is poor and the drugs lifetime short, much higher doses or multiple doses to compensate to obtain the same therapeutic effect. Excessively long lifetimes may indicate a need to monitor for accumulation of the drug. A powerful indicator of metabolic stability is the half-life of a compound in the presence of liver microsomes. Liver microsomes are responsible for primary metabolism through the conversion of compounds into more polar species, these more polar species can then be further processed so that they may be readily excreted. The most common mechanisms of phase 1 metabolism are generally oxidative processes, however there are also a number of reductive

processes as well as carboxylation and hydrolytic mechanisms.¹²⁵ In contrast phase 2 typically involves conjugation based reactions ranging from glucuronic to fatty acids.¹²⁵ There are other important mechanisms of metabolism which will not be identified in microsomal assays such as the effects of renal clearance which may be more important to smaller more polar compounds.

An important factor to consider when testing for microsomal stability is the presence of large differences between species, as can be seen in the results shown in

Table 2.7, there are notable discrepancies between the data from mouse compared to human microsomes. Understanding and appreciating the difference between species is crucial as any successful candidate will be evaluated in mouse *in vivo* disease models before progressing to higher mammal studies. The unsaturated quinolinone ELQ271 (**45**) was used as a comparison against the selected compounds for both measurements.

Microsomal stability, aqueous solubility and anti-parasitic activity data is compiled in **Table 2.7**. In these assays, typically half-lives of below 30 minutes indicate a drug is highly susceptible to metabolism, such as the standard: ketanserin, values between 30 and 120 minutes show moderate metabolic susceptibility and values greater than 120 minutes indicate a compound is metabolically stable.

Table 2.7: Summary of data¹

Compound	Tachy IC ₅₀	Brady IC ₅₀	Aqueous Solubility (pH 7.4)	Microsomal stability Half life (human/mouse)
45	0.03 µM	1.0 - 10 µM	0.15 µM	171.93/448.13 mins
73	1.0-10 µM	>10 µM	ND	ND
72	1.0-10 µM	1.0 - 10 µM	0.94 µM	ND/278.33 mins
57	0.03 µM	1.0 - 10 µM	1.97 µM	146.33/20.97 mins
89	>10 µM	N.D	N.D	N.D
109	0.1 µM	N.D	5.12 µM	ND/>480 mins

¹ Aqueous solubility and microsomal stability assays performed by ChemPartner Ltd (for full experimental details see appendix)

Of the four series successfully synthesised, the most active and competitive with the quinolone-based series were the tetrahydroquinolone; **57** and the 1,7-naphthyrid-4(1H)-one; **109**. Unsurprisingly these were the most similar with respect to shape and electronics to the quinolone **45**. Both of these compounds exhibited potent anti-tachyzoite activity, **57**: 0.03 μM ; **109**: 0.10 μM . These compounds had the additional promise of moderate bradyzoite activity, and, perhaps most importantly, improved aqueous solubility over the unsaturated (quinolone) analogue. While the solubilities are still poor with regards to desirable drug criteria, it validates the initial hypothesis, of increasing F_{sp}^3 and decreasing LogP. Unfortunately metabolic stability of the saturated system remained a liability, especially to mouse microsomes, and would require further optimisation, and it was a priority to establish if this was a result of the unprotected diphenyl ether system or inherent to the saturated ring.

2.2.2 Computational modelling

As discussed in **Chapter 1** computational approaches to drug development are increasingly prevalent and can provide useful insight to accelerate drug development.

In attempt to assist in rationalising the SAR observed, and to determine to utility of computational docking to triage designs prior to synthesis, the compounds synthesised were docked against the proposed target; the Q_i site of cytochrome bc_1 . Currently there are no high-resolution structures of the toxoplasma cytochrome bc_1 complex, as a result it was necessary to construct a homology model in order to perform computational docking studies. The homology model was produced using Phyre 2 (Protein Homology/AnalogY Recognition Engine)¹¹¹ open access service based on the sequence (Uniprot entry O20672). The synthesised compounds were then constructed in Maestro and their binding behaviour modelled using two different docking programmes; Glide and Autodock (see experimental for procedure).^{126,127} The scores generated indicate the affinity of each compound for the protein, with the more negative value indicating better expected binding. Initial docking attempts within Glide generated a wide range of scores and showed no correlation, relative to the observed cellular activity.

Table 2.8: Computational docking results

Compound	XP GScore	XP GScore	pIC ₅₀
	<i>T.gondii</i>	<i>B.taurus</i>	(<i>T.gondii cellular</i>)
45	-2.151	-6.261	7.5
44	-7.527	-7.703	-
85	-5.824	-5.946	6.3
57	-6.257	-6.565	7.5
88	-4.315	-5.111	< 5
87	-5.557	-5.379	< 5
86	-5.918	-6.819	5-6
89	-5.291	-8.299	< 5
109	-2.65	-6.825	7
72	-8.078	-6.615	5-6
73	-8.156	-6.034	5-6

Inspection of the docking poses generated (Table 2.9) revealed binding poses inconsistent with that of the existing ligand protein crystal structure.

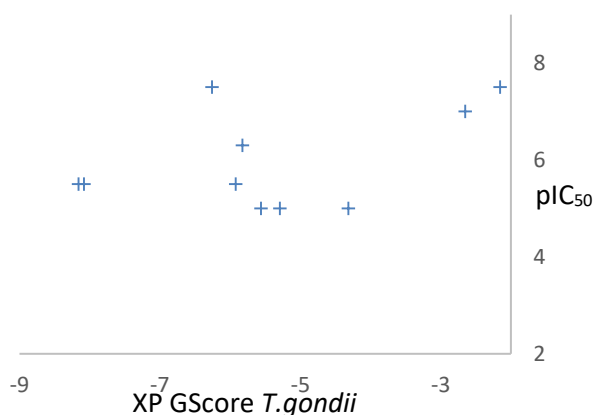
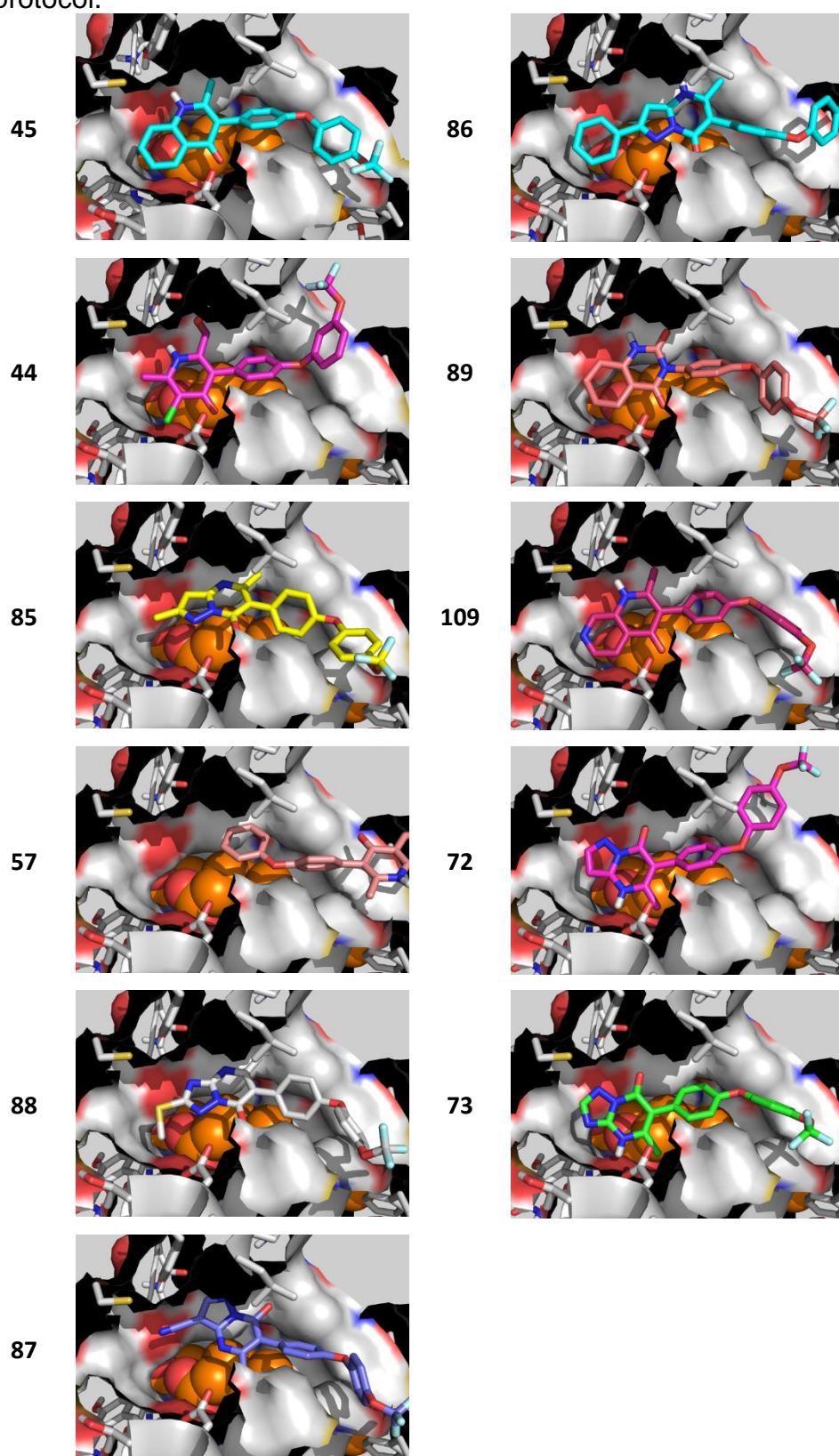


Figure 2.12:

Scatter plot of glidescores vs cellular IC₅₀'s, showing no clear correlation between the two.

Most notably the docking did not model the pyridone moiety, known to be important in binding, in a consistent pose. This combined with the complete absence of correlation (**Figure 2.12**) with observed *in vitro* activity suggests that the binding behaviour is not being accurately reflected by the modelling.

Table 2.9: Lowest energy binding output poses generated from glide docking protocol.



To identify if this was a failure of the modelling software being unable to account for important interactions for this particular binding site, or as a result

of the differences between the mammalian and parasitic complex structures the docking and crystal structure of compound **44** were compared. As can be seen in **Figure 2.13**, the modelling of the binding within the bovine protein appears to replicate the crystal structure to a good approximation, with the pyridone head groups well aligned. The *T.gondii* docking however shows significant differences both in pose and the predicted potency. The docking score suggests that **44** would be selective for the mammalian protein over the parasite and would exhibit very weak affinity for the parasite in particular.

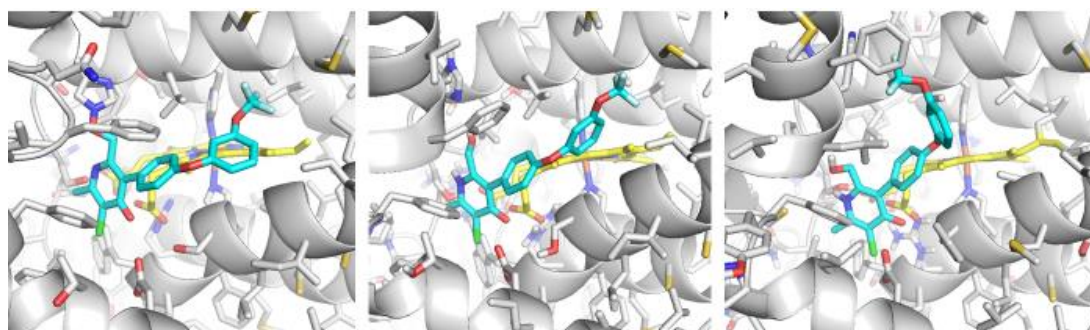


Figure 2.13:

Side by side comparison of cystral structure 4D6U (left), boivine docking model (centre) and *T.gondii* homology docking model (right).

One of the most notable difference between the two protein poses is the position of the histidine (His201), in particular this appears to make a crucial interaction with the hydroxy group of **44** in the crystal structure. In contrast the homology model of the *T.gondii* structure appears to position this residue in a flipped confirmation, resulting in it positioned substantially further from the binding site. This may be a result of the way the homology model was generated, perhaps suggesting that conformational changes occur during ligand binding. It was suspected that this poor correlation and modelling of binding behaviour may be a result of movement of residues during binding; in particular the histidine residue His201 is significantly displaced between the *T.gondii* and *Bovine* dockings.

Unfortunately, it was not possible to refine the docking protocol to achieve a reliable predictive guidance for future designs. As a result computational modelling was restricted to observational assessment.

2.3 Summary and future work

A small number of compounds from five distinct chemical scaffolds were synthesised and evaluated for cellular parasitic activity and aqueous solubility. Pleasingly a number of compounds across several series showed significant anti-parasitic activity ($\leq 1.0 \mu\text{M}$) and performed well with regards to metabolic stability and preliminary toxicity and showed modestly improved solubility. Several of the series explored could have potential but would require more extensive route development to explore adequately enough to establish meaningful SAR. In addition, establishing a practical route to the cyclopenta/hepta-[b]pyrid-4-ones would also be of interest. The additional vectors for substituents and the steric effects would further SAR understanding of the tetrahydroquinolone scaffold and provide interesting alternatives. It would also be of interest to explore the use of 4-amino pyrazoles rather than the 3-amino pyrazoles. These would generate the bridge head at carbon rather than nitrogen and form a closer analogue to the original pyridone scaffold. Other similar examples might include oxazole-based scaffolds, again avoiding the 'N bridge', these provide fewer vectors for substituents but may offer enhanced physicochemical properties desired.

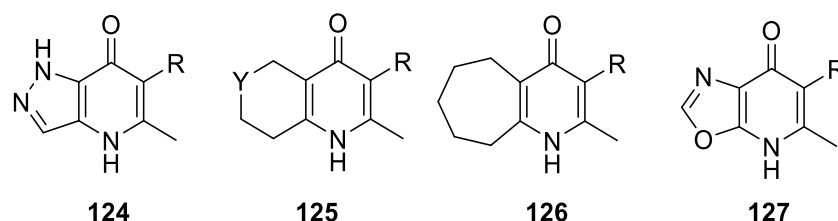


Figure 2.14:
Examples of unexplored scaffolds.

In a similar vein, developing a synthetic route to reach the alternative naphthyridones and other nitrogen enriched systems could also be explored, as these showed potential in reducing the lipophilicity of the compounds. However, if solubility is largely being governed by the high crystallinity, caused by the pyridone moiety as suggested by the observed high melting points, then the modest reductions in lipophilicity these alterations cause may not be sufficient to markedly enhance aqueous solubility.

Overall it is clear that a wide range of scaffolds exist within neighbouring chemical space to the heavily explored quinolone/pyridone/acridone structures, and that exploration of these can provide promising improvements

to the physiochemical liabilities previous scaffolds have been susceptible to. The number partially explored here represent a relatively limited subset of what could be envisaged while making relatively minor changes to the scaffold. Synthetic tractability of some of these scaffolds is perhaps the major hurdle to a more extensive exploration. However, given the biological promise shown by previous series, targeting this complex effectively is a promising pathway to antiparasitic activity.

Unfortunately, the poor correlation between computational modelling and observed inhibition suggests this will not be a valid approach for design optimisation or prioritisation of designs. The homology model does provide a useful reference for visual assessment to guide future designs.

Rewardingly both the THQ and naphthyridone (**57 & 109**) examples exhibited solubilities greater than 1.00 μM and retained potency. The tetrahydroquinolone series in particular was highly potent, and while it did demonstrate significant metabolic liabilities, it was hoped this could be readily optimised in lead development. Further investigation and development of tetrahydroquinolone based compounds is discussed in **Chapters 3 & 4**.

Chapter 3

Design, Synthesis and Optimisation of Tetrahydroquinolones

3.1 Validation of target site

The cellular assays have a number of advantages over enzyme assays, namely; compounds that exhibit activity have demonstrated the ability to reach the site of action, in addition to binding to the protein target site. However a drawback is that it does not specifically identify their mode of action. Given the structural similarities of the series to previous cytochrome *bc₁* inhibitors a reasonable initial assumption was that they operated by the same mechanism. It was therefore felt that obtaining further evidence to support this assumption would be beneficial. Several approaches were taken to establish this by collaborators using compound **57** as a probe, these are described below.

3.1.1 Yeast mutagenic studies

Mutagenic studies are a good method for confirming a specific suspected target site of an inhibitor, as they can be specific to the target site.¹²⁸ Mutagenic studies in general involve generating either point mutations or deletions, these are designed to interfere specifically with inhibitor binding, ideally with minimum disruption to enzyme function. In this case the models most readily available to collaborators were yeast based. Assays were performed by Rima Mcleod research team at the University of Chicago (full experimental details found in the appendix). Modelling of the Q_I site indicated that mutations M221K and M221Q in *S.cerevisiae* (corresponding to F215 and F220 for *T.gondii* and *Bovine* respectively) should result in reduced binding affinity of the inhibitors.

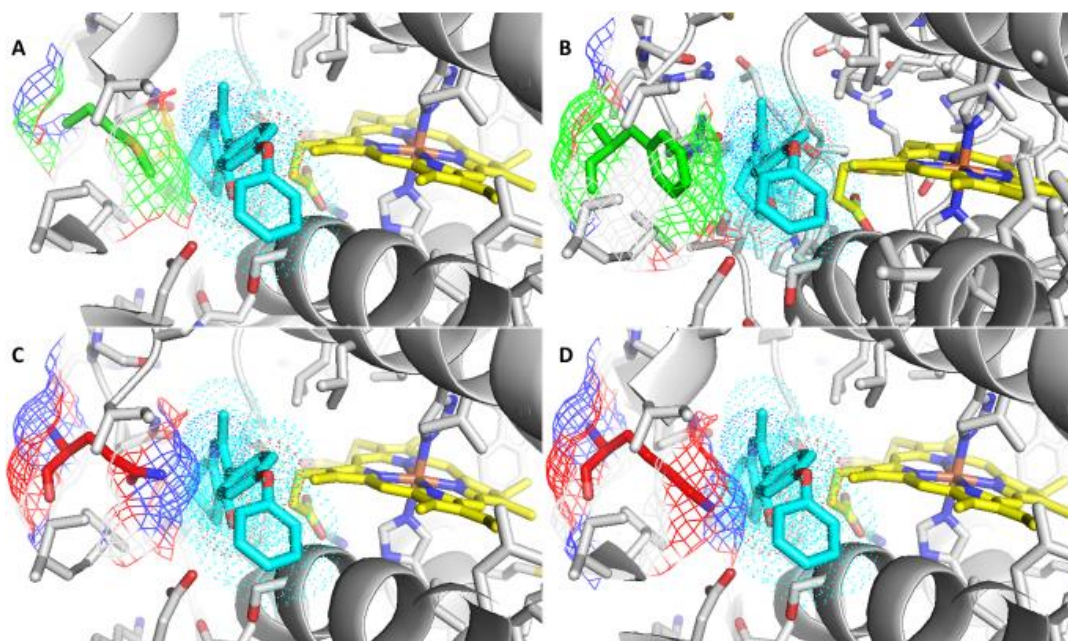


Figure 3.1:

Comparison of yeast mutagens with point of mutation circled in red and expected ligand density shown in teal; A) WT*, B) M221F⁺, C) M221Q⁺, D) M221K⁺. The inhibitory mutants (Red: M221Q/K) can be seen clashing with the expected ligand density of compound **57**. *1KYO, ⁺generated by Pymol from 1KYO.

The results of these assays shown in **Figure 3.2** supported this modelling, showing that both M221K and M221Q were resistant, with regards to the THQ (**57**) and ELQ 271 (**45**). This can be seen in the inhibition circles surrounding the dosage observed in the WT and M221F mutant, while the M221Q mutant is not significantly inhibited even at 1 mM dosage. This supports the conclusion that these compounds act through Q_i site inhibition.

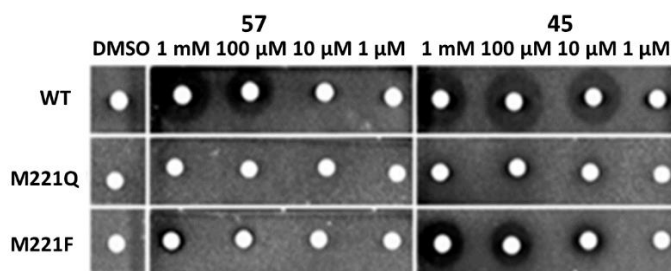


Figure 3.2: Yeast mutagenic studies.⁹⁰

inhibition circles observed surrounding the dosage observed in the WT and M221F mutant, while the M221Q mutant is not significantly inhibited even at 1 mM dosage.

3.1.2 Plasmodium assays

Given the close relationship between plasmodium and toxoplasma species with relation to both their danger as parasitic diseases and homology of their cytochrome b complexes a number of the compounds were tested against strains of the *Plasmodium falciparum* parasite.

Compound **57** was screened against a number of *P.falciparum* cell lines, including known atovaquone resistant strain C2B showing no cross resistance in all cases. In addition compound **57** along with the triazole and pyrazole compounds **72** & **73** were also screened against several common clinically relevant Plasmodial cell lines to further explore their potential as general antiparasitics and provide evidence to support their mechanism of action is not via the Q_o site. Assays carried out by Mark Hickman at the Walter Reed Army Institute of Research (for full assay details see appendix).

Table 3.1: Samples were tested in the Malaria SYBR Green potency assay against 4 different strains of *Plasmodium falciparum*.

Compound	D6 IC ₅₀ (μM)	TM91C235 IC ₅₀ (μM)	W2 IC ₅₀ (μM)	C2B IC ₅₀ (μM)
Chloroquine	0.013	0.18	0.4	0.27
Atovaquone	0.0004	0.001	0.002	6.43
45	0.03	0.07	0.08	0.01
73	0.2	0.58	0.55	0.38
72	0.16	0.57	0.63	0.48
57	0.01	0.03	0.03	0.01

The D6 strain (Sierra Leone) is drug sensitive, the TM91C235 strain (Thailand) is multi-drug resistant, the W2 strain (Thailand) is chloroquine resistant, and the C2B strain is multi-drug resistant with pronounced resistance to atovaquone.

3.1.3 Synergistic studies

Further support for evidence of Q_i site mode of action, was provided during synergistic studies, demonstrating slightly synergistic behaviour with atovaquone a known Q_o site inhibitor, while antagonistic behaviour was observed for the known Q_i inhibitor BRD6323 (**128**).¹²⁹

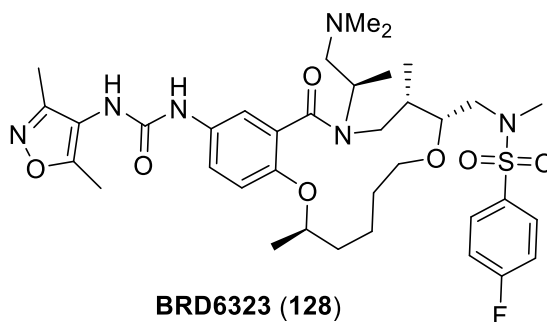


Figure 3.3:
Structure of BRD6323 (**128**), a diversity oriented synthesis generated malarial Q_i site inhibitor.¹²⁹

This is reflected in the Σ FIC values < 1 indicating synergy and >1 indicating antagonism.

Table 3.2: Results of combination dosage experiments, demonstrating THQ (**57**) shows slight synergism with Q₀ inhibitor Atovaquone (**9**) and antagonism and with Q_i inhibitor BRD6323 (**128**).

RATIO	57 & 9			57 & 128		
	FIC (57)	FIC (9)	Σ FIC	FIC (57)	FIC (128)	Σ FIC
8:2	0.47	0.35	0.82	1.60	0.39	2
6:4	0.27	0.52	0.79	0.86	0.55	1.4
4:6	0.16	0.72	0.89	0.60	0.91	1.5
2:8	0.07	0.82	0.89	0.30	1.20	1.5

3.1.4 Co-crystallisation: crystal structure of **57** within bovine Q_i site.

Achieving a cocrystallisation of a compound **57** within the cytochrome *bc*₁ complex of *Toxoplasma gondii*, specifically within its Q_i site, would further support the proposed mode of action. However, crystallisation of parasitic protein has proved challenging due to the difficulty in isolating it in sufficient quantities. As a result studies have been carried out using bovine material, this has been shown to be successful previously, with high resolution crystal structures achieved for a number of GSK compounds including **44**.⁹⁸ To this end the **57** underwent cocrystallisation trials conducted at the University of Liverpool by Michael Capper, Samar Hasnain and Svetlana V. Antonyuk. This resulted in successful cocrystallisation of **57** in the presence of bovine cytochrome *bc*₁. Importantly electron density attributed to the **57** could be clearly identified within the Q_i site of the complex.

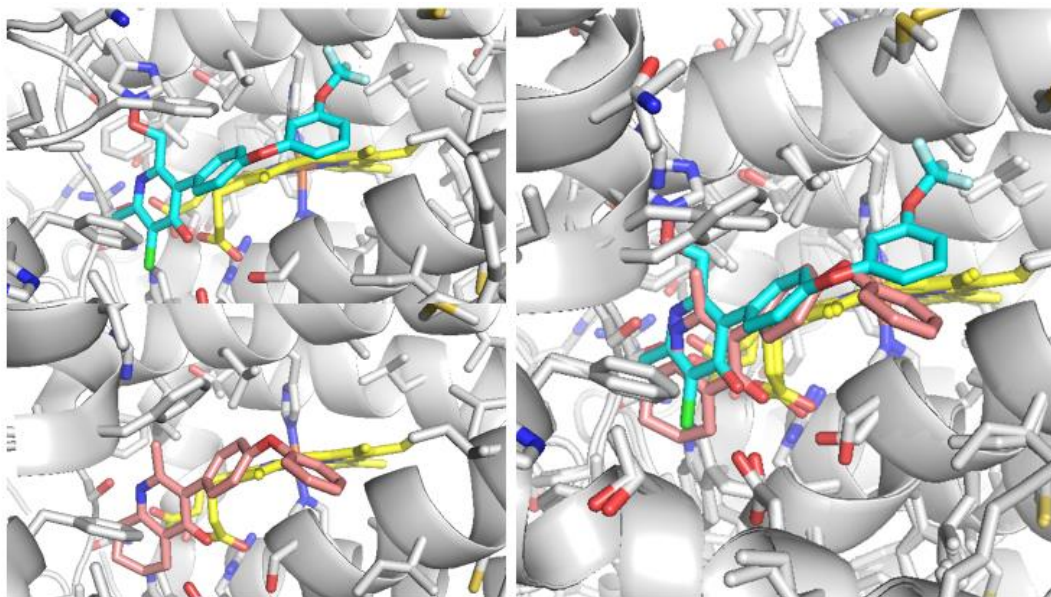


Figure 3.4:
Side by side comparison of inhibitors **44** (top left) and **57** (bottom left) and overlay (right) bound within the Q_i site of bovine cytochrome *bc*₁ complex.

Comparison of the GSK pyridone (**44**) vs tetrahydroquinolone (**57**) (**Figure 3.4**) shows extensive similarities in binding pose between the two ligands, with a slight variation in the diaryl ring positioning, likely a result of the effects of the additional trifluoromethoxy group or possibly an artefact of the flexibility of the ether linker.

3.2 Series development

Having established an initial hit design (**57**), consideration was given to optimisation of this hit to a more lead like candidate. The initial analysis indicated that the most critical deficiency of **57** was its metabolic stability especially in mouse microsomes. As mice were to be the organism of choice for future *in vivo* assessments this was critical to address if the series was to progress further. In addition, a priority would be to continue to improve the limited solubility to reduce potential delivery/administration difficulties. These improvements would need to be achieved without significant loss of potency in the parasitocidal activity demonstrated. A balance of these parameters would be necessary in a candidate compound before progression into *in vivo* testing became viable.

3.2.1 Design of Tetrahydroquinolones Series

A number of key points of diversification were identified from the initial hit (**57**). These positions could be broadly broken down into three main areas; alterations to the 3-position diaryl ether, alterations to the methyl substituent at the two position and finally alterations/decoration of the 'left hand' saturated ring system (highlighted in **Figure 3.5**).

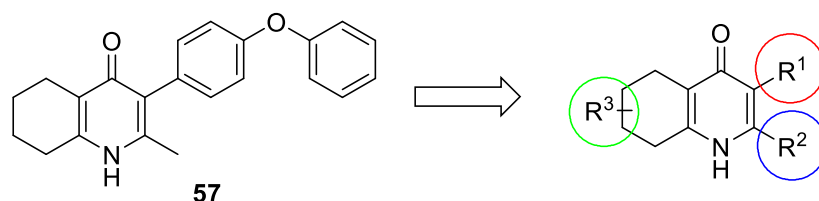


Figure 3.5:
Identification of points of diversification on the tetrahydroquinolone hit.

It was decided that initial efforts should concentrate on variation at the three position (R^1). This had the apparent advantage of being readily amenable to the initial synthetic route, and from preliminary analysis of the binding pocket appeared to be least critical to binding, as it lies in larger more open area of the Q_i site. Given the identified liabilities of the hit compound, the library was designed to concentrate on improving the solubility and metabolic stability. To this end, a library of compounds was designed to investigate the effects of a variety of substituents, with the initial focus on introducing more polar functionality, and identifying and removing sites of metabolic liability. It was thought this could be achieved in a number of ways; by addition of polar moieties such as acid groups onto the terminal ring of the diaryl ether fragment or by introduction of heteroatoms into the fragment at varying positions. In addition a variety of halogen and alkyl-halo groups were also designed to explore steric effects on binding and specifically block likely sites of metabolism.

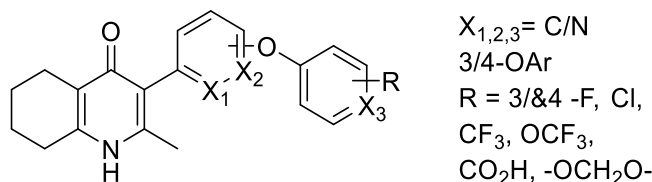


Figure 3.6:
Summary of proposed 3-position variants to be synthesised and evaluated to establish SAR.

3.3 Synthesis of Tetrahydroquinolone series

3.3.1 Retrosynthesis of tetrahydroquinolones

Having established the route to synthesising the hit compound **57** it was felt initially that minimal alteration to the original route would be required. This is illustrated in the simple retrosynthesis shown. It was anticipated that the halo-diaryl ethers could then be attached to the tetrahydroquinolone core via a metal catalysed coupling.

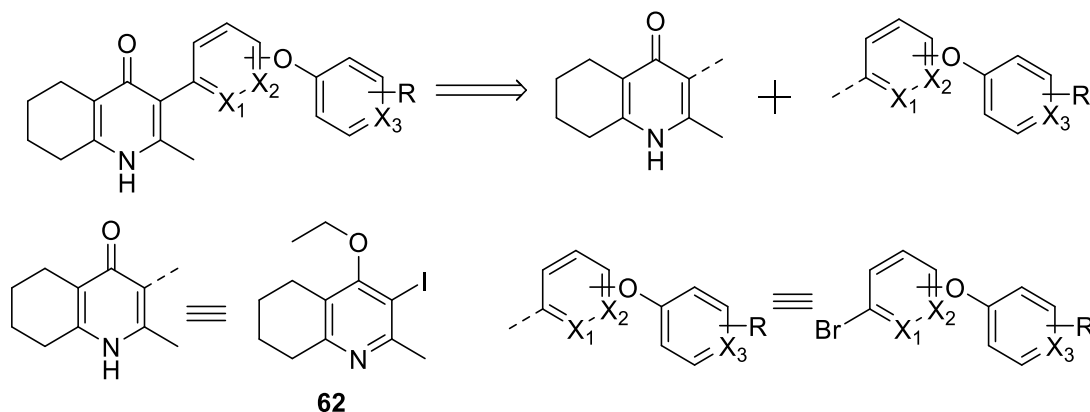
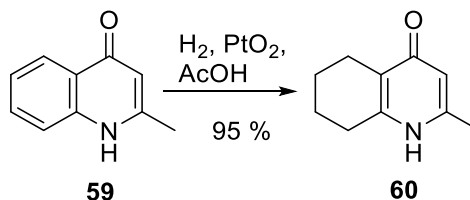


Figure 3.7:
Retrosynthesis of designed tetrahydroquinolone library to identify key intermediates.

It was also considered that by taking this convergent synthetic approach to the synthesis the library, it could then be more easily expanded via a combinatorial coupling of the varied diaryl ethers to a range of modified tetrahydroquinolone cores. This would greatly increase the rate of library synthesis and expand the chemical space explored aiding SAR elucidation. The decision to use the alkylated tetrahydroquinolone core rather than the unprotected quinolone was based upon issues identified in work on the quinolone series, where difficulties were encountered in isolating the product of the Suzuki coupling, due to the highly insoluble nature of the product.¹⁰¹

3.3.2 Synthesis of Tetrahydroquinolone fragment

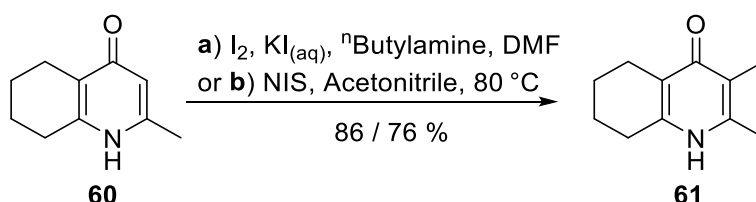
Initially a convergent synthesis was proposed based upon the route used to synthesis the initial hit compound **57**. The synthesis begins with the selective hydrogenation of 2-methylquinolin-4(1H)-one (**59**) using hydrogen atmosphere over Adam's catalyst (PtO_2) in acetic acid.



Scheme 3.1:

Hydrogenation of 4-hydroxy-2-methylquinolone (**59**) using platinum dioxide catalyst and a hydrogen balloon.

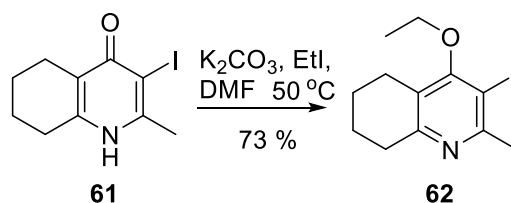
This was found to give the 5,6,7,8 tetrahydroquinolinone product in near quantitative yields, when complete conversion of starting material was achieved. Unfortunately this step was found to be highly sensitive to the batch of catalyst used (commercially supplied), with greatly reduced reaction rates and failure to reach full conversion observed, without any apparent changes in experimental procedure. It proved difficult to identify the precise cause of this variation and this remained a problematic bottle neck for higher throughput.



Scheme 3.2: Iodination of tetrahydroquinolone core **60**.

a) Original method of iodination of tetrahydroquinolone using 10 equivalents of Butylamine and saturated potassium iodide and Iodine. b) alternative method adopted using N-iodosuccinamide in acetonitrile heated to 80°C .

The next step was the iodination at the three position, initially this was conducted with iodine with 10 equivalents of butylamine in DMF, however it was found that the reaction proceeded equally well using NIS in acetonitrile with heating at 80°C . This reaction proceeded in good yield and the product was easily isolated, in both cases, via simple filtration.



Scheme 3.3:

O-Alkylation of tetrahydroquinolone, using iodoethane and potassium carbonate.

The ketone was then protected by alkylation using iodoethane and potassium carbonate, pre-treating the starting material with base and the counter ion of the base, have both been shown to be important in directing the site of alkylation (*N*- vs *O*-). This formed the *O*-substituted tetrahydroquinolinone core, which would then be coupled to the diaryl variants.

3.3.3 Diaryl ether synthesis

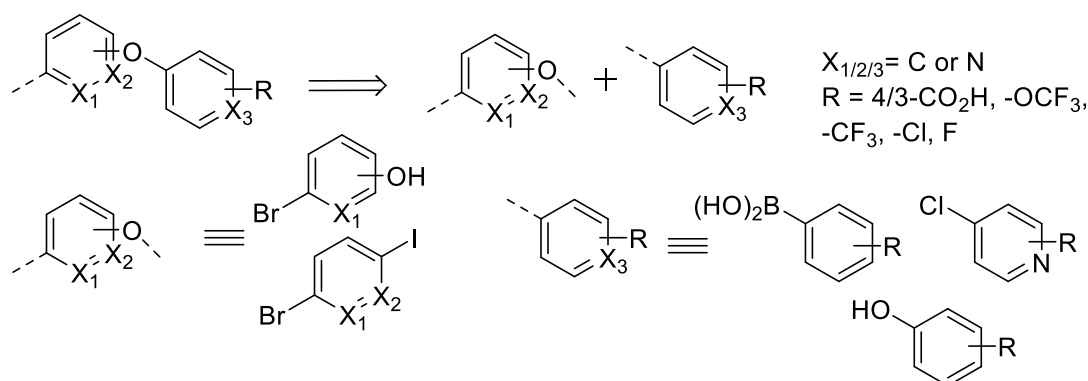


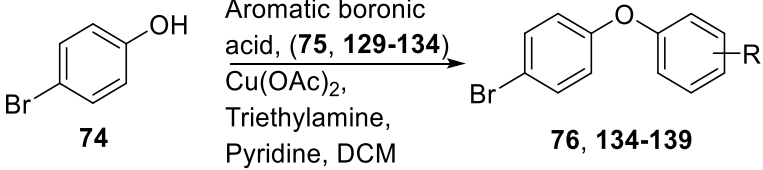
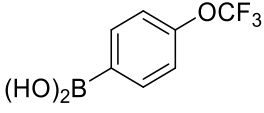
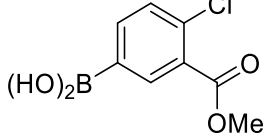
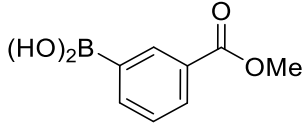
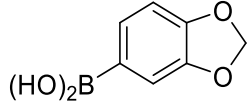
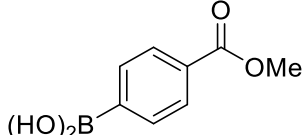
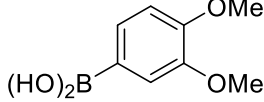
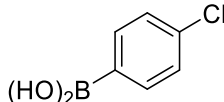
Figure 3.8

Retrosynthesis of diaryl ether side chain, to identify starting reagents and maximise variation for minimal synthetic effort.

Several approaches were taken in synthesising these fragments, largely dependent on availability of starting materials and amenability of chemistry. The systems without heteroaromatic rings were synthesised using bromophenol and the corresponding boronic acid using a Chan lam reaction. This was found to proceed in reasonable yields, however it was observed that there was a high sensitivity to water, with yields severely diminished with some evidence suggesting dependence on the quality/ degree of activation of the molecular sieves used.

Table 3.3:

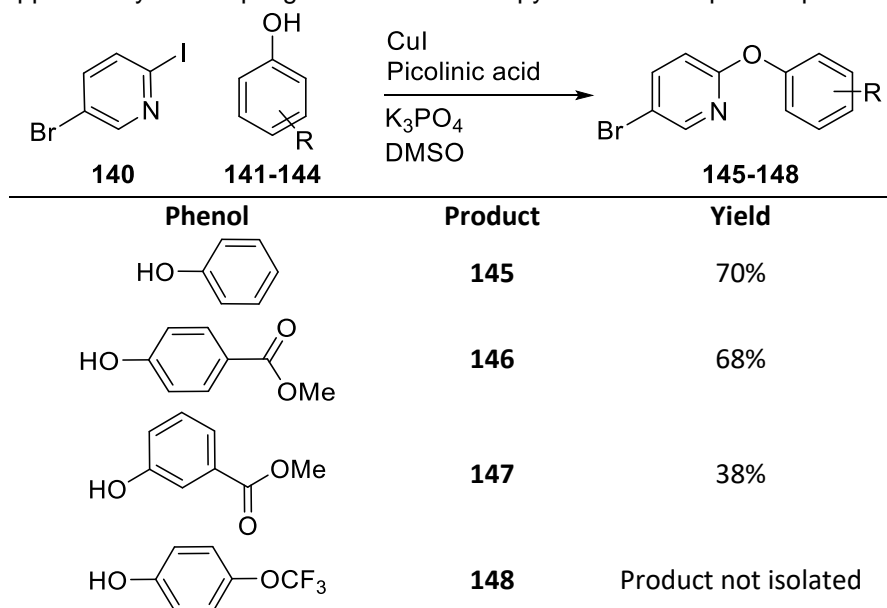
Chan Lam coupling of bromophenol (**74**) to a number of phenylboronic acids (**74**, **129-134**).

			
Boronic Acid	Yield (product)	Boronic Acid	Yield (product)
	70% (76)		19% (137)
	28% (134)		12% (138)⁺
	33% (135)		13% (139)
	20% (136)	-	-

To synthesise the heterocyclic containing compounds a copper iodide catalysed coupling was used taking the 2-iodo-5-bromopyridine and the respective phenol, with addition of picolinic acid and potassium phosphate as base.

Table 3.4:

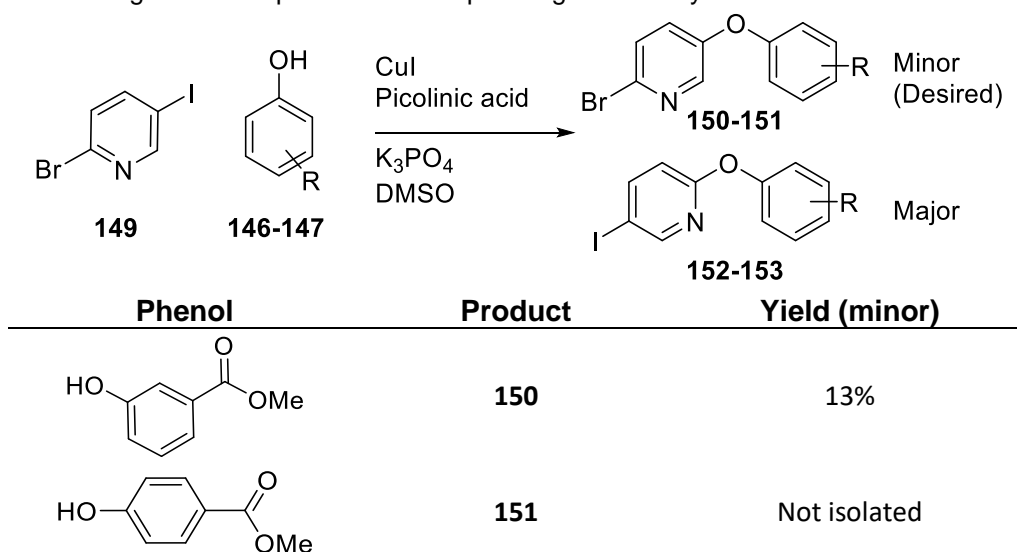
Copper catalysed coupling of 5-bromo-2-iodopyridine with respective phenols.



This reaction proceeded with moderate yields (**Table 3.4**), however in the case of the trifluoromethoxy phenol the product **148** could not be isolated cleanly. In addition it was found that in cases of the 3-iodopyridinyl couplings (**Table 3.5**) the desired regio-selectivity was reversed, with the directing effect of the nitrogen overriding the difference in reactivity of the iodo vs bromo substituents.

Table 3.5:

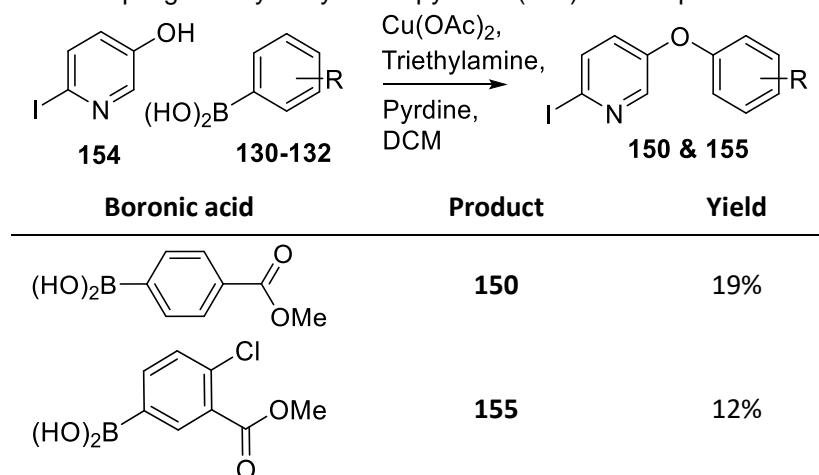
Attempted copper catalysed coupling of 6-bromo-3-iodopyridine with respective phenols showing mixture of products due to poor regioselectivity of reaction.



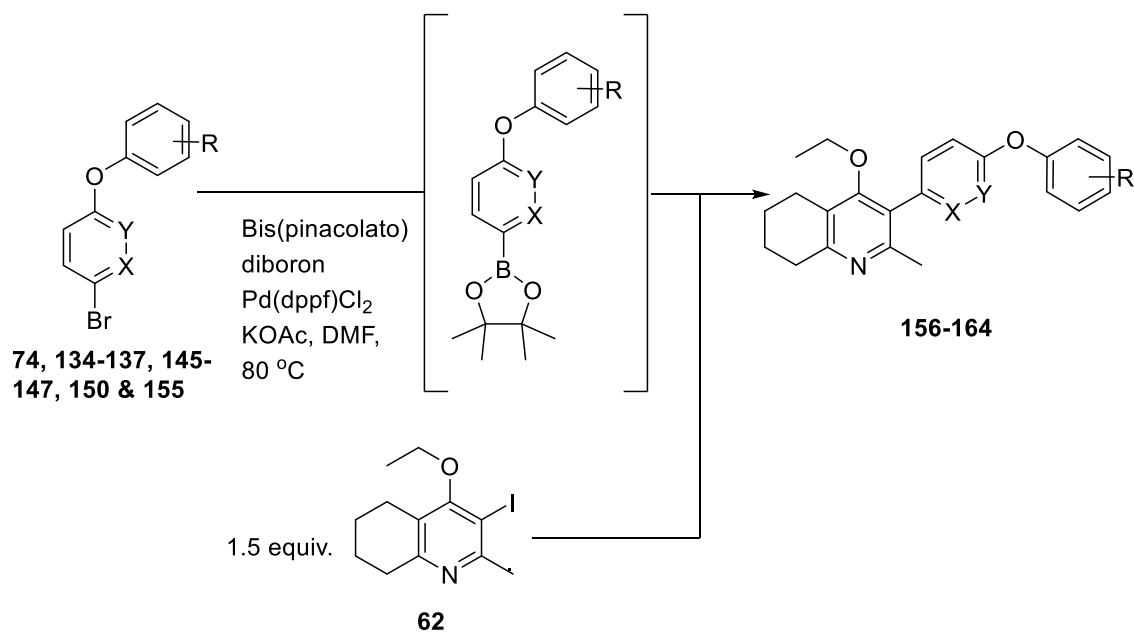
This led to greatly reduced yields of the desired compound in these cases, compounded by the similar retention times during purification. To address this the route for these compounds was revisited, reverting to the Chan-Lam reaction.¹³⁰ This delivered the desired compounds in relatively poor yields, however the lack of regioselectivity problems simplified purification and provide enough material to be carried forward.

Table 3.6:

Chan-Lam coupling of 5-iodo-2-hydroxypyridine (**154**) with respective boronic acids.



Having obtained the diaryl systems the penultimate step in this route was to couple these with the tetrahydroquinolone fragment **62**. This was done using a one-pot Suzuki method, wherein the boronic acid of the aryl ether is formed in situ before addition of the iodotetrahydroquinolone reagent **62**.¹²²

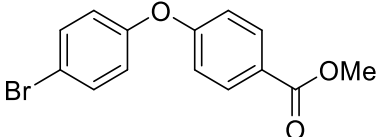
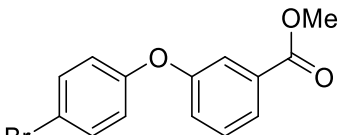
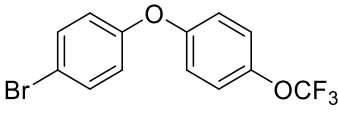
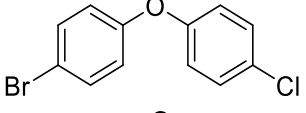
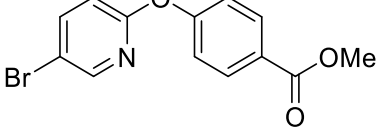
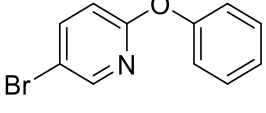
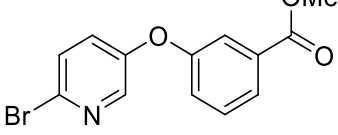
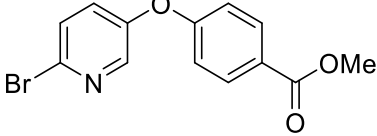
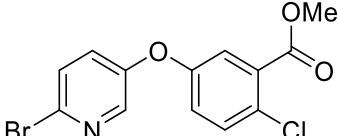


Scheme 3.4:

One-pot Suzuki procedure, with formation of the boronic acid in-situ followed by addition of the tetrahydroquinolone coupling partner.

This procedure was identified as preferable to the stepwise generation and isolation of the boronic acid, as previous work within the group had found difficulty with isolating similar boronic acids in good yield. Of note is the need to use the iodotetrahydroquinolone (**62**) in excess (1.50 equivalents), with respect to the diaryl species, reducing effective yield with a view to library synthesis.

Table 3.7:
Results of one-pot Suzuki couplings with varied diaryl ethers.

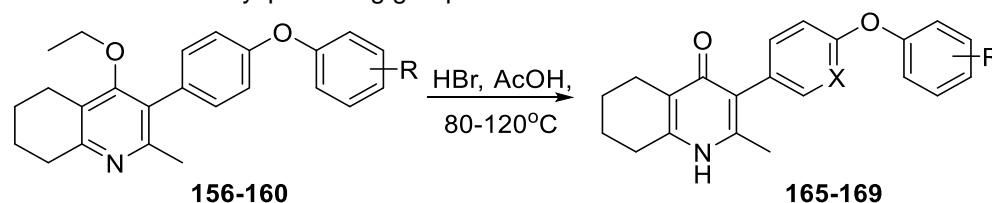
Diaryl ether	Product	Yield
	156	27%
	157	25%
	158	23%
	159	27%
	160	21%
	161	Product not isolated
	162	Product not isolated
	163	Product not isolated
	164	Product not isolated

As can be seen this reaction proceeded, at best, with relatively poor yield (21-27%), especially in respect to the tetrahydroquinolone reagent (**62**), which was required in excess (1.5 equiv.) and not recovered. In the case of the 2-bromopyridine compounds (**162-164**), no product was isolated, it is suspected that this due to the boronic esters propensity to undergo rapid protodeboronation before transmetalation can take place.

The final step in the synthesis was removal of the ethyl group, using hydrobromic acid in acetic acid. Initial attempts were carried out at 80 °C,

however long reaction times, of around 72 hours, were disruptive to rapid library synthesis. Fortunately it was found that simply raising the temperature to 120 °C reduced reaction times to 16 hours, with no noticeable effects on yield. This route delivered a total of five compounds (**Table 3.8**).

Table 3.8:
Removal of O-alkyl protecting group.



Compound no.	Product	Yield
165		45%
166		72%
167		12%
168		95%
169		86%

Overall the route was of limited efficiency, with overall yields less than 10% with respect to the methylquinolone starting material prior to deprotection. The low yields of the one-pot Suzuki coupling would necessitate far larger quantities of both tetrahydroquinolone and diaryl ether than would be feasible

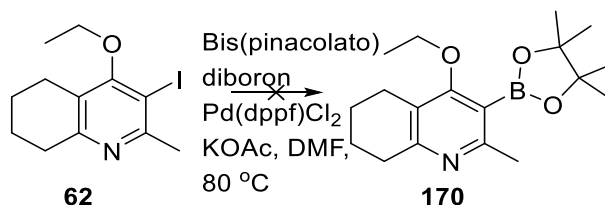
for a combinatorial approach to library diversification. This diminished the advantage of a convergent synthesis to rapid synthesis of compounds.

3.4 Route development/optimisation

As a result of the relatively poor yields observed, it was felt that efforts should be made towards optimisation of the synthesis.

3.4.1 Forming the tetrahydroquinolone boronic ester.

Suspecting protodeboronation of the boronic ester as a possible cause of failure of the pyridine-based couplings, it was decided to explore the possibility of reversing the coupling partners. This would involve forming the boronic ester from the tetrahydroquinolone.



Scheme 3.5:

Unsuccessful attempt at formation of 3-boronate ester from 4-ethoxy-3-iodo-2-methylquinolone.

However unfortunately this appeared to suffer from a similar problem, and the desired product, **170**, was not detected during monitoring of the reaction, with only the conversion of **62** into the dehalogenated material **61** observed.

3.4.2 Stepwise synthesis

Another option explored was to move towards a more linear synthesis introducing diversity in the penultimate step. This may avoid the inefficient one-pot Suzuki coupling, and potentially allow for a simpler method of diversification.

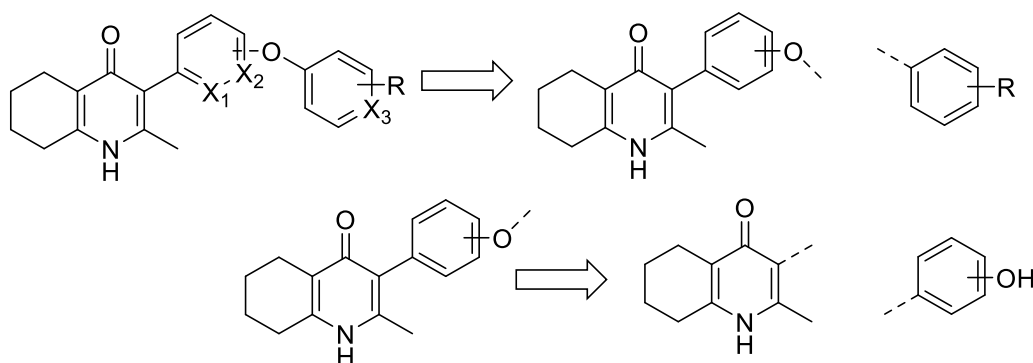
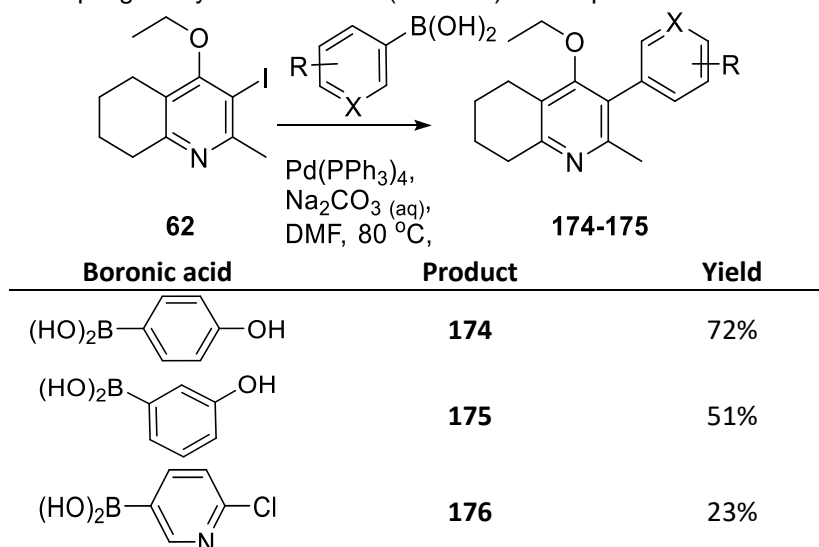


Figure 3.9: Stepwise retrosynthesis of tetrahydroquinolone series.

The route was kept the same, notably including the alkylation step, as this would be required to prevent selectivity issues during the Chan Lam coupling. At this point either the 3 or 4 phenoxy boronic acid could be coupled to the O-alkylated tetrahydroquinolone, **62**, via the Suzuki coupling. In addition, the reaction was also performed with the 2-chloro-pyridine-5-boronic acid as an alternative route to reach pyridine containing products. The isolate yield of the pyridyl coupling product was considerably poorer, than the phenol equivalent. A contributing factor to this may have been the difficulty in isolating the product cleanly through column chromatography due to similar retention times of product and starting material.

Table 3.9:

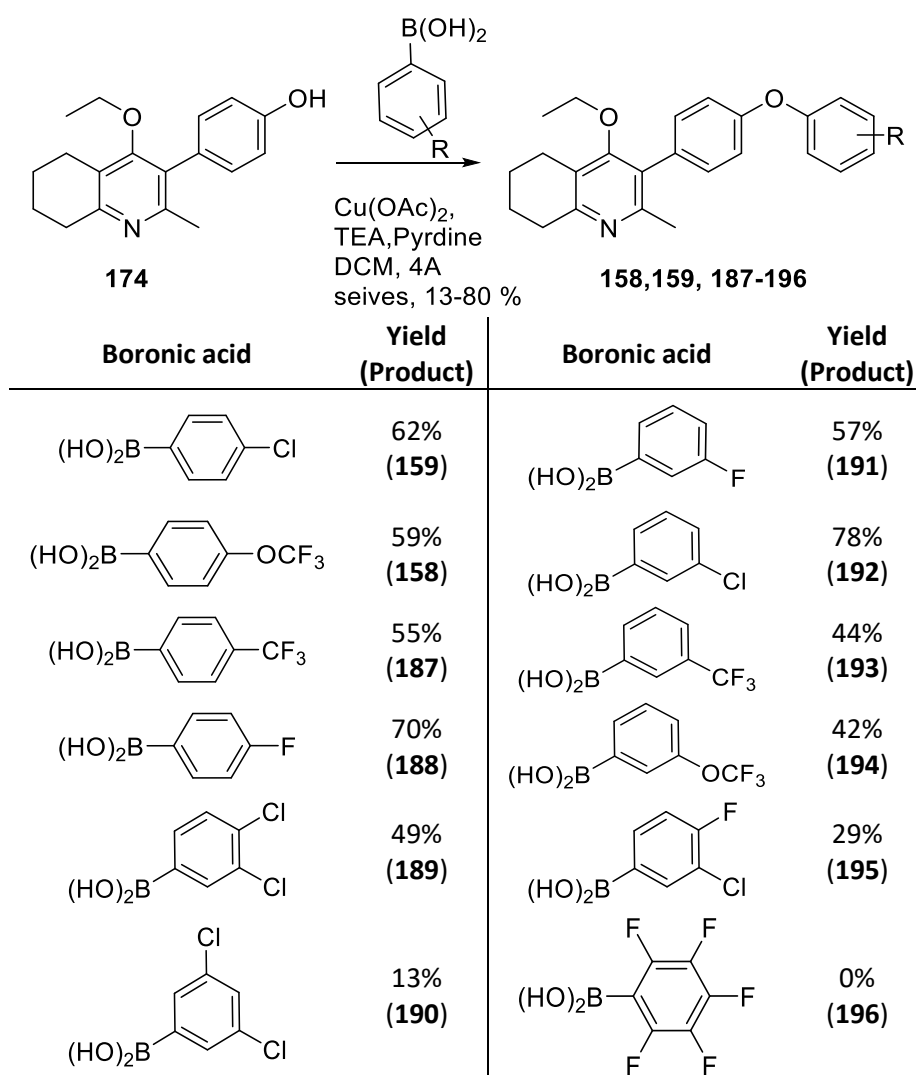
Suzuki coupling of aryl-boronic acids (**171-173**) to compound **62**.



Both the meta and para phenol derivatives could then be coupled with a wide range of boronic acids again using the Chan-Lam reaction. This proceeded in generally acceptable yields in the case of the para phenol couplings, with yields generally lower for the disubstituted boronic acids. The exception being the pentafluoro boronic acid which did not appear to react, this may have been due to poor solubility of the boronic acid or a result of the extensive degree of substitution both sterically and with regards to electron withdrawing effects.

Table 3.10:

Chan Lam coupling of a variety of boronic acids (**75**, **131**, **177-186**) to 4-phenol tetrahydroquinolone **174**.

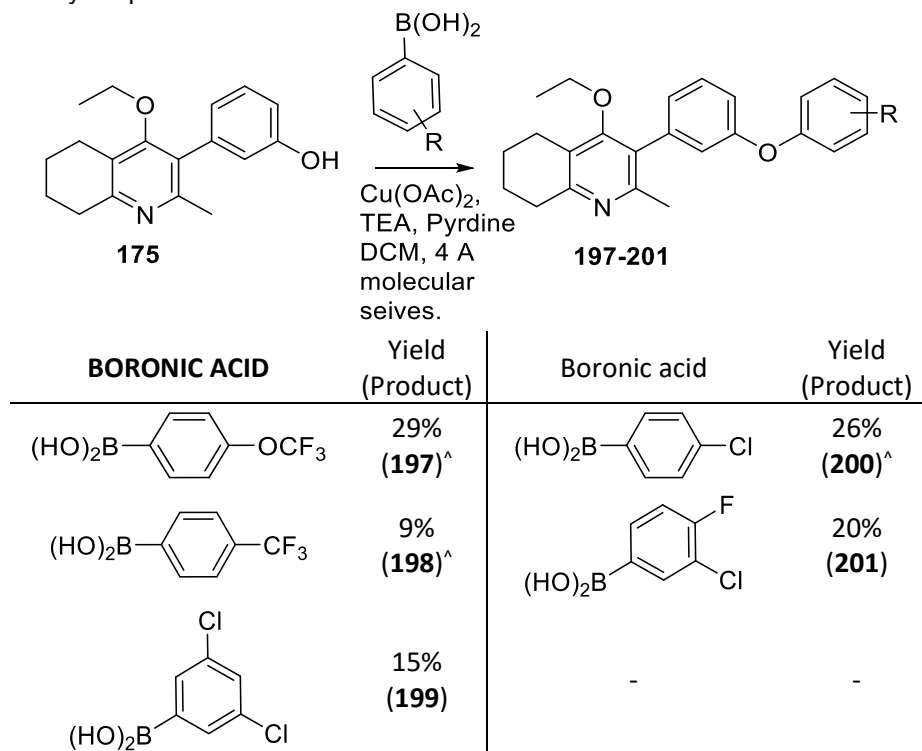


The meta phenol coupling was carried out in the same conditions. This provided sufficient material to access the desired final compounds. But it

was generally notably lower yielding than couplings to the para-phenol analogues, possibly a result of being less sterically favourable.

Table 3.11:

Chan Lam coupling of a variety of boronic acids (**75**, **131**, **177**, **179** & **185**) to 3-phenol tetrahydroquinolone **175**.



This was then followed by the deprotection step as before, yields in this step were highly variable likely a result of isolating the product rather than conversion which appeared to go to completion in all cases.

Table 3.12:

Deprotection of O-alkylated tetrahydroquinolones.

$\text{Starting material (158, 159, 187-201)} \xrightarrow[120\text{ }^\circ\text{C}]{\text{HBr, AcOH}} \text{Product (168, 169, 202-215)}$

Side chain	Yield (Product)	Side chain	Yield (Product)
	86% (169)		66% (208)
	60% (202)		96% (209)
	95% (168)		76% (210)
	58% (203)		13% (211) [^]
	59% (204)		Not isolated (212) [^]
	83% (205)		36% (213)
	66% (206)		96% (214)
	70% (207)		45% (215) [^]

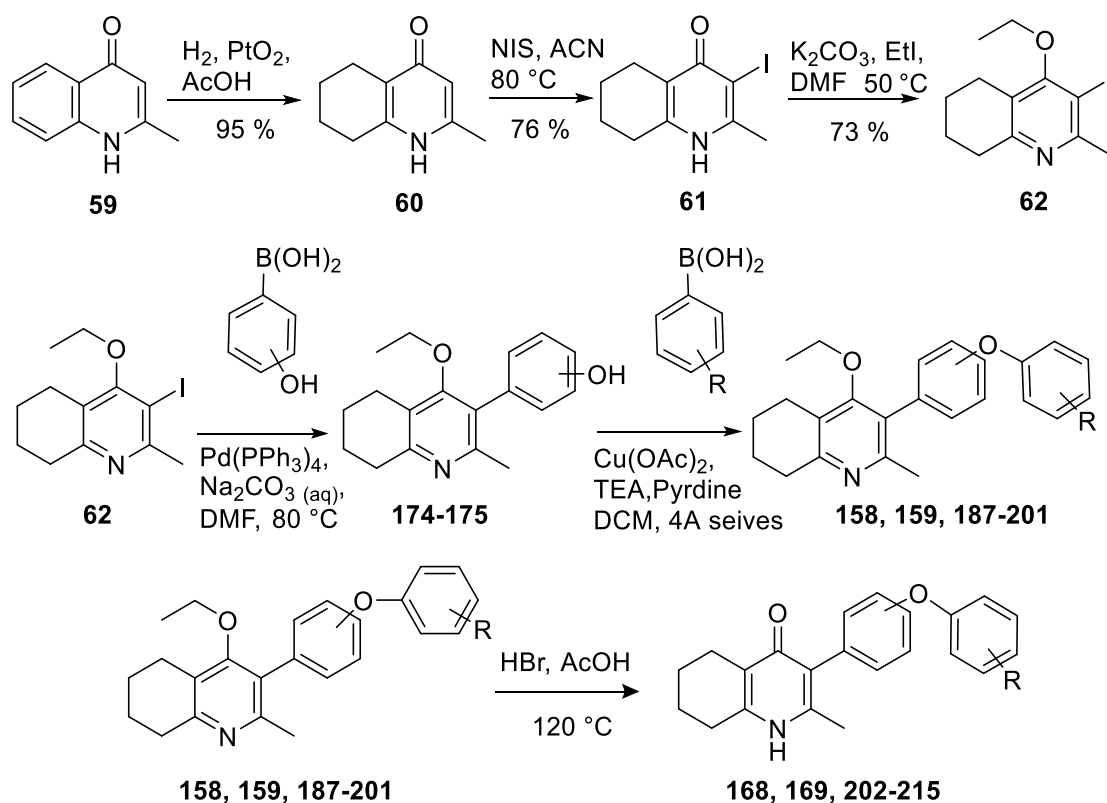
An important observation was made when comparing the O-alkylated intermediates with their final deprotected analogues, namely a marked difference in their melting points. While some difference might be expected from relative Log P it, this highlights the contribution to lattice energy made by the pyridone moiety.

Table 3.13:

Melting point values of THQ's vs their O-alkylated precursors.

Compound	Melting point	O-Alkylated analogue	Melting point
169	>250 °C	158	69.2 - 71.4 °C
203	>250 °C	188	102 - 103 °C
205	>250 °C	190	86.4 - 86.8 °C

Overall this route provided access to fifteen compounds which were then then deprotected as before, using HBr and acetic acid to reach the desired final products.



Scheme 3.6: Final divergent synthetic route.

Six step synthesis from commercial compound **59** to provide compounds **168, 169, 202-215**.

This process was far more efficient with respect to the tetrahydroquinolone core and allowed for simple diversification through addition of a variety of

readily available boronic acids primarily in coupling during the Chan Lam reaction, but also during the Suzuki coupling.

3.4.3 Eliminating the alkylation/dealkylation steps

The next point of optimisation concerned investigating if the isolating difficulties reported in direct Suzuki coupling in formation of the ELQs could be overcome within the THQ series. If so the alkylation of the 4-hydroxyquinolone could be avoided. This would be beneficial as it eliminates two steps; the addition and the removal of the ethyl group, importantly eliminating the harsh conditions used in the de-alkylation step, and potentially improving overall yields and speed of synthesis. This would allow access to a number of diaryl systems (**138**, **139** & **216**) that were expected to be sensitive to the dealkylation conditions.

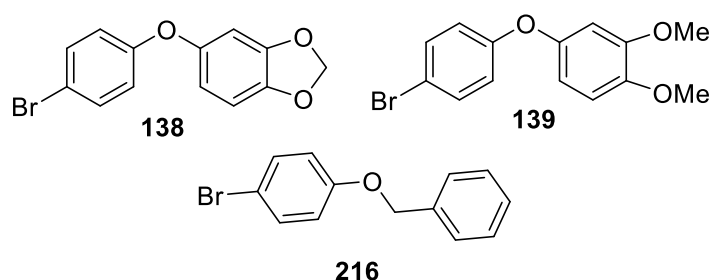
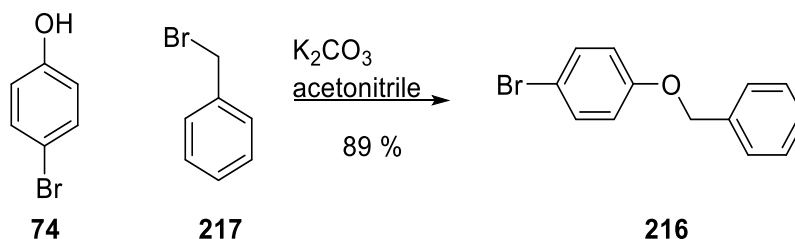


Figure 3.10:

Further diaryl ether systems incompatible with acid deprotection requiring alternative routes.

The diaryl ethers **138** and **139** were synthesised from bromophenol and the appropriate boronic acid as described previously (**Table 3.3**). Compound **216** was synthesised via benzylation of 4-bromophenol.

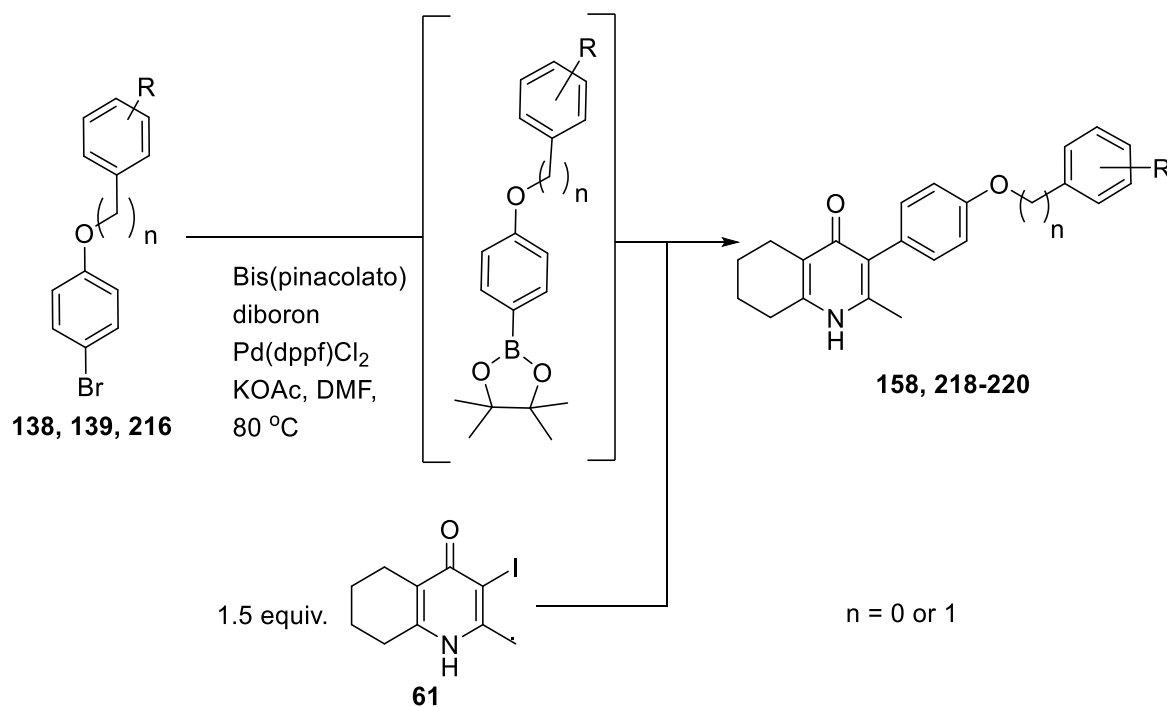


Scheme 3.7:

Formation of **216** via benzylation of 4-bromophenol (**74**) using benzyl bromide (**217**).

The one-pot Suzuki was carried out under the same conditions as previously described with consumption of the diaryl species monitored by TLC before addition of the iodotetrahydroquinolone (**61**). In addition to the three diaryl

ether systems described (**138**, **139** and **216**) the trifluoromethyl derivative **76** was also trialed for comparison.



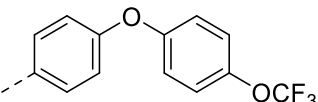
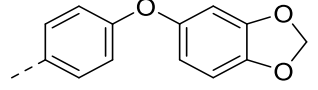
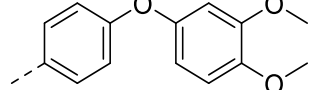
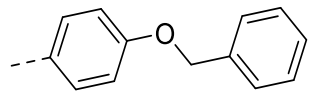
Scheme 3.8:

Direct one-pot Suzuki coupling of the 4-hydroxy-3-iodo-2-methylquinolone.

This route proved successful, allowing access to the compounds below and in a more step efficient manner, without reduction of yield in the coupling. Most importantly it provided access to compounds that would not have survived the conditions used to achieve dealkylation.

Table 3.14:

Products of the one-pot Suzuki reaction shown in **Scheme 3.8**

Product	R	Yield
169		28%
218 ⁺		16%
219		Not isolated
220		5 %

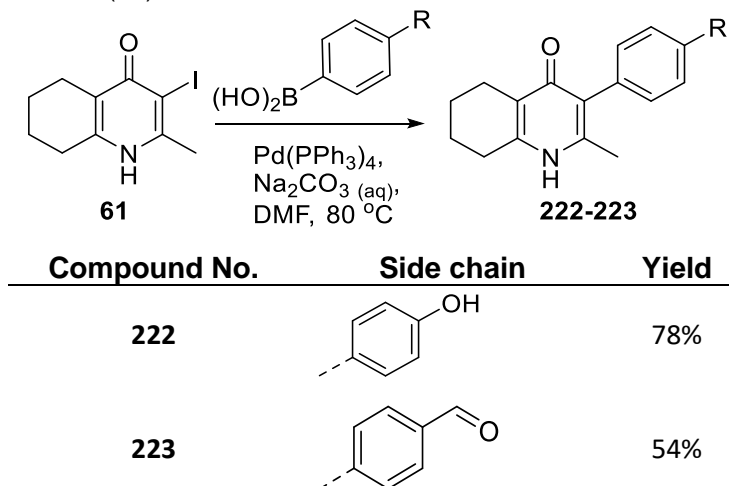
However, as can be seen in **Table 3.14** the reaction was still relatively poor yielding, especially when and the more linear synthesis with late stage diversification was considered more desirable for those ethers that could tolerate the acidic dealkylation conditions.

3.4.4 Other synthesis

A small number of compounds within the series required slight variations to the synthetic routes.

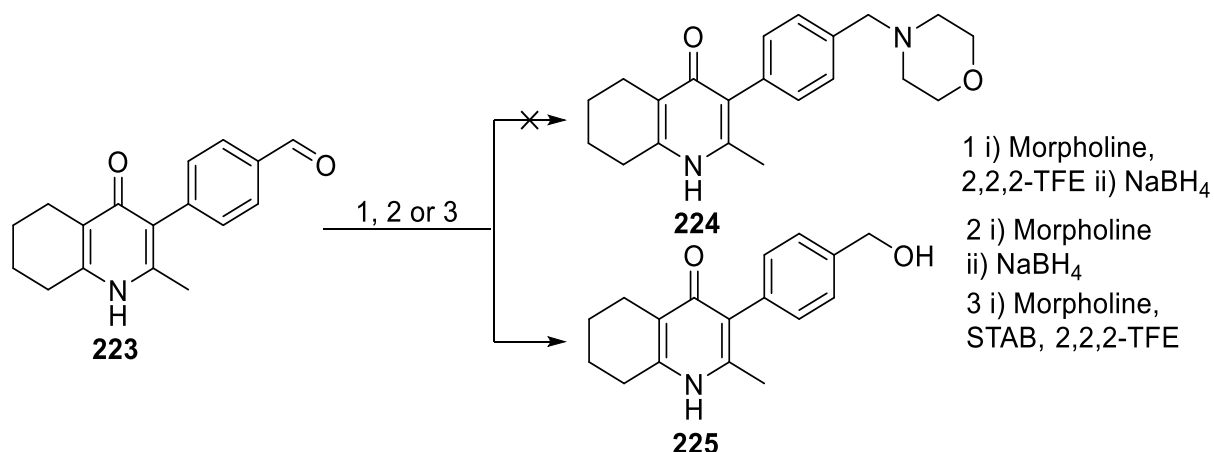
Table 3.15:

Suzuki coupling of phenol and benzaldehyde boronic acids (**171** & **221**) with 3-iodo-2-methylquinolone (**61**).



The aldehyde was carried forward to undergo reductive amination to form the morpholine derivative (**224**). Several conditions/methodologies were trialed without success (Scheme 3.9). Initially the aldehyde and morpholine were combined followed by sodium borohydride, after a delay to allow imine formation, however only the mass of the reduced alcohol was observed (**225**) in under these conditions, suggesting the initial imine formation was not occurring, this was conducted both in solution (2,2,2-TFE) and neat morpholine with the same result. Conducting the reaction in the presence of

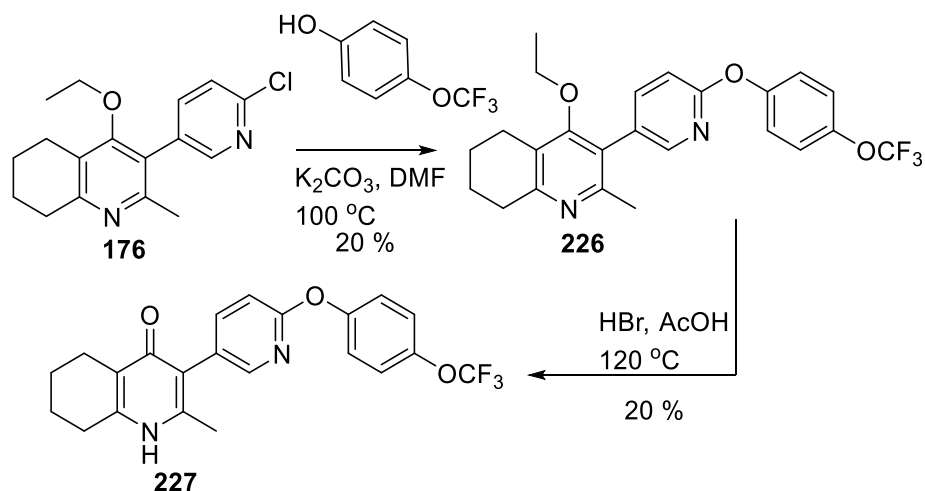
sodium triacetoxyborohydride was also trialled, unfortunately in this case no reaction was observed.



Scheme 3.9:
Unsuccessful reductive amination conditions.

In addition a small number of pyridine-containing compounds were synthesised by slight variations to the route above relying on a S_NAr reaction to couple the two aryl rings.

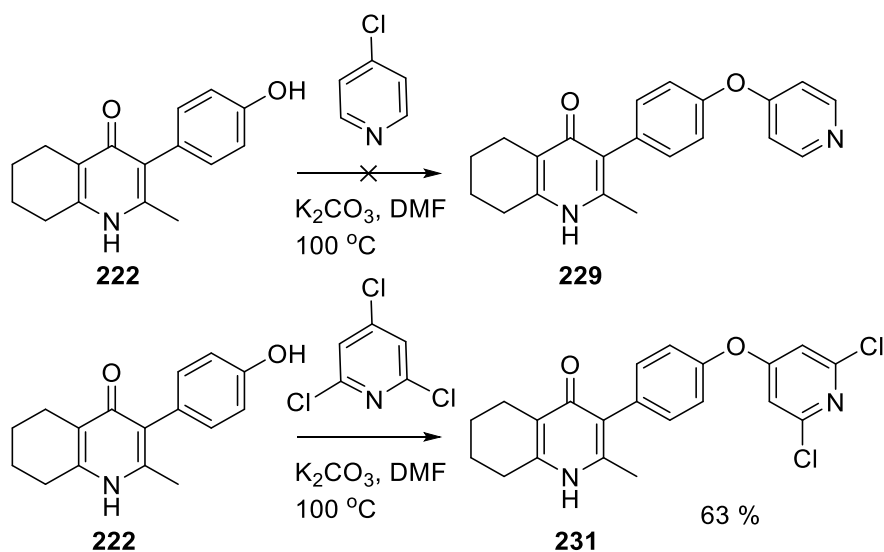
Compound **176** formed via Suzuki reaction discussed earlier (Table 3.9:) provided **226** which, while in poor yield, was then progressed to **227** via acidic deprotection.



Scheme 3.10:
S_NAr reaction conditions used to form compound **226** followed by standard deprotection conditions to reach compound **227**.

Reversing the components and coupling the phenol **222** to of the 4-chloro pyridine **228** was not successful, but did succeed using 2,4,6-trichloropyridine (**230**) as the electrophile to produce a pyridine analogue (**231**) of the 3,5-

dichloro compound **205** with a nitrogen in the 4-position of the terminal ring, shown in **Scheme 3.11**.



Scheme 3.11:

S_NAr conditions used to form 4-pyridyl derivatives.

Happily, the coupling occurred without selectivity issues, exclusively at the *para*-position of the trichloro pyridine, removing concerns over a potentially difficult separation and purification of a mixture of regioisomers.

3.5 Summary of synthesis

A library of twenty-three compounds was synthesised based upon the tetrahydroquinolinone scaffold. The synthetic route was modified a number of times to circumvent unsuccessful reactions, optimise yield and ease of diversification.

Disappointingly the combinatorial approach to synthesising a library of THQ compounds was not found to be practical, without extensive synthesis optimisation.

Further development and optimisation would be required to efficiently broaden the scope of the library, particularly with regard to inclusion of more heterocyclic containing systems. In these systems in particular the metal catalysed couplings, both forming the ether systems and coupling to the THQ core, could benefit from reaction condition optimisation. However the limited examples synthesised did not appear sufficiently promising to warrant extended route optimisation. Synthesis of the tetrahydroquinolone scaffold

remained largely unchanged, although the unreliability of the initial hydrogenation step provided challenges to consistent synthesis.

There remains a wide area of unexplored chemical space around the diaryl ether system, and further synthetic efforts could be directed in increasing the diversity to include *N*- or *S*-linked systems, in addition to longer chain linkages.

3.6 Biological, ADMET and physicochemical evaluation.

3.6.1 Cellular assay results

As before, after synthesis each compound was evaluated for tachyzoite activity as described in **Chapter 2**. An example of data from the cellular assay for a several of these compounds is shown below (Figure 3.11).

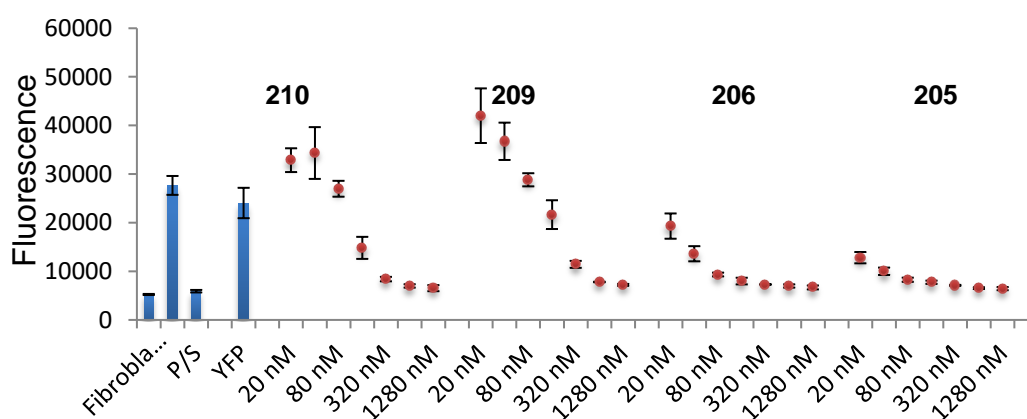
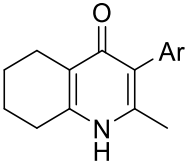
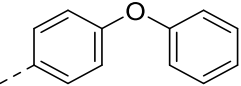
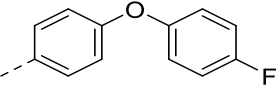
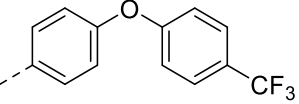
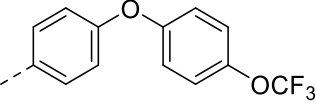
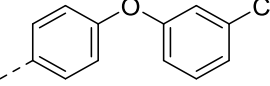
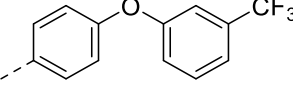
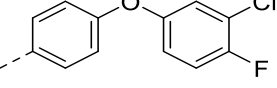
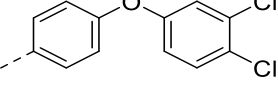
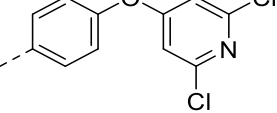
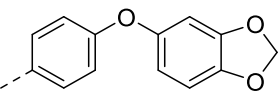
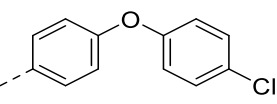
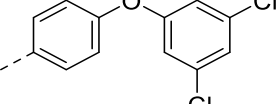
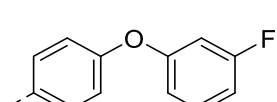
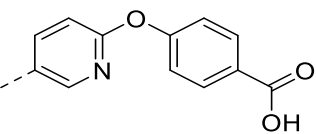
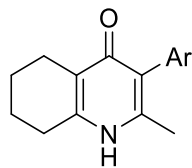


Figure 3.11: Example of data from cellular tachyzoite assay: control bars shown in blue (left to right); untreated fibroblasts, DMSO & pyrimethamine/sulfadoxine. Compound dosage curves are shown in red (left to right); 205, 206, 209 & 210.

The results are summarised for all compounds in Table 3.16.

Table 3.16: *In vitro* tachyzoite inhibition activity

					
No.	Compound	Tachyzoite IC ₅₀	No.	Compound	Tachyzoite IC ₅₀
57		30 nM	203		40 nM
202		195 nM	169		90 nM
208		16 nM	209		260 nM
206		65 nM	204		50 nM
231		275 nM	218		200 nM
168		55 nM	205		30 nM
207		20 nM	165		7.6 μM



No.	Compound	Tachyzoite IC ₅₀	No.	Compound	Tachyzoite IC ₅₀
210		60 nM	166		>10 μM
167		>10 μM	213		200 nM
211		80 nM	215		200 nM
214		60 nM	220		16 nM
227		1.0 μM	-	-	-

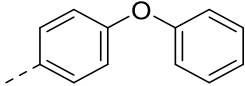
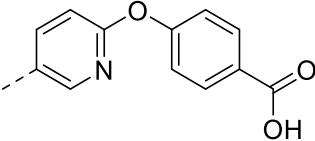
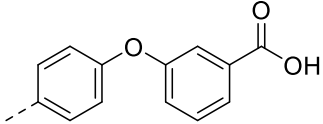
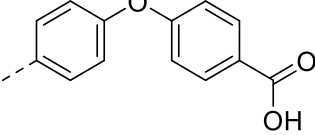
3.6.2 Structure Activity Relationships

There are a number of trends in activity that can be identified from these biological results.

3.6.2.1 Acid moieties

The first noticeable trend is the apparent complete lack of tolerability for any charged or highly polar moieties, this can be seen with the greatly reduced activity of the acid derivatives (compounds **165-167**) in comparison with the hit compound **57**. The limitations of a cellular assay are the inability to distinguish if this loss of activity is a result of detrimental effects on compound enzyme binding or a factor such as membrane penetration, which may be contributing in this case.

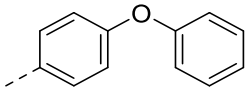
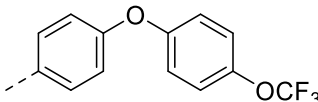
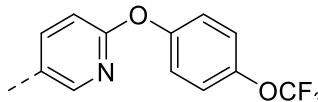
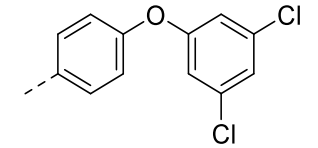
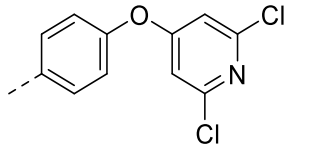
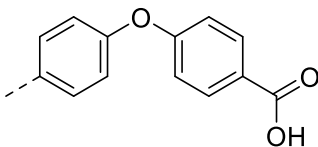
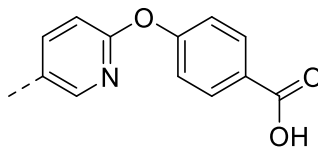
Table 3.17:
Efficacy of 'acidic' diaryl ether.

Side chain	Tachyzoite IC ₅₀	Side chain	Tachyzoite IC ₅₀
	0.030 μM		7.60 μM
	>10.00 μM		>10.00 μM

3.6.2.2 Heterocycles

The addition of heterocyclic ring systems also appears to result in diminished efficacy. These results while disappointing resulted in the move towards less hydrophilic functionalities to explore if potency could be improved sufficiently to tolerate instillation of a solubilising functionality in alternative positions.

Table 3.18:
Efficacy of pyridyl vs benzyl systems

Side chain	Tachyzoite IC ₅₀	Side chain	Tachyzoite IC ₅₀
	0.030 μM	-	-
	0.090 μM		1.00 μM
	0.030 μM		0.275 μM
	>10.00 μM		7.60 μM

3.6.2.3 Terminal ring substitution pattern

With respect to substitution on the 4-position it appears that smaller substituents such as; fluoro & chloro, lead to slightly better activity in comparison to larger groups such as trifluoromethyl or trifluoromethoxy. The smaller 3-position substituents appear to be the most beneficial to binding, with the chloro and fluoro-derivatives exhibiting improved activity relative to any other compounds.

3.6.2.4 *m*- vs *p*- vs extended diaryl linkage

The meta-linked diaryl systems (compounds **211-215**) showed similar activity to the para-linked analogues suggesting that the flexibility of this linkage allows for similar conformations to be adopted, without significant penalisation to binding. The extended system demonstrated improved potency

3.6.3 Mitochondrial assay

The difficulty of interpreting the output from a cellular based assay, is deconvoluting the effects of binding from other factors, such as localisation of the compound, on the observed activity. Conversely there is some advantage to eliminating compounds with strong enzyme inhibition behaviour, but that are ultimately ineffective in an *in vivo* or even cell-based setting.

Towards the end of the project access to a mitochondrial assay was gained, provided by Sylvia Moreno and Zhu-Hong at the University of Georgia. While not an enzymatic assay, this supported the expected mechanism of action in addition to deconvoluting cell penetration issues.

The assay uses a fluorescence readout resulting using safranin O as a readout of membrane potential. (Full assay details are found within the appendix).

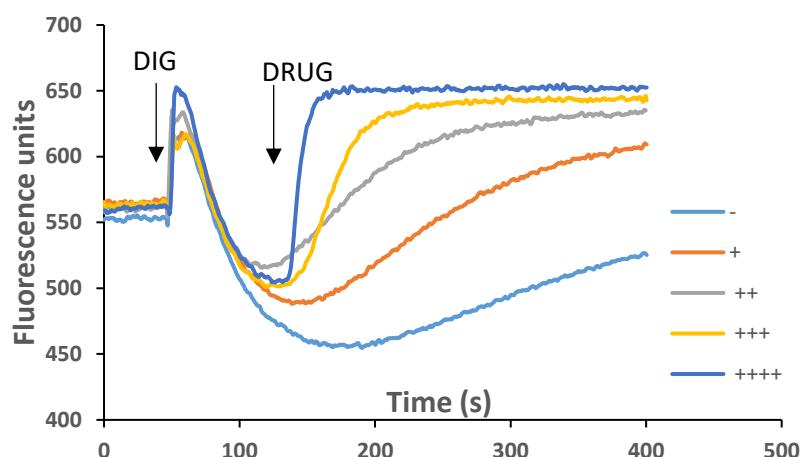


Figure 3.12: Example read outs from mitochondrial assay. DIG indicates administration of digitonin, while drug indicates administration of the inhibitor.

The compounds were screened against both mammalian and parasite-based assays. The assays were performed at a single dose to characterise relative degrees of inhibition between inhibitors.

Table 3.19: Results from mitochondrial assay.

Compound	Mammalian mitochondria activity	<i>T.gondii</i> mitochondria activity	Compound	Mammalian mitochondria activity	<i>T.gondii</i> mitochondria activity
211	++++	++++	213	+++	++++
218	-	++++	227	+++	++++
231	-	-	165	+	-
209	-	++++	166	-	-
215	++++	++++	203	+++	-
206	++++	++++	208	++++	++++
205	++++	++	202	++++	++++
210	++	++++	169	++++	++++
214	++++	++++	168	+++	++++
220	-	+	204	++++	++++
-	-	-	Atovaquone	++++	++++

This identified a number of compounds which appeared to exhibit pronounced selectivity for the *T.gondii* over mammalian mitochondria, specifically compounds **209**, **210** and **218**.

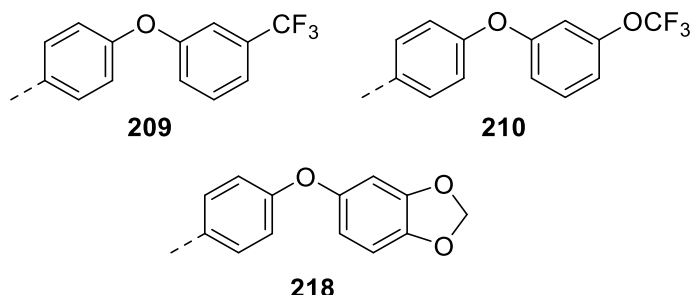


Figure 3.13:
Compounds showing greatest *T.gondii* selectivity in mitochondrial assay.

Interestingly it appears that the greatest selectivity is achieved with large substituents, larger than chloro, at the 3-position for the para linked ethers, but in the 4-position of the meta-linked variants. It can be seen how these 3,4 or 4,3 linkages would position the substituents in similar positions, however this is not observed for compound **69** which would be expected following this reasoning.

While the majority of compounds screened in the mitochondrial assay produced maximal response in *T.gondii* inhibition, and therefore were difficult to differentiate between, this did not always correlate with the cellular assay potencies. Several compounds appeared either significantly more or less potent between the two. The most prominent example being compounds **203**, **205** & **220**.

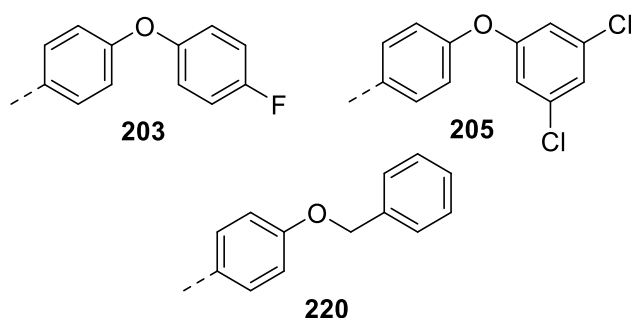


Figure 3.14:
Compounds demonstrating discrepancies between cellular and mitochondrial potency.

It is difficult to determine a clear relationship between these compounds and the differences observed in the mitochondrial assay.

3.6.4 Cytotoxicity assays

Due to the fact *Toxoplasma gondii* requires its host for survival and growth it was important to test compounds for their effects on the host cell (HFF), as compounds which caused host cell death or inhibition would appear as false positives in assessing inhibitor efficacy. These assays were carried out alongside the efficacy studies with compounds. No toxicity was observed across the series, relative to DMSO control, the assay was carried out at doses up to 10 μ M.

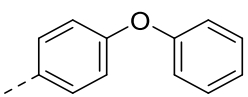
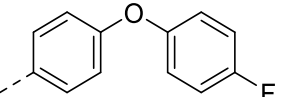
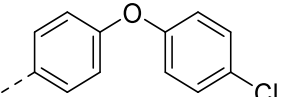
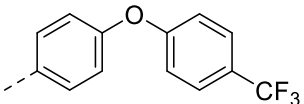
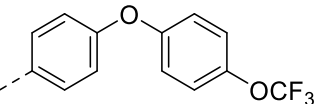
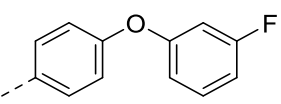
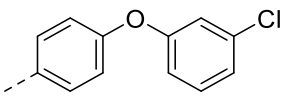
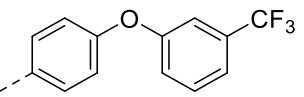
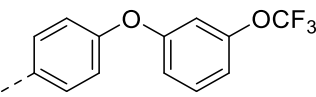
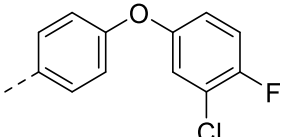
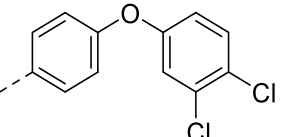
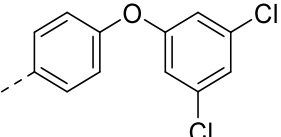
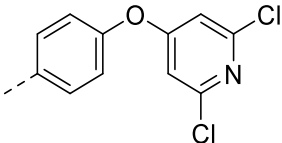
3.6.5 Preliminary ADMET and physicochemical properties

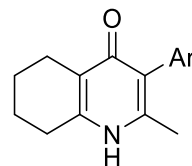
As with the initial screening of series; compounds with sufficient tachyzoite activity were then evaluated for their metabolic stability and their aqueous solubility, to identify any SAR relations with regard to either property.

3.6.6 Metabolic stability

As discussed previously Microsomal stability is an important parameter in drug development and a key deficiency in the THQ compound identified was its susceptibility to microsomal degradation, demonstrating that this problem is not intrinsic to the series as a whole as a result of the saturated ring system was necessary if the series was to be progressed. Microsomal stability was measured externally by ChemPartner using a LCMS/MS technique (see appendix/experimental for full details). Microsomal stability data is compiled in **Table 3.20**.

Table 3.20: Half life of compounds in presence of Human/Mouse liver microsomes.

Compound	Microsomal Stability (M/H)	Compound	Microsomal Stability (M/H)	Compound	Microsomal Stability (M/H)
	21/146 mins		39/263 mins		69/99 mins
	127/537 mins		101/>600 mins		17/202 mins
	12/135 mins		30/- mins		26/- mins
	41/- mins		63/- mins		28/- mins
	25/- mins		-		-



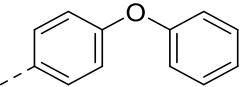
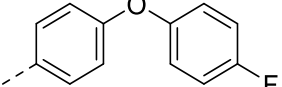
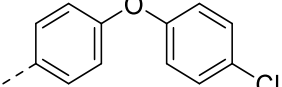
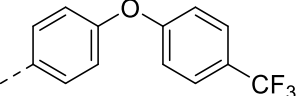
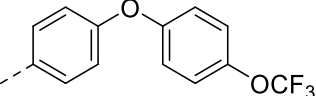
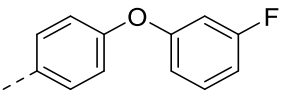
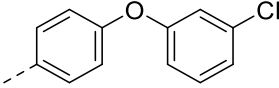
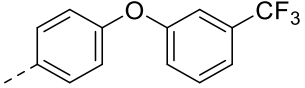
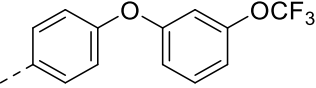
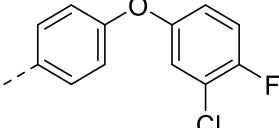
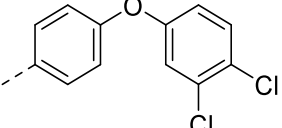
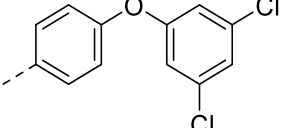
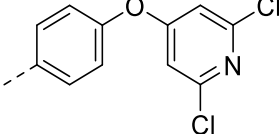
Analysis of the metabolic stability data shows a clear relationship between the size of the substituent in the 4-position of the terminal ring and the half-life of the compound. Increasing the size from a proton to trifluoromethyl/trifluoromethoxy greatly increases a compounds stability. The same is not observed for 3-position substituents where stability appears relatively unchanged. The 3,4-disubstituted compounds demonstrate this with stability improving from singly substituted 3-chloro to 3-chloro4-fluoro to 3,4-dichloro, while the 3,5-dichloro compound retains poor stability.

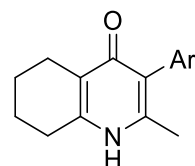
Some variation is observed between mouse and human microsomal activity, notably mouse microsomes, in general, exhibited a much more rapid turnover of compound. This is often a complicating factor in drug discovery and can make predicting PK behaviour extremely challenging between species. Because of the in vivo model any candidate will require reasonable stability in both mice and human microsomal assays to be progressed.

3.6.7 Aqueous solubility

Aqueous solubility was measured externally for a selection of compounds. Aqueous solubility data is compiled in **Table 3.2**.

Table 3.21: Aqueous solubilities measured at pH 7.4

Compound	Aqueous Solubility	Compound	Aqueous Solubility	Compound	Aqueous Solubility
	1.97 μM		2.38 μM		16.41 μM
	0.45 μM		7.07 μM		0.50 μM
	0.33 μM		2.19 μM		0.55 μM
	2.00 μM		0.68 μM		6.25 μM
	5.05 μM	-	-	-	-



Analysis of the solubility did not demonstrate a clear structural relationship, this is likely a result of multiple independent effects, such as hydrophobicity and changes in crystal lattice energies. All compounds exhibited relatively poor solubility with respect to generally accepted requirements of a drug candidate ($\sim 100 \mu\text{M}$). However several compounds showed solubility greater than $5 \mu\text{M}$ including both of the 3,5-dichloro analogues; **213** & **231**, which is a marked improvement over the initial hit compound **57** which exhibited solubility of $1.97 \mu\text{M}$ and a dramatic improvement over the quinolone equivalent, **45**, of $0.15 \mu\text{M}$. Most impressively, both compounds **168** and **169** showed over 50-fold improvements in this regard, while these values are still below ideal parameters, it indicates significant improvement is possible, and further modifications may provide the additional solubility desired.

3.7 Summary

The series was evaluated for tachyzoite activity using a cellular assay. Compounds deemed of sufficient cellular potency were then assayed for aqueous solubility and metabolic stability. The expansion of the series has successfully validated the tetrahydroquinolones as genuine *T.gondii* inhibitors, with a distinct SAR profile.

It is disappointing that no success was had in generating potent inhibitors with more polar character, although this is likely reflection of the hydrophobic nature of the binding site. The overall diversity of the series was also somewhat limited, biased by availability and amenability of the chemistry. Despite this a number of trends were identified as discussed, perhaps most important was the elimination of microsomal liability through alterations to the side chain. If this had not been achieved it would have strongly suggested the point of metabolic weakness was within the saturated ring of the tetrahydroquinolone, and as such, may have proven more difficult to prevent. Frustratingly, the reduction in metabolic susceptibility also resulted in a reduction in efficacy. Less clear was the relationship between substituents and solubility however, there were clear differences between compounds.

Combining this data and compromising between opposing trends in metabolic stability and potency led to compounds **168** and **169** being identified as a promising candidate for further development.

Compounds **169** and **168** both balance potency with metabolic stability as well as exhibiting a notable improvement in solubility in comparison with the rest of the series. Compound **169** was selected preferentially due to its superior mouse microsomal stability data. Further development and evaluation of compound **169** is discussed in **Chapter 4**, with particular focus on improving solubility and the selectivity of the compound.

Chapter 4 Progression of Compound 169 and Further Development of the Tetrahydroquinolone series

4.1 Further evaluation of tetrahydroquinolone-based leads as potential antiparasitics.

Having identified a number of promising compounds that demonstrated potent antiparasitic activity, acceptable *in vitro* metabolic stability, aqueous solubility and toxicity. It was felt that further studies were appropriate. The two primary contenders from the THQ series were compounds **168** & **169**, both having shown low nano-molar level activity, moderate to good metabolic stability and improved solubility.

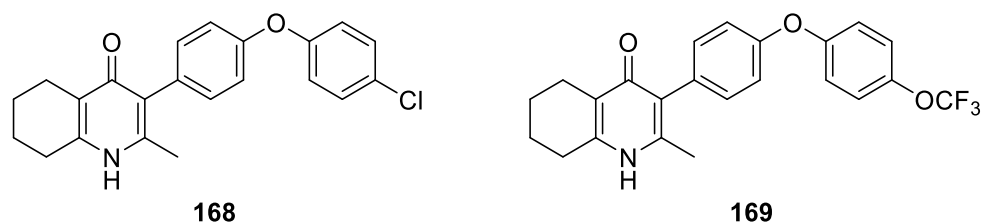


Figure 4.1:
Lead THQ candidates **168** & **169**.

4.1.1 Efficacy vs Bradyzoites *in vitro*

Both compounds were assessed for their activity against the EGS strain of *T.gondii* as a way to ascertain their efficacy against the bradyzoite stage of infection. This produced evidence of statistically significant reduction in cysts, for both compounds, at doses as low as 1.0 μM . This assay was conducted in similar manner to that described for the tachyzoite assay, but efficacy was judged on the elimination or reduction in size of cysts.

4.1.2 Permeability studies

An important factor that dictates a drug's efficacy is its ability to reach its site of action in sufficient quantities/concentration. One of the major barriers to this can be transportation across cell membranes. There are a number of common permeability assays used largely based upon either colorectal adenocarcinoma-2 (Caco-2) or Madin-Darby Canine Kidney (MDCK) cell lines. While both may be used for similar purposes, there are a number difference between the two. One disadvantage of MDCK cell line is the

obvious species mismatch, being a canine cell line. However MDCK has the advantage of rapidly differentiating and therefore is easier to cultivate and lends itself to higher throughput assay formats. An additional major difference between the cell lines is the expression of P-glycoprotein (P-gp), which is an efflux pump that is highly expressed in the MDCK cell line. Jin and co-workers have compared the utility of the two assays for antimalarial drug screening, (and therefore highly applicable to toxoplasmosis) and concluded that the two assays are generally equivalent, but also note the advantage of detecting P-gp substrates.¹³¹ This can include understanding potential drug-drug interactions caused if a compound or co-administered drug is also an inhibitor or substrate of the pump. This is even more advantageous in terms of the identification of drug leads for the treatment of toxoplasmosis, as MDCK has also demonstrated utility as a less laborious alternative in predicting blood-brain-barrier penetration.¹³² As such, it was decided that for the present studies a MDCK based assay would be most appropriate and both the initial hit compound **57** and leads **168**, **169** were assessed, with the results summarised in Table 4.1.

Permeability assays typically measure the speed of transportation across a membrane in both directions, this is important as allows for the calculation of an efflux ratio. The efflux ratio is calculated by dividing the rate of transportation in the B-A direction by that from the A-B value. Values greater than 1 indicate a compound is being effluxed more rapidly than it is being taken up, while values below 1 suggest the opposite. Values significantly higher than 1 indicate a compound is likely an efflux substrate.

Table 4.1: MDCK permeability assay results¹

Compound	Direction	$P_{app} \times 10^6$ cm/sec	Efflux Ratio
Metoprolol	A-B	27.51	0.79
	B-A	21.72	
Atenolol	A-B	1.04	0.64
	B-A	0.67	
Quinidine	A-B	5.96	4.15
	B-A	24.74	
57	A-B	32.12	1.23
	B-A	39.43	
169	A-B	10.80	1.24
	B-A	13.41	
168	A-B	26.93	1.23
	B-A	33.10	

The control compounds used in this assay; Metoprolol, Atenolol and Quinidine, represent a high permeability, low permeability and efflux substrate respectively. The efflux ratios observed indicate that the THQ series compounds are not P-gp substrates, and the P_{app} values indicate that generally the series shows high membrane permeability. Interestingly there appears to be a significant reduction in permeability for compound **169** in comparison with the other two THQ compounds, suggesting the diaryl ether decoration is having a notable impact, this may be a result of the increase in TPSA (Table 4.2), which often has a negative effect on permeability.

Table 4.2: TPSA values for screened compounds

Compound	TPSA*
57	38.33
168	38.33
169	47.56

*Calculate using ChemDraw Prime 16

Without assessing a larger number of the series it is difficult to confidently suggest a SAR. Pleasingly this data suggests the THQ's should not encounter permeability issues and has potential for at least moderate BBB penetration without suffering from at least one of the major efflux contributors.

¹ Performed by ChemPartner Ltd (for full experimental details see appendix).

4.1.3 Protein Binding

An important factor to consider in a drugs development is the fraction that will be 'free' in solution versus that bound to blood plasma proteins (BPP). This ratio will have a substantial influence on the effective concentration of a compound achieved and the lifetime of the compound, potentially complicating the PK profile. As only the 'free' fraction of a compound is able to exert its pharmacological effect. However, the free fraction is also the fraction vulnerable to metabolism and excretion. High BPP binding may suggest risks of low selectivity as a result of high lipophilicity, however it also has the possibility of extending a compounds lifetime with the protein bound fraction acting as a 'reservoir' of the compound prolonging exposure. Compound **169** was tested, and the results shown in **Table 4.3**. The control compounds Warfarin and Quinidine represent known high and low plasma protein binding drugs respectively.

Table 4.3: Plasma protein binding assay results²

Compound	Fraction of Bound (%)
169	99.9
Warfarin	98.9
Quinidine	89.6

As might be expected from relatively lipophilic compound the vast majority of the compound is protein bound, to a higher degree even than highly bound drug warfarin. This is of note as it may present problems with achieving local concentrations required for the compound's efficacy *in vivo*. Conversely this low availability may be beneficial with regards to metabolic life time, as only a small percentage of compound is liable to be metabolised. Another concern with these results is dependent on the accuracy of the assay, as when the unbound fraction is such a small percentage of the total, small difference/errors can represent substantial differences in free fraction concentration.

² Performed by ChemPartner Ltd (for full experimental details see appendix).

4.1.4 CYP450, HERG, and HepG2 studies

An important consideration when assessing a compounds toxicity profile, in addition to the compound's selectivity of parasite over host target site, is the compounds potential to inhibit other important host pathways. Some of the most important and common liabilities include the cytochrome P450 (CYP450) enzymes responsible for metabolism and the human Ether-à-go-go-Related Gene (hERG) channel.¹²⁵

The CYP450 proteins are a super family of heme based proteins named due to the characteristic absorption peak observed at 450 nm when reduced and exposed to carbon monoxide.¹²⁵ There are approximately 500 genes that encode for CYP450 isozymes however of these only 15 are metabolically relevant.¹²⁵ Compound **169** was screened against a panel of five of these isozymes to identify any possible liabilities.

Table 4.4: CYP450 inhibition assay data³

Compound /Isoform	IC ₅₀ (µM)					
	1A2	2C9	2C19	2D6	3A4 (Midazolam)	3A4 (Testosterone)
169	>10	3.80	>10	>10	>10	>10
Reference	0.003	0.459	5.904	0.038	0.015	0.018

From the results it can be seen that there is modest inhibition of the 2C9 P450 isozyme. However, as the level of inhibition is still several fold above the concentration required for anti-parasitic activity and limited to a single isoform this is not critical concern. However, inhibition of CYP450's becomes a more serious concern if the drug is to be administered with a partner or is likely to be given with other medication as this has the potential to lead to drug-drug interactions. This would be a result of one of the drugs CYP450 inhibition interfering with the usual rate of metabolism of the other, leading to reduction in clearance, potential accumulation and resulting toxicity. The results obtained might indicate a problem if a companion drug was required with a similar profile or that required CYP450 isozyme 2C9 to be metabolised.

The hERG protein is a cardiac potassium channel and is important for the electrical regulation of the heartbeat. As a result, inhibition of this channel by

³ Performed by ChemPartner Ltd (for full experimental details see appendix).

a drug molecule is a serious concern for the development of a drugs future development. Accurately assessing a drugs hERG liability can be further complicated by the need to understand the risk associated with either metabolites or prodrugs, especially if administered with known CYP450 inhibitors.

Table 4.5: hERG inhibition assay data. ⁴

Compound	HERG IC ₅₀ (µM)
169	21.78
Cisapride⁵	0.073

The results of the hERG inhibition assay of compound **169** indicate that weak hERG inhibition is observed, however, as with the CYP450 isoform, this is only observed at over 20 times higher than the levels required for tachyzoite inhibition. Therefore, notwithstanding that specific issues with localisation or clearance of the compound may be identified in further PK studies this level of inhibition would be deemed acceptable.

In addition, both **168** and **169** were assessed for their toxicity against HepG2 cells. HepG2 is an immortal liver cancer cell line, it is frequently used in toxicity assays as it is likely to detect toxic effects of metabolites in addition to compound toxicity. Assays carried out by Mark Hickmans team at the Walter Reed Army Institute of Research.

Table 4.6: HepG2 toxicity assay.

Compound	HepG2 IC ₅₀ µM
168	7.1
169	17.7

4.1.5 *In Vivo* efficacy studies.

Having established *in vitro* efficacy against *T.gondii* tachyzoites and achieved acceptable metabolic stability in the mice microsomal studies along with other supporting data it was felt that compound **169** was suitable for *in vivo* studies.

⁴ Performed by ChemPartner Ltd (for full experimental details see appendix).

⁵ The IC₅₀ for cisapride hERG inhibition is ranged from 0.015 to 0.080 µM in literature. Due to cell to cell biological variability, IC₅₀ value within 2-3 folds is considered normal between different runs. Cisapride was used in the experiments to ensure the normal response and good quality of the hERG cells.

These were carried out both against *T.gondii* and *Plasmodium berghei*, a mouse strain of malaria.

With regards to the *T.gondii* assays, (these were carried out by Craig Roberts at the University of Strathclyde) **169** was administered in *in vivo* mice trials at a range of doses, demonstrating excellent efficacy at doses (oral dosage) as low as 5 mg/Kg/day for 14 days. This includes complete elimination of type II tachyzoites in the luminescence studies (**Figure 4.2**).

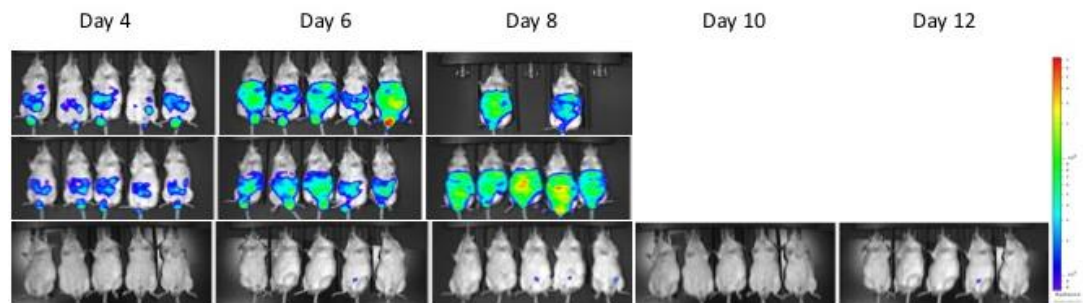


Figure 4.2:
Luminescence in vivo assay top; control, middle; DMSO control, bottom; THQ **169** 5 mg/kg/day (control groups survival = 0 beyond day 8).

The visual results of the luminescence readout provide a striking indication of the compounds efficacy. In addition, when brains of the infected mice from the treatment group were examined, post 30-day survival, significant reduction in normal cysts was observed.

The *Plasmodium berghei* models were carried out by Mark Hickman and team at the Walter Reed Army Institute of Research. These also provided pleasing results; with efficacy against *Plasmodium berghei* achieved down to 0.625 mg/Kg at three doses, leading to 100% survival (at 30 days), and a single dose cure of 2.5 mg/Kg when administered on the day of infection, (note prophylactic administration, i.e. day -1, was not curative at this dose but did prolong survival). IVIS results also showed complete clearance of parasitaemia after up to 72 hours post dosage in all cases.

4.1.6 Mitochondrial toxicity: comparative metabolic assays

Without quantitative enzymatic selectivity data to compare parasite and human *bc₁* inhibition alternative approaches to ascertain the extent of compound toxicity caused via human mitochondrial function inhibition. Giancarlo Biagini and Richard Priestely at The Liverpool School of Tropical Medicine, performed toxicity assays on Hep G2 cells cultured in either glucose or galactose media to control metabolic dependence on either glycolysis or

oxidative phosphorylation (Mitochondrial based).¹³³ By comparing the ratios of toxicity under the two conditions the degree of toxicity caused by mitochondrial inhibition can be ascertained.

The results indicated that both compounds **57** and **169** appear to cause toxicity via inhibition of mitochondrial function, however even in exclusively phosphorylation-based conditions this toxicity remains several fold higher than the observed effective doses for tachyzoite inhibition. Ideally however this therapeutic would need to be broadened to increase confidence in avoiding mitochondrial toxicity.

Table 4.7: Comparative metabolics toxicity assay.

Compound	Glucose IC ₅₀ (μM)	Galactose IC ₅₀ (μM)	Relative potency (fold difference)
Rotenone	4.7 ± 0.7	1.9x10 ⁻² ± 1.1x10 ⁻⁴	250.3 ± 34.0
Tamoxifen	13.2 ± 0.5	10.1 ± 0.5	1.3 ± 0.1
169	43.1 ± 4.9	1.7 ± 0.2	24.7 ± 0.6
57	17.7 ± 2.2	2.4 ± 0.3	7.4 ± 1.2

4.2 Further development of Tetrahydroquinolones.

4.2.1 Increasing selectivity

One of the major concerns noted from literature on the development of the pyridone based systems, such as GSK932121 (**44**) was the risk associated with inadequate selectivity between the parasite and host.¹⁰⁵ The mitochondrial toxicity assays above (4.1.6) confirm that this is a potential issue with the current THQ inhibitors. Observations based on the crystal structure and the ELQ series indicated that this was largely dependent on having a bicyclic system and further enhanced by substituents projecting off the fused ring at the six and seven position specifically.¹⁰¹ It can also be seen in comparison between the bound GSK pyridone (**44**) structure (4D6U) vs the THQ (**57**) structure (5NMI) how the isoleucine (Ile27) is forced to change conformation, twisting to accommodate the larger THQ (**57**) inhibitor.

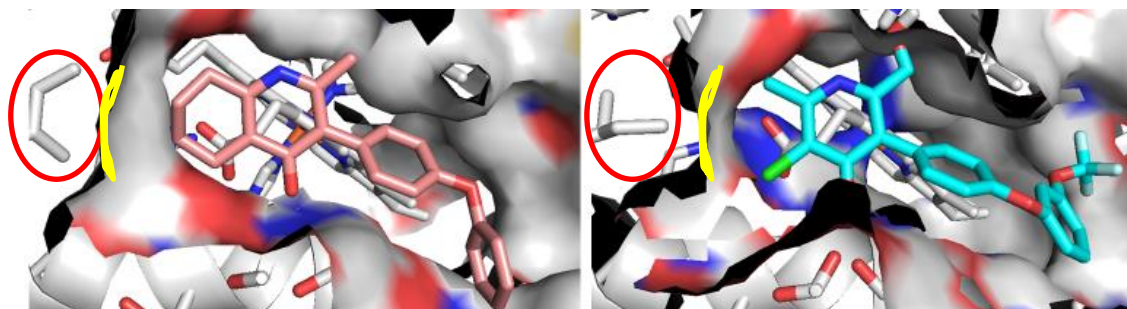


Figure 4.3:
Comparison of binding sites of crystal structures containing pyridone (**44**) (4D6U right)⁹⁸ and THQ (**57**) (5NMI left)⁹⁰ ligands, circled red: isoleucine 27.

When the shape of the protein surface is compared between species in this area (**Figure 4.4**), it can be seen that there is a noticeably larger pocket in the parasite structure compared to that of the mammalian, in the case of *T.gondii* this appears to be a result of the isoleucine being replaced by a valine residue. Interestingly however, this residue is conserved between bovine and malarial sequences (see **Figure 1.17**), suggesting other sequence difference must also be contributing to the observed selectivity.

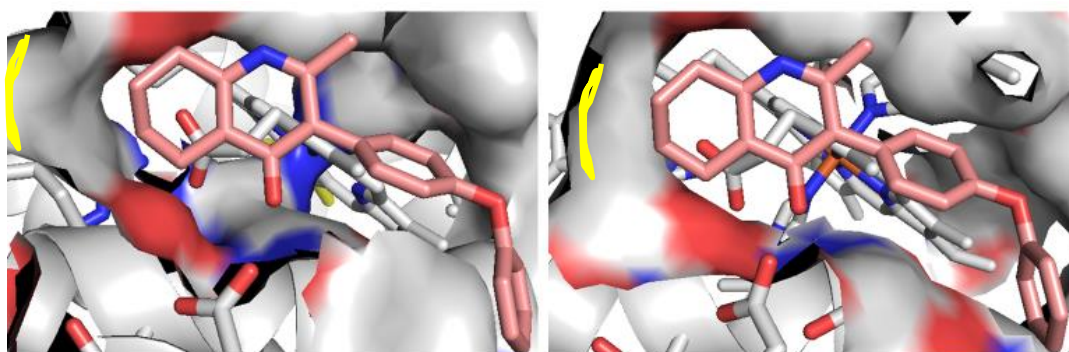


Figure 4.4:
Comparison of **57** positioned within *T.gondi* homology model (left) with crystal structure of **57** (5NMI)⁹⁰ bound within Bovine protein (right).

The ELQ series of inhibitors also demonstrated improved activity of compounds with six and/or seven position derivatives. With lead compounds specifically focusing on the 6-chloro-7-methoxy combination.

4.2.2 Design of more selective THQ inhibitors

Given the potential selectivity concerns and the observations regarding improved selectivity in six and seven substituted ELQ compounds, it was felt the simplest way to address the issue of selectivity was to explore the addition of substituents to analogous positions of the THQ inhibitors. While the structures and shape of quinolones and tetrahydroquinolones are very similar, the effects of moving from planar aromatic systems to the tetrahedral

saturated systems will have a substantial effect on the vectors at which substituents are directed, and therefore could produce different effects on the binding/selectivity. The move away from a planar scaffold with more varied vectors should offer greater ability to tune the binding along with physicochemical properties.

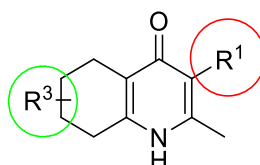
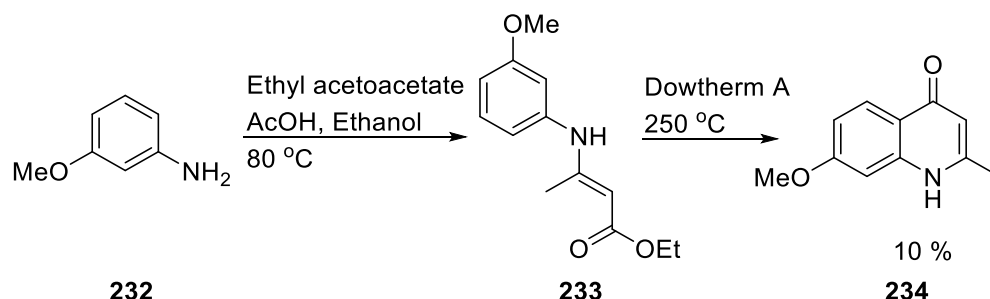


Figure 4.5:

Highlighted possible points of diversification of THQ scaffold. Red: explored within Chapter 3 as areas to modulate PK and solubility, Green: potential area to increase potency and selectivity.

4.2.3 Synthesis of six- and seven-substituted Tetrahydroquinolones

The simplest approach to the formation of the analogous substituted tetrahydroquinolones appeared to be via formation of the substituted quinolone. The quinolone could then be taken forward following the same synthetic pathway as used for the unsubstituted THQ's. There are a number of reported approaches to formation of quinol-4(1H)-ones.¹³⁴ However the Conrad-Limpach cyclisation is ideal for synthesising the desired 2-methyl substituent, and a variety of substituted anilines are commercially available. Initial attempts trialled standard Conrad-Limpach conditions for formation of the quinol-4(1H)-ones, via formation and crude isolation of the aryl enamine (**233**) before thermal cyclisation to reach the desired product (**234**).



Scheme 4.1:

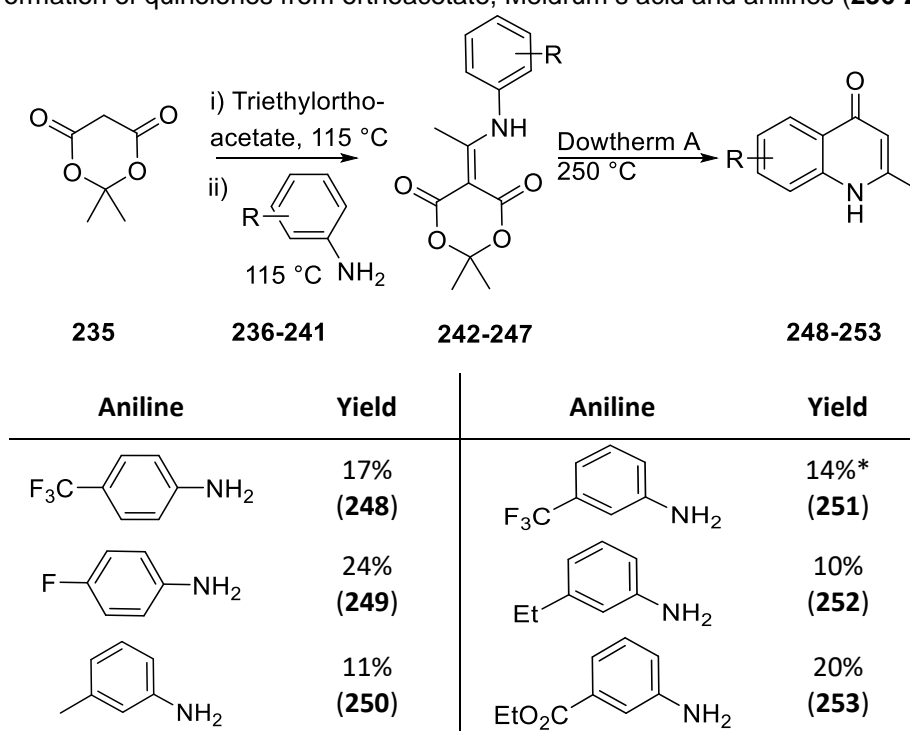
Synthesis of 7-methoxy-2methylquinolone (**234**) via Conrad Limpach cyclisation.

However despite moderate to high yields described in literature, the reaction was found to be poor yielding when attempted across substrates, with isolation of the compound from the solvent proving particularly difficult and

poorly reproducible. In an attempt to address this an alternative route was explored via the arylaminomethylene intermediate. This had the advantage of being easily isolated prior to the thermal cyclisation step. However, as can be seen in **Table 4.8**, the overall yields remained poor, especially for 3-substituted anilines where both 5 and 7-substituted products could be formed, this was compounded by similar retention times making separation of regioisomers difficult.

Table 4.8

Formation of quinolones from orthoacetate, Meldrum's acid and anilines (**236-241**).



*single regiomere not isolated, yield based on ratio of peaks in ¹H NMR.

This was especially problematic with the ethyl carboxylate derivative; while cyclisation proceeded in reasonable yield, only a fraction of the 5-substituted regioisomer was successfully isolated,

Having synthesised the quinolone cores of the substituted inhibitors, the remainder of the synthetic route was maintained as before. In addition, 2,6-dimethylquinol-4(1H)-one (**254**) was commercially available and so was also taken forward.

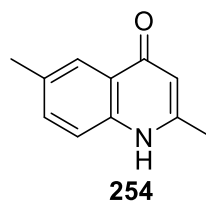


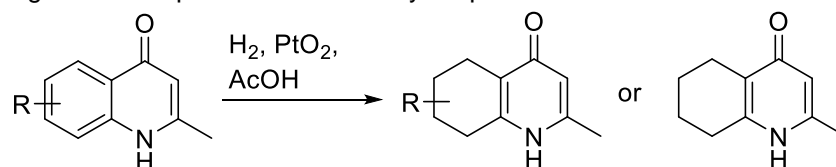
Figure 4.6

Commercially available 2,6-dimethylquinolin-4(1H)-one **254**

Starting with hydrogenation of the unsaturated quinolones **234**, **248-254**, using Adams catalyst in acetic acid as before, to form the tetrahydroquinolones **255-259**. Unfortunately both the fluoro and methoxy derivatives (**234** & **249**) suffered from elimination under these conditions forming the unsubstituted tetrahydroquinolone (**60**). The reduction of the methoxy derivative (**234**) was also trialed in methanol as a solvent, to determine if less acidic conditions could prevent elimination, but this only resulted in slowing the reaction. It was also notable that the hydrogenations did not proceed as readily as with the unsubstituted quinolone (**59 to 60**), however given the poor reproducibility of this reaction overall, it was difficult to confirm this definitively.

Table 4.9

Hydrogenation of quinolones to tetrahydroquinolones.



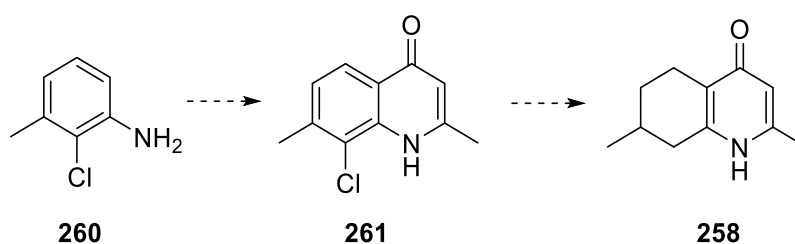
234, 248-254		255-259		60
R group	Yield (Product)	R group	Yield (Product)	
7-OMe	- (60)	6-Me	76% (258)	
7-Me	98% (255)	6-CF ₃	49% (259)	
7-CF ₃	66% (256)*	6-F	- (60)	
7-Et	64% (257)	-	-	

* yield assuming 1:1 ratio of the two regioisomers, as suggested by H¹NMR

At this point compound **256** was successfully isolated from its 5- substituted regioisomer during the chromatographic purification.

As mentioned previously, an issue with the synthesis of seven-substituted quinolones was the production and separation of the seven-substituted

regioisomer from the undesired five-substituted regioisomers. Given the elimination observed of several of the substituents (fluoro and methoxy) during the hydrogenation, one option considered was to use such a substituent as a dummy group, at the 2-position of the aniline. This would prevent cyclisation at this position and therefore lead to only the desired regioisomer, after removal via hydrogenation. The example shown in **Scheme 4.2** uses 2-chloro,-3-methylaniline (**260**) to form exclusively the 7,2-dimethyl-5,6,7,8-tetrahydroquinolone **258**.



Scheme 4.2:

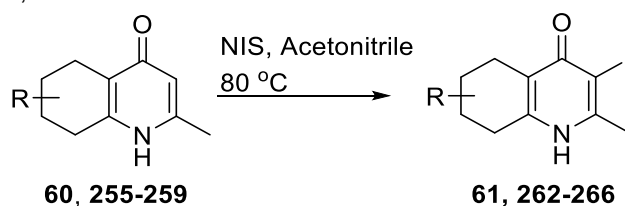
Example of dummy group protecting strategy to reach 7,2-dimethyl-5,6,7,8-tetrahydroquinol-4(1H)-one (**255**).

Unfortunately, the availability of the di-substituted anilines made this infeasible on the scale that would be required to reach final compounds, and so it was not pursued.

The tetrahydroquinol-4(1H)-one derivatives were then iodinated using NIS as before shown in (**Table 4.10**)

Table 4.10

Iodination of tetrahydroquinol-4(1H)-ones **60**, **255-259**, to give 3-iodotetrahydroquinol-4(1H)-ones **61**, **262-266**.



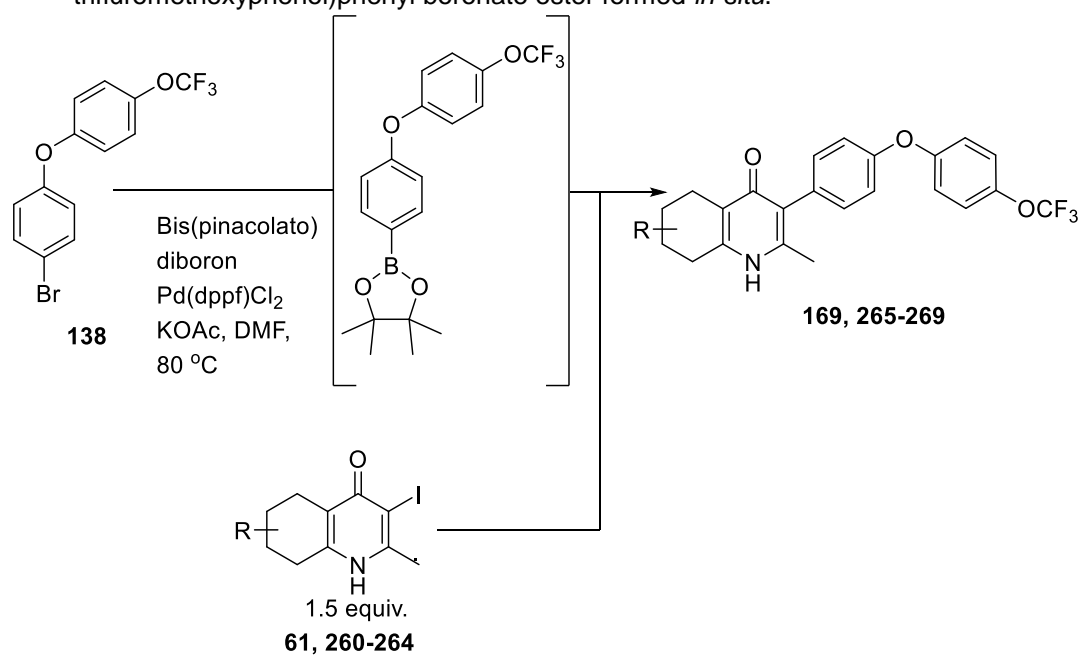
R group	Yield (Product)	R group	Yield (Product)
H	86% (61)	7-Me	71% (262)
6-Me	58% (260)	7-CF ₃	91% (263)
6-CF ₃	84% (261)	7-Et	99% (264)

Given the poor yielding initial step, it was decided to prioritise synthesis of the successful 4-(4-(trifluoromethoxy)phenoxy)benzene-based derivatives over a more combinatorial approach using a variety of diaryl ether side chains. In an

effort increase overall yield, given the limited quantities of the tetrahydroquinolones synthesised, the compounds were synthesised via the one-pot Suzuki reaction discussed in **Chapter 3**. This provided access to the six compounds below.

Table 4.11:

One-pot Suzuki couplings of substituted 3-iodotetrahydroquinolones, with 4-(4-trifluoromethoxyphenyl)phenyl boronate ester formed *in-situ*.



R- group	Yield (Product)	R- group	Yield (Product)
H	28% (169)	7-Me	26% (267)
6-Me	15% (265)	7-CF ₃	30% (268)
6-CF ₃	7% (266)	7-Et	11% (269)

Despite poor to moderate yields throughout the synthesis, five compounds were isolated in sufficient quantities for initial testing. Unfortunately with the quantities obtained enantiomer separation was not deemed feasible, and therefore the compounds were investigated as racemate. The compounds were first evaluated for efficacy against tachyzoites as with the previous generation.

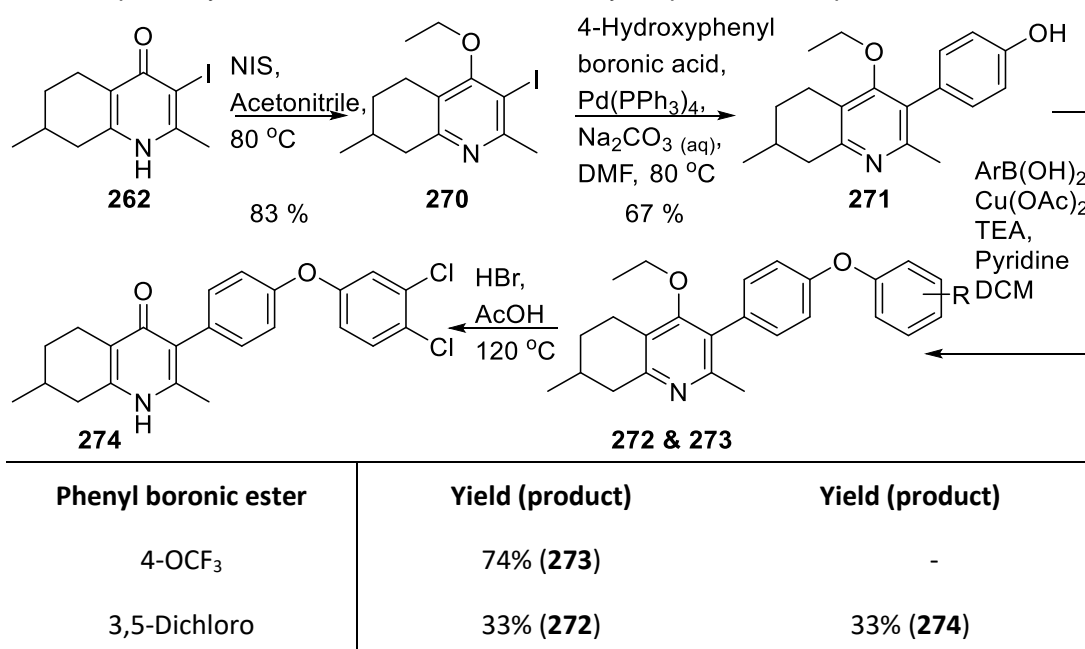
Table 4.12: Tachyzoite activity of 6- and 7-substituted tetrahydroquinolones.

Compound	R- group	Tachy IC ₅₀	Compound	R- group	Tachy IC ₅₀
265	6-Me	2.50 μM	267	7-Me	0.050 μM
266	6-CF ₃	>10.0 μM	268	7-CF ₃	0.30 μM
169	-	0.090 μM	269	7-Et	0.055 μM

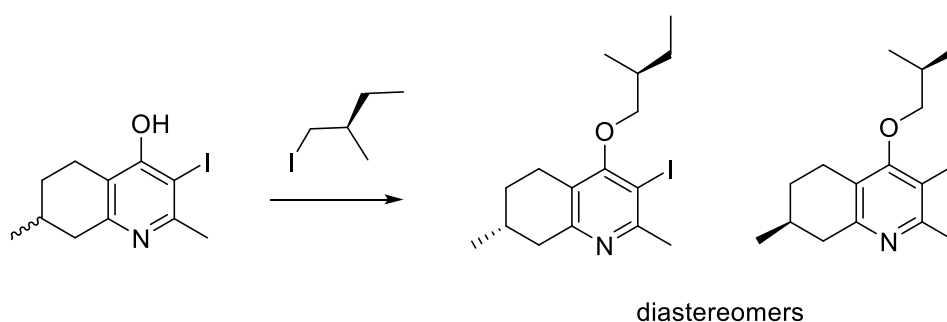
The results demonstrate a clear difference between the effects of six vs seven position substituents, as well as preference for the smaller methyl group over larger trifluoromethyl. Notably this is in contrast to the unsaturated ELQ analogues which show improved activity in both positions relative their unsubstituted analogues.¹⁰¹ It was felt it would be of interest to synthesise further analogues of the 7-methyl compound and to this end the divergent route used for the synthesis of the unsubstituted tetrahydroquinolones, discussed in Chapter 3, was applied.

Table 4.13:

Stepwise synthetic route to substituted tetrahydroquinolone compounds.



Interestingly in the ^1H NMR's of the intermediates **272** and **273** diastereotopic (ABX3) splitting of the CH_2 ethyl protons signal was observed. This highlights a possible advantage to this route with regards to separation of enantiomers. By using a chiral substrate group during the O-protection it would be possible to form respective diastereoisomers which may offer an easier method of separation, without extensive diversion from synthesis route, an example shown in **Scheme 4.3**.



Scheme 4.3:
Example of proposed method for chiral resolution of substituted tetrahydroquinolones.

Compound **274** was only assessed for its tachyzoite activity, however pleasingly as can be seen in **Table 4.14** it was highly potent, however while solubility and microsomal stability were not tested, it is likely to suffer from reduced solubility given the addition of the methyl substituent.

Table 4.14: Tachyzoite activity for Compound **274**

Compound	Tachy IC_{50}
274	0.016 μM

The most interesting results regarding the substituted quinolones came from the mitochondrial assay; **Table 4.15**.

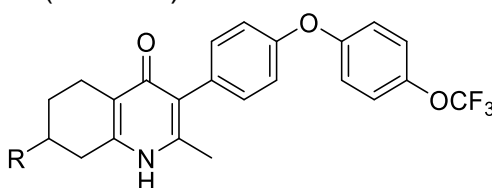
Table 4.15: Mitochondrial activity assay.

Compound	Mammalian mitochondria activity	Toxoplasma mitochondria activity	Compound	Mammalian mitochondria activity	Toxoplasma mitochondria activity
265	+++	++++	268	-	++++
266	-	++++	269	-	+++
267	++++	++++	274	+++	++++

As can be seen, almost all of the 6/7-substituted THQ compounds exhibited selectivity for the *T.gondii* over the mammalian mitochondria. Increasing the

size of the substituent from methyl to trifluoromethyl or ethyl appears to reinforce this effect, pleasingly, supporting the original selectivity hypothesis. The seven position compounds were then assessed to ascertain the effects on solubility and mouse microsomal stability. Given the reduced activity of the 6-substituted THQ's (**265** & **266**) only the 7-substituted compounds (**267-269**) were assessed for solubility and metabolic stability.

Table 4.16: Summary of activity, solubility and metabolic stability data for 7-substituted THQ's (**267-269**)



Compound	R- group	Tachy IC_{50}	Aqueous solubility	$cLog P$	Mouse microsomal stability: Half life
169	H	0.090 μM	7.07 μM	4.47	101 mins
267	Me	0.050 μM	0.03 μM	4.80	112 mins
268	CF ₃	0.300 μM	0.16 μM	5.16	144 mins
269	Et	0.055 μM	0.02 μM	5.21	63 mins

Notably the ethyl group demonstrated a greatly increased susceptibility to microsomal degradation in comparison to either the undecorated or shorter chain substituents. All compounds showed markedly reduced solubility indicating that the increased lipophilicity was not compensated for by any disruption to crystallisation. This reduction in solubility greatly reduced their viability as lead candidates, given regaining and improving on the solubility of lead compound **169** was the main priority for further development of the series.

Improving solubility

Although the change to the saturated ring system showed an initial improvement in solubility to the direct quinolone analogous, the synthetic limitations to the substituents at the six or seven positions did not provide enhancements to solubility as found for some of the ELQ series. This was likely due to the substituents being limited to lipophilic alkyl groups, and in fact as might be expected this reduced overall solubility.

As an alternative route to improved solubility, two further options were considered, firstly; exploring the two-methyl position of the quinolone cores and secondly; the use of a prodrug approach. Importantly, these were not necessarily mutually exclusive considerations, as adaptations to the 2-position if tolerated might also provide an additional 'handle' for prodrug formation.

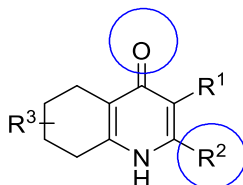


Figure 4.7:
THQ with potential points of modification to enhance solubility circled.

The first approach would be to determine if solubilising moieties might be more easily introduced at this location without detrimental effects to binding, the expectation would be these would aid the solubility of the compounds by reducing their hydrophobicity. Observational analysis of the parasite homology model overlaid with the bovine crystal structure suggests that there is potential for larger substituent in the two-position than the methyl group used in the current series. As such, it was decided to explore the impact of two-position methyl-hydroxyl and carbonate functionalities.

4.2.4 Synthesis of 2-position methyl hydroxy and carboxylate derivatives.

Two potential synthetic options were explored with regards to making the quinolones with 2-position variants. Firstly, installing the modification at the beginning of the synthesis during the formation of the quinolone core. The second option would be to introduce this derivation towards the end of the synthesis, if possible, from a previously constructed intermediate/product.

The first options could be easily achieved via a similar methodology to the original quinolone synthesis. Enamine formation occurs readily from the addition of an aniline with a dialkylactelynedicarboxylate, in this case dimethylactelynedicarboxylate. As can be seen from **Table 4.17**, the intermediate forms in near quantitative yields, however as before the thermal cyclisation remained inefficient, and overall poor yields were obtained for the quinolone.

Table 4.17

Cyclisation of anilines with Dimethyl acetylenedicarboxylate to form 2-carboxyl THQ's

R-Group	Yield (Product)	Yield (Product)
7-Me	98% (275)	7% (278)
7-CF ₃	97% (276)	14% (279)
7-Et	84% (277)	9% (280)

After formation of the respective 2-carboxylatequinolones were then reduced and iodinated. The undecorated compound (**281**) had been previously synthesised by Martin McPhillie within the group and so was also available to be taken forwards.

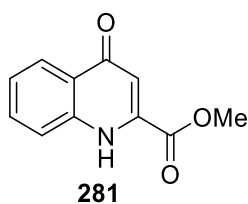


Figure 4.8:

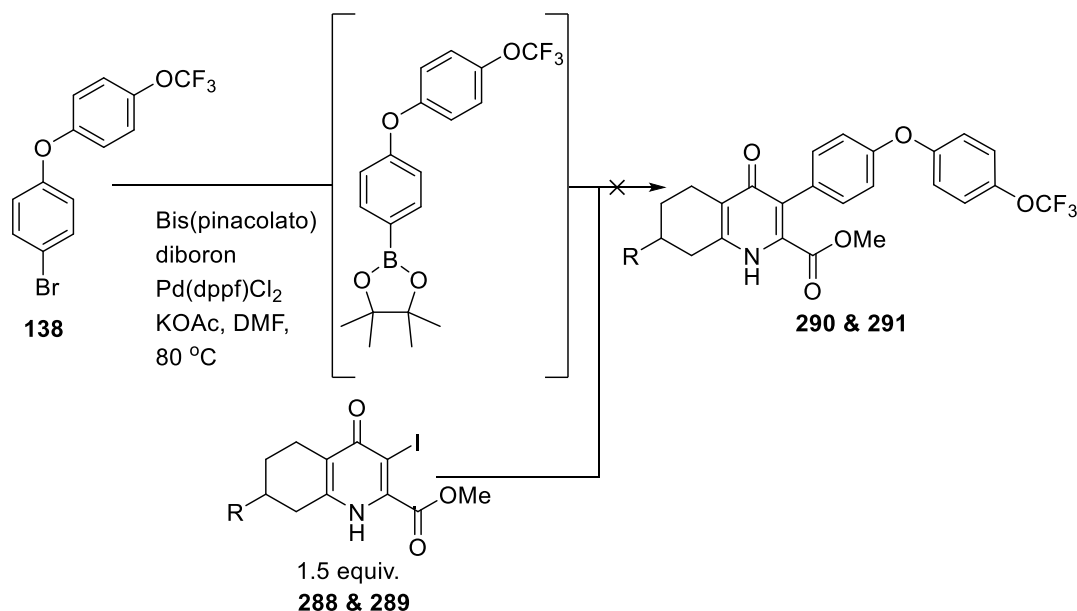
Compound **281** synthesised by Martin McPhillie.

Iodination proceeded as described previously using NIS in acetonitrile, generally yields were poorer than those observed for the 2-methyl analogues.

Table 4.18
Reduction and iodination of 2-carboxyltetrahydroquinolones

R-Group	Yield (Product)	Yield (Product)
7-H	94% (282)	84% (286)
7-Me	96% (283)	55% (287)
7-CF ₃	89% (284)	64% (288)
7-Et	82% (285)	67% (289)

Having isolated the iodinated intermediates (**286-289**) direct one pot Suzuki reactions were attempted on both the trifluoromethyl and ethyl substituted substrates (**288** & **289**). However in both cases the reaction failed and no product was isolated. This suggests that the carboxylate group is detrimental to the reactivity of the system.

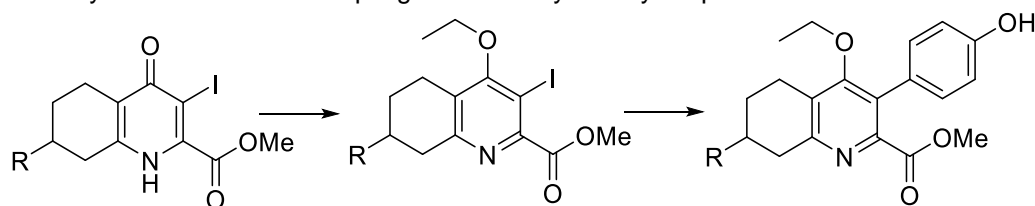


Scheme 4.4:
Unsuccessful one-pot synthesis of methyl-2-carboxylate THQ derivatives.

As a result of the unsuccessful direct coupling, the alternative stepwise route was used, which allowed access to the protected product in acceptable yields across the three steps (Table 4.19 & Table 4.20), although these were somewhat lower than those of the 2-methyl analogue.

Table 4.19

Alkylation and Suzuki coupling of 2-carboxytetrahydroquinolones.

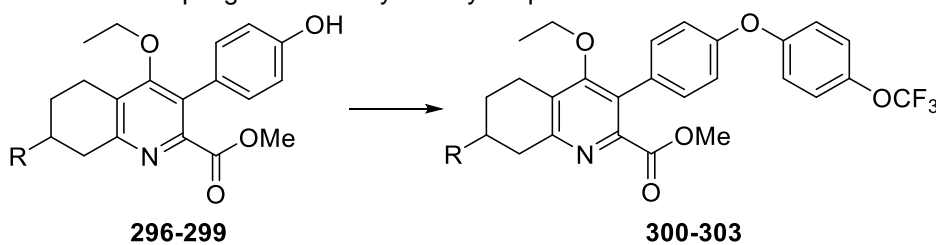


286-289 R-Group	292-295 Yield (Product)	296-299 Yield (Product)
7-H	83% (292)	55% (296)
7-Me	77% (293)	33% (297)
7-CF ₃	74% (294)	49% (298)
7-Et	83% (295)	49% (299)

The Chan-Lam coupling of compounds **296-299** with 4-trifluorophenyl boronic acid (**75**) was carried out in the same manner as previously with similar variable yields 34-78%.

Table 4.20

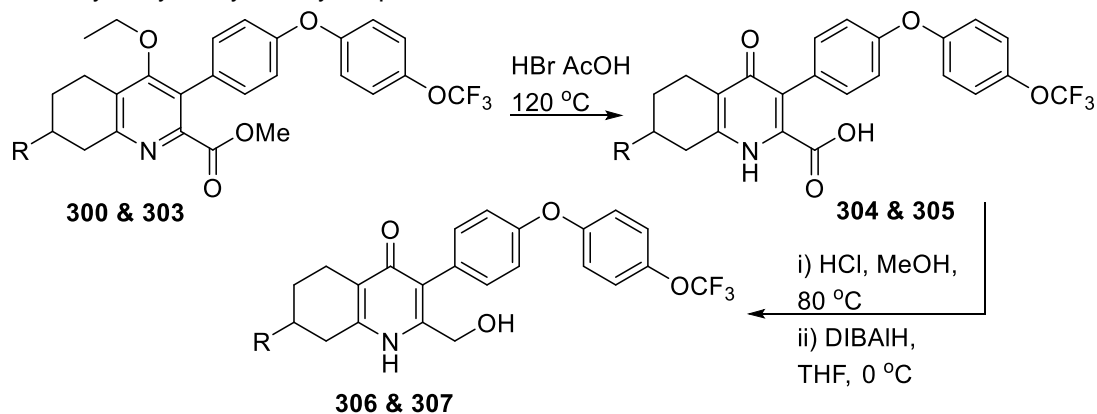
Chan-Lam Coupling of 2-carboxytetrahydroquinolones.



296-299 R-Group	Yield (Product)	300-303 R-Group	Yield (Product)
H	78% (300)	CF ₃	34% (302)
Me	62% (301)	Et	50% (303)

At this point synthesis was varied slightly for each R group in attempts to optimise the route. Initially it was considered desirable to proceed via isolation of the acid as this would be valuable to test.

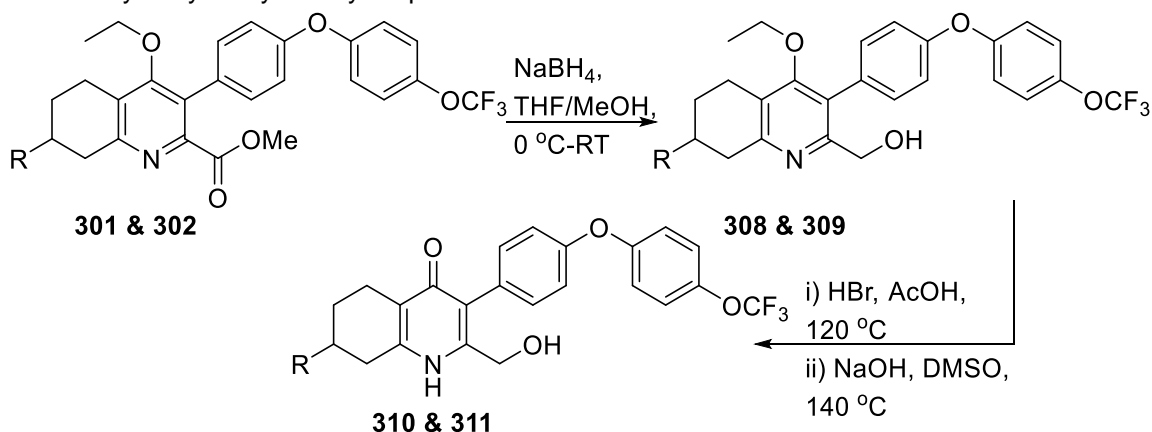
Table 4.21
Hydrolysis and Reduction of 2-carboxyltetrahydroquinolones to 2-hydroxymethyltetrahydroquinolones.



R-Group	Yield (Product)	Yield (Product)
H	43% (304)	55% (306)
Et	100% (305)	61% (307)

However after testing of the unsubstituted compound **304** showed no activity below 1.0 μM , this became less of a priority, and the alternative route shown below in **Table 4.22** was also explored, proceeding via reduction followed by deprotection.

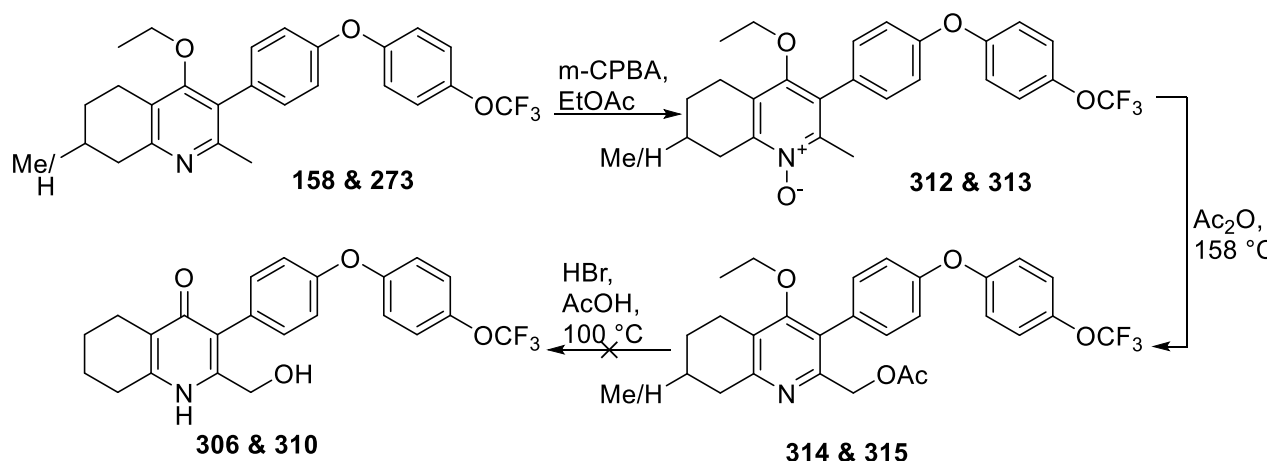
Table 4.22
Reduction and deprotection of 2-carboxyltetrahydroquinolones to 2-hydroxymethyltetrahydroquinolones.



R-Group	Yield (Product)	Yield (Product)
Me	74% (308)	32% (310)
CF ₃	66% (309)	18% (311)

However as can be seen overall yields were not improved, with poor recovery of the target compounds after the final deprotection step (**310 & 311**).

The alternative to installing the solubilising moiety at the beginning of the synthesis; adding the solubilising group towards the end, was also explored. The proposed route would lead on from the penultimate, alkylated compounds. By performing an *N*-oxidation the compounds would be able to undergo a Boekelheide like rearrangement to form the acyl esters.



Scheme 4.5:
Boekelheide like rearrangement based synthesis scheme.

While the rearrangement proceeded relatively efficiently and with the desired selectivity the subsequent deprotection as in the previous example proved problematic, and while product was detected, clean isolation proved difficult. The four 2-hydroxymethyltetrahydroquinolone compounds (**306-307** & **310-311**) were then tested for tachyzoite activity (**Table 4.23**).

Table 4.23:
Tachyzoite activity of 7-substituted-2-hydroxymethyltetrahydroquinolones

Compound	R- group	Tachy IC ₅₀	Compound	R- group	Tachy IC ₅₀
306	H	0.38 μM*	311	CF ₃	2.00 μM
310	Me	0.05 μM*	307	Et	0.38 μM

* Purity < 90% by HPLC

The addition of the hydroxy functionality to the THQ's appears to result in a modest loss in potency against tachyzoites, with the exception of the 7-methyl substituted variant (**310**). Unfortunately the isolated purity for this compound was not sufficient to warrant further assessment without resynthesis.

4.2.5 Prodrugs

The alternative to altering the physiochemical properties of the series itself is, to identify a point of attachment for a detachable solubilising group. This prodrug approach has the advantage of not altering the binding behaviour of the compound which might not otherwise be possible, especially in a case such as this where the target site is particularly hydrophobic. Prodrugs may provide an alternative to extensive and sometimes impossible chemical or formulation efforts.

Prodrugs are relatively common in modern medicine, with greater than 10% of small molecular recent approvals classified as such.¹³⁵ There a number of reasons prodrugs are employed, in addition to improving physiochemical properties, these include; enhancing absorption, permeability, distribution, targeting, tolerability and alteration of metabolic profile.^{136,137}

Prodrugs predominantly take the form of the drug compound conjugated in some way with to a pro-moiety, this drug conjugate will then be transformed in the recipient, usually through enzyme activity, to the active drug. In some cases, this pro-moiety might take the form of another drug, with each drug acting as the pro-moiety for the other, additionally there are bio-precursors, these compounds do not contain the bioactive structure, but rely on transformations occurring within the body to produce the active species, essentially as an active metabolite. A related category, which works in reverse, are what are classified as soft drugs. These are deliberately designed to be metabolised to an inactive form after a set time or upon reaching a target site.

Within these classes a wide range of approaches have been taken. Perhaps the simplest prodrug examples are esters, these can be of either the acid or hydroxyl parent compound. Esters are most commonly used to increase lipophilicity of the parent compound, usually as a means to improve permeability, the compound can then be hydrolysed by one of many esterase's. For improving solubility one of the most common prodrug-moieties is the phosphate ester. Usually attached via an amine or alcohol functionality, the presence of the dianionic phosphate is usually sufficient to greatly boost aqueous solubility. Phosphonate esters also typically exhibit similar rates of hydrolysis across species which is useful for comparing pharmacokinetics.^{137,138}

Unfortunately the highly ionic nature of the prodrug can cause difficulties with effective absorption, often preventing passive diffusion, amongst other effects. This perhaps explains many of the difficulties this kind of approach encounters during development, and why relatively few examples have reached market.¹³⁹ For the purposes of the THQ compounds and the treatment of toxoplasmosis there is the additional complication of the desirability for blood brain barrier penetration, which is likely to be greatly diminished by the presence of dianionic moiety. Other solubility enhancing pro-moieties include the use of sugars and amino acids, both operating in a similar fashion; highly hydrophilic moieties designed to balance against the more lipophilic drug. Prodrugs can complicate development of a drug, largely by convoluting the pharmacokinetics. However if a suitable prodrug resulted in successfully overcoming the major deficiency in this series it may be warranted, especially given the promising in vivo activity of **169**.

In the case of the THQ series a prodrug approach is particularly appealing, with regards to enhancing aqueous solubility, for three reasons. Firstly; the location of the target site; being within the mitochondrial membrane of the parasite, itself within a host cell each with their own membranes, emphasises the requirement for the compound to be highly membrane penetrant, this is another property that can be enhanced with a well-chosen pro-moiety. Secondly; the Q_i binding site is largely hydrophobic and the SAR across series has shown a broad intolerance to introduction of any significant polarity, as such introducing solubilising moieties via a prodrug may be the only option without detrimental effects on activity. Thirdly, a large detrimental factor contributing to series poor aqueous solubility, is their crystallinity. This leads on to a slightly different approach to using prodrugs for improving solubility, that is perhaps underutilised. The 'brick dust to grease ball' approach, less colloquially this approach depends upon reducing the crystallinity of the drug candidate.¹⁴⁰ In this case the intermolecular hydrogen bonding between the carbonyl and NH of the pyridone would be an ideal target for disruption (**Figure 4.9**). This is supported by the difference in melting point observed between the THQ compounds and their ethyl protected intermediates, discussed earlier (Chapter 3).

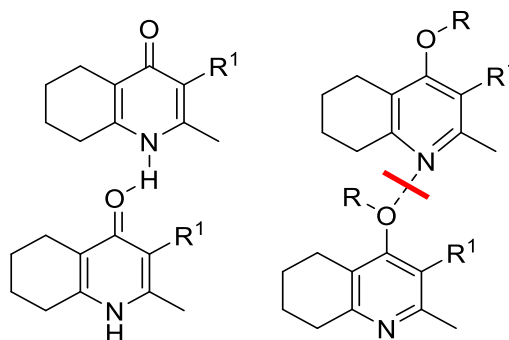
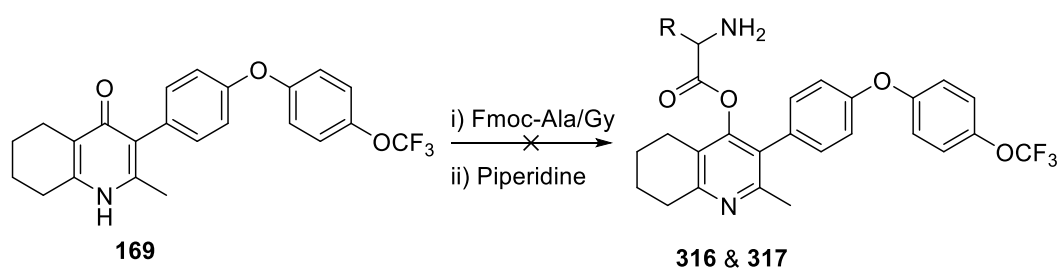


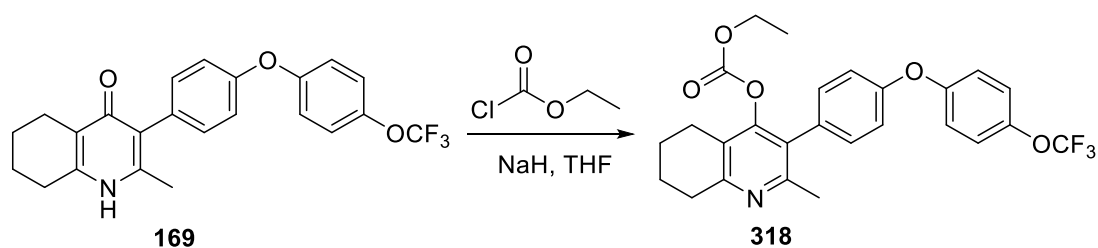
Figure 4.9:
Illustration of disruptive effect on intermolecular H-bonding caused by O-protection.

To disrupt this hydrogen bonding it was decided that the pyridone would, be a preferential point of attachment over any 2-position handles. A limited number of simple and readily available pro-moieties were explored on compound **169**. the pro-moieties used were limited to the amino acids; glycine and alanine, in addition to the ethyl carbonate, explored in the ELQ series.¹⁴¹



Scheme 4.6:
Unsuccessful attempts and formation of amino acid O-linked prodrug.

Unfortunately while formation of the ester appeared successful attempts at removal of the Fmoc resulted in decomposition back to compound **169**.



Scheme 4.7:
Formation of carbonate prodrug of **169**

This was not investigated further but serves to demonstrate this approach is viable within the series and offers an additional avenue of approach to manipulating the series properties.

4.2.6 Cocrystallisation studies of compound **169** in the cytochrome *bc*₁ complex

Pleasingly, further crystallography work at the University of Liverpool, carried out by Kangsa Amporndanai, Samar Hasnain and Svetlana Atonyuk, provided a crystal structure of compound **169** within the bovine complex (Figure 4.10).

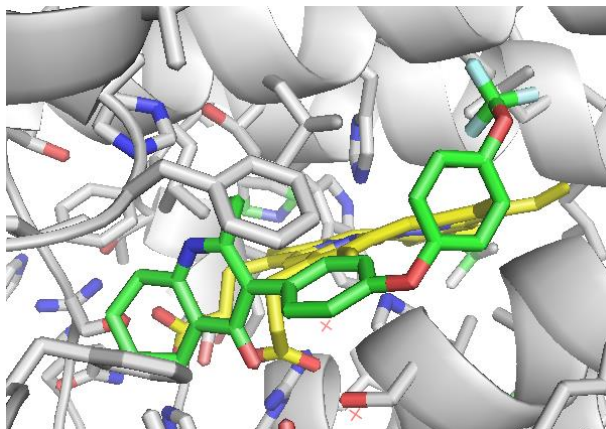


Figure 4.10:
Crystal structure of **169** bound within the Q_i site of the bovine cytochrome *bc*₁.

When compared with the initial hit **57** it can be seen that while both occupy broadly similar space within the pocket, there is a substantial tilt in the positioning of **169**, apparently enforced by the change in position of the 'aryl ether tail' to accommodate the trifluoromethoxy substituent. This may explain the reduction in binding seen for some compounds, as the tail forces a more or less favourable pose for the head group within the binding pocket. How and if this varies in comparison with the *Toxoplasma gondii* structure may also have important effects on selectivity.

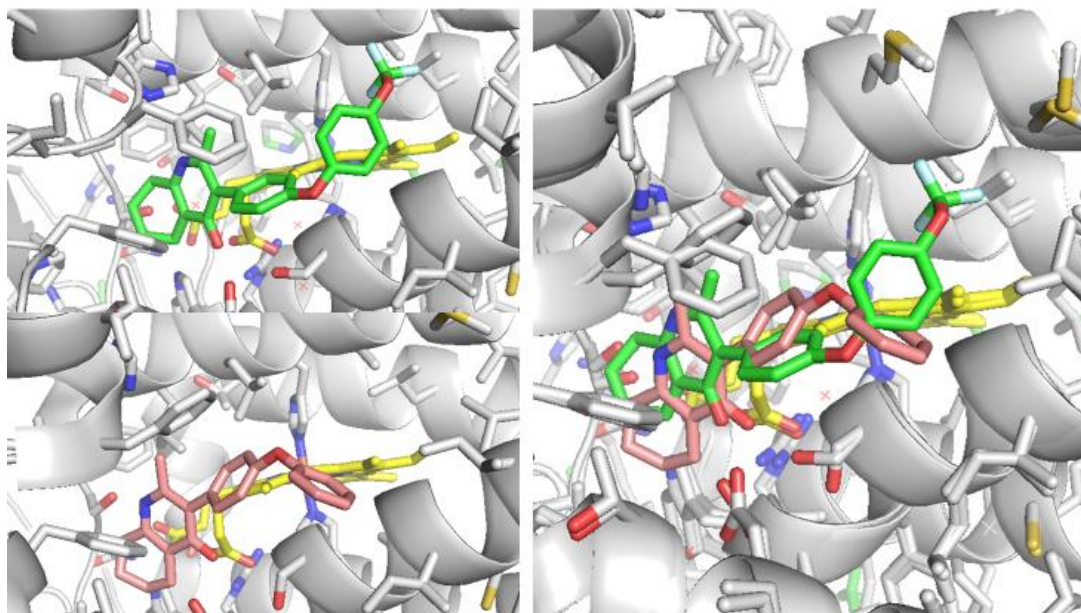


Figure 4.11
Comparison THQ inhibitors **169** (green top left) and **57** (pink bottom left) binding poses within the cytochrome *bc₁* complex.

It also further supports the assertion that the Qi site is the site of action, and it is pleasing to demonstrate this on the lead compound.

4.3 Summary and future work

Lead compound **169** was further assessed for its potential as a anti toxoplasmitic agent, being evaluated for typical early stage pharmacokinetic and pharmacodynamic properties. These included plasma protein binding, membrane permeability, CYP450 inhibition, hERG inhibition and further toxicity evaluation, **169** performed acceptably across these assays and was advanced to evaluation in a number of *in vivo* models for treatment of both *Toxoplasma gondii* and *Plasmodium berghei*. Pleasingly **169** demonstrated excellent potency within both of these models and low doses.

Further development of the THQ series was attempted aimed at addressing the remaining liabilities of species selectivity and solubility. The compound synthesised confirmed the selectivity hypothesis but due to synthetic tractability, the derivatives accessed were not suitable as improvements over lead **169**. Unfortunately attempts to enhance solubility through further modification were unsuccessful. Preliminary investigation of the use of a prodrug approach was initiated and may have further potential, the carbonate having shown to confer some advantage to the ELQ lead; ELQ316 (**44**).

Expanding the range of prodrugs explored and investigating their effects on solubility and Pharmacokinetics.

Perhaps one of the major unexplored advantages remaining to the THQ series is the potential for geminal substitution on the saturated ring of the core, this is not possible on the saturated ELQ series but would perhaps offer the greatest possibility of success with regard to disruption of crystal packing, and thereby solubility. The primary reason it was not investigated is the synthetic tractability, however given the lack of success in more readily accessible areas of chemical space, the additional synthetic efforts may be warranted.

Additionally a crystal structure of lead compound **169** in the bovine complex was obtained, demonstrating how the tail decoration can greatly impact the overall pose of the molecule.

Chapter 5

Conclusions and Future work

4.4 Summary & Achievements

The cytochrome *bc*₁ has been known as a valid target for the treatment of apicomplexan diseases, since the identification of Atovaquone as an inhibitor of its Q_o site.⁴³ The discovery that Atovaquone (**9**) also exhibits some activity against the highly resilient bradyzoite stage of *Toxoplasma gondii*, and the findings that the protein is up regulated in the bradyzoite phenotype expressing EGS strain of the parasite,⁹⁰ both support its value as a target worthy of further drug development. Recent programmes have made some progress in developing new inhibitors, primarily focussed towards malaria, and in this process demonstrated that not only is the Q_o site a valid drug target but in addition the Q_i site is also druggable via traditional small molecule approaches.^{88,98,99,142}

In this project the deficiencies of previous Q_i site inhibitors have been identified; the poor physicochemical properties and concern over parasite/host selectivity, and a combination of knowledge and structure guided approaches utilised in an attempt to develop a novel series, with enhanced drug like properties. To this end a number of novel distinct bicyclic pyridone containing cores were designed.

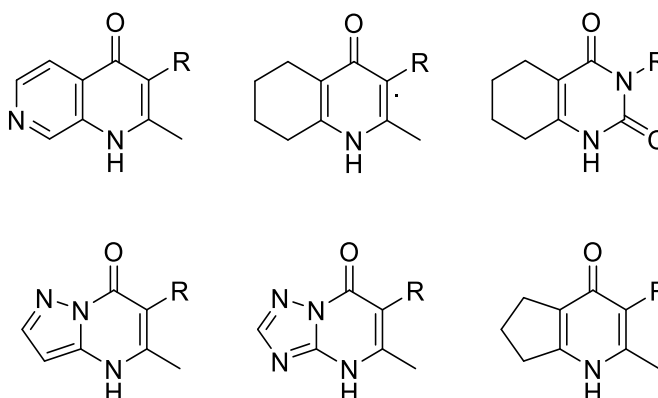


Figure 4.12

Novel bicyclic scaffold designs explored within this work.

Routes to these compounds were developed and a number of these were successfully synthesised; resulting in five distinct cores.

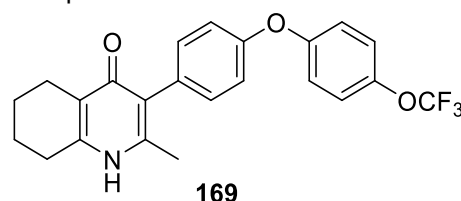
These cores were then evaluated for their anti-parasitic activity. A number of these scaffolds demonstrated potent activity against both *T.gondii* and *P.falciparum*, and several series were investigated further to establish preliminary physiochemical and metabolic stability.

Table 4.24

Data summary of the varied scaffolds.

Compound	Tachy IC ₅₀	Brady IC ₅₀	Aqueous Solubility (pH 7.4)	Microsomal stability Half life (human/mouse)
45	0.03 μM	1.0 - 10 μM	0.15 μM	171.93/448.13 mins
.66	1.0-10 μM	>10 μM	ND	ND
.65	1.0-10 μM	1.0 - 10 μM	0.94 μM	ND/278.33 mins
57	0.03 μM	1.0 - 10 μM	1.97 μM	146.33/20.97 mins
.77	>10 μM	N.D	N.D	N.D
109	0.1 μM	N.D	5.12 μM	ND/>480 mins

The initial THQ hit (**57**) from this investigation was then used successfully as a probe in a variety of *in vitro* and structural experiments, including co-crystallisation, to confirm the series mechanism of action. Supporting the conclusion that, like several of the ELQ and pyridone inhibitors, it acts through inhibition of the Q_i site of the cytochrome *bc*₁ complex. Having established improved solubility in a number of series with regards to a comparative ELQ candidate, the tetrahydroquinolone series was chosen to be taken forward for further development. Work was carried out developing the synthetic route to and expanding the synthesis to produce a library of THQ compounds. SAR studies initially focused around the diaryl side-chain, modification of which delivered the lead candidate **169**. Compound **169** demonstrated similar levels of potency to the initial hit with improved solubility and metabolic properties. The lead compound **169** was assessed further including BPP Binding, MDCK permeability, bradyzoite efficacy, CYP450 inhibition, hERG inhibition, and further toxicity and selectivity assays. Further optimisation was attempted to increase selectivity and solubility, however notable improvements to solubility were not achieved and while there was indication of improvements in selectivity being achievable this came at the expense of detrimental changes to physiochemical properties. Overall profile of **169** shown in Table 4.25.

Table 4.25Summary of data for compound **169**

T.g Tachyzoite IC₅₀ (μM)		0.092
T.g Bradyzoite IC₅₀ (μM)		0.50
P.f activity EC₅₀ (μM)	D6	0.014
	TM91C235	0.061
	W2	0.055
	C2B	0.040
Human FF MTT IC₅₀ (μM)		17.7
hERG IC₅₀ (μM)		22.0
CYP450 IC₅₀ (μM)	1A2	>10
	2C9	3.80
	2C19	>10
	2D6	>10
	3A4	>10
PPB (human)		99.9%
Metabolic stability	Mouse microsomal half-life (min)	101
	Human microsomal half-life (min)	>200
Solubility	Kinetic pH 7.4 (μM)	7.0
Permeability	Caco-2 (PappA-B) cms ⁻¹	10.8 × 10 ⁻⁶
	Efflux Ratio	1.24
In vivo efficacy (mouse)		
T.gondii	Daily dose	5.00 mg/Kg/day
P.berghei	Three doses	0.625 mg/Kg
	Single dose	1.25 mg/Kg

The culmination of the project resulted in the successful *in vivo* testing of novel THQ based inhibitor **169** in both *T.gondii* and *P.berghei* mice models. Compound **169** not only demonstrated excellent efficacy at low dosage, but also achieved single dose curative effects in the malarial model. While exceptionally promising in this regard, the series failed to overcome the physicochemical flaws that have limited similar pyridone containing series and is therefore likely to encounter similar difficulties in progressing, emphasising the need for further development.

4.4.1 Future work.

Development of inhibitors against the cytochrome *bc*₁ would greatly benefit from further structural information on the target. Currently the lack of protozoan crystal structure, limits the reliability of structure-based design, especially using computational models to predict ligand binding, given the poor correlation between computational and actual values. This highlights the importance of progress within the field of structural biology to gain access to difficult to capture structural information. Whether this is through X-ray crystallography, NMR or cryogenic electron microscopy this information will undoubtedly aid in future drug design. Cryogenic EM is already being used to elucidate the structure of cytochrome *bc*₁ in bovine down to resolutions of 4.1 Å, and demonstrating this can be achieved with significantly less protein, one of the major hurdles to imaging of the protein parasite.⁵⁸

While the tetrahydroquinolones generally appeared to demonstrate improved solubility and compound **169** demonstrated highly promising potent in vivo efficacy, the solubility of the **169** and the series in general did not reach the levels hoped for, as an improvement over other series in development such as the ELQ's.

As mentioned one area which was not explored was investigating geminal substituents as a method of disrupting crystallinity, however this is likely to be synthetically challenging to achieve.

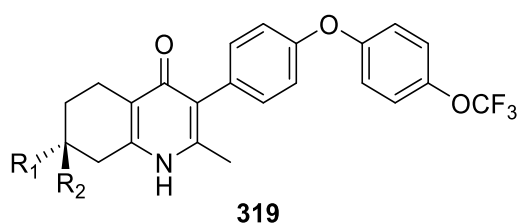


Figure 4.13:
Example of a possible geminally substituted THQ **319**

Without a distinct physiochemical advantage, there is a risk of the series encountering the same fundamental problems as encountered by the ELQ series. It is worth noting that prodrug approaches have been investigated for both the pyridone GSK series and the ELQ's.^{141,143}

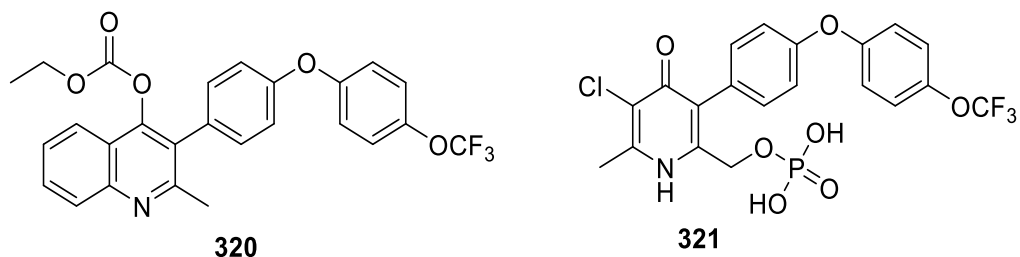


Figure 4.14:
Prodrugs of ELQ300: **320** and GSK932121: **321**

There remains the possibility that the lattice energy of the pyridone system remains too dominant a factor to achieve the level of solubility required, and that methods of disrupting this are incompatible with maintaining potency with this pharmacophore.

Due to limited time and resources, not all compounds synthesised were profiled completely with regard to solubility and microsomal stability, this additional information would help define the SAR of the series. The diversity of both the substituents on the saturated ring system and the variety in the diaryl-ether tail were limited and would benefit from further expansion. To develop the series further, improving the synthesis both with respect to efficiency and flexibility, would be a priority. A major bottle neck in the efficient synthesis of the THQ library was the hydrogenation of the quinolone, looking into a more robust methodology such as a H-cube may be a prudent approach. Not only did this impose significant restriction on the choice of substituents it proved repeatedly problematic with regards to reliability, scale and expense of catalyst. Developing a route to access a broader range of substituted THQ would also greatly enhance the series potential.

The naphthyridone and pyrazolopyrimidones cores could also benefit from further development. These compounds demonstrated potential in preliminary assays (tachyzoite efficacy at concentrations < 100 nM), and with some synthetic development, could be expanded to independent series, while their deviations from the quinolone scaffolds are relatively modest, they offer additional diversity in areas previously unexplored. There were also a number of alternative scaffolds designed that proved synthetically challenging or were not initially prioritised that could be investigated. While these cores may not be as synthetically tractable with regards to library expansion as the quinolone and pyridones, they may offer the opportunity to capture the promising biological activity without the undesirable physicochemical properties.

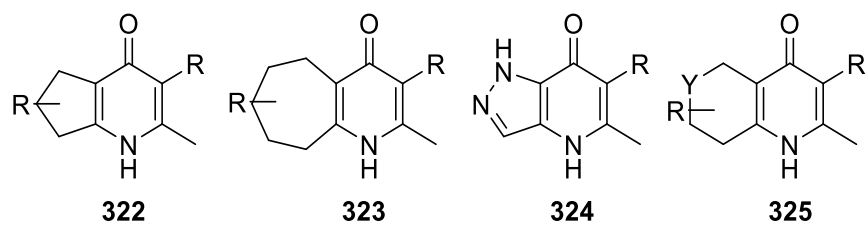


Figure 4.15
cyclopentane- (**66**), cycloheptane- (**316**), alternative pyrazolo- (**317**) and saturated heterocycles- (**318**) pyridone, scaffolds, either unexplored or unsynthesised.

Given the challenges encountered with improving solubility, prioritising this as an initial screening criterion at a higher threshold may be beneficial to preventing the pursuit of further series with undesirable physiochemical properties.

Chapter 5 Experimental

5.1 General procedures

All reactions were carried out at room temperature under standard atmospheric conditions and were stirred with a magnetic stirrer unless otherwise stated. All reagents were obtained from commercial sources and were used without further purification. Anhydrous solvents were obtained from a PureSolv MD6 solvent purification system.

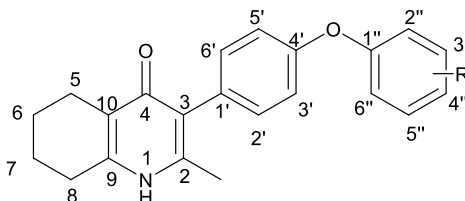
Thin layer chromatography (TLC) analysis was performed on aluminium pre-coated silica gel plates (254 μm) supplied by Merck chemicals and visualised by ultraviolet light (254 nm).

High resolution mass spectrometry (HRMS) was carried out using a Bruker MaXis Impact Time of Flight spectrometer using electron spray ionisation (ES $^{+/-}$), giving masses correct to four decimal places.

HPLC was performed on an Agilent 1290 Infinity Series equipped with a UV detector. Instrument – Agilent 1290 Infinity with Diode Array Detection; Column – Ascentis Express C18, 50 x 2.1mm, 2.7 μm particle size; Mobile Phase – Acetonitrile + 0.1% TFA, Water + 0.1% TFA; Gradient – 5-95% Acetonitrile over 5 mins; Flow Rate – 0.5ml/min

Proton (^1H) and carbon (^{13}C) NMR spectra were recorded at 500/400 MHz and 126/101 MHz respectively on a Bruker Advance 500 Fourier transform spectrometer. Spectra were recorded at room temperature unless otherwise stated. Chemical shifts (δ) are reported in parts per million (ppm) and are reported with reference to the residual solvent peak. In some cases due to poor solubility addition of TFA or a CDCl_3 was required and are noted by respective assignments.

Assignment of tetrahydroquinolones is based on the numbering shown below;



Multiplicities are reported with coupling constants and are given to the nearest 0.1 Hz. Apparent multiplicities are denoted by app. followed by the splitting

pattern. Where needed, two-dimensional correlation spectroscopy (2D-COSY), heteronuclear single quantum coherence spectroscopy (HSQC), heteronuclear multiple bond correlation spectroscopy (HMBC) and Distortionless enhancement by polarization transfer (DEPT) were used in order to aid assignment. Numbering in assignment is based upon compound names. NMR data was processed using MestReNova software, in cases where quaternary carbons could not be specifically assigned they are denoted as C_q. Infrared spectra (IR) were recorded in solid phase on a Bruker Alpha Platinum ATR FTIR spectrometer with vibrational frequencies given in cm⁻¹. Melting points were measured on a Stuart SMP30.

Protein images were created using PyMol.¹⁴⁴

* required addition of CD₃Cl to solubilise.

+ required addition of TFA to solubilise.

5.2 Experimental: Chapter 2

5.2.1 General method A (Cyclisation of pyrazoles/triazoles)

To a solution of ethyl 3-oxo-2-(4-(trifluoromethoxy)phenoxy)phenyl)butanoate (1.00 equiv.) in acetic acid (2.00 mL) was added 3-amino—pyrazole/triazole (1.00 equiv.). The solution was heated to 120 °C and refluxed for 4 hours. The reaction mixture was then allowed to cool. Addition of H₂O (2.00 mL) caused precipitation of a white solid. Precipitate was filtered and washed with H₂O.

5.2.2 General method B (Deprotection)

To a solution of the 4-ethoxy-3-(diaryl ether)-hydroxyquinolone (1.00 equiv.) in acetic acid (2.00 mL mmol⁻¹) was added hydrogen bromide (>48% w/v (aq)) (1.00 mL mmol⁻¹). The reaction mixture was then heated to reflux for 72 hours. The reaction mixture was neutralised with sodium hydroxide (2.00 M, 30.00 mL) and precipitate formed. The reaction mixture was then filtered to afford the title compound.

5.2.3 General method C (Naphthyridone formation)

2,2-Dimethyl-1,3-dioxane-4,6-dione (1.50 equiv.) was dissolved in trimethyl orthoacetate (2.00 equiv.) and heated to 115 °C for 2 hrs. The reaction was cooled to allow the addition of the amino aniline (1.00 equiv.) before being heated to 115 °C for a further 2 hrs. The reaction mixture was then allowed to cool and was concentrated *in vacuo*, remaining solvent was washed off with cold methanol. The precipitate was then dissolved in minimum volume of Dowtherm A and refluxed at 250 °C for 1.5 hours. The reaction mixture was allowed to cool and the precipitate filtered followed by washing with hexane to afford the title compound.

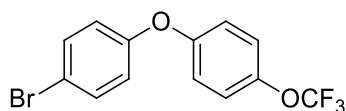
5.2.4 General method D (iodination)

Tetrahydroquinolone/Naphthyridone (1.00 equiv.) and N-Iodosuccinimide (1.20 equiv.) were dissolved in acetonitrile (5.00 mL mmol⁻¹) and stirred and heated at 80 °C for 3 hours. The reaction mixture was then allowed to cool and the mixture filtered, the precipitate was then washed with water (15.00 mL) to afford the title compound as a colourless solid.

5.2.5 General method E (O-alkylation)

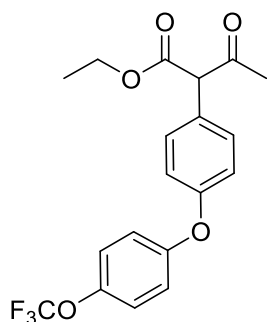
A suspension of the 3-iodo-tetrahydroquinolin/naphthyrid-4(1H)-one (1.00 equiv.) and potassium carbonate (2.00 equiv.) in DMF (20.00 mL) was heated to 50 °C and stirred for 45 minutes. The reaction mixture was removed from the heat and ethyl iodide (1.50 equiv.) was added dropwise. The reaction mixture was then heated and kept at 50 °C with stirring for a further 18 hrs. Formation of a yellow emulsion was observed. The reaction mixture was then quenched with water (40.00 mL). The organic phase was extracted using the polar extraction technique (ethyl acetate, 3 × 40.00 mL), and the resulting organic layers were combined and dried over MgSO₄ and concentrated *in vacuo* to afford the title compound.

1-Bromo-4-(4-(trifluoromethoxy)phenoxy)benzene (76).



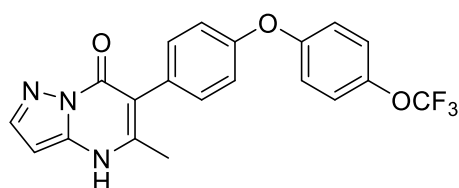
Triethylamine (1.68 mL, 12.15 mmol), and pyridine (0.98 mL, 12.15 mmol) was added to a solution of 4-bromophenol (0.42 g, 2.43 mmol), 4-trifluoromethoxy benzene boronic acid (1.00 g, 4.68 mmol) and copper (II) acetate (0.44g, 2.43 mmol) over heat-activated 4 Å molecular sieves (1.00 g). The reaction mixture was stirred over 16 hours at room temperature. The reaction mixture was quenched with HCl (0.50 M, 44.60 mL) and filtered through a pad of Celite. Organics were extracted with DCM (3 × 15.00 mL) and combined, followed by repeated washing with water (25.00 mL). The combined organic layers were washed with brine, dried over magnesium sulphate, and concentrated *in vacuo*. Purification by silica gel chromatography (hexane) afforded the title compound as a colourless oil (70%, 0.53 g, 1.63 mmol). **HPLC**; 2.95 min (100% reference area); **R_f**; 0.56 (hexane); **δ H NMR** (500 MHz, Chloroform-d) δ 7.37 (d, J = 9.0 Hz, 2H, H-2 & 6), 7.10 (d, J = 9.1 Hz, 2H, H-2' & 6'), 6.91 (d, J = 9.1 Hz, 2H, H-3' & 5'), 6.80 (d, J = 9.0 Hz, 2H, H-3 & 5); **δ C NMR** (126 Hz, Chloroform-d,); δ 156.1 (C-4), 155.5 (C-4'), 145.0 (C-1') 132.8 (C-2' & 6'), 122.7 (C-2 & 6), 120.8 (q, J = 268.1 Hz, CF₃) 120.6 (C-3' & 5'), 119.7 (C-3 & 5), 116.4 (C-1); **v_{max}/cm⁻¹** (oil) 3066, 1582, 1498, 1480, 1260, 1236, 1218, 1203. H¹NMR data in agreement with literature.¹⁴⁵

Ethyl 3-oxo-2-(4-(4-(trifluoromethoxy)phenoxy)phenyl)butanoate (78).



To a solution of 1-Bromo-4-(4-(Trifluoromethoxy)Phenoxy)Benzene (0.30 g, 0.90 mmol) in toluene (2 mL) was added ethyl acetoacetate (0.25 mL, 0.99 mmol), palladium acetate (0.01 g, 5.00 mol%), John Phos (26.8 mg, 10.00 mol%) and potassium phosphate (0.25 g, 1.20 mmol). The reaction mixture was heated to 90 °C for 16 hours. The reaction mixture was then allowed to cool and diluted in DCM (15.00 mL) followed by filtration through Celite. The reaction mixture was then concentrated *in vacuo* and purified using silica gel chromatography. The title compound was obtained (0.1653 g, 0.43 mmol, 47%) as an orange oil, **R_f**; 0.50 (Pet ether: ethyl acetate, 10:1); **δ H NMR** (500 MHz, Chloroform-d); δ 7.33 (d, J = 8.6 Hz, 2H, H-2 & 6), 7.19 (d, J = 8.5 Hz, 2H, H-3 & 5), 7.05-6.94 (m, 4H, H-2', 3', 5' & 6'), 4.61 (s, 1H, R₃CH), 4.27-4.15 (m, 2H, CH₃CH₂O), 2.21 (s, 3H, OCM_e), 1.28 (q, 3H, CH₃CH₂O); **δ ¹³C NMR** (126 MHz, CDCl₃) δ 201.3 (C=O), 168.5 (C=O₂Me), 157.0 (C_q), 155.3 (C_q), 144.8 (C_q), 132.7 (C_q), 130.9 (C-2 & 6), 122.7 (C-3' & 5'), 120.1 (C-3 & 5), 119.0 (C-2' & 6'), 64.9 (CH₃CH₂O), 61.7 (CHR₃), 28.8 ((OC)Me), 14.0 (CH₃CH₂O); **ν_{max} /cm⁻¹**; 2937, 1736, 1720, 1641, 1600, 1496, 1236, 1156; **M/Z** (ESI+); 383.11 (Found MH⁺, 383.1112, C₁₉H₁₉F₃O₅ requires 383.1100);

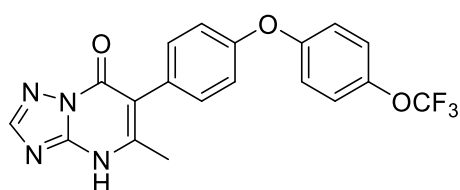
5-Methyl-6-(4-(4-(trifluoromethoxy)phenoxy)phenyl)pyrazolo[1,5-a]pyrimidin-7(4H)-one (72)*



The title compound was synthesised from 3-amino pyrazole (41 mg, 0.50 mmol) according to general procedure B (recrystallized in EtOAc) and isolated as colourless platelets (96 mg, 0.24 mmol, 48%). **MP**; >250 °C; **HPLC**; 3.18 mins (100% reference area); **¹H NMR**

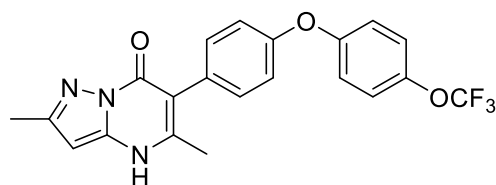
(500 MHz, DMSO); δ 7.88 (d, J = Hz, 1H, H-2), 7.43 (d, J = Hz, 2H, H-2' & 6'), 7.56 (d, J = Hz, 2H, H-3'' & 5''), 7.20 (d, J = Hz, 2H, H-2'' & 6''), 7.11 (d, J = Hz, 2H, H-2' & 6'), 6.15 (d, J = Hz, 1H, H-3), 2,21 (s, 3H, Me); **δ C NMR** (126 MHz, DMSO); 156.1 (C_q), 155.6 (C_q), 155.3 (C_q), 146.9 (C-5), 143.7 (C_q), 143.0 (C-2), 140.8 (C_q), 139.0 (C_q), 133.1 (C-2' & 6'), 129.8 (C_q), 123.0 (C-3'' & 5''), 120.0 (C-2'' & 6''), 118.4 (C-3' & 5'), 107.0 (C_q), 87.9 (C-3), 18.3 (Me); **$\nu_{\max}/\text{cm}^{-1}$** ; 3153, 1650, 1569, 1496, 1348, 1288, 1239; **M/Z** (ESI); 402.11 (Found MH⁺; 402.1065 C₂₀H₁₅F₃N₃O₃ requires 402.1060).

5-Methyl-6-(4-(4-(trifluoromethoxy)phenoxy)phenyl)-[1,2,4]triazolo [1,5-a]pyrimidin-7(4H)-one (73).



The title compound was synthesised from 3-amino triazole (40 mg, 0.47 mmol) according to general procedure **A**, (recrystallized in EtOAc) and isolated as colourless platelets (45 mg, 0.11 mmol, 24%). **MP**; >250 °C; **HPLC**; 3.11 (100% reference area); **$^1\text{H NMR}$** (400 MHz, DMSO) δ 13.32 (s, 1H, NH), 8.24 (s, 1H, C-2), 7.43 (d, J = 8.9 Hz, 2H, 3'' & 5''), 7.36 (d, J = 8.5 Hz, 2H, 2' & 6'), 7.19 (d, J = 8.9 Hz, 2H, 2'' & 6''), 7.12 (d, J = 8.5 Hz, 2H, 3' & 5'), 2.22 (s, 3H, Me); **$^{13}\text{C NMR}$** (101 MHz, DMSO) δ 156.3 (C_q), 156.1 (C_q), 155.9 (C_q), 152.7 (C-2), 150.2 (C_q), 149.1 (C_q), 144.3 (C_q), 133.3 (C-2' & 6'), 129.4 (C_q), 123.5 (C-3'' & 5''), 120.6 (C-2'' & 6''), 118.9 (C-3' & 5'), 110.9 (C_q), 18.8 (Me); **$\nu_{\max}/\text{cm}^{-1}$** ; 2723, 1686, 1649, 1563, 1494, 1343; **M/Z** (ESI); 403.10 (Found MH⁺ 403.1014 C₁₉H₁₄F₃N₄O₃ requires 403.1013).

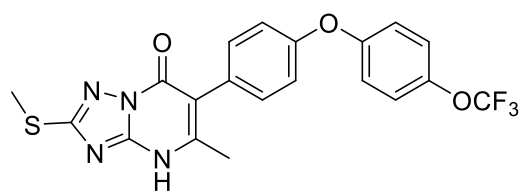
2,5-Dimethyl-6-(4-(4-(trifluoromethoxy)phenoxy)phenyl)pyrazolo[1,5-a]pyrimidin-7(4H)-one (85).



The title compound was synthesised from 3-amino-5 methyl-pyrazole (30 mg, 0.31 mmol) according to general procedure **A** (recrystallized in EtOAc) to afford the title compound as

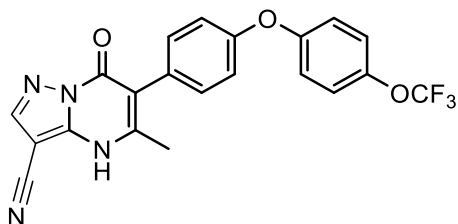
colourless platelets (47 mg, 0.11 mmol, 36%). **MP**; >250 °C; **CHN**; (Found; C, 60.8; H, 3.80; N, 10.1; C₂₁H₁₆F₃N₃O₃ requires; C, 60.7; H, 3.88; N, 10.1%); **HPLC**; 2.95 min (100% reference area); **δ H NMR** (500 MHz, CDCl₃); δ 7.27 (d, J = 8.6 Hz, 2H, H-3'' & 5''), 7.16 (d, J = 8.7 Hz, 2H, H-2' & 6'), 6.99 (d, J = 8.9 Hz, 2H, H-3' & 5'), 6.95 (d, J = 8.6 Hz, 2H, H-2'' & 6''), 5.80 (s, 1H, H-3), 2.34 (s, 3H, 2-Me), 2.21 (s, 3H, 5-Me); **δ C NMR** (126 MHz, DMSO); 157.8 (C_q), 156.5 (C_q), 155.2 (C_q), 153.6 (C_q), 148.2 (C_q), 144.8 (C_q), 141.8 (C_q), 132.8 (C-3'' & 5''), 129.1 (C_q), 122.6 (C-2' & 6'), 120.5 (q, J= 255 Hz, OCF₃), 120.2 (C-2'' & 6''), 118.4 (C-3' & 5'), 107.6 (C_q), 89.3 (C-3), 18.6 (5-Me), 14.6 (C-2Me); **$\nu_{\max}/\text{cm}^{-1}$** ; 2937, 1652, 1631, 1562, 1495, 1243, 1218, 1188, 1164; **M/Z** (ESI); 416.12 (Found MH⁺ 416.1221, C₂₁H₁₇F₃N₃O₃ requires 416.1217).

5-Methyl-2-(methylthio)-6-(4-(4-(trifluoromethoxy)phenoxy)phenyl)-[1,2,4]triazolo [1,5-a]pyrimidin-7(4H)-one (88).



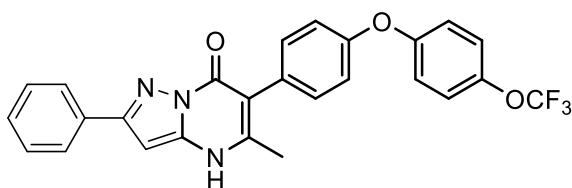
The title compound was synthesised from 3-amino-5-methyl-1,2,4-triazole (30 mg, 0.31 mmol) according to general procedure **A** to afford the title compound as colourless flake crystals (recrystallized EtOAc) (54 mg, 0.12 mmol, 39%); **MP**; 205.5-206.0 °C; **CHN**; (Found; C, 53.8; H, 3.30; N, 12.2; C₂₀H₁₅F₃N₄O₃S requires; C, 53.6; H, 3.37; N, 12.5%); **HPLC**; 3.13 min (100% ref area); **δ H NMR** (500 MHz, CDCl₃); δ 7.30 (d, J = 8.6 Hz, 2H, H-3'' & 5''), 7.22 (d, J = 8.7 Hz, 2H, C-2' & 6'), 7.09 (d, J = 8.7 Hz, 2H, H-3' & 5'), 7.07 (d, J = 8.6 Hz, 2H, H-2'' & 6''), 2.74 (s, 3H, Me-S), 2.49 (s, 2H, Me-5); **δ C NMR** (126 MHz, CDCl₃); 170.7 (C-2), 163.9 (C_q), 157.8 (C_q), 155.2 (C_q), 150.7 (C_q), 146.4 (C_q), 144.9 (C_q), 132.5 (C-3'' & 5''), 127.3 (C_q), 122.7 (C-2' & 6'), 120.4 (C-2'' & 6''), 118.6 (C-3' & 5'), 112.9 (C_q), 19.3 (Me-S), 14.2 (Me-5); **$\nu_{\max}/\text{cm}^{-1}$** ; 2827, 1693, 1572, 1497, 1270, 1235, 1211, 1184, **M/Z** (ESI); 449.09 (Found MH⁺ 449.0893, C₂₀H₁₆F₃N₄O₃S requires 449.0893).

5-Methyl-7-oxo-6-(4-(4-(trifluoromethoxy)phenoxy)phenyl)-4,7-dihydropyrazolo[1,5-a]pyrimidine-3-carbonitrile (87).



The title compound was synthesised from 3-amino-4-carbonitrile-1,2-pyrazole (45 mg, 0.42 mmol) according to general procedure **A** to afford the title compound as white flake crystals (recrystallized EtOAc), (43 mg, 0.10 mmol, 23%); **MP**; > 250 °C; **CHN**; (Found; C, 59.2; H, 3.00; N, 13.1; C₂₁H₁₃F₃N₄O₃ requires; C, 59.2; H, 3.07; N, 13.1%); **¹H NMR** (500 MHz, DMSO) δ 8.49 (s, 1H, H-2), 7.51 (d, *J* = 8.9 Hz, 2H, H-2'' & 6''), 7.44 (d, *J* = 8.6 Hz, 2H, H-2' & 6'), 7.28 (d, *J* = 8.9 Hz, 2H, H-3'' & 5''), 7.20 (d, *J* = 8.6 Hz, 2H, H-3' & 5'), 2.32 (s, 3H, Me). **^δ C NMR** (126 MHz, DMSO) δ 155.7 (C_q), 155.4 (C_q), 155.1 (C_q), 148.3 (C_q), 145.0 (C-2), 144.1 (C_q), 143.8 (C_q), 132.8 (C-2' & 6'), 128.6 (C_q), 123.0 (C-2'' & 6''), 120.2 (C-3'' & 5''), 120.1 (q, *J* = 255 Hz, OCF₃), 118.4 (C-3' & 5'), 112.8 (C-nitrile), 110.5 (C_q), 74.1 (C-3), 18.11 (Me-6); **v_{max}/cm⁻¹**; 2817, 2228, 1665, 1631, 1565, 1493, 1276, 1238; **M/Z** (ESI+); 427.10 (Found MH⁺ 427.1018, C₂₁H₁₄F₃N₄O₃ requires 427.1012).

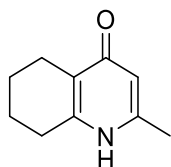
5-Methyl-2-phenyl-6-(4-(4-(trifluoromethoxy)phenoxy)phenyl)pyrazolo[1,5-a]pyrimidin-7(4H)-one (86).



The title compound was synthesised from 3-amino-4-carbonitrile-1,2-pyrazole (67 mg, 0.42 mmol) according to general procedure **A** (recrystallized in DMSO) to afford the title compound as a grey micro crystals (150 mg, 0.31 mmol, 74%) **MP**; > 250 °C; **CHN**; (Found; C, 65.2; H, 3.70; N, 8.7; C₂₆H₁₈F₃N₃O₃ requires; C, 65.4; H, 3.80; N, 8.8%); **HPLC**; 2.47 (90% ref area); **¹H NMR** (500 MHz, DMSO) δ 12.47 (s, 1H, NH), 8.01 (d, *J* = 6.8 Hz, 2H, H-2* & 6*), 7.53 – 7.40 (m, 5H, H-3*, 4*, 5*, 2' & 6'), 7.38 (d, *J* = 8.7 Hz, 2H, H-2'' & 6''), 7.20 (d, *J* = 9.1 Hz, 2H, H-3' & 5'), 7.11 (d, *J* = 8.7 Hz, 2H, H-3'' & 5''), 6.62 (s, 1H, H-3), 2.22 (s, 3H, Me); **¹³C NMR** (126 MHz, DMSO) δ 155.9 (C_q), 155.6 (C_q), 155.4 (C_q), 153.3

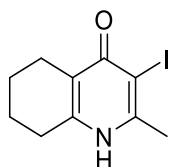
(C_q), 146.8 (C_q), 143.9 (C_q), 142.1 (C_q), 133.0 (C-2'' & 6''), 132.6 (C_q), 129.8 (C_q), 128.8 (C-4*), 128.6 (C-3* & 5*), 126.2 (C-2* & 6*), 122.8 (C-2' & 6'), 120.1 (C-3' & 5'), 118.3 (C-3'' & 5''), 107.6 (C_q), 85.1 (C_q), 18.3 (Me); $\nu_{\max}/\text{cm}^{-1}$; 3130, 1660, 1630, 1566, 1496, 1278; **M/Z** (ESI+); 478.1378 (Found MH⁺, C₂₆H₁₉F₃N₃O₃ requires 478.1373).

2-Methyl-5,6,7,8-tetrahydroquinolin-4(1H)-one (60).



A solution of 4-hydroxyl 2-methyl-quinilone (1.00 g, 6.28 mmol) in acetic acid (10.00 mL) was catalytically hydrogenated over platinum dioxide (0.10 g, 0.44 mmol) for 12 hours. The resulting suspension was filtered through a pad of Celite and washed with ethyl acetate (10.00 mL). The filtrate was concentrated *in vacuo* to afford a yellow/brown oil. Purification by column chromatography (CHCl₃:MeOH) afforded the title compound as colourless amorphous solid. (1.02 g, 6.25 mmol, 99%). **Lit MP**; 246 °C.¹⁴⁶ **MP**; 249-250 °C, **R_f**; 0.05 (10% methanol, DCM); **LCMS**; 1.10 (100% ref area) **δ H NMR**; (500 MHz, Chloroform-d); δ 6.29 (s, 1H, H-3), 2.71 (t, J = 6.1 Hz, 2H, H-8), 2.48 (t, J = 6.1 Hz, 2H, H-8), 2.32 (s, 3H, H-Me), 1.78-1.69 (m, 4H, H-6 & 7); **δ C NMR**; (126 MHz, Chloroform-d) δ 176.6 (C-4), 148.1 (C-9), 147.8 (C-2), 122.0 (C-10), 111.9 (C-3), 26.9 (C-8), 21.8 (C-5), 21.6 & 21.7 (C-6 & 7), 18.7 (Me); $\nu_{\max}/\text{cm}^{-1}$; 2946, 1622, 1518, 1438, 1394, 1202; **M/Z** (ESI+); 164.1122 (Found MH⁺, 164.11 C₁₀H₁₄NO requires 164.1075).

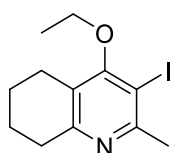
3-Iodo-2-methyl-5,6,7,8-tetrahydroquinolin-4(1H)-one (61).



Saturated potassium iodide solution (sat aq, 5.60 mL) and n-butylamine (5.80 mL, 58.3 mmol) was added to a solution of 2-methyl-5,6,7,8-tetrahydroquinolin-4(1H)-one (0.95 g, 5.83 mmol) and iodine (1.48 g, 5.83 mmol) in DMF (10.00 mL). The reaction mixture was stirred at room temperature for 16 hours. Observed colour change from dark purple to orange. Sodium thiosulphate (0.25 g in 10.00 mL water) was then added

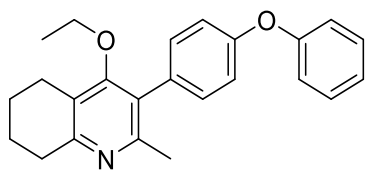
followed by filtration (washed 2 × 10.00 mL water) to afford the title compound as colourless microcrystals (1.45 g, 5.02 mmol, 86%). **MP**; decomposed; **HPLC**: 1.63 (100% reference area) **δ H NMR** (500 MHz, MeOD); δ 2.53 (t, J = 6.1 Hz, 2H, H-8), 2.44 (s, 3H, Me), 2.30 (t, J = 6.1 Hz, 2H, H-5), 1.73-1.67 (m, 2H, H-7), 1.67-1.61 (m, 2H, H-6); **δ C NMR** (126 MHz, MeOD); 173.5 (C-4), 143.4 (C_q), 142.1 (C_q), 132.8 (C-10), 111.9 (C-3), 25.8 (C-8) 24.7 (C-5), 22.5 (C-7), 21.7 (C-6), 21.4 (Me); **$\nu_{\max}/\text{cm}^{-1}$** ; 2850, 1620, 1640, 1495; **M/Z** (ESI+); 290.00 (Found MH⁺, 290.0037 C₁₀H₁₃INO requires 290.0036).

4-Ethoxy-3-iodo-2-methyl-5,6,7,8-tetrahydroquinoline (62).



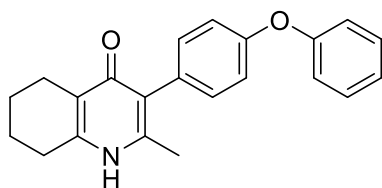
A suspension of 4(1H), 3-iodo-2-methyl, 5,6,7,8-tetrahydroquinolinone (2.20 g, 7.61 mmol) and Potassium carbonate (2.10 g, 15.20 mmol) in DMF (20.00 mL) was heated to 50 °C and stirred for 45 minutes. The reaction mixture was removed from the heat and ethyl iodide (0.89 mL, 11.40 mmol) was added dropwise. The reaction mixture was then heated to 50 °C and stirred for a further 18 hours. Formation of a yellow emulsion was observed. The reaction mixture was then quenched with water (40.00 mL). The organic phase was extracted using the polar extraction technique (ethyl acetate, 3 × 40.00 mL), and the resulting organic layers were combined and dried over MgSO₄ and concentrated *in vacuo* to afford the title compound as an orange oil. (2.00 g, 6.32 mmol, 83%). **HPLC**; 1.84 (90% reference area); **δ H NMR** (500 MHz, CDCl₃); δ 3.96 (q, J = 7.0 Hz, 2H, MeCH₂O), 2.84 (t, J = 6.3 Hz, 2H, H-5), 2.74 (t, J = 6.3 Hz, 2H, H-8), 2.71 (s, 3H, 2-Me), 1.89-1.82 (m, 2H, H-6), 1.78-1.72 (m, 2H, H-7), 1.49 (t, J = 7.0 Hz, 3H, CH₃CH₂O); **δ C NMR** (126 MHz, CDCl₃); 163.9 (C-4), 158.8 (C_q), 158.2 (C_q), 124.5 (C-10), 90.9 (C-3), 68.3 (MeCH₂O), 32.0 (C-5), 29.3 (2-Me), 23.5 (C-8), 22.8 (C-6), 22.3 (C-7), 14.5 (CH₃CH₂O); **$\nu_{\max}/\text{cm}^{-1}$** ; 2932, 1738, 1680, 1560, 1539, 1431, 1410, 1376, 1328, 1241; **M/Z** (ESI+); 318.04 (Found MH⁺, 318.0350, C₁₂H₁₈INO requires 318.0349).

4-Ethoxy-2-methyl-3-(4-phenoxyphenyl)-5,6,7,8-tetrahydroquinoline (63).



A solution of 4-ethoxy, 3-iodo, 2-methyl, 5,6,7,8-tetrahydro, quinolone (1.00 g, 3.16 mmol), 4-phenoxy phenyl boronic acid (1.01 g, 4.73 mmol), Palladium (II) tetra(tri-phenyl-phosphine) (0.18 g, 0.16 mmol) and dipotassium carbonate (2.00 M, 6.40 mL) dissolved in degassed DMF (20.00 mL) was heated to 85 °C and stirred for 12 hours. Observed colour change from yellow to black. The reaction mixture was allowed to cool to room temperature before dilution with ethyl acetate (15.00 mL). The organic layer was extracted using polar extraction technique, before being collected and dried over MgSO₄. The solution was then concentration *in vacuo* and purified via column chromatography to afford the title compound as colourless fine needles (0.45 g, 1.25 mmol, 40%). **MP**; 59.5-60.0 °C **HPLC**; 2.38 (100% ref area); **R_f**; 0.17 (Pet ether : ethyl acetate, 3 : 1); **δ H NMR** (126 MHz, CDCl₃); δ 7.35 (t, J = 7.6 Hz, 2H, H-3'' & 5''), 7.23 (d, J = 8.5 Hz, 2H, H-2' & 6'), 7.11 (t, J = 7.6 Hz, 1H, H-4''), 7.05 (d, 4H, H-3', 5', 2'' & 6'') 3.42 (q, J = 7.0 Hz, 2H, CH₃CH₂O), 2.82 (t, J = 6.4 Hz, 2H, H-5), 2.62 (t, J = 6.3 Hz, 2H, H-8), 2.23 (s, 3H, Me-2), 1.80-1.74 (m, 2H, H-6), 1.73-1.67 (m, 2H, H-7), 1.49 (t, J = 7.0 Hz, 3H, CH₃CH₂O); **δ C NMR** (126 MHz, CDCl₃); 162.2 (C_q), 157.4 (C_q) 157.2 (C_q), 156.5 (C_q), 154.9 (C_q), 131.5 (C-2'' & 6''), 131.2 (C_q), 129.8 (C-3'' & 5''), 126.9 (C_q), 123.5 (C_q), 119.02 (C-3' & 5'), 118.6 (C-2'' & 6''), 68.2 (CH₃CH₂O) 32.5 (C-5), 23.1 (C-8), 23.1(2-Me), 23.0 (C-6), 22.5 (C-7), 15.6 (CH₃CH₂O); **$\nu_{\max}/\text{cm}^{-1}$** ; 2931, 1577, 1551, 1489, 1430, 1328, 1227; **M/Z** (ESI+); 360.20 (Found MH⁺, 360.1963, C₂₄H₂₇NO₂ requires 360.1958).

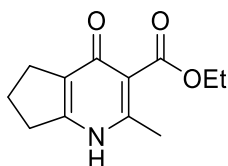
2-Methyl-3-(4-phenoxyphenyl)-5,6,7,8-tetrahydroquinolin-4(1H)-one (57).



The title compound was synthesised from 4-ethoxy,3-(4-phenoxy, benzene),2-methyl,5,6,7,8-hydroquinolone (0.43 g, 1.20 mmol) following general procedure **B** to afford the title compound as colourless microcrystals (0.39 g, 1.20 mmol, 99%). **MP**; > 250 °C; **HPLC**; 2.38

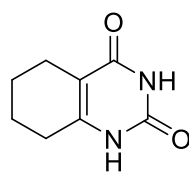
min (100% reference area); **¹H NMR** (500 MHz, DMSO-d₆); δ 7.38 (t, J = 7.9 Hz, 2H, H-3'' & 5''), 7.17 (d, J = 8.5 Hz, 2H, H-2' & 6'), 7.14 (t, J = 7.4 Hz, 1H, H-4''), 7.05 (d, J = 7.9 Hz, 2H, H-2'' & 6''), 6.98 (d, J = 8.5 Hz, 2H, H-3' & 5'), 2.56 (t, J = 5.9 Hz, 2H, H-8), 2.30 (t, J = 6.1 Hz, 2H, H-5), 2.08 (s, 3H, 2-Me), 1.75-1.68 (m, 2H, H-7), 1.68-1.62 (m, 2H, H-6); **^δ C NMR** (500 MHz, DMSO); 175.4 (C-4), 156.5 (C_q), 154.8 (C_q), 143.0 (C_q), 142.1 (C_q), 132.4 (C-2' & 6'), 131.5 (C_q), 129.7 (C-3'' & 5''), 123.7 (C_q), 123.3 (C-4''), 121.2 (C_q), 118.6 (C-3' & 5'), 117.6 (C-2'' & 6''), 26.2 (C-8), 21.9 (C-6), 21.8 (C-5), 21.5 (C-7), 17.7 (2-Me); **v_{max}/cm⁻¹**; 2992, 1618, 1588, 1535, 1351, 1233; **M/Z** (ESI+); 332.17 (Found MH⁺, 332.1673, C₂₂H₂₂NO₂ requires 332.1650).

Ethyl-2-carboxyl-1,5,6,7-Tetrahydro-4H-cyclopenta[b]pyridin-4-one (70).



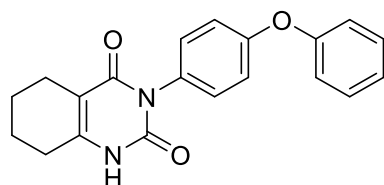
Ethyl-3-aminocrotonate (5.00 mL, 39.53 mmol) and ethyl-2-oxocyclopentanonecarboxylate (5.87 mL, 39.53 mmol) were added to a nitrogen flushed flask of Toluene (20.00 mL) and 4 Å molecular sieves (2.00 g) connected to Dean Stark apparatus. The reaction mixture was stirred at reflux under Nitrogen for 96 hours, after which heating was stopped and the reaction allowed to cool. Precipitate was formed and washed with petroleum ether (20.00 mL) to afford the title compound as pale-yellow powder (4.58 g, 20.72 mmol, 52%). **MP**; >250 °C; **HPLC**; **¹H NMR** (500 MHz, CDCl₃) δ 11.97 (s, 1H, NH), 4.48 (q, J = 7.1 Hz, 2H, CH₃CH₂O), 3.00 (t, J = 7.7 Hz, 2H, H-7), 2.93 (t, J = 7.4 Hz, 2H, H-5), 2.78 (s, 3H, 2-Me), 2.22 – 2.10 (m, 2H, H-6), 1.48 (t, J = 7.1 Hz, 3H, CH₃CH₂O); **¹³C NMR** (101 MHz, CDCl₃) δ 171.7 (C-4), 169.8 (C=O₂Et), 165.0 (C_q), 144.9 (C_q), 121.8 (C_q), 107.3 (C_q), 62.0 (OCH₂CH₃), 35.2 (C-7), 27.0 (C-5 & 2-Me), 22.4 (C-6), 14.2 (OCH₂CH₃); **v_{max}/cm⁻¹**; 2925, 1626, 1512, 1402, 1342, 1309, 1277, 1253; **M/Z** (ESI); 244.09 (Found MNa⁺; 244.0941, C₁₂H₁₆NO₃ requires 244.0944).

1,2,3,4,5,6,7,8-Octahydroquinazoline-2,4,dione (90).



Urea (0.48 g, 8.00 mmol) and ethyl-2-oxocyclohexancarboxylate (1.00 g, 6.00 mmol) were dissolved in ethanol (10.00 mL). Sodium methoxide (3.00 mL, 12.00 mmol) was added and the reaction mixture refluxed at 80 °C for 15 hours. The reaction mixture was allowed to cool and the resulting precipitate was washed with diethyl ether (2 × 10.00 mL) to afford the title compound as a white solid. (0.53 g, 3.17 mmol, 53%). **MP**; >250 °C; **HPLC**; 1.18 mins (100% reference area); **¹H NMR** (501 MHz, DMSO) δ 10.72 (s, 1H, H-1), 8.50 (s, 1H, H-3), 2.28 (t, *J* = 6.2 Hz, 2H, H-8), 2.12 (t, *J* = 6.2 Hz, 2H, H-5), 1.69 – 1.60 (m, 2H, H-7), 1.59 – 1.51 (m, 2H, H-6); **¹³C NMR** (126 MHz, DMSO) δ 166.2 (C_q), 164.4 (C_q), 159.7 (C-9), 105.6 (C-10), 25.7 (C-5), 21.3 (C-8), 21.0 (C-7), 20.5 (C-6); **v_{max}/cm⁻¹**; 2828, 1607, 1418, 1357; **M/Z** (ESI+); 167.08 (Found MH⁺; 167.0815, C₈H₁₁N₂O₂ requires 167.0815).

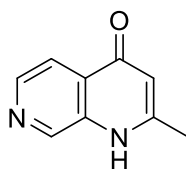
3-(4-Phenoxypheyl)-1,2,3,4,5,6,7,8-octahydroquinazoline-2,4,dione (89)



1,2,3,4,5,6,7,8-Octahydroquinazoline-2,4,dione (0.30 g, 1.80 mmol), 4phenoxyphenyl boronic acid (0.60 g, 2.70 mmol) and copper acetate (0.33 g, 1.80 mmol) were dissolved in ethanol (20.00 mL). Triethylamine (1.20 mL, 9.00 mmol), and pyridine (0.66 mL, 9.00 mmol) were added immediately and the reaction stirred overnight. The reaction was filtered through Celite and neutralised with HCl (0.50 M, 60.00 mL) to give crude solid, this was then recrystallized in DCM to afford product as colourless needles (0.06 g, 0.18 mmol, 10%). **MP**; >250 °C; **HPLC**; 2.68 min (100% reference area); **¹H NMR** (500 MHz, DMSO) δ 11.04 (s, 1H, NH), 7.45 (t, *J* = 7.1 Hz, 2H, H-3'' & 5''), 7.20 (d, *J* = 7.5 Hz, 3H, H-2'', 6'' & 4''), 7.09 (d, *J* = 7.8 Hz, 2H, H-2' & 6'), 7.04 (d, *J* = 7.9 Hz, 2H, H-3' & 5'), 2.39 (s, 2H, H-8), 2.22 (s, 2H, H-5), 1.68 (m, 4H, H-6 & 7); **¹³C NMR** (101 Hz, DMSO); 163.9 (C_q), 156.8 (C_q), 156.7 (C_q), 151.2 (C_q), 146.7 (C_q), 131.1 (C_q), 131.0 (C-2' & 6'),

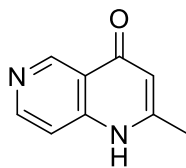
130.7 (C-3'' & 5''), 124.4 (C-4''), 119.6 (C-3' & 5'), 118.7 (C-2'' & 6''), 106.1 (C_q), 26.19 (C-8), 21.8 (C-5), 21.6 (C-7), 21.4 (C-6); $\nu_{\max}/\text{cm}^{-1}$; 2930, 1713, 1633, 1588, 1486, 1422, 1292, 1237; **M/Z** (ESI+); 335.14 (Found MH⁺; 335.1394, C₂₀H₁₉N₂O₃ requires 335.1390).

2-Methyl-1,7-naphthyrid-4(1H)-one (98).



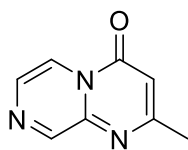
The title compound was synthesised using 3-amino pyridine (3.00 g, 32.00 mmol) following general procedure **C** and purified by column chromatography (DCM:MeOH) and isolated as a colourless solid (0.49 g, 3.10 mmol, 10%). **MP**; >250 °C; **HPLC**; 0.46 mins (100% reference area); **¹H NMR** (500 MHz, CDCl₃) δ 8.52 (s, 1H, H-8), 7.72 (d, J = 8.0 Hz, 1H, H-5), 7.59 – 7.31 (m, 1H, H-6), 6.18 (s, 1H, H-3), 2.28 (s, 3H, 2-Me); **¹³C NMR** (101 MHz, MeOD) δ 178.0 (C-4), 151.9 (C_q), 146.6 (C-6), 138.8 (C_q), 136.6 (C_q), 126.9 (C-8), 126.5 (C-5), 111.0 (C_q), 18.4 (2-Me); $\nu_{\max}/\text{cm}^{-1}$; 2715, 1637, 1550, 1498, 1408, 1329, 1220; **M/Z** (ESI+); 183.05 (Found MNa⁺; 183.0528, C₉H₈N₂ONa requires 183.0529).

1,6-Naphthyrid-(1H)4-one (97).



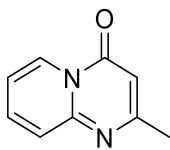
The title compound was synthesised from 4-aminopyridine (2.50 g, 26.60 mmol) according to general procedure **C** purified by column chromatography (CHCl₃:MeOH) and was isolated as a colourless solid (1.40 g, 8.75 mmol, 33%). **MP**; >250 °C; **HPLC**; 0.45 mins (100% reference area); **¹H NMR** (400 MHz, DMSO) δ 11.79 (s, 1H, NH), 9.14 (s, 1H, H-5), 8.56 (d, J = 5.8 Hz, 1H, H-7), 7.37 (d, J = 5.8 Hz, 1H, H-8), 6.04 (s, 1H, H-3), 2.34 (s, 3H, 2-Me); **¹³C NMR** (101 MHz, DMSO) δ 177.1 (C-4), 151.8 (C_q), 150.3 (C-7), 149.2 (C-5), 145.0 (C_q), 119.8 (C_q), 112.1 (C-8), 111.8 (C-3), 20.0 (2-Me); $\nu_{\max}/\text{cm}^{-1}$; 3279, 3118, 2656, 1617, 1557, 1476, 1404, 1321; **M/Z** (ESI); 161.07 (Found MH⁺ 161.0705 C₉H₉N₂O requires 161.0709).

2-Methylpyrazino[1,2-a]pyrimidin-4-one (104).



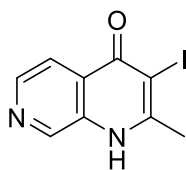
The title compound was synthesised from aminopyrazine (2.00 g, 21.00 mmol) according to general procedure **C** and was isolated as a yellow powder (0.26 g, 1.63 mmol, 7.8%). **MP**; 116.0-117.2 °C; **HPLC**; 0.92 mins (100% ref area); **δ H NMR** (400 MHz, DMSO) δ 9.06 (s, 1H, H-8), 8.63 (d, J = 4.6 Hz, 1H, H-6), 8.19 (d, J = 4.6 Hz, 1H, H-5), 6.56 (s, 1H, H-3), 2.44 (s, 3H, 2-Me); **δ C NMR** (101 MHz, DMSO) δ 165.7 (C-4), 156.3 (C_q), 153.3 (C-8), 144.2 (C_q), 131.9 (C-5), 117.6 (C-6), 107.0 (C-3), 24.5 (2-Me); **$\nu_{\max}/\text{cm}^{-1}$** ; 3097, 1651, 1567, 1503, 1391, 1201; **M/Z** (ESI); 162.07 (Found MH⁺ 162.0659, C₉H₉N₂O requires 162.0662).

2-Methylpyrido[1,2-a]pyrimidin-4-one (96).[^]



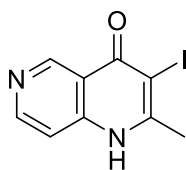
The title compound was synthesised from 2-aminopyridine (3.00 g, 31.90 mmol) according to general procedure **C** and was isolated as a pale-yellow solid (0.05 g, 3.13 mmol, 32%). **MP**; 129.6-130.4 °C; **HPLC**; 0.53 mins (90% reference area); **$^1\text{H NMR}$** (400 MHz, DMSO) δ 8.92 (d, J = 7.0 Hz, 1H, H-5), 8.00 – 7.87 (m, 1H, H-7), 7.61 (d, J = 8.9 Hz, 1H, H-8), 7.31 (t, J = 6.5 Hz, 1H, H-6), 6.29 (s, 1H, H-3), 2.37 (s, 3H, 2-Me); in line with literature **$^{13}\text{C NMR}$** (101 MHz, DMSO) δ 165.2 (C-4), 157.3 (C_q), 150.8 (C_q), 137.8 (C-7), 127.3 (C-5), 125.9 (C-8), 116.3 (C-6), 102.5 (C-3), 24.6 (2-Me); **$\nu_{\max}/\text{cm}^{-1}$** ; 3037, 1699, 1529, 1468, 1405, **M/Z** (ESI); 161.07 (Found MH⁺ 161.0705 C₉H₉N₂O requires 161.0709).

3-Iodo-2-methyl-1,7-naphthyrid-4(1H)-one (118).



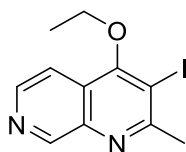
The title compound was synthesised using 2-Methyl-1,7-naphthyrid-4(1H)-one (0.48 mg, 3.00 mmol) following general procedure **D** and was isolated as a colourless solid (0.74 g, 2.60 mmol, 86%). **MP**; >250 °C; **HPLC**; 0.92 min (100% reference area); **¹H NMR** (500 MHz, CDCl₃) δ 8.36 – 7.91 (m, 1H, H-8), 7.49 (dd, *J* = 8.4, 1.1 Hz, 1H, H-5), 7.18 (dd, *J* = 8.6, 4.2 Hz, 1H, H-6), 2.27 (s, 3H, 2-Me); **¹³C NMR** (101 MHz, CDCl₃) δ 172.8 (C-4), 151.6 (C_q), 147.2 (C-8), 136.0 (C_q), 135.8 (C_q), 127.1 (C-7), 126.9 (C-6), 90.2 (C-3), 26.6 (2-Me); **v_{max}/cm⁻¹**; 2898, 1560, 1488, 1412; **M/Z** (ESI+); 286.97 (Found MH⁺; 286.9685 C₉H₈INO₂ requires 286.9676).

3-Iodo-1,6-naphthyrid-4(1H)-one (117).



The title compound was synthesised from 1,6-naphthyrid-4(1H)-one (1.30 g, 8.13 mmol) according to general procedure **D** and was isolated as a colourless solid (2.05 g, 7.12 mmol, 86%). **MP**; 248 °C decolouration; **HPLC**; 0.96 mins (95% reference area); **¹H NMR** (400 MHz, DMSO) δ 12.36 (s, 1H, NH), 9.19 (s, 1H, H-5), 8.63 (d, *J* = 5.8 Hz, 1H, H-7), 7.43 (d, *J* = 5.8 Hz, 1H, H-8), 2.64 (s, 3H, 2-Me). **¹³C NMR** (101 MHz, DMSO) δ 173.3 (C-4), 153.7 (C_q), 150.4 (C-7), 149.8 (C-5), 143.8 (C_q), 115.9 (C-10), 111.9 (C-8), 89.5 (C-3), 26.8 (2-Me); **v_{max}/cm⁻¹**; 3249, 1681, 1622, 1554, 1469, 1379, 1307; **M/Z** (ESI); 286.97 (Found MH⁺ 276.9676 requires C₉H₈INO₂ requires 286.9676).

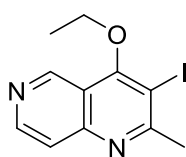
4-Ethoxy-3-iodo-2-methyl-1,7-naphthyridine (119).



The title compound was synthesised using, 3-Iodo-2-methyl-naphthyrid-4(1H)-one (0.72 g, 2.50 mmol) following general procedure **E**. To give the title compound as brown gum (0.24 g, 0.80 mmol, 33%). **MP**; 57.6-

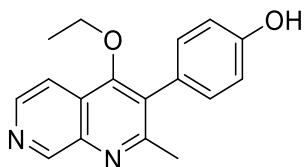
58.0 °C; **HPLC**; 2.05 mins (93% reference area); **¹H NMR** (500 MHz, CDCl₃) δ 8.87 (dd, *J* = 4.0, 1.5 Hz, 1H, H-8), 8.31 (dd, *J* = 8.5, 1.6 Hz, 1H, H-5), 7.63 (dd, *J* = 8.5, 4.1 Hz, 1H, H-6), 4.84 (q, *J* = 7.0 Hz, 2H, OCH₂CH₃), 3.00 (s, 3H, 2-Me), 1.59 (t, *J* = 7.0 Hz, 3H, OCH₂CH₃) **¹³C NMR** (126 MHz, CDCl₃) δ 162.5 (C_q), 162.4 (C_q), 148.8 (C-8), 144.1 (C_q), 136.9 (C-10), 136.6 (C-5), 124.7 (C-6), 92.9 (C-3), 71.9 (CH₂CH₃), 30.8 (2-Me), 16.1 (CH₂CH₃). **v_{max}/cm⁻¹**; 2923, 1561, 1480, 1457, 1367, 1346; **M/Z** (ESI+); 315.00 (Found MH⁺; 314.9991, C₁₁H₁₂IN₂O requires 314.9989).

4-Ethoxy-3-iodo-2-methyl-1,6-naphthyridine (122).



The title compound was synthesised from 3-iodo-1,6-naphthyrid-4(1H)-one (2.00 g, 7.02 mmol) according to general procedure **E** and was isolated as a brown solid (0.60 g, 0.19 mmol, 27%). **MP**; >250 °C; **HPLC**; 1.05 mins (97% reference area); **¹H NMR (400 MHz, DMSO)** δ 9.30 (d, *J* = 1.6 Hz, 1H, H-5), 8.37 (dd, *J* = 7.1, 1.6 Hz, 1H, H-7), 7.63 (d, *J* = 7.1 Hz, 1H, H-8), 4.50 (q, *J* = 7.2 Hz, 2H, CH₃CH₂O), 2.64 (s, 3H, Me), 1.48 (t, *J* = 7.2 Hz, 3H, CH₃CH₂O); **¹³C NMR (101 MHz, DMSO)** δ 171.9 (C_q), 167.5 (C_q), 154.1 (C_q), 145.7 (C-5), 137.5 (C-7), 123.6 (C-8), 119.3 (C-10), 92.8 (C-3), 54.3 (CH₃CH₂O), 31.9 (2-Me), 16.8 (CH₃CH₂O); **v_{max}/cm⁻¹**; 3774, 3389, 1642, 1557, 1373, 1289; **M/Z** (ESI); 315.00 (Found MH⁺ 314.9987, C₁₁H₁₂IN₂O requires 314.9989).

4-Ethoxy-3-phenol-2-methyl-1,7-naphthyridine (120).

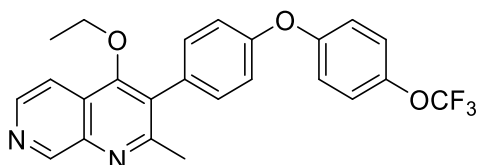


To a nitrogen flushed flask charged with the 4-Ethoxy-3-iodo-2-methyl-1,7-naphthyridine (0.23 g, 0.73 mmol), 4-hydroxybenzene boronic acid (0.15 g, 1.10 mmol) and palladium tetra(triphenylphosphine) (0.05 g, 0.06 mmol) was added degassed DMF (5.00 mL). Potassium carbonate_(aq) (0.90 mL, 2.00 M) was added and the reaction mixture brought up to 80 °C and stirred for 3 hours. The reaction mixture was then cooled to

room temperature and diluted with water (10.00 mL). The organic phase was then extracted using ethyl acetate (3 × 10.00 mL). The organic phases were combined and washed with water (3 × 10.00 mL) and then dried with brine (1 × 10.00 mL) and MgSO₄, before concentration *in vacuo*. A red brown gum was obtained which was washed with minimum volume of DCM to give the title compound as an orange powder (0.08 g, 0.80 mmol, 28%). **MP**; 238.6-239.8 °C; **HPLC** 1.60 min (100% reference area); **¹H NMR** (400 MHz, MeOD) δ 8.78 (dd, *J* = 4.1, 1.4 Hz, 1H, H-8), 8.24 (dd, *J* = 8.6, 1.4 Hz, 1H, H-5), 7.64 (dd, *J* = 8.6, 4.2 Hz, 1H, H-6), 7.08 (d, *J* = 8.5 Hz, 2H, H-2' & 6'), 6.84 (d, *J* = 8.5 Hz, 2H, H-3' & 5'), 4.12 (q, *J* = 7.0 Hz, 2H, CH₃CH₂O), 2.39 (s, 3H, 2-Me), 1.05 (t, *J* = 7.0 Hz, 3H, CH₃CH₂O); **¹³C NMR** (101 MHz, MeOD) δ 161.5 (C_q), 159.5 (C_q), 157.2 (C_q), 149.0 (C-8), 143.1 (C_q), 138.1 (C_q), 135.7 (C-5), 130.8 (C-2' & 6'), 130.3 (C_q), 125.9 (C-1'), 124.5 (C-6), 115.0 (C-3' & 5'), 70.4 (CH₃CH₂O), 23.3 (2-Me), 14.3 (CH₃CH₂O). **v_{max}/cm⁻¹**; 2965, 1581, 1512, 1458, 1375, 1343, 1265; **M/Z** (ESI+); 282.13 (Found MH⁺; 281.1282 C₁₇H₁₈N₂O₂ requires 281.1285).

4-Ethyl-3-(4-(4-trifluoromethoxyphenoxy)phenyl)-2-methyl-1,7-naphthyridone

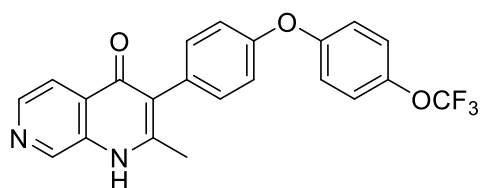
(121)



To an oven dried flask was added 4-ethoxy-3-iodo-2-methyl-1,7-naphthyridine (0.07 g, 0.25 mmol), 4-trifluoromethoxybenzenboronic acid (0.08 g, 0.38 mmol) and copper acetate (0.05 mg, 0.25 mmol) and 4 Å molecular sieves (0.15 g). DCM (5.00 mL) was then added immediately, followed by triethylamine (0.17 mL, 1.25 mmol) and pyridine (0.10 mL, 1.25 mmol). The reaction was stirred at room temperature under air. On completion the reaction mixture was quenched with HCl (2.50 mL, 0.50 M) and filtered through a pad of Celite, followed by repeated washing with DCM (3 × 5.00 mL). The organic layer was extracted with brine, dried over magnesium sulphate, and concentrated *in vacuo*. Purification by silica gel chromatography (ethyl acetate/hexane; 50:50) afforded the title compound as a red crystalline solid (34 mg, 0.08 mmol, 20%). **MP**; 75.2-75.4 °C; **HPLC** 3.23 mins (97% reference area); **¹H NMR** (400 MHz, CDCl₃) δ 8.90 (dd, *J* = 4.0,

1.3 Hz, 1H, H-8), 8.33 (dd, $J = 8.5, 1.3$ Hz, 1H, H-5), 7.61 (dd, $J = 8.5, 4.1$ Hz, 1H, H-6), 7.31 (d, $J = 8.5$ Hz, 2H, H-2' & 6'), 7.24 (d, $J = 8.7$ Hz, 2H, H-2'' & 6''), 7.13 (d, $J = 8.7$ Hz, 2H, H-3' & 5'), 7.10 (d, $J = 9.1$ Hz, 2H, H-3'' & 5''), 4.43 (q, $J = 7.0$ Hz, 2H, OCH_2CH_3), 2.54 (s, 3H, Me), 1.19 (t, $J = 7.0$ Hz, 3H, OCH_2CH_3); $^{13}\text{C NMR}$ (101 MHz, CDCl_3) δ 160.4 (C_q), 159.4 (C_q), 156.4 (C_q), 155.5 (C_q), 148.9 (C-8), 144.7 (C_q), 144.0 (C_q), 138.4 (C_q), 136.6 (C-5), 131.5 (C-2' & 6'), 131.1 (C_q), 129.2 (C_q), 124.3 (C-6), 122.7 (C-2'' & 6''), 120.52 (q, $J = 256$ Hz, OCF_3) 120.0 (C-3'' & 5''), 118.7 (C-3' & 5'), 71.0 (OCH_2CH_3), 25.0 (Me), 15.7 (OCH_2CH_3). $\nu_{\text{max}}/\text{cm}^{-1}$; 2980, 1585, 1498, 1477, 1376, 1351, 1244, 1206; **M/Z** (ESI+); 441.14 (Found MH^+ ; 442.1414 $\text{C}_{24}\text{H}_{20}\text{F}_3\text{N}_2\text{O}_3$ requires 441.1421).

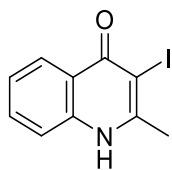
3(4-(4-Trifluoromethoxyphenoxy)phenyl)-2-methyl-1,7-naphthyrid-4(1H)-one
(109)



4-Ethyl-3(4-(4-

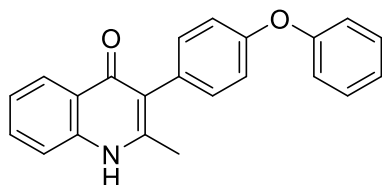
trifluoromethoxyphenoxy)phenyl)-2-methyl-1,7-naphthyridone (31 mg, 0.07 mmol) was dissolved in acetic acid (1.00 mL), hydrobromic acid (0.50 mL, 40% aq) was then added and reaction heated to reflux until complete conversion observed. The reaction mixture was neutralised with sodium hydroxide (2.00 M, 30.00 mL) and precipitate formed. The reaction mixture was then filtered to afford the title compound to give the title compound as a colourless solid (13 mg, 0.03 mmol, 45%). **MP**; 182.4.0-184.0 °C; **HPLC**; 2.83 mins (97% reference area); $^1\text{H NMR}$ (400 MHz, CDCl_3) δ 8.44 (d, $J = 3.6$ Hz, 1H, H-8), 7.75 (d, $J = 8.2$ Hz, 1H, H-5), 7.36 (dd, $J = 8.3, 4.1$ Hz, 1H, H-6), 7.02 (d, $J = 8.6$ Hz, 2H, H-2' & 6'), 6.96 (d, $J = 8.5$ Hz, 2H, H-2'' & 6''), 6.83 (d, $J = 9.2$ Hz, 4H, H-3', 5', 3'' & 5''), 2.09 (s, 3H, Me); $^{13}\text{C NMR}$ (101 MHz, CDCl_3) δ 180.2 (C-4), 160.1 (C_q), 159.8 (C_q), 150.6 (C-8), 148.4 (C_q), 143.1 (C_q), 139.9 (C_q), 136.1 (C-2' & 6'), 134.5 (C_q), 130.9 (C-5), 130.2 (C-6), 128.1 (C_q), 126.4 (C-3'' & 5''), 125.7 (C_q), 123.6 (C-3' & 5'), 122.9 (C-2'' & 6''), 22.7 (Me); $\nu_{\text{max}}/\text{cm}^{-1}$; 2913, 1497, 1263, 1239; **M/Z** (ESI+); 413.11 (Found MH^+ ; 413.11105, $\text{C}_{22}\text{H}_{16}\text{F}_3\text{N}_2\text{O}_3$ requires 413.1108).

3-Iodo-2-methylquinol-4(1H)-one



2-Methylquinol-4(1H)-one (0.10 g, 0.63 mmol) and NIS (0.17 g, 0.76 mmol) were dissolved in acetonitrile (10.00 mL) and heated to reflux. The reaction was allowed to cool and diluted with water (10.00 mL) causing the product to precipitate to crash out as a colourless powder (0.16 g, 0.55 mmol, 87%). **MP**; >250 °C; **HPLC**; 1,73 mins (98% reference area); **¹H NMR** (400 MHz, DMSO) δ 12.14 (s, 1H, NH), 8.08 (d, $J = 7.7$ Hz, 1H, H-5), 7.68 (t_(app), $J = 7.6$ Hz, 1H, H-7), 7.56 (d, $J = 8.2$ Hz, 1H, H-8), 7.36 (t, $J = 7.5$ Hz, 1H, H-6), 2.65 (s, 3H, 2-Me); **¹³C NMR** (101 MHz, DMSO) δ 173.4 (C-4), 151.8 (C-2), 139.4 (C-9), 132.4 (C-7), 126.0 (C-5), 124.3 (C-6), 121.0 (C-8), 118.1 (C-10), 86.5 (C-3), 26.6 (2-Me); **$\nu_{\max}/\text{cm}^{-1}$** ; 2915, 1629, 1544, 1470, 1346, **M/Z** (ESI); 285.97 (Found MH⁺ 285.9719, C₁₀H₉INO requires 285.9723).

2-Methyl-3-(4-phenoxyphenyl)quinol-4(1H)-one (45)



A solution of 3-Iodoquinol-4(1H)-one (0.14 g, 0.50 mmol) 4-phenoxy phenyl boronic acid (0.17 g, 0.75 mmol), Palladium (II) tetra(tri-phenyl-phosphine) (0.03 g, 0.03 mmol) and dipotassium carbonate (2.00 M, 0.75 mL) dissolved in degassed DMF (2.00 mL) was heated to 85 °C and stirred for 12 hours. The reaction mixture was filtered through Celite, followed by dilution with water causing precipitation a solid. The solid was filtered and washed with ethyl acetate to give a grey powder (84 mg, 0.26 mmol, 51%). **MP**; >250 °C; **HPLC**; 3.11 mins (100% reference area); **¹H NMR** (400 MHz, DMSO) δ 8.09 (dd, $J = 8.1, 1.2$ Hz, 1H, H-5), 7.65 – 7.57 (m, 1H, H-7), 7.53 (d, $J = 8.0$ Hz, 1H, H-8), 7.47 – 7.37 (m, 2H, H-3'' & 5''), 7.30 – 7.22 (m, 3H, H-6, 2' & 6'), 7.16 (t, $J = 7.4$ Hz, 1H, H-4''), 7.07 (d, $J = 7.7$ Hz, 2H, H-2'' & 6''), 7.01 (d, $J = 8.6$ Hz, 2H, 3' & 5'), 2.25 (s, 3H, 2-Me); **¹³C NMR** (101 MHz, DMSO) δ 175.1 (C-4), 157.3 (C_q), 155.6 (C_q), 147.9 (C_q), 140.7 (C_q), 133.1 (C-2' & 6'), 132.3 (C_q), 131.5 (C-7), 130.5 (C-3'' & 5''), 125.8 (C-5), 125.1

(C_q), 123.8 (C-4''), 122.9 (C-6), 120.5 (C_q), 119.1 (C-2'' & 6''), 118.9 (C-8), 118.3 (C-3' & 5'), 19.9 (2-Me); $\nu_{\max}/\text{cm}^{-1}$; 2914, 1628, 1584, 1485, 1349, 1294, 1234; **M/Z** (ESI); 328.14 (Found MH⁺; 328.1352, C₂₂H₁₈NO₂ requires 328.1332).

5.3 Experimental: Chapter 3

5.3.1 General method F (Chan Lam)

Copper (II) acetate (1.00 equiv.), triethylamine (5.00 equiv.), and pyridine (5.00 equiv.) was added to a solution of the boronic acid (1.50 equiv.) and phenol (1.00 equiv.) in dichloromethane (10.00 mL mmol⁻¹) over heat-activated 4 Å molecular sieves. The reaction mixture was stirred at room temperature, monitored by LCMS. The reaction mixture was quenched with HCl (0.50 M, 10.00 equiv.) and filtered through a pad of Celite, followed by repeated washing with DCM (3 × 10.00 mL mmol⁻¹). The organics were combined and washed with water (3 × 10.00 mL mmol⁻¹) followed by brine (10.00 mL mmol⁻¹), then dried over magnesium sulphate, and concentrated *in vacuo*. Purification by silica gel chromatography (ethyl acetate/hexane) afforded the title compound.

5.3.2 General method G (Copper coupling)

To a flask containing aryl iodide (1.70 mmol, 1.00 equiv.), phenol (2.10 mmol, 1.20 equiv.), copper (I) iodide (0.17 mmol, 0.10 equiv.), picolinic acid (0.34 mmol, 0.20 equiv.), and potassium phosphate (3.40 mmol, 2.00 equiv.) was added dry DMSO (4.00 mL). The reaction mixture was heated to 80 °C, stirred overnight, and allowed to cool to room temperature. The reaction was then diluted with ethyl acetate (10.00 mL) and water (10.00 mL) and separated. The aqueous phase was extracted with ethyl acetate (2 × 20.0 mL). The combined organic phases were treated with brine, dried over magnesium sulphate, concentrated *in vacuo*. The resulting residue was purified by silica gel chromatography (ethyl acetate/petroleum ether).

5.3.3 General method H (One Pot Suzuki alkylated)

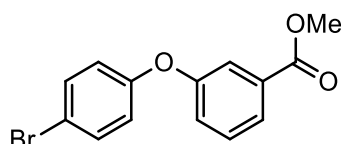
A flask charged with the 4-bromo-diarylether (1.00 equiv.), bispinocolatodiborane (1.10 equiv.), potassium acetate (3.00 equiv.) and Pd(dppf)Cl₂ (3.00 mol%) was flushed with nitrogen. DMF (2.00 mL) was added and the reaction was stirred at 80 °C for 18 hours. After cooling the solution to room temperature, 4-ethoxy-3-iodotetrahydroquinoline (2.00 equiv.), PdCl₂(dppf) (3.00 mol%) and Na₂CO₃ (2.00 M, 5.00 equiv.) were added and

the mixture was stirred at 80 °C under nitrogen for a further 24 hours. The solution was cooled to room temperature, the product was extracted with Et₂O (15.00 mL). The organic layers were combined and washed with H₂O (15.00 mL), brine and dried over MgSO₄ and concentrated *in vacuo*. This was followed by purification by silica gel chromatography (ethyl acetate/petroleum ether).

5.3.4 General method I (One Pot Suzuki)

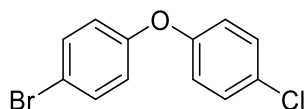
A flask charged with the bromo-diarylether (1.00 equiv.), bispinocolatodiborane (1.10 equiv.), KOAc (3.00 equiv.) and Pd(dppf)Cl₂ (3.00 mol%) was flushed with nitrogen. DMF (2.00 mL) was added and the reaction was stirred at 80 °C for 18 hours. After cooling the solution to room temperature, 3-iodotetrahydroquinoline (2.00 equiv.), PdCl₂(dppf) (3.00 mol%) and Na₂CO₃ (2.00 M, 5.00 equiv.) were added and the mixture was stirred at 80 °C under nitrogen for a further 24 hours. The solution was cooled to room temperature, the product was extracted with Et₂O (15.00 mL). The organic layers were combined and washed with H₂O (15.00 mL), brine and dried over MgSO₄ and concentrated *in vacuo*. This was followed by purification by silica gel chromatography (ethyl acetate/petroleum ether).

Methyl 3-(4-bromophenoxy)benzoate (134)



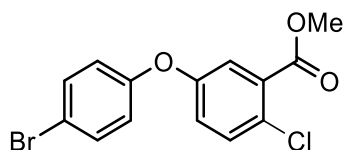
The title compound was synthesised, from 4-bromo-phenol (0.42 g, 2.43 mmol) and 3-methoxycarbonyl phenyl boronic acid (0.43 g, 2.43 mmol), according to general procedure **F** and was isolated as colourless glassy solid (0.21 g, 0.69 mmol, 28%). **Lit MP**; 68-69 °C.¹⁴⁷ **MP**; 62.5-65.3 °C; **HPLC**; 2.60 (100% reference area); **¹H NMR** (500 MHz, CDCl₃) δ 7.73 (dt, *J* = 7.7, 1.2 Hz, 1H, H-6), 7.59 – 7.53 (m, 1H, H-2), 7.38 (d, *J* = 9.0 Hz, 2H, H-3' & 5'), 7.34 (t, *J* = 8.4 Hz, 2H, H-5), 7.13 (ddd, *J* = 8.4, 2.5, 0.9 Hz, 1H, H-4), 6.82 (d, *J* = 9.0 Hz, 2H, H-2' & 6'), 3.83 (s, 3H, Me); **¹³C NMR** (125 MHz, CDCl₃) δ 166.4 (C=O), 157.0 (C-3), 156.0 (C-1'), 132.9 (C-3' & 5'), 132.1 (C-1), 129.9 (C-5), 124.8 (C-6), 123.4 (C-4), 120.7 (C-2' & 6'), 119.6 (C-2), 116.3 (C-4'), 52.3 (methoxy); **v_{max}/cm⁻¹**; 2951, 1720, 1576, 1480, 1437, 1268, 1228; **R_f**; 0.4 (petroleum ether : ethyl acetate, 10 : 1); **M/Z** (ESI+); 307.00 (Found MH⁺, 306.9962 C₁₄H₁₂BrO₃ requires; 306.9964).

1-Bromo-4-(4-chlorophenoxy)benzene (136).



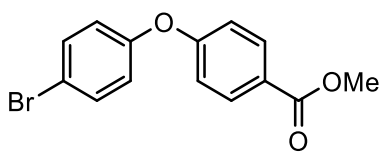
The title compound was synthesised, from 4-bromophenol (0.50 g, 2.80 mmol) and 4-trifluoromethoxy benzene boronic acid (0.60 g, 4.20 mmol), according to general procedure **F** and was isolated as colourless needles (0.16 g, 0.56 mmol, 20%). **Lit MP**; 36.0 °C (ethanol).¹⁴⁸ **MP**; 35.1-36.0 °C ; **HPLC**; 2.72 mins (100% reference area); **¹H NMR** (500 MHz, CDCl₃) δ 7.43 (d, *J* = 9.0 Hz, 2H, H-2 & 6), 7.30 (d, *J* = 9.0 Hz, 2H, H-3' & 5'), 6.93 (d, *J* = 9.0 Hz, 2H, H-2' & 6'), 6.86 (d, *J* = 9.0 Hz, 2H, H-3 & 5); **¹³C NMR** (126 MHz, CDCl₃); δ 156.2 (C-4), 155.4 (C-1'), 132.8 (C-2 & 6), 129.9 (C-3' & 5'), 128.8 (C-4'), 120.5 (C-3 & 5), 120.2 (C-2' & 6'), 116.1 (C-1); **v_{max}/cm⁻¹**; 1891, 1581, 1477, 1238; **R_f**; 0.40 (hexane).

Methyl 5-(4-bromophenoxy)-2-chlorobenzoate (137).



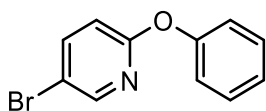
The title compound was synthesised, from 4-bromophenol (0.42 g, 2.43 mmol) and 4-chloro-3-methoxycarbonyl phenyl boronic acid (0.52 g, 2.43 mmol), according to general procedure **F** and was isolated as colourless oil (0.16 g, 0.47 mmol, 19%). **HPLC**; 2.62 mins (84% reference area) ; **¹H NMR** (500 MHz, CDCl₃) δ 7.49 – 7.44 (m, 2H, H-3' & 5'), 7.42 (d, *J* = 3.0 Hz, 1H, H-3), 7.40 (d, *J* = 8.8 Hz, 1H, H-6), 7.05 (dd, *J* = 8.8, 3.0 Hz, 1H, H-5), 6.92 – 6.85 (m, 2H, H-2' & 6'), 3.90 (s, 3H, MeO); **¹³C NMR** (126 MHz, CDCl₃) δ 165.4 (C=O), 155.6 & 155.4 (C-4 & 1'), 133.0 (C-3' & 5'), 132.4 (C-6), 131.3 (C-2), 128.0 (C-1), 122.9 (C-5), 121.2 (C-3), 120.8 (C-2' & 6'), 116.7 (C-4'), 52.6 (C-Me); **v_{max}/cm⁻¹**; 1734, 1571, 1482, 1434, 1228; **R_f**; 0.41 (petroleum ether : ethyl acetate, 10 : 1); **M/Z** (ESI+); 340.96 (Found MH⁺, 340.9569 C₁₄H₁₁BrClO₃ requires 340.9575).

Methyl 4-(4-bromophenoxy)benzoate (135).



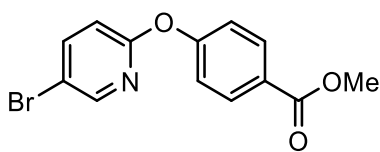
The title compound was synthesised, from 4-bromo-phenol (0.42 g, 2.43 mmol) and 4-methoxycarbonyl phenyl boronic acid (0.43 g, 2.43 mmol), according to general procedure **F** and was isolated as colourless plate crystals (0.25 g, 0.81 mmol, 33%). **Lit MP** 91-92 °C (ethanol).¹⁴⁹ **MP**; 87.5-88.3°C; **HPLC**; 2.60 (100% ref area); **¹H NMR** (500 MHz, CDCl₃) δ 7.94 (d, J = 8.9 Hz, 2H, H-2 & 6), 7.41 (d, J = 8.9 Hz, 2H, H-3' & 5'), 6.91 (d, J = 8.8 Hz, 2H, H-3 & 5), 6.87 (d, J = 8.9 Hz, 2H, H-2' & 6'), 3.83 (s, 3H); **¹³C NMR** (126 MHz, CDCl₃) δ 166.5 (C=O), 161.2 (C-4), 154.9 (C-1'), 133.0 (C-3' & 5'), 131.8 (C-2 & 6), 125.0 (C-1), 121.7 (C-2' & 6'), 117.5 (C-3 & 5), 117.1 (C-4'), 52.1 (C-Me); **v_{max}/cm⁻¹**; 2948, 1712, 1584, 1478, 1434, 1276; **R_f**; 0.33 (petroleum ether : ethyl acetate, 10 : 1); **M/Z** (ESI+); 307.00 (Found MH⁺, 306.9961 C₁₄H₁₂BrO₃ requires 306.9964).

5-Bromo-2-phenoxy pyridine (145).



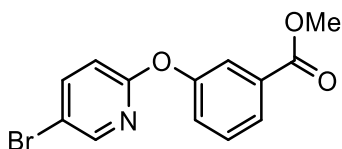
The title compound was synthesised from phenol (0.20 g, 2.10 mmol) and 5-bromo-2-iodopyridine (0.50 g, 1.70 mmol) according to general procedure **G** and was isolated as a colourless oil (295 mg, 1.18 mmol, 70%). **HPLC**; 2.42 (100% reference area); **¹H NMR** (500 MHz, CDCl₃) δ 8.25 – 8.20 (m, 1H, H-6), 7.76 (dd, J = 8.7, 2.6 Hz, 1H, H-4), 7.44 – 7.35 (m, 2H, H-3' & 5'), 7.25 – 7.18 (m, 1H, H-3), 7.16 – 7.09 (m, 2H, H-2' & 6'), 6.83 (dd, J = 8.7, 0.5 Hz, 1H, H-2); **¹³C NMR** (126 MHz, CDCl₃) δ 161.6 (C-2), 152.8 (C-1'), 147.4 (C-2), 140.9 (C-3), 128.7 (C-3' & 5'), 124.0 (C-4), 120.1 (C-2' & 6'), 112.5 (C-5), 112.0 (C-4'); **v_{max}/cm⁻¹**; 3064, 1574, 1490, 1450, 1364 and 1237; **R_f**; 0.40 (Petrol ether : Ethyl Acetate, 10 : 1); **M/Z** (ESI+); 249.99 (Found MH⁺, 249.9853 C₁₁H₉BrNO requires 249.9862). Spectroscopic data in agreement with literature.¹⁵⁰

Methyl 4-((5-bromopyridin-2-yl)oxy)benzoate (146).



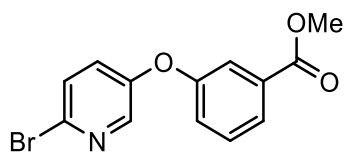
The title compound was synthesised from methyl-4-hydroxybenzoate (0.32 g, 2.10 mmol) and 5-bromo-2-iodopyridine (0.50 g, 1.70 mmol) according to general procedure **G** and was isolated as colourless flakes (0.36 g, 1.16 mmol, 68%). **MP**; 102.3-102.8 °C; **HPLC**; 2.41 (100% reference area); **¹H NMR** (500 MHz, CDCl₃) δ 8.17 (d, *J* = 2.5 Hz, 1H, H-6), 8.02 (d, *J* = 8.7 Hz, 2H, H-3'&5'), 7.75 (dd, *J* = 8.7, 2.5 Hz, 1H, H-4), 7.10 (d, *J* = 8.7 Hz, 2, H-2'&6'), 6.83 (d, *J* = 8.7 Hz, 1H, H-3), 3.85 (s, 3H, Me); **¹³C NMR** (126 MHz, CDCl₃) δ 166.4 (C=O₂Me), 161.7 (C-2'), 157.8 (C-4), 148.5 (C-6'), 142.3 (C-4'), 131.5 (C-2&6), 126.6 (C-1), 120.5 (C-3&5), 114.4 (C-5'), 113.8 (C-3'), 52.1 (OMe); **v_{max}/cm⁻¹**; 2950, 1714, 1578, 1504, 1458, 1434, 1363, 1268, 1238; **Rf**; 0.24 (petroleum ether : ethyl acetate, 10 : 1); **M/Z** (ESI+); 307.99 (Found MH⁺, 307.9914 C₁₃H₁₁BrNO₃ requires 307.9917).

Methyl 3-(5-bromopyridin-2-yl)oxy)benzoate (147)



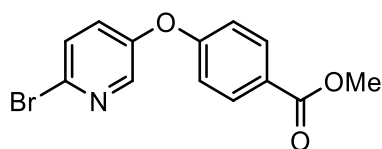
The title compound was synthesised from methyl-3-hydroxybenzoate (0.32 g, 2.10 mmol) and 5-bromo-2-iodopyridine (0.50 g, 1.70 mmol) according to general procedure **G**. The title compound was isolated as colourless flakes (0.20 g, 0.65 mmol, 38%). **MP**; 53-54 °C; **HPLC**; 2.41 mins (100% reference area); **¹H NMR** (500 MHz, CDCl₃) δ 8.13 (dd, *J* = 2.5, 0.5 Hz, 1H, H-6), 7.86 – 7.80 (m, 1H, H-4'), 7.75 – 7.69 (m, 2H, H-4 & 2'), 7.40 (t, *J* = 7.9 Hz, 1H, H-5'), 7.26 (ddd, *J* = 8.1, 2.5, 1.0 Hz, 1H, H-6'), 6.81 (dd, *J* = 8.7, 0.5 Hz, 1H, H-2), 3.84 (s, 3H, Me); **¹³C NMR** (126 MHz, CDCl₃) δ 166.3 (C=O₂Me), 162.1 (C-2'), 153.8 (C-3), 148.4 (C-6'), 142.2 (C-4'), 131.9 (3'), 129.7 (C-5'), 126.2 (C-6), 125.8 (C-4), 122.3 (C-2'), 114.0 (C-5'), 113.3 (C-3'), 52.3 (C-Me); **v_{max}/cm⁻¹**; 2947, 1720, 1573, 1429, 1360, 1264; **Rf**; 0.24 (petroleum ether : ethyl acetate, 10 : 1) **M/Z** (ESI+); 307.99 (Found MH⁺, 307.9914 C₁₃H₁₀BrNO₃ requires 307.9917).

Methyl 3-((6-bromopyridin-3-yl)oxy)benzoate (150)



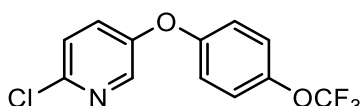
The title compound was synthesised from methyl-3-hydroxybenzoate (0.32 g, 2.10 mmol) and 2-bromo-5-iodopyridine (0.50 g, 1.70 mmol) according to general procedure **G** and was isolated as a colourless oil (0.07 g, 0.23 mmol, 13%). **HPLC**; 2.35 mins (100% reference area); **¹H NMR** (500 MHz, CDCl₃) δ 8.17 (d, *J* = 3.1 Hz, 1H, H-2'), 7.88 – 7.83 (m, 1H, H-6), 7.66 (dd, *J* = 2.3, 1.6 Hz, 1H, H-2), 7.46 (t, *J* = 8.1 Hz, 1H, H-5), 7.45 (d, *J* = 8.6 Hz, 1H, H-5'), 7.23 (ddd, *J* = 8.1, 2.5, 0.9 Hz, 1H, H-4), 7.19 (dd, *J* = 8.6, 3.1 Hz, 1H, H-4'), 3.91 (s, 3H, CO₂Me); **¹³C NMR** (126 MHz, CDCl₃) δ 156.2 (CO₂Me), 153.3 (C-3), 150.3 (C-3'), 141.5 (C-2'), 135.2 (C-6'), 132.4 (C-1), 130.3 (C-5), 128.8 & 128.7 (C-4'&5'), 125.6 (C-6), 123.5 (C-4), 119.7 (C-2), 52.4 (C-Methoxy); **v_{max}/cm⁻¹**; 3069, 2951, 1721, 1567, 1440, 1267; **Rf**; 0.17 (petroleum ether : ethyl acetate, 10 : 1) **M/Z** (ESI+); 307.99 (Found MH⁺, 307.9914 C₁₃H₁₁BrNO₃ requires 307.9917).

Methyl 3-((6-bromopyridin-3-yl)oxy)benzoate (151)



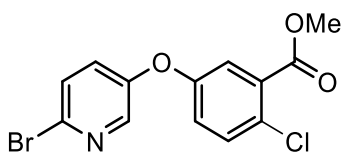
The title compound was synthesised, from 2-bromo-5-hydroxypyridine (0.30 g, 1.70 mmol) and 4-methoxycarbonyl phenyl boronic acid (0.30 g, 1.70 mmol), according to general procedure **F** and was isolated as colourless crystals (0.10 g, 0.33 mmol, 19%). **MP**; 79.0-79.6 °C; **HPLC**; 2.35 mins (100% reference area); **¹H NMR** (500 MHz, CDCl₃) δ 8.14 (s, 1H, H-2'), 7.98 (d, *J* = 8.8 Hz, 2H, H-2&6), 7.42 (d, *J* = 8.6 Hz, 1H, 5'), 7.18 (dd, *J* = 8.4, 2.7 Hz, 1H, 4'), 6.95 (d, *J* = 8.8 Hz, 2H, 3&5), 3.84 (s, 3H, CO₂Me); **¹³C NMR** (126 MHz, CDCl₃) δ 166.23 (CO₂Me), 160.24 (C-4), 152.31 (C-3'), 142.25 (C- 2'), 136.01 (C-6'), 132.02 (C-3&5), 129.68 (C-4'), 128.91 (C-5'), 125.98 (C-1), 117.70 (C-2&6), 52.18 (CO₂Me); **v_{max}/cm⁻¹**; 3032, 1712, 1601, 1504, 1445, 1376, 1255, 1232; **Rf**; 0.17 (petroleum ether : ethyl acetate, 10 : 1); **M/Z** (ESI+); 307.99 (Found MH⁺, 307.9918, C₁₃H₁₀BrNO₃ requires 307.9917).

2-Chloro-5-(4-(trifluoromethoxy)phenoxy)pyridine ()



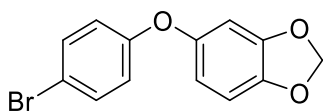
The title compound was synthesised from 4-trifluoromethoxy phenol (0.37 g, 2.10 mmol) and 5-iodoo-2-chloropyridine (0.41 g, 1.70 mmol) according to general procedure **G**. The title compound was isolated as colourless oil (0.18 g, 0.62 mmol, 37%). **HPLC**; 2.94 mins (100% reference area); **¹H NMR** (500 MHz, CDCl₃) δ 8.17 (s, 1H, H-6), 7.29 (m, 2H, H-3 & 4), 7.23 (d, *J* = 9.0 Hz, 2H, H-2' & 6'), 7.03 (d, *J* = 9.0 Hz, 2H, H-3'&5'); **¹³C NMR** (126 MHz, CDCl₃) δ 154.6 (C-1'), 152.8 (C-5), 145.5 (C-4'), 140.8 (C-6), 128.8 & 125.0 (C-3 & 4), 123.0 (C-2' & 6'), 120.5 (q, *J* = 257, OCF₃), 119.9 (C-3' & 5'); **v_{max}/cm⁻¹**; 1500, 1452, 1372, 1210; **R_f**; 0.39, (petroleum ether : ethyl acetate, 10 : 1); **M/Z** (ESI+); 290.02 (Found MH⁺, 290.0187 C₁₂H₈ClF₃NO₂ requires 290.0190).

Methyl 5-((6-bromopyridin-3-yl)oxy)-2-chlorobenzoate (155)



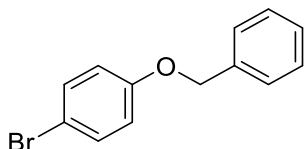
The title compound was synthesised, from 2-bromo-5-hydroxypyridine (0.42 g, 2.43 mmol) and 4-chloro-3-methoxycarbonyl phenyl boronic acid (0.52 g, 2.43 mmol), according to general procedure **F**. The title compound was isolated as colourless oil (0.10 g, 0.29 mmol, 12%). **HPLC**; 2.39 (100% ref area); **¹H NMR** (500 MHz, CDCl₃) δ 8.10 (d, *J* = 3.0 Hz, 1H, H-2'), 7.41 – 7.37 (m, 3H, H-3,6&5'), 7.13 (dd, *J* = 8.6, 3.1 Hz, 1H, H-4), 7.03 (dd, *J* = 8.8, 3.0 Hz, 1H, H-4'), 3.85 (s, 3H, CO₂Me); **¹³C NMR** (126 MHz, CDCl₃) δ 165.1 (CO₂Me), 154.5 (C-5), 152.8 (C-3'), 141.5 (C-2'), 135.7 (6'), 132.8 (3), 131.6 (C-2), 129.1 (C-1), 128.9 (C-5'), 128.8 (C-4), 122.9 (C-4'), 121.3 (C-6), 52.7; **v_{max}/cm⁻¹**; 1732, 1566, 1448, 1366, 1228; **R_f**; 0.22 (petroleum ether : ethyl acetate, 10 : 1); **M/Z** (ESI+); 341.95 (Found MH⁺, 341.9528, C₁₃H₁₀BrClNO₃ requires 341.9527).

5-(4-Bromophenoxy)-2H-1,3-benzodioxole (138).⁺



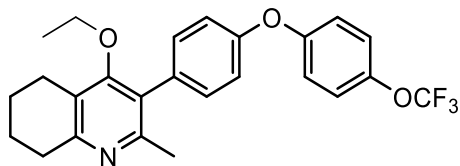
The title compound was synthesised, from 4-bromophenol (0.50 g, 2.89 mmol) and 3,4-methylenedioxy-phenylboronic acid (0.72 g, 4.34 mmol) according to general procedure **F**. The title compound was isolated as a pale-yellow oil (0.20 g, 0.67 mmol, 23%). **HPLC**; 3.28 mins (86%); δ **¹H NMR** (500 MHz, CDCl₃) δ 7.43 (d, J 8.5 Hz, 2H, H-2 & 6), 6.86 (d, J 8.5 Hz, 2H, H-3 & 5), 6.79 (d, J 8.5 Hz, 1H, 5'), 6.59 (d, J 2.5 Hz, 1H, H-2'), 6.51 (dd, J 8.5 & 2.5 Hz, 1H, H-6'), 6.00 (s, 2H, OCH₂O); **¹³C NMR** (126 MHz, CDCl₃) δ 157.5 (C-4), 150.9 (C-1'), 148.5 (C-3'), 144.1 (C-4'), 132.6 (C-2 & 6), 119.4 (C-3 & 5), 115.1 (C-1), 112.1 (C-6'), 108.4 (C-5'), 102.2 (C-4'), 101.6 (OCH₂O); $\nu_{\text{max}}/\text{cm}^{-1}$; 2890, 1583, 1500, 1471, 1355, 1211; **M/Z (ESI)**; not detected.

1-Bromo-4-(phenylmethoxy)benzene (216)



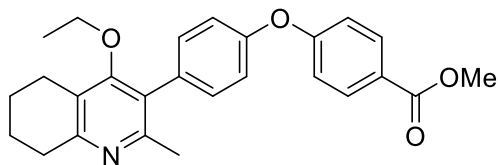
To a suspension of 4-bromophenol (0.26 g, 1.50 mmol) and potassium carbonate (0.29 g, 1.50 mmol) in acetonitrile (10.00 mL) was added benzyl bromide (0.20 mL, 1.65 mmol). The reaction was stirred at room temperature for 16 hours before being concentrated *in vacuo* and purified via column chromatography (Pet:EtOAc) and was isolated as a colourless solid (0.35 g, 1.33 mmol, 89%). **MP**; 58.2-58.7 °C; **¹H NMR**; (400 MHz, CDCl₃) δ 7.44 – 7.31 (m, 7H, H-2, 6, 2', 3', 5' & 6'), 6.86 (d, J = 9.0 Hz, 2H, H-3 & 5), 5.04 (s, 2H, CH₂); **¹³C NMR** (101 MHz, CDCl₃) δ 157.9 (C-4), 136.6 (C-1'), 132.3 (C-2 & 6), 128.7 (C-2' & 6'), 128.1 (C-4'), 127.5 (C-3' & 5'), 116.7 (C-3 & 5), 113.2 (C-1), 70.3 (CH₂); $\nu_{\text{max}}/\text{cm}^{-1}$; 1574, 1451, 1377, 1312, 1238; **M/Z (ESI)**; not detected.

4-Ethoxy-2-methyl-3-(4-(4-(trifluoromethoxy)phenoxy)phenyl)-5,6,7,8-tetrahydroquinoline (158).



The title compound was synthesised from 1-Bromo-4-(4-(trifluoromethoxy)phenoxy)benzene (0.10 g, 0.30 mmol) according to general procedure **H** and was isolated as a colourless solid (0.03 mg, 0.07 mmol, 23%). **MP**: 69.2-71.4; **HPLC**; 2.41 mins (82% reference area); **¹H NMR** (500 MHz, Acetone) δ 7.28 (d, J = 8.7 Hz, 2H, H-2' & 6'), 7.26 (d, J = 9.1 Hz, 2H, H-2'' & 6''), 7.09 (d, J = 9.1 Hz, 2H, H-3'' & 5''), 7.07 (d, J = 8.7, 2H, H-3' & 5'), 3.52 (q, J = 7.0 Hz, 2H, CH₃CH₂O), 2.85 (t, J = 6.5 Hz, 2H, H-8), 2.78 (t, J = 6.2 Hz, 2H, H-5), 2.26 (s, 3H, 2-Me), 1.89 – 1.81(m, 2H, H-7), 1.81– 1.72 (m, 2H, H-6), 0.93 (t, J = 7.0 Hz, 3H, CH₃CH₂O); **δ ¹³C NMR** (126 MHz, Acetone) δ 161.9 (C-4), 157.1 (C_q), 156.5 (C_q), 156.0 (C_q), 154.5 (C_q), 145.3 (C_q), 132.5 (C_q), 132.0 (C-2' & 6'), 126.7 (C_q), 123.0 (C-2'' & 6''), 119.8 (C-3'' & 5''), 119.0 (C-3' & 5'), 68.0 (CH₃CH₂O), 32.5 (C-8), 23.0 (C-5), 22.9 (2-Me), 22.7 (C-7), 22.5 (C-6), 15.1 (CH₃CH₂O); **$\nu_{\max}/\text{cm}^{-1}$** ; 2932, 1578, 1497, 1434, 1329, 1237; **M/Z** (ESI+); 444.18 (Found MH⁺, 444.1792 C₂₅H₂₅F₃NO₃ requires 444.1781).

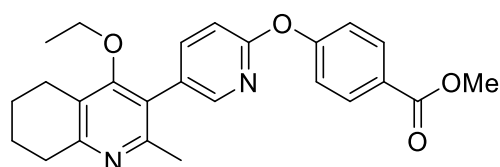
4-Ethoxy-2-methyl-3-(4-(4-methylbenzoate)phenyl)-5,6,7,8-tetrahydroquinoline)phenoxy)benzoate (156).



The title compound was synthesised from methyl 4-(4-bromophenoxy)benzoate (0.15 g, 0.49 mmol) according to general procedure **H** and was isolated as colourless microcrystals (0.06 g, 0.13 mmol, 27%). **MP**; 112.2-112.8 °C; **HPLC**; 2.31 mins (100% reference area); **¹H NMR** (500 MHz, CDCl₃) δ 8.03 (d, J = 8.7 Hz, 2H, H-3'' & 5''), 7.29 (d, J = 8.4 Hz, 2H, H-2' & 6'), 7.11 (d, J = 8.4 Hz, 2H, H-3' & 5'), 7.03 (d, J = 8.7 Hz, 2H, H-2'' & 6''), 3.90 (s, 3H, MeO), 3.51(q, J = 7.0 Hz, 2H, CH₃CH₂O), 2.91 (t, J = 6.2 Hz, 2H, H-5), 2.72 (t, J = 6.0 Hz, 2H, H-8), 2.32 (s, 3H, 2-Me), 1.91-1.84 (m, 2H, H-6), 1.83-1.76 (m, 2H, H-7), 1.04 (t, J = 7.0 Hz, 3H,

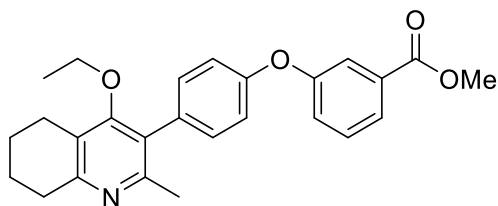
CH₃CH₂O); ¹³C NMR (126 MHz, CDCl₃); δ 166.6 (C=O), 162.2 (C_q), 161.6 (C_q), 157.4 (C_q), 154.9 (C_q), 154.7 (C_q), 132.6 (C_q), 131.8 (C-3' & 5'', 2' & 6'), 126.7 (C_q), 124.7 (C_q), 123.5 (C_q), 119.8 (C-3' & 5'), 117.4 (C-2'' & 6''), 68.3 (CH₃CH₂O), 52.1 (MeO), 32.5 (C-5), 23.1 (C-8), 23.1 (2-Me), 22.9 (C-6), 22.5 (C-7), 15.5 (CH₃CH₂O); $\nu_{\max}/\text{cm}^{-1}$; 2931, 1718, 1579, 1502, 1434, 1287, 1251; **Rf**; 0.30 (Petroleum ether: ethyl acetate, 10:1); **M/Z**; 418.20 (ESI+); (Found MH⁺, 418.2037 C₂₆H₂₈NO₄ requires 418.2018).

4-Ethoxy-2-methyl-3-(4-(4-methylbenzoate)pyrid-3yl)-5,6,7,8-tetrahydroquinoline)phenoxy)benzoate (160).



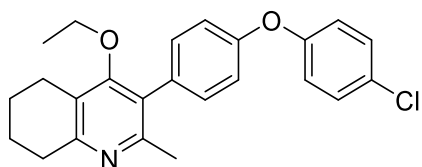
The title compound was synthesised from methyl 4-((5-bromopyridin-2-yl)oxy)benzoate (0.10 g, 0.33 mmol) according to general procedure **H** and was isolated as a colourless gum/semisolid (0.03 g, 0.07 mmol, 21%). ¹H NMR (500 MHz, CDCl₃) δ 8.13 (d, J = 2.3 Hz, 1H, H-2'), 8.10 (d, J = 8.7 Hz, 2H, H-3'' & 5''), 7.67 (dd, J = 8.4, 2.4 Hz, 1H, H-6'), 7.24 (d, J = 8.7 Hz, 2H, H-2'' & 6''), 7.05 (d, J = 8.4 Hz, 1H, H-5'), 3.91 (s, 3H, CO₂Me), 3.53 (q, J = 7.0 Hz, 2H, CH₃CH₂O), 2.92 (t, J = 6.3 Hz, 2H, H-8), 2.71 (t, J = 6.2 Hz, 2H, H-5), 2.27 (s, 3H, 2-Me), 1.84-1.80 (m, 2H, H-7), 1.76-1.71 (m, 2H, H-6), 1.06 (t, J = 7.0 Hz, 3H, CH₃CH₂O); ¹³C NMR (126 MHz, CDCl₃) δ 166.5 (CO₂Me), 162.4 (C_q), 162.0 (C_q), 158.3 (C_q), 158.1 (C_q), 154.8 (C_q), 148.5 (C-2'), 141.6 (C-6'), 131.5 (C-3'' & 5''), 127.8 (C_q), 126.4 (C_q), 123.7 (C_q), 123.6 (C_q), 120.6 (C-2'' & 6''), 111.7 (C-5'), 68.4 (CH₃CH₂O), 52.1 (CO₂Me), 32.6 (C-5), 23.2 (2-Me), 23.1 (C-8), 22.9 (C-6), 22.4 (C-7), 15.5 (CH₃CH₂O); $\nu_{\max}/\text{cm}^{-1}$; 2924, 1719, 1624, 1592, 1434, 1347, 1241; **Rf**; 0.40 (petroleum ether: ethyl acetate, 5:2) **M/Z** (ESI+); 419.20 (Found MH⁺, 419.1993 C₂₅H₂₇N₂O₄ requires 419.1970).

4-Ethoxy-2-methyl-3-(4-(3-methoxybenzoate)phenyl)-5,6,7,8-tetrahydroquinoline)phenoxy)benzoate (157)



The title compound was synthesised from methyl-3-(4-bromophenoxy)benzoate (0.15 g, 0.49 mmol) according to general procedure **H** and was isolated as colourless crystals (0.05 g, 0.12 mmol, 25%). **MP**; 60.0-60.7 °C; **HPLC**; 2.35 mins (100% reference area); **¹H NMR** (500 MHz, CDCl₃) δ 7.84 (d, *J* = 7.7 Hz, 1H, H-4''), 7.72 (s, 1H, H-2''), 7.46 (t, *J* = 7.9 Hz, 1H, H-5), 7.19 (m, 3H, H-6'', 2' & 6'), 7.09 (d, *J* = 8.6 Hz, 2H, H-3' & 5'), 3.83 (s, *J* =, 3H, CO₂Me), 3.45 (q, *J* = 7.0 Hz, 2H, CH₃CH₂O), 2.85 (t, *J* = 6.3 Hz, 2H, H-5), 2.65 (t, *J* = 6.2 Hz, 2H, H-8), 2.26 (s, 3H, 2-Me), 1.88 – 1.78 (m, 2H, H-7), 1.76 – 1.67 (m, 2H, H-6), 0.99 (t, *J* = 7.0 Hz, 3H, CH₃CH₂O); **¹³C NMR** (126 MHz, CDCl₃); δ 166.7 (C=O₂Me), 160.2 (C_q), 157.2 (C_q), 156.0 (C_q), 154.8 (C_q), 145.1 (C_q), 132.0 (C_q), 131.7 (C-2' & 6'), 129.9 (C_q), 129.2 (C-5''), 128.5 (C_q), 126.8 (C_q), 124.6 (C-4''), 123.5 (C-6''), 120.1 (C-2''), 118.8 (C-3' & 5'), 68.3 (CH₃CH₂O), 52.3 (MeO), 32.5 (C-5), 23.1 (2-Me), 23.0 (C-8), 22.5 (C-6), 22.1 (C-7), 15.6 (CH₃CH₂O); **v_{max}/cm⁻¹**; 2921, 1718, 1578, 1485, 1433, 1295, 1227; **R_f**; 0.30 (Petroleum ether: ethyl acetate, 5:1); **M/Z** (ESI+); 418.20 (Found MH⁺ 418.2030, C₂₆H₂₈NO₄ requires 418.2018).

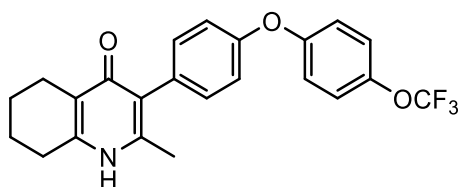
3-(4-(4-Chlorophenoxy)phenyl)-4-ethoxy-2-methyl-5,6,7,8-tetrahydroquinoline (159).



The title compound was synthesised from 1-bromo-4-(4-chlorophenoxy)benzene (0.07 g, 0.24 mmol) according to general procedure **H** and was isolated as colourless oil (0.02 g, 0.05 mmol, 27%). **HPLC**; 2.36 mins (100% reference area); **¹H NMR** (500 MHz, CDCl₃) δ 7.25 (d, *J* = 8.9 Hz, 2H, H-3'' & 5''), 7.17 (d, *J* = 8.7 Hz, 2H, H-2' & 6'), 6.98 (d, *J* = 8.7 Hz, 2H, H-3' & 5'), 6.93 (d, *J* = 8.9 Hz, 2H, H-2'' & 6''), 3.45 (q, *J* = 7.0 Hz,

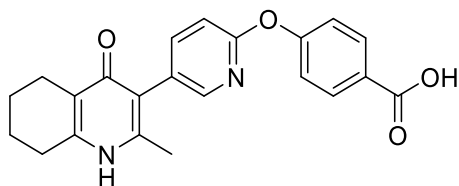
2H, CH₃CH₂O), 2.89 (t, *J* = 6.3 Hz, 2H, H-5), 2.65 (t, *J* = 6.1 Hz, 2H, H-8), 2.28 (s, 3H, 2-Me), 1.90 – 1.61 (m, 4H, H-6 & 7), 0.98 (t, *J* = 7.0 Hz, 3H, CH₃CH₂O); ¹³C NMR (126 MHz, CDCl₃) δ 156.4 (C_q), 155.6 (C_q), 154.51 (C_q), 131.6 (C-2' & 6'), 129.9 (C-3'' & 5''), 128.6 (C_q), 126.8 (C_q), 123.9 (C_q), 120.3 (C-2'' & 6''), 119.1 (C_q), 118.6 (C-3' & 5'), 68.5 (CH₃CH₂O), 31.9 (C-5), 23.0 (C-8), 22.7 (2-Me), 22.7 (C-6) 22.3 (C-7), 15.6 (CH₃CH₂O); *v*_{max}/cm⁻¹; 2932, 1736, 1575, 1506, 1434, 1405, 1329; **Rf**; 0.40 (petroleum ether : ethyl acetate, 5 : 1); **M/Z** (ESI+); 394.16 (Found MH⁺ 394.1575, C₂₄H₂₅ClNO₂ requires 394.1568).

2-Methyl-3-(4-(4-(trifluoromethoxy)phenoxy)phenyl)-5,6,7,8-tetrahydroquinolin-4(1H)-one (169).



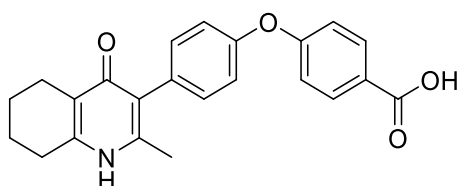
The title compound was synthesised from 4-ethoxy-2-methyl-3-(4-(4-(trifluoromethoxy)phenoxy)phenyl)-5,6,7,8-tetrahydroquinoline (0.03 g, 0.07 mmol) according to general procedure **B** and isolated as a colourless solid (0.03 g, 0.06 mmol, 86%). **MP**; >250 °C; **HPLC**; 2.78 mins (100% reference area); ¹H NMR (500 MHz, DMSO) δ 11.07 (s, 1H, NH), 7.40 (d, *J* = 8.5 Hz, 2H, H-2' & 6'), 7.19 (d, *J* = 8.5 Hz, 2H, H-3'' & 5''), 7.13 (d, *J* = 9.0 Hz, 2H, H-3' & 5'), 7.02 (d, *J* = 8.5 Hz, 2H, H-2'' & 6''), 2.54 (t, *J* = 6.0 Hz, 2H, H-8), 2.28 (t, *J* = 5.9 Hz, 2H, H-5), 2.07 (s, 3H, 2-Me), 1.71 (m, 2H, H-7), 1.65 (m, 2H, H-6); ¹³C NMR; (126 MHz, DMSO) δ 175.7 (C-4), 155.9 (C_q), 154.5 (C_q), 143.5 (C_q), 143.2 (C_q), 142.2 (C_q), 132.5 (C-3'' & 5''), 132.2 (C_q), 123.6 (C_q), 123.0 (C-2' & 6'), 121.3 (C_q), 119.6 (C-3' & 5'), 118.2 (C-2'' & 6''), 26.2 (C-8), 21.9 (C-7) 21.8 (C-5), 21.5 (C-6), 17.7 (2-Me); *v*_{max}/cm⁻¹; 2933, 1619, 1500, 1464, 1241; **M/Z** (ESI+); 416.15 (Found MH⁺, 416.1492 C₂₃H₂₁F₃NO₃ requires 416.1473).

4-(4-(2-Methyl-4-oxo-,5,6,7,8-tetrahydroquinolin-3-yl)pyrid-2-oxo)benzoic acid (165).



The title compound was synthesised from 4-Ethoxy-2-methyl-3-(4-(4-methylbenzoate)pyrid-3yl)-5,6,7,8-tetrahydroquinoline)phenoxy)benzoate (30 mg, 0.07 mmol) according to general procedure **B**, and was isolated as colourless solid (13 mg, 0.03 mmol, 45%). **MP**; > 250 °C **HPLC**; 0.96 mins (100% reference area); **¹H NMR** (500 MHz, DMSO) δ 12.83 (s, 1H, NH), 11.03 (s, 1H, CO₂H), 8.00 (d, J = 8.7 Hz, 2H, H-3'' & 5''), 7.99 (s, 1H, H-2'), 7.73 (dd, J = 8.4, 2.4 Hz, 1H, H-6'), 7.24 (d, J = 8.7 Hz, 2H, H-2'' & 6''), 7.12 (d, J = 8.4 Hz, 1H, H-5'), 2.56 (t, J = 5.8 Hz, 2H, H-8), 2.30 (t, J = 5.8 Hz, 2H, H-5), 2.11 (s, 3H, 2-Me), 1.82 – 1.51 (m, 4H, H-6 & 7); **¹³C NMR** (126 Hz, DMSO) δ 166.7 (C-4), 160.7 (C=O), 158.1 (C_q), 148.6 (C-6'), 143.7 (C_q), 143.1 (C_q), 142.8 (C-4'), 131.2 (C-3'' & 5''), 128.0 (C_q), 126.5 (C_q), 121.3 (C_q), 120.4 (C-2'' & 6''), 120.2 (C_q), 111.1 (C-3'), 26.2 (C-5''), 21.8 (C-8''), 21.7 (C-6''), 21.4 (C-7''), 17.7 (2-Me); **ν_{\max} /cm⁻¹**; 2924, 1680, 1593, 1461, 1253; **M/Z** (ESI+); 377.15 (Found MH⁺, 377.1497 C₂₂H₂₁N₂O₄ requires 377.1496).

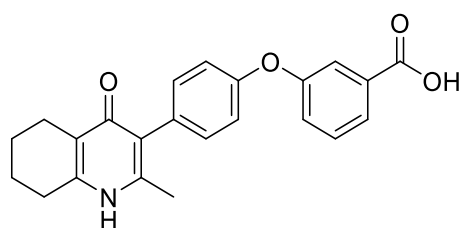
4-(4-(2-Methyl-4-oxo-1,4,5,6,7,8-hexahydroquinolin-3-yl)phenoxy)benzoic acid (166).



The title compound was synthesised from 4-Ethoxy-2-methyl-3-(4-(4-methylbenzoate)phenyl)-5,6,7,8-tetrahydroquinoline)phenoxy)benzoate (50 mg, 0.12 mmol) according to general procedure **B**, and was isolated as colourless crystals (33 mg, 0.09 mmol, 72%). **MP**; 249.0-250.0 °C; **HPLC**; 0.98 mins (97% reference area); **¹H NMR** (500 MHz, DMSO) δ 13.79 (s, 1H, NH), 12.80 (s (b), 1H, CO₂H), 7.99 (d, J = 8.8 Hz, 2H, H-3'' & 5''), 7.36 (d, J = 8.7 Hz, 2H, H-2' & 6'), 7.24 (d, J = 8.7 Hz, 2H, H-3' & 5'), 7.14 (d, J = 8.8 Hz, 2H, H-2'' & 6''), 2.92 (t, J = 5.1 Hz,

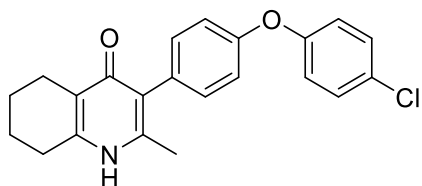
2H, H-8), 2.62 (t, $J = 5.0$ Hz, 2H, H-5), 2.31 (s, 3H, 2-Me), 1.90-1.76 (m, 4H, H-6 & 7); $^{13}\text{C NMR}$ (126 MHz, DMSO) δ 166.8 (C_q), 166.7 (C_q), 160.6 (C_q), 155.4 (C_q), 149.9 (C_q), 148.8 (C_q), 132.2 (C-2' & 6'), 131.7 (C-3'' & 5''), 127.8 (C_q), 125.6 (C_q), 123.4 (C_q), 120.9 (C_q), 120.1 (C-3' & 5'), 117.6 (C-2'' & 6''), 26.7 (C-8), 21.8 (C-5), 20.7 (C-7), 20.5 (C-6), 18.0 (2-Me); $\nu_{\text{max}}/\text{cm}^{-1}$; 3370, 2835, 1687, 1595, 1504, 1425, 1293, 1246; **M/Z** (ESI+); 376.16 (Found MH⁺, 376.1550, C₂₃H₂₂NO₄ requires 376.1543).

3-(4-(2-methyl-4-oxo-5,6,7,8-tetrahydroquinolin-3-yl)phenoxy)benzoic acid
(167).



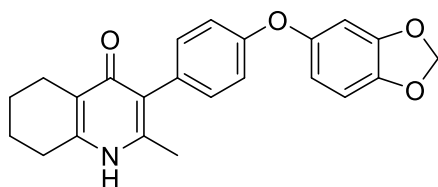
The title compound was synthesised from compound 4-Ethoxy-2-methyl-3-(4-(3-methoxybenzoate)phenyl)-5,6,7,8-tetrahydroquinoline)phenoxy)benzoate (50 mg, 0.12 mmol) according to general procedure **B**, and was isolated as colourless crystals (7 mg, 0.02 mmol, 12%). **MP**; >250 °C; **HPLC**; 0.86 mins (100% reference area); $^1\text{H NMR}$ (500 MHz, DMSO) δ 13.00 (s, 1H, NH), 11.31 (s, 1H, CO₂H), 7.70 (d, $J = 7.9$ Hz, 1H, H-4''), 7.52 (t, $J = 7.9$ Hz, 1H, H-5''), 7.48 (dd, $J = 2.2, 1.6$ Hz, 1H, H-2''), 7.31 (dd, $J = 7.9, 1.6$ Hz, 1H, H-6''), 7.21 (d, $J = 8.6$ Hz, 2H, H-2' & 6'), 7.04 (d, $J = 8.6$ Hz, 2H, H-3' & 5'), 2.58 (t, $J = 5.8$ Hz, 2H, H-5), 2.32 (t, $J = 5.8$ Hz, 2H, H-8), 2.09 (s, 3H, Me), 1.76 – 1.59 (m, 4H, H-6 & 7); $^{13}\text{C NMR}$ (126 MHz, DMSO) δ 166.6 (C-4), 157.1 (CO₂H), 154.6 (C_q), 144.1 (C_q), 143.1 (C_q), 132.7 (C-2' & 6'), 132.4 (C_q), 131.5 (C_q), 130.4 (C-5''), 124.1 (C-4''), 123.6 (C_q), 122.9 (C-6''), 121.2 (C_q), 118.4 (C-3' & 5'), 118.3 (C-2''), 26.3 (C-5), 21.8 (C8), 21.7 (C-6), 21.4 (C-7), 17.8 (2-Me); $\nu_{\text{max}}/\text{cm}^{-1}$; 3390, 2922, 1699, 1618, 1504, 1443, 1238; **M/Z** (ESI+); 376.15 (Found MH⁺ 376.1547, C₂₃H₂₂NO₄ requires 376.1543).

Formation of: 3-(4-(4-chlorophenoxy)phenyl)-2-methyl-5,6,7,8-tetrahydroquinolin-4(1H)-one (168).



The title compound was synthesised from 3-(4-(4-chlorophenoxy)phenyl)-4-ethoxy-2-methyl-5,6,7,8-tetrahydroquinoline (20 mg, 0.05 mmol) according to general procedure **B** and was isolated as colourless solid (18 mg, 0.05 mmol, 95%). **MP**; >250 °C; **HPLC** 1.01 (100% ref area); **¹H NMR** (500 MHz, DMSO) δ 10.99 (s, 1H, NH), 7.44 (d, J = 8.9 Hz, 2H, H-2' & 6'), 7.18 (d, J = 8.6 Hz, 2H, H-3'' & 5''), 7.05 (d, J = 8.9 Hz, 2H, H-3' & 5'), 7.04 (d, J = 8.6 Hz, 2H, H-2'' & 6''), 2.56 (t, J = 5.3 Hz, 2H, H-5), 2.29 (t, J = 5.3 Hz, 2H, H-8), 2.07 (s, 3H, 2-Me), 1.78 – 1.55 (m, 4H, H-6 & 7); **¹³C NMR** (126 MHz, DMSO) δ 171.9 (C-4), 155.8 (C_q), 154.7 (C_q), 142.8 (C_q), 132.4 (C-3'' & 5''), 130.0 (C_q), 129.9 (C-2' & 6'), 127.0 (C_q), 123.6 (C_q), 121.2 (C_q), 120.1 (C-3' & 5'), 118.6 (C_q), 118.1 (C-2'' & 6''), 26.3 (C-5), 21.8 (C-8), 21.7 (C-7), 21.4 (C-6), 17.8 (2-Me); **ν_{\max} /cm⁻¹**; 2940, 1619, 1504, 1461, 1273, 1237; **M/Z** (ESI+); 366.13 (Found MH⁺ 366.1262, C₂₂H₂₁ClNO₂ requires 366.1253).

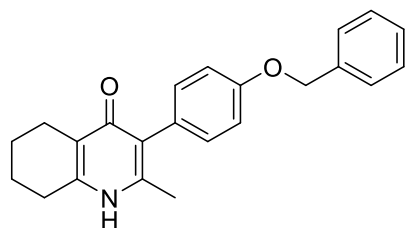
3-[4-(2H-1,3-benzodioxol-5-yloxy)phenyl]-2-methyl-5,6,7,8-tetrahydroquinolin-4(1H)-one (218).⁺



The title compound was synthesised from 5-(4-bromophenoxy)-2H-1,3-benzodioxole (200 mg, 0.68 mmol) and 3-iodo-5,6,7,8-tetrahydroquinolin-4(1H)-one (288 mg, 1.02 mmol) according to general procedure **I** and was isolated as a pale grey solid (40 mg, 0.11 mmol, 16%). **HPLC**; 3.28 mins (86% reference area); **MP**; >250 °C; **¹H NMR** (400 MHz, CDCl₃)⁺ δ 12.89 (s, 1H, NH), 7.20 (q, J = 8.7 Hz, 4H, H-2', 3', 5' & 6'), 6.86 (d, J = 8.3 Hz, 1H, H-5''), 6.67 (d, J = 2.2 Hz, 1H, H-3''), 6.62 (dd, J = 8.3, 2.2 Hz, 1H, H-6''), 6.05 (s, 2H, OCH₂O), 2.99 (t, J = 5.3 Hz, 2H, H-8), 2.75 (t, J = 5.6 Hz, 2H, H-5), 2.41 (s, 3H, 2-Me), 2.03 – 1.79 (m, 4H, H-6 & 7); **δ ¹³C**

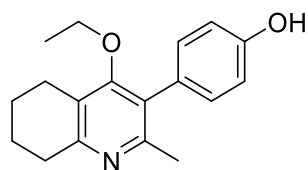
NMR (101 MHz, CDCl₃)⁺ δ 164.7 (C-4), 160.9 (C_q), 152.2 (C_q), 150.2 (C_q), 149.3 (C_q), 148.7 (C_q), 144.9 (C_q), 131.4 (C-2' & 6'), 123.3 (C_q), 121.6 (C_q), 120.7 (C_q), 118.9 (C-3' & 5'), 113.3 (C-6''), 108.7 (C-5''), 103.0 (C_q), 101.8 (OCH₂O), 26.9 (C-5), 21.5 (C-8), 20.6 (C-7), 20.6 (C-6), 18.0 (2-Me). **v_{max}/cm⁻¹**; 3428, 3270, 3077, 3062, 3002, 2923, 2856, 2837, 2799, 1712, 1633, 1619, 1602, 1537, 1504, 1463; **M/Z** (ESI); 375.1563, (C₂₃H₂₂NO₄ requires 375.1471).

3-[4-(benzyloxy)phenyl]-2-methyl-5,6,7,8-tetrahydro-1H-quinolin-4-one (220).



The title compound was synthesised from 1-bromo(4-benzyloxy)benzene (132 mg, 0.50 mmol) 3-iodo-2-methyl-5,6,7,8-tetrahydroquinolin-4(1H)-one (150 mg, 0.75 mmol) according to general procedure I and was isolated as an orange solid (8 mg, 0.02 mmol, 5%). **MP** >250 °C; **HPLC**; 2.55 mins (100% reference area); **¹H NMR** (501 MHz, CDCl₃) δ 7.22 (d, *J* = 7.4 Hz, 2H, H-2'' & 6''), 7.15 (t, *J* = 7.1 Hz, 2H, H-3'' & 5''), 7.09 (t, *J* = 7.9 Hz, 1H, H-4''), 6.89 (d, *J* = 8.4 Hz, 2H, H-2' & 6'), 6.78 (d, *J* = 8.4 Hz, 1H, H-3' & 5'), 4.87 (s, 1H, PhCH₂O), 2.40 (t, *J* = 4.8 Hz, 2H, H-5), 2.28 (t, *J* = 5.5 Hz, 2H, H-8), 1.89 (s, 3H, 2-Me), 1.62-1.57 (m, 2H, H-7), 1.57-1.51 (m, 2H, H-6); **¹³C NMR** (101 MHz, CDCl₃/MeOH) δ 181.4 (C_q), 161.8 (C_q), 148.5 (C_q), 147.8 (C_q), 141.0 (C_q), 135.5 (C-2' & 6'), 132.4 (C-3'' & 5''), 131.9 (C_q), 131.8 (C-4''), 131.3 (C-2'' & 6''), 129.8 (C_q), 126.9 (C_q), 118.5 (C-3' & 5'), 73.9 (PhCH₂O), 30.6 (C-5), 25.9 (C-6), 25.7 (C-8), 25.6 (C-7), 21.5 (2-Me); **v_{max}/cm⁻¹**; 2924, 1608, 1562, 1513, 1451, 1327, 1268, 1238; **M/Z (ESI)**; 346.18 (Found MH⁺; 346.1809, C₂₃H₂₄NO₂ requires 346.1801).

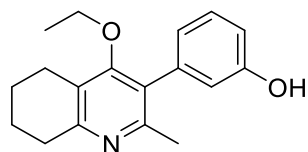
4-(4-Ethoxy-2-methyl-5,6,7,8-tetrahydroquinolin-3-yl)phenol (174).



To a nitrogen flushed flask charged with 4-ethoxy-3-iodo-2-methyl-5,6,7,8-tetrahydroquinoline (0.40 g, 1.26 mmol), 4-hydroxybenzene boronic acid (0.26 g, 1.89 mmol) and palladium

tetra(triphenylphosphine) (0.07 mg, 0.06 mmol) was added degassed DMF (10.00 mL). Potassium carbonate (aq) (3.00 mL, 2.00 M) was added and the reaction mixture brought up to 80 °C and stirred for 3 hours. The reaction mixture was then cooled to room temperature and diluted with water (10.00 mL). The organic phase was then extracted using ethyl acetate (3 x 20.00 mL). The organic phases were combined and washed with water (3 x 20.00 mL) and then dried with brine (1 x 10.00 mL) and MgSO₄, before concentration *in vacuo*. The resulting reddish-brown solid was then recrystallized in ethyl acetate. To yield the title compound as a colourless solid (0.22 g, 0.78 mmol, 61%). **MP**; 225-226 °C; **HPLC**; 1.98 mins (100% reference area); **¹H NMR** (500 MHz, MeOD) δ 7.07 (d, *J* = 8.6 Hz, 2H, H-3 & 5), 6.86 (d, *J* = 8.6 Hz, 2H, H-2 & 6), 3.51 (q, *J* = 7.0 Hz, 2H, CH₃CH₂O), 2.83 (t, *J* = 6.3 Hz, 2H, H-8'), 2.72 (t, *J* = 6.1 Hz, 2H, H-5'), 2.23 (s, 3H, 2-Me), 1.95 – 1.72 (m, 4H, H-6' & 7'), 1.00 (t, *J* = 7.0 Hz, 3H, CH₃CH₂O); **¹³C NMR** (126 MHz, MeOD) δ 164.0 (C_q), 158.1 (C_q), 157.4 (C_q), 156.1 (C_q), 132.2 (C-2' & 6'), 129.1 (C_q), 127.9 (C_q), 124.9 (C_q), 116.2 (C-3' & 5'), 69.1 (CH₃CH₂O), 32.7 (C-5), 23.9 (C-8), 23.8 (C-6), 23.4 (C-7), 22.3 (Me), 15.7 (CH₃CH₂O); **v_{max}/cm⁻¹**; 2978, 2942, 1609, 1557, 1514, 1439, 1331, 1294, 1248. **RF**; 0.22 (EtOAc); **M/Z** (ESI+); 284.17 (Found MH⁺ 284.1664, C₁₈H₂₂NO₂ requires 284.1651).

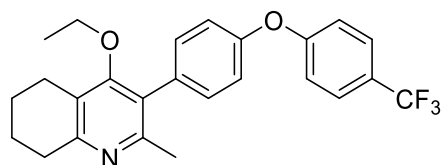
3-(4-Ethoxy-2-methyl-5,6,7,8-tetrahydroquinolin-3-yl)phenol (175).



To a nitrogen flushed flask charged with 4-ethoxy-3-iodo-2-methyl-5,6,7,8-tetrahydroquinoline (1.28 g, 4.03 mmol), 3 hydroxybenzene boronic acid (0.84 g, 6.05 mmol) and palladium tetra(triphenylphosphine) (0.23 g, 0.20 mmol) was added degassed DMF (15.00 mL). Potassium carbonate (aq) (5.00 mL, 2.00 M) was added and the reaction mixture brought up to 80 °C and stirred for 3 hours. The reaction mixture was then cooled to room temperature and diluted with water (10.00 mL). The organic phase was then extracted using ethyl acetate (3 x 20.00 mL). The organic phases were combined and washed with water (3 x 20.00 mL) and then dried with brine (1 x 10.00 mL) and MgSO₄, before concentration *in vacuo*. The resulting solid was recrystallized from toluene and isolated as

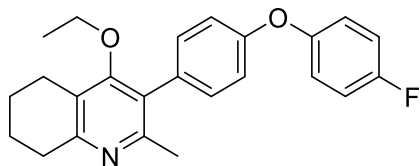
pale-yellow microcrystals (0.58 g, 2.05 mmol, 51%). **MP**; 250.4-251.5 °C; **HPLC**; 2.03 mins (86% reference area); **¹H NMR** (400 MHz, MeOD) δ 7.26 (t, $J = 7.8$ Hz, 1H, H-5'), 6.83 (dd, $J = 8.1, 1.8$ Hz, 1H, H-6'), 6.77 – 6.67 (m, 2H, H-2' & 4'), 3.57 (q, $J = 7.0$ Hz, 2H, CH₃CH₂O), 2.86 (t, $J = 6.3$ Hz, 2H, H-8), 2.73 (t, $J = 6.1$ Hz, 2H, H-5), 2.24 (s, 3H, Me), 1.90 (dd, $J = 7.6, 3.4$ Hz, 2H, H-7), 1.86 – 1.71 (m, 2H, H-6), 1.03 (t, $J = 7.0$ Hz, 3H, CH₃CH₂O); **¹³C NMR** (101 MHz, MeOD) δ 162.4 (C_q), 157.2 (C_q), 156.4 (C_q), 154.4 (C_q), 137.2 (C_q), 129.1 (C-5'), 127.8 (C_q), 123.6 (C_q), 121.0 (C-4'), 116.7 (C-2'), 114.2 (C-6'), 68.1 (CH₃CH₂O), 31.4 (C-8), 22.7 (C-5), 22.5 (C-7), 22.1 (C-6), 21.1 (Me), 14.6 (CH₃CH₂O); **v_{max}/cm⁻¹**; 2932, 1607, 1447, 1260; **M/Z (ESI)**; 284.17 (284.1757, C₁₈H₂₁NO₂ requires 284.1651).

4-Ethoxy-2-methyl-3-(4-(4-(trifluoromethyl)phenoxy)phenyl)-5,6,7,8-tetrahydroquinoline (187).



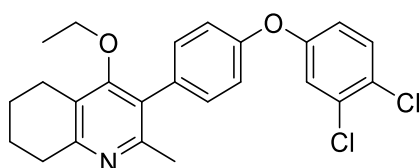
The title compound was synthesised from 4-(4-ethoxy-2-methyl-5,6,7,8-tetrahydroquinolin-3-yl)phenol (60 mg, 0.21 mmol) and 4-trifluoromethylbenzene boronic acid (62 mg, 0.29 mmol), according to general procedure **F**, and isolated as a viscous orange oil (47 mg, 0.11 mmol, 55%). **R_f**; 0.4 (1:1 Pet:EtOAc); **HPLC**; 3.28 (93% reference area); **¹H NMR** (500 MHz, CDCl₃) δ 7.61 (d, $J = 8.7$ Hz, 2H, H-3'' & 5''), 7.28 (d, $J = 8.5$ Hz, 2H, H-2' & 6'), 7.15 – 7.06 (m, 5H, H-3', 5', 2'' & 6''), 3.54 (q, $J = 7.0$ Hz, 2H, CH₃CH₂O), 2.98 (t, $J = 6.3$ Hz, 2H, H-8), 2.72 (t, $J = 6.2$ Hz, 2H, H-5), 2.37 (s, 3H, Me), 1.94 – 1.85 (m, 2H, H-6), 1.84 – 1.77 (m, 2H, H-7), 1.06 (t, $J = 7.0$ Hz, 3H, CH₃CH₂O); **¹³C NMR** (126 MHz, CDCl₃) δ 163.4 (C_q), 160.0 (C_q), 156.3 (C_q), 155.5 (C_q), 154.1 (C_q), 131.8 (C-2' & 6'), 127.3 (q, $J = 3.7$ Hz, C-3'' & 5''), 126.8 (C_q), 125.2 (d, $J = 7.4$ Hz, C-4''), 124.4 (C_q), 123.1 (C_q), 119.6 (C-2'' & 6''), 118.3 (C-3' & 5'), 68.71 (CH₃CH₂O), 31.3 (C-8), 23.0 (C-5), 22.4 (C-6 & 7), 22.2 (2-Me), 15.6 (CH₃CH₂O); **v_{max}/cm⁻¹**; 2938, 1599, 1577, 1504, 1433, 1319, 1288, 1238, 1202 **M/Z (ESI+)**; 428.18 (Found MH⁺ 428.1842, C₂₅H₂₅F₃NO₂ requires 428.1832).

4-Ethoxy-3-(4-(4-fluorophenoxy)phenyl)-2-methyl-5,6,7,8-tetrahydroquinoline (188).



The title compound was synthesised from 4-(4-ethoxy-2-methyl-5,6,7,8-tetrahydroquinolin-3-yl)phenol (60 mg, 0.21 mmol) and 4-fluorobenzene boronic acid (45 mg, 0.31 mmol), according to general procedure **F**, and was isolated as pink micro crystals (55 mg, 0.15 mmol, 70%). **MP**; 102-103 °C; **R_f**; 0.56 (1:1 Pet:EtOAc); **¹H NMR** (500 MHz, CDCl₃) δ 7.14 (d, *J* = 8.6 Hz, 2H, H-2' & 6'), 6.97 (m, 6H, H-3', 5', 2'', 3'', 5'' & 6''), 3.44 (q, *J* = 7.0 Hz, 2H, CH₃CH₂O), 2.87 (t, *J* = 6.2 Hz, 2H, H-5), 2.64 (t, *J* = 6.1 Hz, 2H, H-8), 2.26 (s, 3H, Me), 1.78 (m, 4H, H-6 & 7), 0.97 (t, *J* = 7.0 Hz, 3H, CH₃CH₂O); **¹³C NMR** (75 MHz, CDCl₃) δ 161.6 (d, *J* = 242.0 Hz, C-4''), 157.4 (C_q), 157.1 (C_q), 156.7 (C_q), 154.6 (C_q), 152.6 (d, *J* = 2.4 Hz, C-1''), 131.5 (C-2' & 6'), 130.6 (C_q), 126.8 (C_q), 123.8 (C_q), 120.8 (d, *J* = 8.2 Hz, C-2'' & 6''), 117.9 (C-3' & 5'), 116.4 (d, *J* = 23.4 Hz, C-3'' & 5''), 68.4 (CH₃CH₂O), 32.0 (C-8), 23.0 (C-5), 22.7 (2-Me), 22.7 (C-7), 22.3 (C-8), 15.6 (CH₃CH₂O); **M/Z** (ESI+); 378.19 (Found MH⁺ 378.1877, C₂₄H₂₅FNO₂ requires).

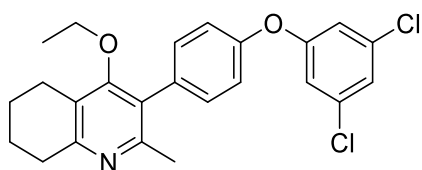
4-Ethoxy-3-(4-(3,4-dichlorophenoxy)phenyl)-2-methyl-5,6,7,8-tetrahydroquinoline (189).



The title compound was synthesised from 4-(4-ethoxy-2-methyl-5,6,7,8-tetrahydroquinolin-3-yl)phenol (100 mg, 0.34 mmol) and 3,4-dichlorobenzene boronic acid (93 mg, 0.51 mmol), according to general procedure **F**, and was isolated as an orange oil (70 mg, 0.16 mmol, 49%). **HPLC**: 3.40 mins (98% Reference area); **LCMS**; 428 (100% reference area); **rt**; 2.30 min; **¹H NMR** (300 MHz, CDCl₃) δ 7.34 (d, *J* = 8.8 Hz, 1H, H-5''), 7.20 (dd, *J* = 7.1, 1.6 Hz, 2H, H-2' & 6'), 7.06 (d, *J* = 2.8 Hz, 1H, H-2''), 7.03 – 6.97 (m, 2H, H-3' & 5'), 6.85 (dd, *J* = 8.8, 2.8 Hz, 1H, H-6''), 3.46 (q, *J* = 7.0 Hz, 2H, CH₃CH₂O), 2.91 (t, *J* = 6.2 Hz, 2H, H-8), 2.65 (t, *J* = 6.1 Hz, 2H, H-5), 2.29 (s, 3H, 2-Me), 1.90 – 1.62 (m, 4H, H-6 & 7), 0.99 (t, *J* = 7.0 Hz, 3H,

CH₃CH₂O); ¹³C NMR (126 MHz, CDCl₃) δ 163.2 (C_q), 156.5 (C_q), 156.2 (C_q), 155.8 (C_q), 154.2 (C_q), 133.3 (C_q), 131.8 (C-2' & 6'), 131.4 (C_q) 131.2 (C-5''), 126.9 (C_q), 126.8 (C_q), 124.2 (C_q), 120.6 (C-2''), 119.1 (C-3' & 5'), 118.3 (C-6''), 68.6 (CH₃CH₂O), 31.5 (C-8), 23.0 (C-5), 22.5 (C-7), 22.2 (C-6), 22.2 (2-Me), 15.6 (CH₃CH₂O); **v_{max}/cm⁻¹**; 2929, 1578, 1505, 1465, 1430, 1327, 1254, 1227; **M/Z** (ESI+); 428.12 (Found MH⁺; 428.1202, C₂₄H₂₄Cl₂NO₂ requires 428.1184).

3-[4-(3,5-Dichlorophenoxy)phenyl]-4-ethoxy-2-methyl-5,6,7,8-tetrahydroquinoline (190).

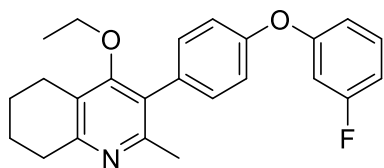


The title compound was synthesised from 4-(4-

ethoxy-2-methyl-5,6,7,8-tetrahydroquinolin-3-yl)phenol (250 mg, 0.88 mmol) and 3,5-dichlorophenylboronic acid (278 mg, 1.32 mmol according to general procedure **F**, and was isolated as a yellow solid (50 mg, 0.12 mmol, 13%).

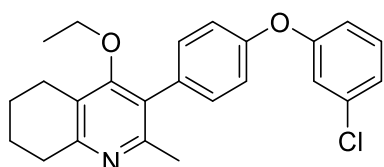
MP: 86.4-86.8 °C; **HPLC;** 3.50 mins (91% reference area); **¹H NMR** (500 MHz, CDCl₃) δ 7.23 (d, J = 8.4 Hz, 2H, H-2' & 6'), 7.13-7.11 (m, 3H, H-3',5' & 4''), 6.93 (d, J = 1.8 Hz, 2H, H-2'' & 6''), 3.54 (q, J = 7.0 Hz, 2H, OCH₂CH₃), 2.94 (t, J = 6.1 Hz, 2H, H-8), 2.75 (t, J = 6.3 Hz, 2H, H-5), 2.39 (s, 3H, 2-Me), 1.95-1.81 (m, 4H, H-6 & 7), 1.08 (t, J = 7.0 Hz, 3H, OCH₂CH₃); **¹³C NMR** (126 MHz, CDCl₃) δ 162.1 (C_q), 158.8 (C_q), 157.5 (C_q), 154.7 (2 × C_q), 135.7 (C_q), 132.9 (C-3'' & 5''), 131.9 (C-2' & 6'), 126.7 (C_q), 123.6 (C_q), 123.3 (C-4''), 119.6 (C-3' & 5'), 116.9 (C-2'' & 6''), 68.3 (OCH₂CH₃), 32.5 (C-8), 23.1 (C-5), 23.1 (C-7), 23.0 (2-Me), 22.5 (C-6), 15.5 (OCH₂CH₃).; **v_{max}/cm⁻¹**; 2935, 1717, 1577, 1506, 1433, 1247; **M/Z** (ESI); 428.12 (Found; 428.1194, C₂₄H₂₄Cl₂NO₂ requires 428.1179).

4-Ethoxy-3-(4-(3-fluorophenoxy)phenyl)-2-methyl-5,6,7,8-tetrahydroquinoline
(191)



The title compound was synthesised from 4-(4-ethoxy-2-methyl-5,6,7,8-tetrahydroquinolin-3-yl)phenol (250 mg, 0.88 mmol) and 3-fluorobenzene boronic acid (184 mg, 1.32 mmol), according to general procedure **F**, and was isolated as a yellow oil, that solidified on extensive drying to a pale orange solid (190 mg, 0.50 mmol, 57%). **MP**: 80.0-85.0 °C; **R_f**; 0.37 (1:1 Pet:EtOAc); **HPLC**; 3.22 mins (80% reference area); **¹H NMR** (500 MHz, CDCl₃) δ 7.25 (dd, *J* = 15.0, 8.2 Hz, 1H, H-5''), 7.18 (d, *J* = 8.6 Hz, 2H, H-2' & 6'), 7.04 (d, *J* = 8.6 Hz, 2H, H-3' & 5'), 6.81 – 6.75 (m, 2H, H-4'' & 6''), 6.69 (dt, *J* = 10.1, 2.3 Hz, 1H, H-2''), 3.49 (q, *J* = 7.0 Hz, 2H, CH₃CH₂O), 3.04 (m, 2H, H-8), 2.65 (t, *J* = 6.2 Hz, 2H, H-5), 2.39 (s, 3H, 2-Me), 1.87 – 1.79 (m, 2H, H-7), 1.79 – 1.70 (m, 2H, H-6), 1.02 (t, *J* = 7.0 Hz, 3H, CH₃CH₂O); **¹³C NMR** (126 MHz, CDCl₃) δ 163.7 (d, *J* = 246.8 Hz, H-3''), 162.4 (C_q), 158.8 (d, *J* = 10.3 Hz, C-1''), 157.4 (C_q), 155.71 (C_q), 154.9 (C_q), 132.1 (C_q), 131.8 (C-2' & 6'), 130.7 (d, *J* = 9.6 Hz, C-5''), 126.9 (C_q), 123.7 (C_q), 119.3 (C-3' & 5'), 114.2 (d, *J* = 2.3 Hz, C-6''), 110.2 (d, *J* = 21.3 Hz, C-4''), 106.3 (d, *J* = 24.5 Hz, C-2''), 68.4 (CH₃CH₂O), 32.5 (C-8), 23.2 (C-5), 23.2 (C-7), 23.0 (2-Me), 22.6 (C-6), 15.7 (CH₃CH₂O). **v_{max}/cm⁻¹**; 2932, 1580, 1555, 1506, 1470, 1430, 1329, 1262, 1229; **M/Z** (ESI+); 378.19 (Found MH⁺ 378.1877, C₂₄H₂₅FNO₂ requires).

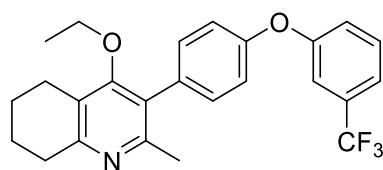
3-(4-(3-Chlorophenoxy)phenyl)-4-ethoxy-2-methyl-5,6,7,8-
tetrahydroquinoline (192)



The title compound was synthesised from 4-(4-ethoxy-2-methyl-5,6,7,8-tetrahydroquinolin-3-yl)phenol (250 mg, 0.88 mmol) and 3-chlorobenzene boronic acid (205 mg, 1.32 mmol), according to general procedure **F**, and was isolated as a viscous orange oil (270 mg, 0.68 mmol, 78%). **R_f**; 0.35 (1:1 Pet:EtOAc); **HPLC**; 3.28 mins (93% reference area); **¹H**

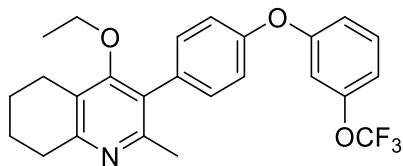
NMR (500 MHz, CDCl₃) δ 7.19 (dt, *J* = 6.0, 3.8 Hz, 3H, H- 2', 6' & 5''), 7.05 – 6.97 (m, 3H, H-3', 5' & 4''), 6.94 (t, *J* = 2.0 Hz, 1H, H-2''), 6.86 (dd, *J* = 8.1, 1.9 Hz, 1H, H-6''), 3.43 (q, *J* = 7.0 Hz, 2H, CH₃CH₂O), 2.83 (t, *J* = 6.2 Hz, 2H, H-8), 2.64 (t, *J* = 6.0 Hz, 2H, H-5), 2.25 (s, 3H, 2-Me), 1.87 – 1.77 (m, 2H, H-7), 1.77 – 1.64 (m, 2H, H-6), 0.97 (t, *J* = 7.0 Hz, 3H, CH₃CH₂O); **¹³C NMR** (101 MHz, CDCl₃) δ 162.1 (C_q), 158.2 (C_q), 157.4 (C_q), 155.5 (C_q), 154.8 (C_q), 135.1 (C_q), 132.1 (C_q), 131.7 (C-2' & 6'), 130.6 (C-5''), 126.7 (C_q), 123.5 (C_q), 123.4 (C-4''), 119.1 (C-3' & 5'), 118.9 (C-2''), 116.8 (C-6''), 68.2 (CH₃CH₂O), 32.6 (C-8), 23.2 (C-5), 23.1 (2-Me), 23.0 (C-7), 22.5 (C-6), 15.6 (CH₃CH₂O); **v_{max}/cm⁻¹**; 2932, 1579, 1554, 1505, 1470, 1430, 1329, 1267, 1228; **M/Z** (ESI+); 394.16 (Found MH⁺; 394.1588, C₂₄H₂₅ClNO₂ requires 394.1574).

4-Ethoxy-3-(4-(3-trifluoromethylphenoxy)phenyl)-2-methyl-5,6,7,8-tetrahydroquinoline (193)



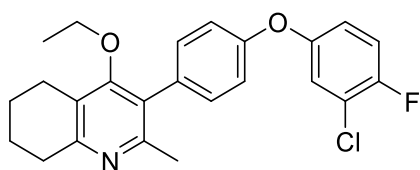
The title compound was synthesised from 4-(4-ethoxy-2-methyl-5,6,7,8-tetrahydroquinolin-3-yl)phenol (300 mg, 1.06 mmol) and 3-trifluoromethylphenyl boronic acid (302 mg, 1.59 mmol) according to general procedure **F**, and was isolated as a yellow oil (198 mg, 0.46 mmol, 44%). **HPLC**; 3.27 mins (71% reference area); **¹H NMR** (400 MHz, CDCl₃) δ 7.44 – 7.38 (m, 1H, H-5''), 7.32 (d, *J* = 7.8 Hz, 1H, H-4''), 7.19 (s, 1H, H-2''), 7.16 (d, *J* = 8.3 Hz, 1H, H-6''), 7.12 (d, *J* = 8.3 Hz, 2H, H-2' & 6'), 7.01 (d, *J* = 8.4 Hz, 2H, H-3' & 5'), 3.45 (q, *J* = 7.0 Hz, 2H, OCH₂CH₃), 2.85 (t, *J* = 6.0 Hz, 2H, H-8), 2.62 (t, *J* = 5.7 Hz, 2H, H-5), 2.25 (s, 3H, 2-Me), 1.73 (m, 4H, H-6 & 7), 1.00 (t, *J* = 7.0 Hz, 3H, OCH₂CH₃); **¹³C NMR** (101 MHz, CDCl₃) δ 157.4 (C_q), 156.0 (2 × C_q), 153.9 (C_q), 138.3 (C_q), 131.7 (C-2' & 6'), 130.9 (C_q), 130.5 (C-5''), 128.0 (C_q), 126.8 (C_q), 122.0 (C-6''), 120.1 (C-4''), 119.2 (C-3' & 5'), 115.5 (C-2''), 68.9 (OCH₂CH₃), 31.1 (C-8), 22.8 (C-5), 22.3 (C- 6 & 7), 22.0 (2-Me), 15.5 (OCH₂CH₃); **v_{max}/cm⁻¹**; 2937, 1591, 1507, 1448, 1325, 1236; **M/Z** (**ESI**); 427.19 (found MH⁺ 427.1852, C₂₅H₂₅F₃NO₂ requires 427.1759).

4-Ethoxy-3-(4-(3-trifluoromethoxyphenoxy)phenyl)-2-methyl-5,6,7,8-tetrahydroquinoline (194).



The title compound was synthesised from 4-(4-ethoxy-2-methyl-5,6,7,8-tetrahydroquinolin-3-yl)phenol (200 mg, 0.71 mmol) and 3-trifluoromethoxyphenylboronic acid (218 mg, 1.06 mmol) according to general procedure **F**, and was isolated as a purple/brown oil (132 mg, 0.32 mmol, 42%); **HPLC**: 3.40 mins (93% reference area); **¹H NMR** (400 MHz, CDCl₃) δ 7.29 (t, *J* = 8.3 Hz, 1H, H-5''), 7.21 (d, *J* = 8.3 Hz, 2H, H-2' & 6'), 7.03 (d, *J* = 8.2 Hz, 2H, H-3' & 5'), 6.90 (d, *J* = 8.2 Hz, 2H, H-4'' & 6''), 6.81 (s, 1H, H-2''), 3.44 (q, *J* = 7.0 Hz, 2H, OCH₂CH₃), 2.84 (t, *J* = 6.2 Hz, 2H, H-8), 2.65 (t, *J* = 6.0 Hz, 2H, H-5), 2.25 (s, 3H, 2-Me), 1.86 – 1.78 (m, 2H, H-7), 1.70-1.77 (m, 2H, H-6), 0.97 (t, *J* = 7.0 Hz, 3H, OCH₂CH₃); **¹³C NMR** (101 MHz, CDCl₃) δ 162.1 (C_q), 158.6 (C_q), 157.4 (C_q), 155.3 (C_q), 154.8 (C_q), 150.2 (C_q), 132.3 (C_q), 131.7 (C-2' & 6'), 130.5 (C-5''), 126.7 (C_q), 123.5 (C_q), 119.3 (C-3' & 5'), 116.6 (C-6''), 115.3 (C-4''), 111.3 (C-2''), 68.2 (OCH₂CH₃), 32.5 (C-8), 23.1 (2-Me), 23.1 (C-5), 23.0 (C-7), 22.5 (C-6), 15.5 (OCH₂CH₃); **v_{max}/cm⁻¹**; 2934, 1578, 1485, 1434, 1329, 1250, 1206; **M/Z (ESI)**; 444.18 (found 444.1781, C₂₅H₂₅F₃NO₃ requires 444.1781).

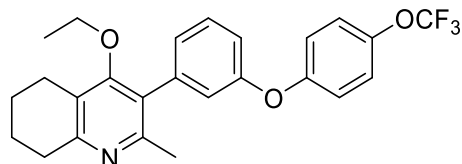
4-Ethoxy-3-(4-(3-chloro-4-fluorophenoxy)phenyl)-2-methyl-5,6,7,8-tetrahydroquinoline (195).



The title compound was synthesised from 4-(4-ethoxy-2-methyl-5,6,7,8-tetrahydroquinolin-3-yl)phenol (250 mg, 0.88 mmol) and 3-chloro-4-fluorophenylboronic acid (230 mg, 1.32 mmol), according to general procedure **F**, and was isolated as a pale orange solid (104 mg, 0.25 mmol, 29%). **MP**; 118.0-119.0; **HPLC**: 3.26 min (94% reference area); **¹H NMR** (400 MHz, CDCl₃) δ 7.26 (d, *J* = 8.2 Hz, 2H, H-2' & 6'), 7.17 – 7.11 (t, *J* = 8.7 Hz, 1H, H-5''), 7.09 (dd, *J* = 6.1, 2.9 Hz, 1H, H-2''), 7.04 (d, *J* = 8.3 Hz, 2H, H-3' & 5'), 6.97 – 6.91 (m, 1H, H-6''), 3.50 (q, *J* = 7.0 Hz, 2H,

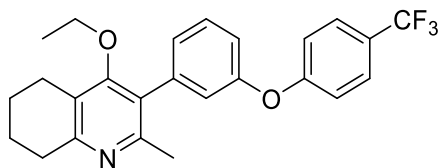
OCH₂CH₃), 2.91 (t, *J* = 6.2 Hz, 2H, H-8), 2.72 (t, *J* = 5.9 Hz, 2H, H-5), 2.31 (s, 3H, 2-Me), 1.95 – 1.84 (m, 2H, H-7), 1.81 (m, 2H, H-6), 1.04 (t, *J* = 7.0 Hz, 3H, OCH₂CH₃); ¹³C NMR (101 MHz, CDCl₃) δ 162.2 (C_q), 157.6 (C_q), 156.2 (C_q), 154.9 (C_q), 154.6 (d, *J* = 242.2 Hz, C-4''), 153.3 (C_q), 132.1 (C_q), 131.9 (C-2' & 6'), 126.8 (C_q), 123.6 (C_q), 121.1 (C-2''), 118.6 (C-3' & 5'), 118.6 (d, *J* = 6.8 Hz, C-6''), 117.3 (d, *J* = 22.8 Hz, C-5''), 68.4 (OCH₂CH₃), 32.8 (C-8), 23.3 (C-5), 23.2 (2-Me), 23.1 (C-7), 22.6 (C-6), 15.7 (OCH₂CH₃); *v*_{max}/cm⁻¹; 2929, 1578, 1490, 1329, 1252, 1212; **M/Z** (ESI+); 412.15 (Found MH⁺; 412.1474 C₂₄H₂₄ClFNO₂ requires 412.1474).

4-ethoxy-2-methyl-3-(3-(4-(trifluoromethoxy)phenoxy)phenyl)-5,6,7,8-tetrahydro quinolone (197).[^]



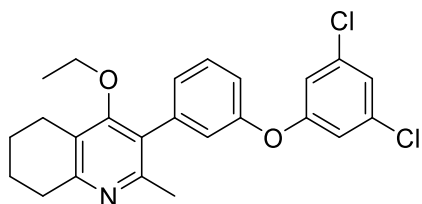
The title compound was synthesised from (4-ethoxy-2-methyl-5,6,7,8-tetrahydroquinolin-3-yl)phenol (200mg, 0.71 mmol) and 4-trifluoromethoxybenzene boronic acid (218 mg, 1.06 mmol) according to general procedure F and was isolated as a yellow oil (91 mg, 0.20 mmol, 29%). **HPLC**; 3.32 mins (94% reference area); **R_f** 0.36 (19:1 DCM:MeOH); **¹H NMR** (500 MHz, CDCl₃) δ 7.34 (t, *J* = 7.9 Hz, 1H, H-5'), 7.11 (d, *J* = 8.8 Hz, 2H, H-3'' & 5''), 7.01-6.96 (m, 2H, H-4' & 6'), 6.94 (d, *J* = 9.0 Hz, 2H, H-2'' & 6''), 6.88 (s, 1H, H-2'), 3.47 (q, *J* = 7.0 Hz, 2H, CH₃CH₂O), 2.83 (t, *J* = 6.3 Hz, 2H, H-8), 2.64 (t, *J* = 6.1 Hz, 2H, H-5), 2.22 (s, 3H, Me), 1.83 – 1.67 (m, 4H, H-6 & 7), 0.99 (t, *J* = 7.0 Hz, 3H, CH₃CH₂O); **¹³C NMR**; 157.8 (C_q), 156.7 (C_q), 155.9 (C_q), 154.4 (C_q), 138.3 (C_q), 132.2 (C_q), 129.8 (C-5'), 128.7 (C_q), 122.7 (C-4'), 122.6 (C-2'' & C-6''), 120.8 (C-2'), 119.4 (C-3'' & C-5''), 118.1 (C-6'), 116.2 (C_q), 68.4 (CH₃CH₂O), 32.2 (C-8), 23.0 (C-5), 22.8 (2-Me), 22.7 (C-7), 22.4 (C-6), 15.6 (CH₃CH₂O); *v*_{max}/cm⁻¹; 3247, 3156, 3075, 2994, 2935, 1613, 1575, 1500, 1432, 1353, 1306; **M/Z (ESI)**; 444.18 (Found MH⁺ 444.1762, C₂₅H₂₄F₃NO₃ requires 444.1781).

4-ethoxy-2-methyl-3-(3-(4-(trifluoromethyl)phenoxy)phenyl)-5,6,7,8-tetrahydroquinolone (198).[^]



The title compound was synthesised from 3-(4-ethoxy-2-methyl-5,6,7,8-tetrahydroquinolin-3-yl)phenol (200mg, 0.71 mmol) and 4trifluoromethylbenzne boronic acid (201 mg, 1,06 mmol) according to general procedure **F** and was isolated as an orange oil (27 mg, 0.06 mmol, 9%). **R_f** 0.08 (19:1 DCM:MeOH); **¹H NMR** (500 MHz, CDCl₃) δ 7.61 (d, *J* = 8.5 Hz, 2H, H-3'' & 5''), 7.49 (t, *J* = 8.1 Hz, 1H, H-6'), 7.25 – 7.07 (m, 3H, H-6', 2'' & 6''), 7.02 (s, 1H, H-2'), 6.94 (d, *J* = 8.3 Hz, 1H, H-4'), 3.59 (dd, *J* = 13.9, 7.0 Hz, 2H, CH₃CH₂O), 2.94 (t, *J* = 5.8 Hz, 2H, H-8), 2.75 (t, *J* = 5.5 Hz, 1H, H-5), 2.33 (s, 3H), 1.89 (d, *J* = 4.9 Hz, 2H, H-7), 1.82 (d, *J* = 5.4 Hz, 2H, H-6), 1.11 (t, *J* = 7.0 Hz, 3H, CH₃CH₂O); **¹³C NMR** (126 MHz, CDCl₃) δ 162.4 (C_q), 160.4 (d, *J* = 6.5 Hz, C-1''), 157.4 (C_q), 155.7 (C_q), 154.3 (C_q), 138.3 (C_q), 130.0 (C-6'), 127.2 (C-3'' & 5''), 125.1 (C_q), 124.0 (C_q), 121.6 (C-2'), 119.0 (C_q), 117.9 (C-2'' & 6''), 115.7 (C-4'), 68.5 (CH₃CH₂O), 31.8 (C-8), 23.0 (C-5), 22.7 (2-Me), 22.4 (C-7), 22.3 (C-6), 15.6 (CH₃CH₂O). **v_{max}/cm⁻¹**; 2943, 1573, 1429, 1335, 1291, 1212; **M/Z** (ESI+); 428.18 (Found MH⁺ 428.1838, C₂₅H₂₅F₃NO₂ requires 428.1832).

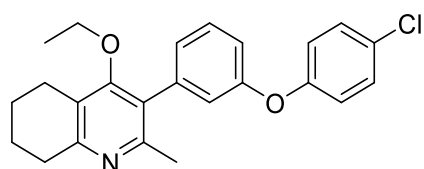
3-[3-(3,5-Dichlorophenoxy)phenyl]-4-ethoxy-2-methyl-5,6,7,8-tetrahydroquinoline (199).



The title compound was synthesised from 3-(4-ethoxy-2-methyl-5,6,7,8-tetrahydroquinolin-3-yl)phenol (142 mg, 0.5 mmol) and 3,5-dichlorobenzene boronic acid (147 mg, 0.75 mmol) according to general procedure **F**. The title compound was isolated as a colourless oil (33 mg, 0.08 mmol, 15%). **HPLC**: 3.46 mins (56% reference area); **¹H NMR** (500 MHz, CDCl₃) δ 7.38 (t, *J* = 7.9 Hz, 1H, H-5'), 7.05 (d, *J* = 7.5 Hz, 1H, H-6'), 6.98 (d, *J* = 9.5 Hz, 2H, H-2' & 4''), 6.90 (s, 1H, H-4'), 6.79 (s, 2H, H-2'' & 6''),

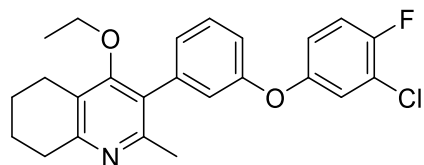
3.46 (q, $J = 7.0$ Hz, 2H, CH₃CH₂O), 2.83 (t, $J = 6.3$ Hz, 2H, H-8), 2.64 (t, $J = 6.0$ Hz, 2H, H-5), 2.23 (s, 3H, 2-Me), 1.80 (dt, $J = 11.7, 5.7$ Hz, 2H, H-7), 1.75 – 1.63 (m, 2H, H-6), 0.99 (t, $J = 7.0$ Hz, 3H CH₃CH₂O); ¹³C NMR; (101 MHz, CDCl₃) δ 161.8 (C_q), 159.1 (C_q), 157.8 (C_q), 155.3 (C_q), 154.4 (C_q), 138.8 (C_q), 135.6 (C-3'' & 5''), 130.0 (C-5'), 126.7 (C-6'), 126.6 (C_q), 123.5 (C_q), 123.1 (C-4''), 121.7 (C-2'), 118.9 (C-4'), 116.7 (C-2'' & 6''), 68.4 (CH₃CH₂O), 32.5 (C-8), 23.1 (2-Me), 23.0 (C-5), 22.9 (C-6), 22.4 (C-7), 15.6 (CH₃CH₂O); $\nu_{\max}/\text{cm}^{-1}$; 2930, 1572, 1484, 1428, 1328, 1238; **M/Z (ESI)**; 428.12 (Found MH⁺ 428.1188, C₂₄H₂₄Cl₂NO₂ requires 428.1179)

4-ethoxy-2-methyl-3-(3-(4-chlorophenoxy)phenyl)-5,6,7,8-tetrahydroquinolone (200)[^]



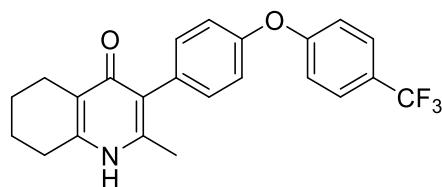
The title compound was synthesised from (4-ethoxy-2-methyl-5,6,7,8-tetrahydroquinolin-3-yl)phenol (230 mg, 0.81 mmol) and 4-chlorobenzene boronic acid (190 mg, 1.22 mmol) according to general procedure F and was isolated as a pale-yellow oil (308 mg, 0.78 mmol, 96%). **R_f** 0.38 (19:1 DCM:MeOH); ¹H NMR (500 MHz, CDCl₃) δ 7.42 (t, $J = 7.9$ Hz, 1H, H-2'), 7.32 – 7.27 (m, 2H, H-3'' & 5''), 7.07 (d, $J = 7.6$ Hz, 1H, H-6'), 7.03 (dd, $J = 8.2, 2.3$ Hz, 1H, H-4'), 7.00-6.90 (m, 3H, H-2', 2'' & 6''), 3.56 (q, $J = 7.0$ Hz, 2H, CH₃CH₂O), 2.93 (t, $J = 6.3$ Hz, 2H, H-8), 2.73 (t, $J = 6.1$ Hz, 2H, H-5), 2.32 (s, 3H, 2-Me), 2.02 – 1.84 (m, 2H, H-7), 1.84 – 1.66 (m, 2H, H-6), 1.08 (t, $J = 7.0$ Hz, 3H, CH₃CH₂O); ¹³C NMR; (126 MHz, CDCl₃) δ 162.0 (C_q), 157.5 (C_q), 156.8 (C_q), 155.9 (C_q), 154.4 (C_q), 138.4 (C_q), 129.9 (C-5'), 129.8 (C-3'' & 5''), 128.3 (C_q), 126.9 (C_q), 125.5 (C-6'), 123.6 (C_q), 120.7 (C-2'), 120.0 (C-2'' & 6''), 117.9 (C-4'), 68.3 (CH₃CH₂O), 32.3 (C-8), 23.1 (C-5 & 7), 22.9 (Me), 22.4 (C-6), 15.6 (CH₃CH₂O); $\nu_{\max}/\text{cm}^{-1}$; 3063, 1608, 1482, 1231 **M/Z (ESI)**; 394.16 (Found 394.1568, C₂₄H₂₅ClNO₂ requires 394.1568).

4-Ethoxy-3-(3-(3-chloro-4-fluorophenoxy)phenyl)-2-methyl-5,6,7,8-tetrahydroquinoline (201).



The title compound was synthesised from 3-(4-ethoxy-2-methyl-5,6,7,8-tetrahydroquinolin-3-yl)phenol (142 mg, 0.50 mmol) and 3-chloro-4-fluorobenzene boronic acid (130 mg, 0.75 mmol) according to general procedure F and was isolated as a yellow oil (42 mg, 0.10 mmol, 20%). **HPLC**; 3.20 mins (97% reference area); **¹H NMR** (500 MHz, CDCl₃) δ 7.44 (t, *J* = 7.9 Hz, 1H, H-5'), 7.12 (t, *J* = 8.7 Hz, 1H, H-5''), 7.09 (d, *J* = 7.7 Hz, 1H, H-6'), 7.08 – 7.05 (m, 1H, H-2''), 7.03 (dd, *J* = 7.7, 1.9 Hz, 1H, H-4'), 6.96 – 6.94 (m, 1H, H-2'), 6.94 – 6.90 (m, 1H, H-6''), 3.55 (q, *J* = 7.0 Hz, 2H, CH₃CH₂O), 2.92 (t, *J* = 6.3 Hz, 2H, H-8), 2.73 (t, *J* = 6.2 Hz, 2H, H-5), 2.32 (s, 3H, 2-Me), 1.90 (dt, *J* = 10.5, 5.4 Hz, 2H, H-7), 1.86 – 1.75 (m, 2H, H-6), 1.08 (t, *J* = 7.0 Hz, 3H, CH₃CH₂O); **¹³C NMR** (126 MHz, CDCl₃) δ 161.8 (C_q), 157.7 (C_q), 156.7 (C_q), 154.5 (C_q), 154.3 (d, *J* = 244.5 Hz, C-4''), 153.47 (d, *J* = 2.8 Hz, C-1''), 138.67 (C_q), 129.8 (C-5'), 126.65 (C-6'), 125.79 (C_q), 123.5 (C_q), 121.59 (d, *J* = 19.4 Hz, C-3''), 120.63 (d, *J* = 7.6 Hz, C-2' & 2''), 118.19 (d, *J* = 7.0 Hz, C-6''), 117.79 (C-4'), 117.12 (d, *J* = 22.7 Hz, C-5''), 68.30 (CH₃CH₂O), 32.63 (C-8), 23.2 (2-Me), 23.1 (C-5), 23.0 (C-6), 22.5 (C-7), 15.6 (CH₃CH₂O); **v_{max}/cm⁻¹**; 2933, 1579, 1492, 1201; **M/Z (ESI)**; 412.15 (Found MH⁺ 412.1473, C₂₄H₂₄ClFNO₂ requires 412.1474).

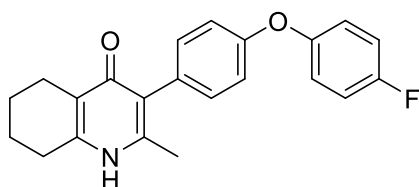
2-Methyl-3-(4-(4-(trifluoromethyl)phenoxy)phenyl)-5,6,7,8-tetrahydroquinolin-4(1H)-one (202)



The title compound was synthesised from 4-ethoxy-2-methyl-3-(4-(4-(trifluoromethyl)phenoxy)phenyl)-5,6,7,8-tetrahydroquinoline (47 mg, 0.12 mmol) according to general procedure B and was isolated as a colourless solid (25 mg, 0.07 mmol, 60%). **MP**; >250 °C; **HPLC**; 2.86 mins (73% reference area); **¹H NMR** (500 MHz, DMSO) δ 11.14 (s, 1H, NH), 7.77 (d, *J* = 8.6 Hz, 2H, H-3' & 5''), 7.26 (d, *J* = 8.6 Hz, 2H, H-2')

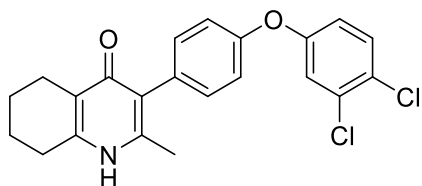
&6'), 7.19 (d, $J = 8.6$ Hz, 2H, H-), 7.12 (d, $J = 8.6$ Hz, 2H, H-), 2.59 (t, $J = 5.8$ Hz, 2H, H-5), 2.33 (t, $J = 6.4$ Hz, 2H, H-8), 2.14 (s, 3H, 2-Me), 1.80-1.65(m, 4H, H-6 & 7); $^{13}\text{C NMR}$ (126 MHz, DMSO) δ 172 (C-4), 160.4 (C_q), 153.8 (C_q), 143.9 (C_q), 132.53 (C-2' & 6'), 127.45 (q, $J = 3.8$ Hz, C-3'' & 5''), 123.5 (C_q), 123.2 (broad, C-4''), 121.2 (C_q), 119.3 (C-2'' & 6''), 119.1 (C_q), 118.0 (C-3' & 5'), 26.3 (C-5), 21.8 (C-8), 21.6 (C-6), 21.3 (C-7), 17.8 (2-Me); $\nu_{\text{max}}/\text{cm}^{-1}$; 2932, 1598, 1501, 1353, 1241; **M/Z** (ESI+); 400.15 (Found MH⁺; 400.1528, C₂₃H₂₁F₃NO₂ requires 400.1519).

3-(4-(4-Fluorophenoxy)phenyl)-2-methyl-5,6,7,8-tetrahydroquinolin-4(1H)-one (203).



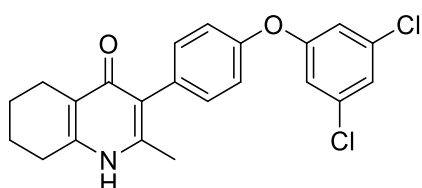
The title compound was synthesised from 4-ethoxy-3-(4-(4-fluorophenoxy)phenyl)-2-methyl-5,6,7,8-tetrahydroquinoline (45 mg, 0.12 mmol) according to general procedure **B**, and was isolated as colourless solid (25 mg, 0.07 mmol, 58%) **MP**; >250 °C; **HPLC**; 2.73 mins (90% reference area); **LCMS rt**; 1.80 min; $^1\text{H NMR}$ (500 MHz, DMSO) δ 11.00 (s, 1H, NH), 7.25 (t, $J = 8.7$ Hz, 2H, H-3'' & 5''), 7.17 (d, $J = 8.5$ Hz, 2H, H-2' & 6'), 7.11 (dd, $J = 8.9, 4.5$ Hz, 2H, H-2'' & 6''), 6.96 (d, $J = 8.5$ Hz, 2H, H-3' & 5'), 2.59 – 2.53 (m, 2H, H-5), 2.30 (t, $J = 5.2$ Hz, 2H, H-8), 2.08 (s, 3H, 2-Me), 1.72 (m, 2H, H-6), 1.66 (m, 2H, H-7); $^{13}\text{C NMR}$ (126 MHz, DMSO) δ 175.6 (C-4), 158.1 (C_q), 155.5 (C_q), 152.7 (d, $J = 2.1$ Hz, C-1''), 143.0 (C_q), 142.1 (C_q), 132.3 (C-2' & 6'), 131.4 (C_q), 123.7 (C_q), 121.2 (C_q), 120.6 (d, $J = 8.5$ Hz, C-2'' & 6''), 117.2 (C-3' & 5'), 116.5 (d, $J = 23.3$ Hz, C-3'' & 5''), 26.2 (C-5), 21.9 (C-8), 21.8 (C-6), 21.5 (C-7), 17.7 (2-Me); $\nu_{\text{max}}/\text{cm}^{-1}$; 2923, 1620, 1585, 1505, 1464, 1278, 1233 **M/Z** (ESI+); 350.16 (Found MH⁺ 350.1562, C₂₂H₂₁FNO₂ requires 350.1550).

3-(4-(3,4-Dichlorophenoxy)phenyl)-2-methyl-5,6,7,8-tetrahydroquinolin-4(1H)-one (204)



The title compound was synthesised from 4-ethoxy-3-(4-(3,4-dichlorophenoxy)phenyl)-2-methyl-5,6,7,8-tetrahydroquinoline (60 mg, 0.15 mmol) according to general procedure **B**, and was isolated as colourless solid (35 mg, 0.08 mmol, 59%). **MP**; >250 °C; **HPLC**; 2.96 mins (95% reference area); **¹H NMR** (500 MHz, DMSO) δ 10.95 (s, 1H, NH), 7.66 (d, J = 8.5 Hz, 1H, H-5''), 7.31 (s, 1H, H-2''), 7.23 (d, J = 8.2 Hz, 2H, H-2' & 6'), 7.08 (d, J = 7.6 Hz, 2H, H-3' & 5'), 7.04 (d, J = 8.9 Hz, 1H, H-6''), 2.55 (m, 2H, H-5), 2.30 (m, Hz, 2H, H-8), 2.09 (s, 3H, 2-Me), 1.72 (m, 2H, H-6), 1.66 (m, 2H, H-7); **¹³C NMR** (126 MHz, MeOD)* δ 176.9 (C-4), 156.6 (C_q), 154.9 (C_q), 144.7 (C_q), 143.7 (C_q), 132.8 (C_q), 132.0 (C-2' & 6'), 131.3 (C_q), 130.8 (C-5''), 126.1 (C_q), 125.1 (C_q), 122.9 (C_q), 119.9 (C-2''), 118.9 (C-3' & 5'), 117.8 (C-6''), 26.5 (C-5), 21.8 (C-8), 21.6 (C-6), 21.4 (C-7), 17.40 (2-Me); **$\nu_{\max}/\text{cm}^{-1}$** ; 2703, 1620, 1462, 1253, 1228; **M/Z** (ESI+); 400.09 (Found MH⁺; 400.0881, C₂₂H₂₀Cl₂NO₂ requires 400.0866).

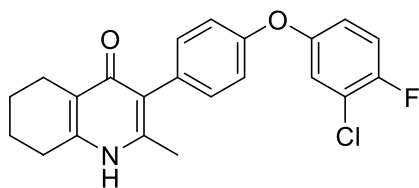
3-[4-(3,5-dichlorophenoxy)phenyl]-2-methyl-5,6,7,8-tetrahydro-1H-quinolin-4(1H)-one (205)



The title compound was synthesised from 3-[4-(3,5-dichlorophenoxy)phenyl]-4-ethoxy-2-methyl-5,6,7,8-tetrahydroquinoline (40 mg, 0.93 mmol) according to general procedure **B**, and was isolated as colourless solid (31 mg, 0.08 mmol, 83%). **MP**; >250 °C **HPLC**; 2.98 mins (93% reference area); **δ ¹H NMR** (500 MHz, DMSO) δ 11.13 (s, 1H, NH), 7.38 (t, J = 1.6 Hz, 1H, H-4''), 7.25 (d, J = 8.5 Hz, 2H, H-3' & 5'), 7.11 (d, J = 8.5 Hz, 2H, H-2' & 6'), 7.07 (d, J = 1.7 Hz, 2H, H-2'' & 6''), 2.59 – 2.55 (m, 2H, H-8), 2.30 (t, J = 6.3 Hz, 2H, H-5), 2.09 (s, 3H, 2-Me), 1.77-1.70 (m, 2H, H-7),

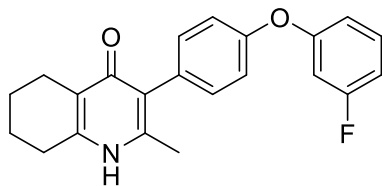
1.70-1.63 (m, 2H, H-6); ^{13}C NMR; (101 MHz, DMSO) δ 173.5 (C-4), 159.4 (C_q), 153.7 (C_q), 143.7 (C_q), 142.8 (C_q), 135.4 (C-3'' & 5''), 133.7 (C_q), 133.2 (C-2' & 6'), 124.0 (C_q), 123.2 (C-4''), 121.8 (C C_q), 119.4 (C-3' & 5'), 117.2 (C-2'' & 6''), 26.7 (C-5), 22.3 (C-8), 22.3 (C-7), 22.0 (C-6), 18.2 (Me); $\nu_{\text{max}}/\text{cm}^{-1}$; 2928, 1620, 1574, 1504, 1463, 1427, 1246, 1200; **M/Z (ESI)**; 400.87 (Found MH⁺; 400.0874, C₂₂H₂₀Cl₂NO₂ requires 400.0866).

3-(4-(3,4-Dichlorophenoxy)phenyl)-2-methyl-5,6,7,8-tetrahydroquinolin-4(1H)-one (206).



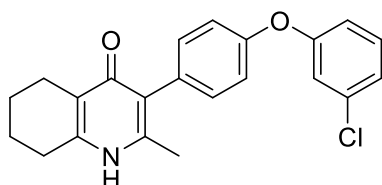
The title compound was synthesised from 4-Ethoxy-3-(4-(3-chloro-4-fluorophenoxy)phenyl)-2-methyl-5,6,7,8-tetrahydroquinoline (90 mg, 2.18 mmol) according to general procedure **B**, and was isolated as a pale grey precipitate (55 mg, 0.14 mmol, 66%). **MP**; >250 °C; **HPLC**; 3.26 min (86% reference area); ^1H NMR (501 MHz, DMSO) δ 11.10 (s, 1H, NH), 7.44 (t, J = 8.8 Hz, 1H, H-5''), 7.28 (dd, J = 5.9, 3.0 Hz, 1H, H-2''), 7.18 (d, J = 8.4 Hz, 2H, H-2' & 6'), 7.10 – 7.04 (m, 1H, H-6''), 7.01 (d, J = 8.3 Hz, 2H, H-3' & 5'), 2.56 (t, J = 5.8 Hz, 2H, H-5), 2.30 (t, J = 5.0 Hz, 2H, H-8), 2.07 (s, 3H, 2-Me), 1.70 (dd, J = 8.8, 4.8 Hz, 2H, H-6), 1.65 (dd, J = 8.1, 4.4 Hz, 2H, H-7); ^{13}C NMR (101 MHz, CDCl₃)⁺ δ 164.8 (C-4), 159.8 (C_q), 155.4 (d, J = 246.6 Hz, C-4''), 152.25 (C_q), 151.14 (d, J = 3.1 Hz, C-1''), 150.12 (C_q), 131.7 (C-2' & 6'), 123.18 (C_q), 122.56 (C_q), 122.20 (d, J = 19.5 Hz, C-3''), 121.79 (d, J = 7.5 Hz, C-2''), 119.96 (d, J = 7.1 Hz, C-5''), 119.5 (C-3' & 5'), 117.60 (d, J = 22.9 Hz, C-6''), 27.1 (C-1), 21.5 (C-5), 20.6 (C-7), 20.5 (C-6), 18.1 (Me); $\nu_{\text{max}}/\text{cm}^{-1}$; 2929, 1620, 1466, 1213; **M/Z (ESI)**; 384.1167, (C₂₂H₂₀ClFNO₂ requires 384.1161).

3-(4-(3-Fluorophenoxy)phenyl)-2-methyl-5,6,7,8-tetrahydroquinolin-4(1H)-one (207).



The title compound was synthesised from 4-ethoxy-3-(4-(3-fluorophenoxy)phenyl)-2-methyl-5,6,7,8-tetrahydroquinoline (170 mg, 0.45 mmol) according to general procedure **B**, and was isolated as colourless solid (110 mg, 0.31 mmol, 70%). **MP**: >250 °C; **HPLC**: 2.72 mins (97% reference area); **¹H NMR** (500 MHz, DMSO) δ 7.47 (dt, J = 8.6, 7.1 Hz, 1H, H-5''), 7.31 (d, J = 8.7 Hz, 2H, H-2' & 6'), 7.17 (d, J = 8.7 Hz, 2H, H-3' & 5'), 7.02 (tdd, J = 8.5, 2.3, 0.7 Hz, 1H, H-4''), 6.97 – 6.88 (m, 2H, H-2'' & 6''), 2.83 (t, J = 6.1 Hz, 2H, H-5), 2.54 (t, J = 5.8 Hz, 2H, H-8), 2.25 (s, 3H, 2-Me), 1.87 – 1.69 (m, 4H, H-6 & 7); **¹³C NMR** (126 MHz, DMSO) δ 168.9 (C-4), 163.9 (C_q), 161.9 (C_q), 158.2 (d, J = 10.9 Hz, C-1''), 155.5 (C_q) 147.7 (d, J = 134.7 Hz, C-3''), 132.2 (C-2' & 6'), 131.4 (d, J = 10.0 Hz, C-5''), 128.6 (C_q), 123.5 (C_q), 121.0 (C_q), 119.2 (C-3' & 5'), 114.4 (d, J = 2.9 Hz, C-6''), 110.2 (d, J = 21.1 Hz, C-4''), 105.9 (d, J = 24.5 Hz, C-2''), 26.6 (C-5), 21.8 (C-8), 21.0 (C-6), 20.7 (C-7), 18.0 (2-Me); **ν_{max} /cm⁻¹**; 2839, 1597, 1504, 1462, 1267, 1217; **M/Z** (ESI+); 350.16 (Found MH⁺; 350.1569, C₂₂H₂₁FNO₂ requires 350.1556).

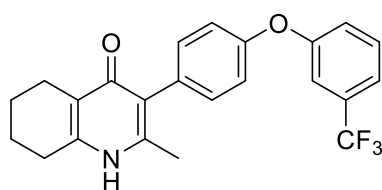
3-(4-(3-Chlorophenoxy)phenyl)-2-methyl-5,6,7,8-tetrahydroquinolin-4(1H)-one (208)



The title compound was synthesised from 3-(4-(3-chlorophenoxy)phenyl)-4-ethoxy-2-methyl-5,6,7,8-tetrahydroquinoline (200 mg, 0.51 mmol) according to general procedure **B**, and was isolated as a colourless solid (120 mg, 0.33 mmol, 66%). **MP**: >250 °C; **HPLC**: 2.91 mins (95% reference area); **¹H NMR** (500 MHz, DMSO) δ 11.71 (s, 1H, NH), 7.44 (t, J = 8.2 Hz, 1H, H-5''), 7.25 (d, J = 8.6 Hz, 2H, H-2' & 6'), 7.22 (ddd, J = 8.0, 1.9, 0.8 Hz, 1H, H-4''), 7.10 (t, J = 2.0 Hz, 1H, H-2''), 7.09 (d, J = 8.6 Hz, 2H, H-3' & 5'), 7.03 (ddd, J = 8.2, 2.3, 0.6, 1H, H-6''), 2.65 (t, J = 5.9 Hz, 2H, H-5),

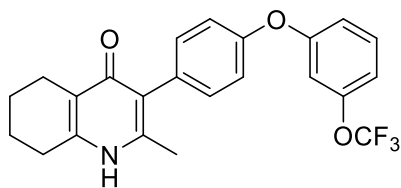
2.39 (t, $J = 5.2$ Hz, 2H, H-8), 2.14 (s, 3H, Me), 1.84 – 1.59 (m, 4H, H-6 & 7); $^{13}\text{C NMR}$ (101 MHz, DMSO); δ 176.0 (C-4), 158.6 (C_q), 154.6 (C_q), 143.8 (C_q), 142.8 (C_q), 135.2 (C_q), 134.4 (C_q), 133.0 (C-2' & 6'), 131.9 (C-5''), 123.6 (C-4''), 121.8 (C_q), 120.4 (C_q), 118.9 (C-3' & 5'), 118.5 (C-2''), 117.3 (C-6''), 26.7 (C-5), 22.3 (C-8), 22.3 (C-6), 22.0 (C-7), 18.2 (2-Me); $\nu_{\text{max}}/\text{cm}^{-1}$; 2923, 1620, 1585, 1505, 1464, 1277, 1233; **M/Z** (ESI+); 366.13 (Found MH⁺ 366.1262, C₂₂H₂₁ClNO₂ requires 366.1255).

3-(4-(3,4-Dichlorophenoxy)phenyl)-2-methyl-5,6,7,8-tetrahydroquinolin-4(1H)-one (209)



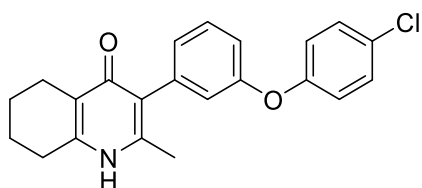
The title compound was synthesised from 4-ethoxy-3-(4-(3-trifluoromethylphenoxy)phenyl)-2-methyl-5,6,7,8-tetrahydroquinoline (193 mg, 0.45 mmol) according to general procedure **B** and was isolated as a colourless solid (174 mg, 0.44 mmol, 96%) **MP**; >250 °C; **HPLC**; 2.84 mins (96% reference area); $^1\text{H NMR}$ (501 MHz, DMSO) δ 10.95 (s, 1H, NH), 7.63 (t, $J = 8.6$ Hz, 1H, H-5''), 7.48 (d, $J = 8.2$ Hz, 1H, H-4''), 7.30 (s, 2H, H-2'' & 6''), 7.22 (d, $J = 8.4$ Hz, 2H, H-2' & 6'), 7.07 (d, $J = 8.4$ Hz, 2H, H-3' & 5'), 2.56 (t, $J = 3.3$ Hz, 2H, H-5), 2.30 (t, $J = 5.3$ Hz, 2H, H-8), 2.08 (s, 3H, 2-Me), 1.71 (dd, $J = 6.0, 4.6$ Hz, 2H, H-6), 1.68 – 1.60 (m, 2H, H-7); $^{13}\text{C NMR}$ (101 MHz, DMSO) δ 176.1 (C-4), 158.1 (C_q), 154.4 (C_q), 143.6 (C_q), 142.7 (C_q), 133.1 (C_q), 133.1 (C-2' & 6'), 131.9 (C-5''), 124.0 (C_q), 122.5 (C-6''), 121.8 (C_q), 120.12 (q, $J = 3.8$ Hz, C-4''), 119.0 (C-3' & 5'), 114.9 (q, $J = 3.8$ Hz, C-2''), 26.7 (C-5), 22.3 (C-8), 22.3 (C-6) 22.0 (C-7), 18.2 (Me); $\nu_{\text{max}}/\text{cm}^{-1}$; 2922, 1619; **M/Z** (ESI+); 400.15 (Found MH⁺; 400.1519 requires C₂₃H₂₁F₃NO₂ requires 400.1519).

3-(4-(3,4-Dichlorophenoxy)phenyl)-2-methyl-5,6,7,8-tetrahydroquinolin-4(1H)-one (210).



The title compound was synthesised from 4-ethoxy-3-(4-(3-trifluoromethoxyphenoxy)phenyl)-2-methyl-5,6,7,8-tetrahydroquinoline (100 mg, 0.23 mmol) according to general procedure **B** and was isolated as a colourless solid (72 mg, 0.16 mmol, 76%). **MP**; > 250 °C; **HPLC**; 2.91 (91% reference area); **¹H NMR** (501 MHz, DMSO) δ 11.27 (s, 1H, NH), 7.51 (t, *J* = 8.3 Hz, 1H, H-5''), 7.22 (d, *J* = 8.5 Hz, 2H, H-2' & 6'), 7.12 (d, *J* = 7.6 Hz, 1H, H-4''), 7.07 (d, *J* = 8.5 Hz, 2H, H-3' & 5'), 7.03 (dd, *J* = 8.6, 1.7 Hz, 1H, H-6''), 7.00 (s, 1H, H-2''), 2.58 (t, *J* = 5.2 Hz, 2H, H-5), 2.32 (t, *J* = 6.2 Hz, 2H, H-8), 2.09 (s, 3H, Me), 1.76 – 1.69 (m, 2H, H-6), 1.69 – 1.61 (m, 2H, H-7); **¹³C NMR** (126 MHz, DMSO) δ 174.4 (C-4), 158.3 (C_q), 154.1 (C_q), 149.3 (C_q), 144.1 (C_q), 143.1 (C_q), 132.5 (C-2' & 6'), 131.9 (C_q), 131.5 (C-5''), 123.6 (C_q), 121.2 (C_q), 118.7 (C-3' & 5'), 116.9 (C-6''), 115.3 (C-4''), 110.9 (C-2''), 26.3 (C-5), 21.8 (C-8), 21.7 (C-6), 21.4 (C-7), 17.8 (Me); **v_{max}/cm⁻¹**; 2922, 1619, 1461, 1447, 1326, 1239; **M/Z** (ESI+); 416.15 (Found MH⁺; 416.1469, C₂₃H₂₁F₃NO₃ requires 416.1468).

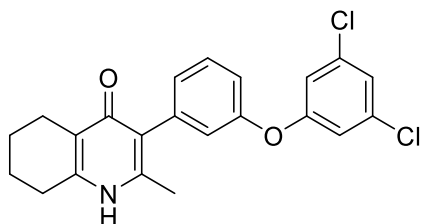
2-Methyl-3-(3-(4-Chlorophenoxy)phenyl)-5,6,7,8-tetrahydroquinolin-4(1H)-one (211).



The title compound was synthesised from 4-ethoxy-2-methyl-3-(3-(4-chlorophenoxy)phenyl)-5,6,7,8-tetrahydroquinoline (300 mg, 0.76 mmol) according to general procedure **B**, and was isolated as a colourless solid (38 mg, 0.10 mmol, 13%). **MP**; >250 °C; **HPLC**; 2.76 mins (100% reference area). **¹H NMR**; (500 MHz, MeOD) δ 7.31 (t, *J* = 7.9 Hz, 1H, H-5'), 7.22 (dd, *J* = 6.8, 2.1 Hz, 2H, H-3'' & 5''), 6.95 – 6.91 (m, 2H, H-2'' & 6''), 6.90 (d, *J* = 7.7 Hz, 1H, H-6'), 6.87 (dd, *J* = 8.2, 2.4 Hz, 1H, H-4'), 6.77 (d, *J* = 1.5 Hz, 1H, H-2'), 2.57 (t, *J* = 5.6 Hz, 2H, H-5), 2.39 (t, *J* = 6.0 Hz, 2H, H-

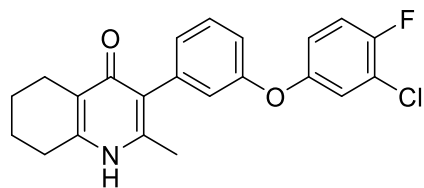
8), 2.04 (s, 3H Me), 1.77-1.65 (m, 4H, H-6 & 7); $^{13}\text{C NMR}$ (101 MHz, MeOD) δ 177.3 (C-4), 156.7 (C_q), 156.1 (C_q), 144.8 (C_q), 143.6 (C_q), 137.6 (C_q), 129.5 (C-5', 3'' & 5''), 128.0 (C_q), 126.0 (C-6'), 125.5 (C_q), 123.1 (C_q), 121.0 (C-2'), 119.9 (C-2'' & 6''), 117.5 (C-4'), 26.6 (C-5), 21.9 (C-8), 21.7 (C-6), 21.6 (C-7), 17.4 (Me); $\nu_{\text{max}}/\text{cm}^{-1}$; 2857, 1619, 1572, 1487, 1309, 1273, 1227; **M/Z (ESI)**; 366.13 (Found MH⁺ 366.1256, C₂₂H₂₀ClNO₂ requires 366.1255).

3-[3-(3,5-dichlorophenoxy)phenyl]-2-methyl-5,6,7,8-tetrahydro-1H-quinolin-4(1H)-one (213).



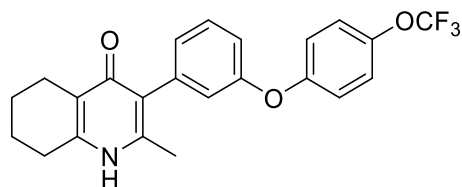
The title compound was synthesised from 3-[3-(3,5-dichlorophenoxy)phenyl]-4-ethoxy-2-methyl-5,6,7,8-tetrahydroquinoline (30 mg, 0.07 mmol) according to general procedure **B**, and was isolated as a colourless powder (11 mg, 0.03 mmol, 36%). **MP**: >250 °C; **HPLC**; 2.96 mins (98% reference area); $^1\text{H NMR}$ (400 MHz, CDCl₃)⁺ δ 13.25 (s, 1H, NH), 7.66 (t, J = 8.0 Hz, 1H, H-5'), 7.24 (dd, J = 8.4, 1.7 Hz, 1H, H-6'), 7.22 (s, 1H, H-4''), 7.10 (d, J = 7.5 Hz, 1H, H-4'), 7.01 – 6.94 (m, 3H, 2', 3'' & 5''), 3.02 (t, J = 5.1 Hz, 2H, H-5), 2.75 (t, J = 5.3 Hz, 2H, H-8), 2.45 (s, 3H, Me), 2.03 – 1.84 (m, 4H, H-6 & 7); $^{13}\text{C NMR}$ (101 MHz, CDCl₃) δ 164.2 (C-4), 158.2 (C_q), 157.0 (C_q), 152.6 (C_q), 150.0 (C_q), 136.1 (C-3'' & 5''), 132.6 (C-5'), 130.0 (C_q), 125.1 (C-4'), 124.8 (C-4''), 122.8 (C_q), 121.8 (C_q), 120.7 (C-6'), 120.0 (C-2'), 118.2 (C-2'' & 6''), 27.0 (C-5), 21.5 (C-8), 20.6 (C-6), 20.6 (C-7), 18.1 (Me); $\nu_{\text{max}}/\text{cm}^{-1}$; 2932, 1572, 1502, 1306; **M/Z (ESI)**; 400.09 (Found MH⁺ 400.0864, C₂₂H₂₀Cl₂NO₂ requires 400.0866).

3-(3-(3,4-Dichlorophenoxy)phenyl)-2-methyl-5,6,7,8-tetrahydroquinolin-4(1H)-one (214).



The title compound was synthesised from 3-(3-(3-Chloro-4-fluorophenoxy)phenyl)-4-ethoxy-2-methyl-5,6,7,8-tetrahydroquinoline (39 mg, 0.10 mmol) according to general procedure **B**, and was isolated as a white solid (35 mg, 0.09 mmol, 96%). **MP**; >250 °C; **HPLC**; 2.72; **¹H NMR** (501 MHz, DMSO) δ 11.14 (s, 1H, NH), 7.42 (t, J = 9.1 Hz, 1H, H-5''), 7.37 (t, J = 7.9 Hz, 1H, H-5'), 7.25 (dd, J = 6.2, 3.0 Hz, 1H, H-6'), 7.03 (dt, J = 3.4, 9.0 Hz, 1H, H-6''), 6.96 (d, J = 7.6 Hz, 1H, H-2''), 6.93 (dd, J = 8.1, 2.4 Hz, 1H, H-4'), 6.84 – 6.81 (m, 1H, H-2'), 2.52 (t, J = 6.3 Hz, 2H, H-5), 2.26 (t, J = 6.1 Hz, 2H, H-8), 2.05 (s, 3H, Me), 1.68 (m, 2H, H-6), 1.62 (m, 2H, H-7); **¹³C NMR** (101 MHz, DMSO) δ 174.0 (C-4), 156.1 (C_q), 155.9 (d, J = 242 Hz, C-4''), 153.9 (d, J = 2.2 Hz, C-1'''), 143.8 (C_q), 142.8 (C_q), 139.1 (C_q), 129.8 (C-5'), 127.1 (C-6''), 124.1 (C_q), 121.9 (C_q), 121.7 (C-6'), 120.8 (C-4'), 120.66 (d, J = 19.5 Hz, C-3''), 119.25 (d, J = 7.2 Hz, C-2''), 118.25 (d, J = 22.4 Hz, H-5''), 117.1 (C-2'), 26.7 (C-5), 22.3 (C-8), 22.3 (C-7), 22.0 (C-6), 18.1 (Me); **ν_{\max} /cm⁻¹**; 2855, 1619, 1484, 1247; **M/Z (ESI)**; 384.12 Found MH⁺; 384.1167, C₂₂H₁₉ClFNO₂ requires 384.1161)

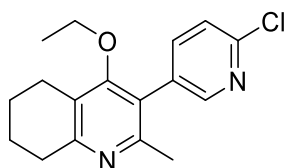
2-Methyl-3-(3-(4-(trifluoromethoxy)phenoxy)phenyl)-5,6,7,8-tetrahydroquinolin-4(1H)-one (215).[^]



The title compound was synthesised from 4-ethoxy-2-methyl-3-(3-(4-(trifluoromethoxy)phenoxy)phenyl)-5,6,7,8-tetrahydroquinoline (86 mg, 0.19 mmol) according to general procedure **B**, and was isolated as a colourless powder (35 mg, 0.08 mmol, 45%). **MP**; >250 °C; **HPLC**; 2.91 mins (100% reference area); **¹H NMR** (500 MHz, MeOD)* δ 7.31 (t, J = 7.9 Hz, 1H, H-5''), 7.14 (d, J = 8.6 Hz, 2H, H-3'' & 5''), 7.03 – 6.95 (d, J = 9.1 Hz, 2H, H-2'' & 6'''), 6.91 (d, J = 7.6 Hz, 1H, H-6'), 6.88 (dd, J = 8.2,

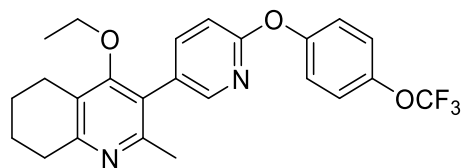
1.7 Hz, 1H, H-4'), 6.82 – 6.75 (m, 1H, H-2'), 2.55 (t, $J = 6.1$ Hz, 2H, H-5), 2.38 (t, $J = 6.0$ Hz, 2H, H-8), 2.03 (s, 3H, Me), 1.84 – 1.52 (m, 4H, H-6 & 7); ^{13}C NMR (126 MHz, MeOD) δ 178.6 (C-4), 158.0 (C_q), 157.8 (C_q), 146.6 (C_q), 145.6 (C_q), 145.4 (C_q), 139.2 (C_q), 130.9 (C-5'), 127.5 (C-6'), 126.8 (C_q), 124.2 (C_q), 123.8 (C-2'' & 6''), 122.8 (C-2'), 120.6 (C-3'' & 5''), 119.1 (C-4'), 27.8 (C-5), 23.12 (C-8), 23.1 (C-6), 22.8 (C-7), 18.0 (C-Me); $\nu_{\text{max}}/\text{cm}^{-1}$; 2937, 1614, 1500, 1432, 1256, 1221; **M/Z (ESI)**; 416.15 (Found MH⁺ 416.1467, C₂₃H₂₁F₃NO₃ requires 416.1468).

4-Ethoxy-3-(6-chloropyridin-3-yl)-2-methyl-5,6,7,8-tetrahydroquinoline (176)



To a nitrogen flushed flask charged with 4-ethoxy-3-iodo-2-methyl-5,6,7,8-tetrahydroquinoline (1.50 g, 4.70 mmol), 2-chloropyridine-5-boronic acid (1.12 g, 7.10 mmol) and palladium tetra(triphenylphosphine) (0.27 g, 0.24 mmol) was added degassed DMF (20.00 mL). Potassium carbonate_(aq) (3.00 mL, 2.00 M) was added and the reaction mixture brought up to 80 °C and stirred for 3 hours. The reaction mixture was then cooled to room temperature and diluted with water (10.00 mL). The organic phase was then extracted using ethyl acetate (3 x 20.00 mL). The organic phases were combined and washed with water (3 x 20.00 mL) and then dried with brine (1 x 10.00 mL) and MgSO₄, before concentration *in vacuo*. The resulting residue was purified by column chromatography (Pet:EtOAc), to afford the title compound as yellow platelets (0.33 g, 1.09 mmol, 23%). **HPLC**; 2.17 min (100% reference area); **MP**; 114.5-115.5 °C; **¹H NMR** (500 MHz, CDCl₃) δ 8.33 (d, $J = 2.4$ Hz, 1H, C-2'), 7.60 (dd, $J = 8.2, 2.4$ Hz, 1H, C-6'), 7.44 – 7.42 (d, $J = 8.2$, 1H, C-5'), 3.53 (q, $J = 7.0$ Hz, 2H, CH₃CH₂O), 2.98 (t, $J = 6.2$ Hz, 2H, H-8), 2.72 (t, $J = 6.2$ Hz, 2H, H-5), 2.35 (s, 3H, Me), 1.93 – 1.85 (m, 2H, H-7), 1.84 – 1.76 (m, 2H, H-6), 1.06 (t, $J = 7.0$ Hz, 3H, CH₃CH₂O); ^{13}C NMR (126 MHz, CDCl₃) δ 162.2 (C_q), 158.9 (C_q), 154.5 (C_q), 150.6 (C_q), 150.4 (C-2'), 140.4 (C-6'), 131.2 (C_q), 123.9 (C-5'), 123.8 (C_q), 123.0 (C_q), 68.5 (CH₃CH₂O), 32.6 (C-8), 23.1 (C-5), 23.1 (C-7), 22.9 (C-6), 22.3 (2-Me), 15.5 (CH₃CH₂O); $\nu_{\text{max}}/\text{cm}^{-1}$; 2934, 1548, 1433, 1412, 1326; **M/Z (ESI+)**; 303.13 (Found MH⁺; 303.1266, C₁₇H₂₀ClN₂O requires 303.1259).

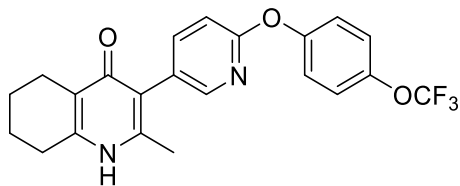
4-Ethoxy-3-(6-(4-trifluoromethoxyphenoxy)pyridin-3-yl)-2-methyl-5,6,7,8-tetrahydroquinoline (226).



4-Ethoxy-3-(6-chloropyridin-3-yl)-2-methyl-

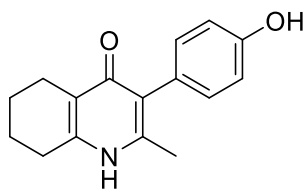
5,6,7,8-tetrahydroquinoline (0.25 g, 0.82 mmol), 4-trifluoromethoxyphenol (0.18 g, 1.00 mmol) and potassium carbonate (0.28 g, 1.70 mmol) were dissolved in DMF (5.00 mL) and refluxed at 110 °C for 24 hours. The reaction mixture was then cooled to room temperature and diluted with water (10.00 mL). The organic phase was then extracted using ethyl acetate (3 × 20.00 mL). The organic phases were combined and washed with water (3 × 20.00 mL) and then dried with brine (1 × 10.00 mL) and MgSO₄, before concentration *in vacuo*. The resulting residue was purified by reverse phase column chromatography (H₂O : acetonitrile), to yield the title compound as a yellow oil (0.075 g, 0.17 mmol, 20%). **MP**; 75.2-75.4 °C; **HPLC**; 3.23 mins (96% reference area); **¹H NMR** (400 MHz, CDCl₃) δ 8.03 (d, *J* = 2.2 Hz, 1H, H-2'), 7.58 (dd, *J* = 8.4, 2.2 Hz, 1H, 6'), 7.29 – 7.07 (m, 4H, C-2'', 3'', 5'' & 6''), 6.95 (d, *J* = 8.4 Hz, 1H, 5'), 3.46 (q, *J* = 7.0 Hz, 2H, CH₃CH₂O), 2.85 (t, *J* = 6.3 Hz, 2H, H-8), 2.64 (t, *J* = 6.1 Hz, 2H, H-5), 2.25 (s, 3H, Me), 1.81 (dt, *J* = 12.2, 6.3 Hz, 2H), 1.77 – 1.68 (m, 2H), 0.99 (t, *J* = 7.0 Hz, 3H, CH₃CH₂O); **¹³C NMR** (100 MHz, CDCl₃) δ 162.5 (C_q), 162.4 (C_q), 158.2 (C_q), 154.8 (C_q), 152.3 (C_q), 148.3 (C-2'), 145.7 (C_q), 145.7 (C_q), 141.5 (C-6'), 127.4 (C_q), 123.8 (C_q), 122.4 (C-2'', 3'', 5'' & 6''), 111.2 (C-5'), 68.4 (CH₃CH₂O), 32.5 (C-5), 23.1 (C-8), 23.1 (Me), 22.9 (C-6), 22.4 (C-7), 15.5 (CH₃CH₂O); **M/Z** (ESI+); 445.18 (Found MH⁺; 445.1759, C₂₄H₂₄F₃N₂O₃ requires 445.1739).

3-(6-(4-Trifluoromethoxyphenoxy)pyridin-3-yl)-2-methyl-5,6,7,8-tetrahydroquinolin-4(1H)-one (227).



The title compound was synthesised from 4-ethoxy-3-(6-(4-trifluoromethoxyphenoxy)pyridin-3-yl)-2-methyl-5,6,7,8-tetrahydroquinoline (70 mg, 0.15 mmol) according to general procedure **B** and was isolated as colourless solid (13 mg, 0.03 mmol, 20%). **MP**; 250-251 °C; **HPLC**; 2.73 min (100% reference area); **¹H NMR** (400 MHz, DMSO) δ 11.07 (s, 1H, NH), 7.94 (d, *J* = 2.2 Hz, 1H, H-2'), 7.70 (dd, *J* = 8.4, 2.4 Hz, 1H, H-6'), 7.43 (d, *J* = 8.7 Hz, 2H, H-3'' & 5''), 7.29 (d, *J* = 9.0 Hz, 2H, H-3'' & 6''), 7.09 (d, *J* = 8.4 Hz, 1H, H-5'), 2.56 (t, *J* = 5.1 Hz, 2H, H-5), 2.30 (t, *J* = 5.9 Hz, H, H-8), 2.10 (s, 3H, Me), 1.79 – 1.57 (m, 4H, H-6 & 7); **¹³C NMR** (101 MHz, DMSO) δ 175.9 (C-4), 161.6 (C_q), 153.2 (C_q), 148.8 (C-2'), 145.0 (q, *J* = 1.8 Hz, C-4''), 144.1 (C_q), 143.4 (C_q), 143.2 (C-6'), 128.0 (C_q), 123.3 (C-2'' & 6''), 123.0 (C-3'' & 5''), 121.8 (C_q), 120.7 (C_q), 111.0 (C-5'), 26.7 (C-5), 22.3 (C-8), 22.2 (C-6), 21.9 (C-7), 18.2 (Me); **v_{max}/cm⁻¹**; 2933, 1621, 1463, 1253; **M/Z** (ESI+); 417.14 (Found MH⁺; 417.1432, C₂₂H₂₀F₃N₂O₃ requires 417.1421).

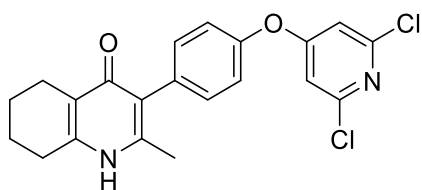
3-(Phen-4-ol)-2-methyl-5,6,7,8-tetrahydroquinolin-4(1H)-one (222).



3-Iodo-2-methyl-5,6,7,8-tetrahydroquinolin-4(1H)-one (0.40 g, 1.39 mmol), 4-hydroxybenzen boronic acid (0.29 g, 2.08 mmol) and palladium tetrakis (0.08 g, 0.07 mmol) were charged into a nitrogen flushed flask and dissolved in DMF (5.00 mL), sodium carbonate solution (1.75 mL, 2.00 M) was then added and reaction heated to 80 °C. The organic phase was then extracted using ethyl acetate (3 x 20.00 mL). The organic phases were combined and washed with water (3 x 20.00 mL) and then dried with brine (1 x 10.00 mL) and MgSO₄, before concentration *in vacuo*. The title compound was isolated as a colourless solid (0.28 g, 1.08 mmol, 78%). **MP**; >250 °C; **HPLC**; 1.50 mins (83% reference area); **¹H NMR** (400 MHz, MeOD) δ 6.91 (d,

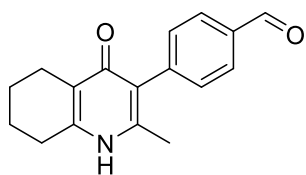
$J = 8.6$ Hz, 2H, H-2' & 6'), 6.71 (d, $J = 8.6$ Hz, 2H, H-3' & 5'), 2.57 (t, $J = 6.0$ Hz, 2H, H-5), 2.39 (t, $J = 5.6$ Hz, 2H, H-8), 2.03 (s, 3H, Me), 1.77 – 1.61 (m, 4H, H-6 & 7); $^{13}\text{C NMR}$ (101 MHz, MeOD) δ 177.7 (C-4), 156.5 (C_q), 144.7 (C_q), 144.1 (C_q), 131.4 (C-2' & 6'), 126.2 (C_q), 122.5 (C_q), 114.8 (C-3' & 5'), 26.4 (C-8), 21.8 (C-5), 21.7 (C-7), 21.5 (C-6), 16.7 (Me); $\nu_{\text{max}}/\text{cm}^{-1}$; 2932, 1607, 1447, 1260; **M/Z** (ESI+); 256.13 (Found MH⁺; 256.1330, C₁₆H₁₇NO₂ requires 256.1332).

3-{4-[(2,6-dichloropyridin-4-yl)oxy]phenyl}-2-methyl-5,6,7,8-tetrahydro-1H-quinolin-4-one (231)⁺



The title compound was synthesised as follows; 3-phenol-2-methyl-5,6,7,8-tetrahydroquinolin-4(1H)-one (120 mg, 0.47 mmol) and potassium carbonate (78 mg, 0.56 mmol) were dissolved in DMF (3.00 mL) and the reaction mixture was stirred for 15 mins. Following this, 2,4,6-Trichloropyridine (86 mg, 0.47 mmol) was added and the mixture was heated to 100 °C and stirred for 18 hours under an inert atmosphere. The reaction mixture was allowed to cool to room temperature and was diluted with water (5.00 ml). The resulting pale grey precipitate was collected by vacuum filtration, washed with water (5 ml) and dried (118 mg, 0.29 mmol, 63%). **MP**; >250 °C; **HPLC**; 2.52 mins; $^1\text{H NMR}$ (500 MHz, TFA) δ 7.66 (d, $J = 8.5$ Hz, 2H, H-2'' & 6''), 7.56 (d, $J = 8.5$ Hz, 2H, H-3' & 5'), 7.44 (s, 2H, H-2' & 6'), 3.10 (t, $J = 5.0$ Hz, 2H, H-5), 2.90 (t, $J = 5.0$ Hz, 2H, H-8), 2.55 (s, 3H, Me), 2.10-2.08 (m, 4H, H-6 & 7); $^{13}\text{C NMR}$: (126 MHz TFA) δ 171.6 (C-4), 155.5 (C_q), 154.9 (C_q), 137.6 (C_q), 136.3 (C-2' & 6'), 135.7 (C_q), 128.4 (C_q), 126.7 (C_q), 124.3 (C_q), 124.0 (C-3' & 5'), 122.2 (C-3), 114.7 (C-2'' & 6''), 112.9 (C-10), 30.3 (C-8), 25.5 (C-5), 25.3 (C-7), 25.2 (C-6), 21.2 (Me); **M/Z** (ESI); 400.08 (MH⁺ found; 400.0826, C₂₁H₁₉Cl₂N₂O₂ requires 400.0745).

3-(benzyl-4-adehyde)-2-methyl-5,6,7,8-tetrahydroquinolin-4(1H)-one (223)



4(1H), 3-iodo-2-methyl-5,6,7,8-tetrahydroquinolin-

4(1H)-one (1.00 g, 3.46 mmol), 4-formylbenzene boronic acid (0.78 g, 5.20 mmol) and palladium tetrakis (0.20 g, 0.17 mmol) were charged into a nitrogen flush flask, and dissolved in DMF (5.00 mL), sodium carbonate solution (1.75 mL, 2.00 M) was then added and reaction heated to 80 °C. The reaction was monitored by LCMS, on completion the reaction mixture was allowed to cool and was dilute with water (10.00 mL) before filtering. The title compound was isolated as a colourless solid (0.48 g, 1.78 mmol, 51%). **MP**; >250 °C; **HPLC**; 1.56 mins (94% reference area); **¹H NMR** (500 MHz, MeOD) δ 8.73 (s, 1H, HCO), 6.66 (d, *J* = 8.0 Hz, 2H, H-3' & 5'), 6.15 (d, *J* = 8.0 Hz, 2H, H-2' & 6'), 1.40 (t, *J* = 6.1 Hz, 2H, H-5), 1.21 (t, *J* = 6.0 Hz, 2H, H-8), 0.86 (s, 3H, Me), 0.53 (dd, *J* = 25.0, 5.4 Hz, 4H, H-6 & 7); **¹³C NMR** (126 MHz, MeOD) δ 193.9 (HCO), 178.4 (C-4), 146.9 (C_q), 145.5 (C_q), 144.1 (C_q), 136.8 (C_q), 132.7 (C-2' & 6'), 130.7 (C-3' & 5'), 126.5 (C_q), 124.3 (C_q), 27.8 (C-5), 23.1 (C-8), 23.0 (C-6), 22.8 (C-7), 18.0 (Me); **v_{max}/cm⁻¹**; 2923, 1708, 1620, 1470, 1207; **M/Z** (ESI+); 268.13 (Found MH⁺; 268.1330 C₁₇H₁₈NO₂ requires 268.1332).

5.4 Experimental: Chapter 4.

5.4.1 General procedure J (Quinolone formation)

2,2-Dimethyl-1,3-dioxane-4,6-dione (1.50 equiv.) was dissolved in triethyl orthoacetate (2.00 equiv.) and heated to 115 °C for 2 hours. The reaction was cooled to allow the addition of the aniline (1.00 equiv.) before being heated to 115 °C for a further 2 hours. The reaction mixture was then allowed to cool and was concentrated *in vacuo*, remaining solvent was washed off with cold methanol. The precipitate was then dissolved in minimum volume of Dowtherm A and refluxed at 250 °C for 1.5 hours. The reaction mixture was allowed to cool and the precipitate filtered followed by washing with hexane to afford the title compound.

5.4.2 General method K (Hydrogenation)

The 4-hydroxylquinolone (1.00 equiv.) was dissolved in acetic acid (10.00 mL) under inert conditions and platinum dioxide (5.00% weight equiv.) was added. A hydrogen balloon was attached and reaction vessel exposed to hydrogen. The reaction was monitored by LCMS. On completion the resulting suspension was filtered through a pad of Celite and washed with ethyl acetate (10.00 mL). The filtrate was concentrated *in vacuo* to afford a yellow/brown oil. Purification by column chromatography (CHCl₃:MeOH) afforded the title compound.

5.4.3 General method L (Iodination)

The tetrahydroquinolin-4(1H)-one (1.00 equiv.) and N-iodosuccinimide (1.20 equiv.) were dissolved in acetonitrile (5.00 mL mmol⁻¹) and stirred and heated at 80 °C for 3 hours. The reaction mixture was then allowed to cool and the mixture filtered, the precipitate was then washed with water (15.00 mL) to afford the title compound.

5.4.4 General method M (One Pot Suzuki)

A flask charged with the 4-bromo-diarylether (1.00 equiv.), bispinocolatodiborane (1.10 equiv.), KOAc (3.00 equiv.) and Pd(dppf)Cl₂ (3.00 mol%) was flushed with nitrogen. DMF (2.00 mL) was added and the reaction was stirred at 80 °C for 18 hours. After cooling the solution to room

temperature, 3-iodotetrahydroquinoline (2.00 equiv.), PdCl₂(dppf) (3.00 mol%) and Na₂CO₃ (2.00 M, 5.00 equiv.) were added and the mixture was stirred at 80 °C under nitrogen for a further 24 hours. The solution was cooled to room temperature, the product was extracted with Et₂O (15.00 mL). The organic layers were combined and washed with H₂O (15.00 mL), brine and dried over MgSO₄ and concentrated *in vacuo*. This was followed by purification by silica gel chromatography (ethyl acetate/petroleum ether) afford the title compound.

5.4.5 General method N (Suzuki)

To a nitrogen flushed flask charged with the 4-ethoxy-3-iodo-tetrahydroquinoline (1.00 equiv.), 4-hydroxybenzene boronic acid (1.50 equiv.) and palladium tetra(triphenylphosphine) (0.05 equiv.) was added degassed DMF (5.00 mLmmol⁻¹). Potassium carbonate_(aq) (2.00 M, 2.50 equiv.) was added and the reaction mixture brought up to 80 °C and stirred for 3 hours. The reaction mixture was then cooled to room temperature and diluted with water (5.00 mL). The organic phase was then extracted using ethyl acetate (3 × 10.00 mL). The organic phases were combined and washed with water (3 × 10.00 mL) and then dried with brine (1 × 10.00 mL) and MgSO₄, before concentration *in vacuo* and purified by column chromatography to afford the title compound.

5.4.6 General method O (Conjugate addition)

Aniline (1.00 equiv.) was dissolved in methanol (0.75 mLmmol⁻¹), Dimethyl acetylenedicarboxylate (1.20 equiv.) was then added slowly and reaction stirred. Exotherm was allowed to cool and reaction stirred and monitored by TLC. Reaction was concentrated and purified by column chromatography when necessary, afford the title compound.

5.4.7 General method P (Thermal cyclisation)

Dimethyl 2-phenylaminofumarate (1.00 equiv.) was dissolved in Dowtherm A (1.00 mLmmol⁻¹) and heated to 250 °C for 1 hour. The reaction mixture was allowed to cool and purified by column chromatography.

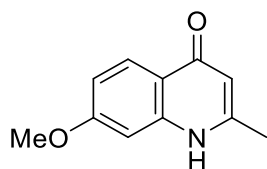
5.4.8 General method Q (N-Oxide formation)

m-Chloroperoxybenzoic acid (70%, 2.00 equiv.) was dissolved in ethyl acetate (5.00 mL mmol⁻¹) and washed with brine (5.00 mL mmol⁻¹), the organic phase was then dried with magnesium sulphate and filtered. The solution of *m*-chloroperoxybenzoic acid in ethyl acetate was then added to the 4-ethoxy-3-(4-(4-trifluoromethoxyphenoxy)phenyl)-5,6,7,8-tetrahydroquinoline (1.00 equiv.) and stirred for 16 hours at room temperature. The solution was then concentrated *in vacuo* before trituration with cold petrol to cause a colourless solid to precipitate. Precipitate was filtered and washed with cold petrol to give the afford the title compound

5.4.9 General method R (Boekelheide rearrangement)

The N-Oxide (1.00 equiv.) was dissolved in acetic anhydride (25.00 mL mmol⁻¹) and heated to 158 °C for 4 hours. The solvent was then removed under reduced vacuum and the residue purified by column chromatography to afford the title compound.

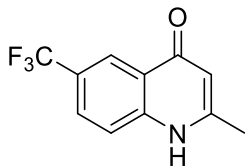
7-Methoxyquinolin-(4H)-one (234).



m-Anisidine (1.00 mL, 10.90 mmol) and ethyl acetoacetate (1.55 mL, 12.10 mmol) were added to ethanol (anhydrous, 7.00 mL), acetic acid (0.70 mL) was added and the reaction heated to reflux with stirring for 18 hours. The reaction mixture was then allowed to cool and concentrated *in vacuo* before purification of the intermediate via column chromatography to give a red oil. The oil was then added to a flask of Dowtherm A (7.00 mL) and heated to 250 °C for 10 minutes, after cooling a precipitate formed and was filtered. Precipitate was then purified by column chromatography (EtOAc:MeOH) (0.20 g, 1.05 mmol, 10%). **MP**; 237.0-238.2 °C; **HPLC**; 1.45 mins (100% reference area); **¹H NMR**; (400 MHz, MeOD) δ 7.98 (d, *J* = 9.1 Hz, 1H, H-5), 6.87 (dd, *J* = 9.1, 2.3 Hz, 1H, H-6), 6.80 (d, *J* = 2.2 Hz, 1H, H-8), 6.01 (s, 1H, H-3), 3.80 (s, 3H, OMe), 2.33 (s, 3H, Me); **¹³C NMR**; (101 MHz, MeOD) δ 178.8 (C-4), 163.1 (C-7), 151.0 (C_q), 142.1 (C_q), 126.3 (C-5), 118.2 (C_q), 114.1 (C-6), 107.8 (C_q), 98.1 (C-8), 54.7 (OMe), 18.4 (Me); **v_{max}/cm⁻¹**;

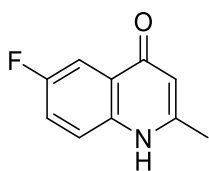
2788, 1609, 1469, 1216; **M/Z (ESI)**; 190.09 (Found MH⁺: 190.863 C₁₁H₁₂NO₂ requires 190.0863).

2-Methyl-6-(trifluoromethyl)quinolin-4(1H)-one (248).



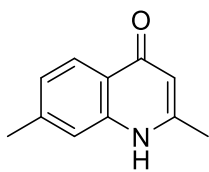
The title compound was synthesised from 4-trifluoromethyl aniline (2.00 g, 12.4 mmol) according to general method **J** and was isolated as a colourless solid (0.47 g, 2.05 mmol, 17%). **MP**; >250 °C; **HPLC**; 3.42 min (95% reference area); **R_f**; 0.21 (10% MeOH)*; **¹H NMR** (300 MHz, MeOD) δ 8.42 (s, 1H, H-5), 7.81 (dd, *J* = 8.8 Hz, 2.1 Hz, 1H, H-7), 7.60 (d, *J* = 8.8 Hz, 1H, H-8), 6.16 (s, 1H, H-3), 2.40 (s, 3H, 2-Me); **¹³C NMR** (126 MHz, MeOD) δ 179.9 (C-4), 154.0 (C_q), 143.34 (C_q), 129.1 (q, *J* = 3.2 Hz, C-7), 126.64 (q, *J* = 33.5 Hz, C-6), 124.8 (C_q), 123.98 (q, *J* = 4.2 Hz, C-5), 120.27 (C-8), 110.59 (C_q), 19.82 (Me); **v_{max}/cm⁻¹**; 2974, 1646, 1600, 1562, 1488, 1408, 1324, 1296, 1238; **M/Z (ESI+)**; 228.06 (Found MH⁺ 228.0634, C₁₁H₉F₃NO requires 228.0630).

2-Methyl-6-fluoroquinolin-(4H)-one (249).



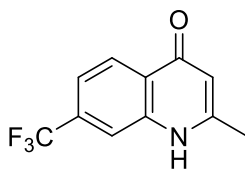
The title compound was synthesised from 4-fluoroaniline (2.00 mL, 20.10 mmol) according to general procedure **J**, and was isolated as brown microcrystals (0.84 g, 4.75 mmol, 24%). **MP**; > 250 °C; **HPLC**; 1.26 mins (100% reference area); **¹H NMR**; (400 MHz, MeOD) δ 7.72 (dd, *J* = 9.3, 2.8 Hz, 1H, H-5), 7.50 (dd, *J* = 9.1, 4.5 Hz, 1H, H-8), 7.42 – 7.28 (m, 1H, H-7), 6.11 (s, 1H, H-3), 2.37 (s, 3H, 2-Me); **¹³C NMR**; (101 MHz, MeOD) δ 178.0 (C-4), 159.3 (d, *J* = 244.0 Hz, C-6'), 151.9 (C-2), 136.8 (C-9), 125.1 (d, *J* = 7.1 Hz, C-10), 120.9, (d, *J* = 26.0 Hz, C-7), 120.2 (d, *J* = 8.3 Hz, C-8), 108.6 (d, *J* = 22.9 Hz, C-5), 107.6 (C-3), 18.4 (2-Me); **v_{max}/cm⁻¹**; 2745, 1646, 1603, 1550, 1517, 1479, 1408, 1364, 1297, 1247; **M/Z (ESI)**; 178.07 (Found MH⁺; 178.0664 C₁₀H₉FNO requires 178.0663).

2,7-Dimethylquinolin-4(1H)-one (250).



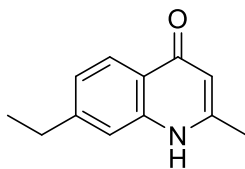
The title compound was synthesised from 3-methylaniline (4.00 mL, 37.4 mmol) according to general procedure **J**, and was isolated as a colourless solid (0.70 g, 4.05 mmol, 11%). **MP**; > 250 °C; **HPLC**; 1.43 mins (92% reference area); **¹H NMR** (400 MHz, CDCl₃) δ 9.58 (s, 1H, NH), 8.24 (d, *J* = 8.3 Hz, 1H, H-5), 7.22 (s, 1H, H-8), 7.16 (d, *J* = 8.3 Hz, 1H, H-6), 6.15 (s, 1H, H-3), 2.46 (s, 3H, Me), 2.41 (s, 3H, Me). **¹³C NMR** (126 MHz, MeOD)* δ 180.4 (C-4), 152.6 (C_q), 144.5 (C_q), 141.7 (C-7), 126.7 (C-5), 125.8 (C-8), 123.2 (C_q), 118.2 (C-6), 109.3 (C_q), 21.7 (7-Me), 19.7 (2-Me); **v_{max}/cm⁻¹**; 2916, 1603, 1509, 1467, 1309; **M/Z** (ESI+); 174.09 (Found MH⁺;174.0911, C₁₁H₁₂NO requires 174.0913).

7-Trifluoromethyl-2-methylquinolin-4(1H)-one (251).



The title compound was synthesised following general procedure **K** from 3-trifluoromethyl-aniline (3.00 mL, 24.0 mmol). The title compound was isolated with its regioisomer and separation was not achieved and so was carried forwards as a mixture of both regioisomers (1.50 g, 6.61 mmol, 28% combined).

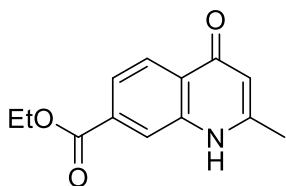
7-Ethyl-2-methylquinolin-4(1H)-one (252).



The title compound was synthesised from 3-ethylaniline (1.40 mL, 11.1 mmol) according to general procedure **J**, and was isolated as a colourless solid (0.21 g, 1.12 mmol, 10%). **MP**; >204.2-206.0 °C; **HPLC**; 1.69 min (100% reference area); **¹H NMR** (500 MHz, CDCl₃) δ 9.72 (s, 1H, NH), 8.17 (d, *J* = 8.3 Hz, 1H, H-8), 7.16 (s, 1H, H-8), 7.10 (d, *J* = 8.3 Hz, 1H, H-6), 6.07 (s, 1H, H-3), 2.66 (q, *J* = 7.6 Hz, 2H, CH₂CH₂), 2.33 (s, 3H, 7-Me), 1.18

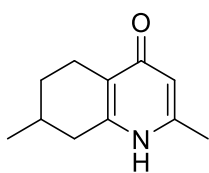
(t, $J = 7.6$ Hz, 3H, CH_2CH_3); ^{13}C NMR (101 MHz, CDCl_3) δ 178.8 (C-4), 150.0 (C-7), 148.8 (C_q), 140.6 (C_q), 125.4 (C-5), 124.4 (C-6), 123.0 (C_q), 116.3 (C-8), 109.0 (C_q), 29.0 (CH_3CH_2), 20.2 (Me), 15.1 (CH_3CH_2); $\nu_{\text{max}}/\text{cm}^{-1}$; 2922, 1644, 1604, 1546, 1511, 1464; **M/Z** (ESI+); 188.11 (Found MH^+ ; 188.1068 $\text{C}_{12}\text{H}_{14}\text{NO}$ requires 188.1070).

Ethyl-2-methylquinolin-4(1H)-one-7-carboxylate (253).



The title compound was synthesised from Methyl-3-carboxylaniline (2.60 g, 17.22 mmol) according to general procedure K, and was isolated as colourless solid a mixture of the two regioisomers (0.84 g, 3.32 mmol, 20%). **MP**; >250 °C; **HPLC**; 1.71 mins (91% reference area); ^1H NMR (400 MHz, MeOD) δ 8.17 (d, $J = 8.5$ Hz, 1H, H-5), 8.11 (d, $J = 1.0$ Hz, 1H, H-8), 7.83 (dd, $J = 8.5, 1.4$ Hz, 1H, H-6), 6.15 (s, 1H, H-3), 4.33 (q, $J = 7.1$ Hz, 2H, $\text{CH}_3\text{CH}_2\text{O}$), 2.39 (s, 3H, Me), 1.33 (t, $J = 7.1$ Hz, 3H, $\text{CH}_3\text{CH}_2\text{O}$). ^{13}C NMR (101 MHz, MeOD) δ 178.6 (C-4), 165.5 (CO_2Me), 152.7 (C_q), 139.7 (C_q), 133.5 (C-7), 126.5 (C-10), 125.2 (C-8), 123.1 (C-6), 119.6 (C-5), 109.1 (C_q), 61.4 ($\text{CH}_3\text{CH}_2\text{O}$), 18.5 (Me), 13.1 ($\text{CH}_3\text{CH}_2\text{O}$); **M/Z** (ESI); 254.08 (Found MNa^+ ; 254.0788, $\text{C}_{13}\text{H}_{14}\text{NO}_3$ requires 254.0788).

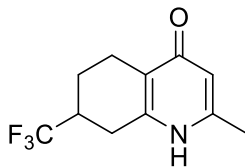
2,7-Dimethyl-5,6,7,8-tetrahydroquinolin-4(1H)-one (255).



The title compound was synthesised from 2,7-dimethylquinolin-4(1H)-one (0.68 g, 4.00 mmol) according to general procedure K, and was isolated as a colourless solid (0.69 g, 3.90 mmol, 98%). **MP**; >250 °C; **HPLC**; 1.48 mins (100% reference area); ^1H NMR (400 MHz, MeOD) δ 6.16 (s, 1H, H-3), 2.81 – 2.58 (m, 2H, H-5 & 8), 2.43 – 2.23 (m, 5H, H-5, 8 and 2-Me), 1.99 – 1.84 (m, 2H, H-6 & 7), 1.33 (qd, $J = 11.2, 5.9$ Hz, 1H, H-7), 1.11 (d, $J = 6.5$ Hz, 1H); ^{13}C NMR (126 MHz, MeOD) δ 180.8 (C-4), 148.6 (C_q), 147.4 (C_q), 123.2 (C_q), 113.9 (C_q), 35.9 (C-8), 31.2 (C-6), 29.4 (C-7), 22.6 (C-

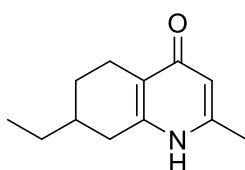
5), 21.5 (7-Me), 18.7 (2-Me) $\nu_{\max}/\text{cm}^{-1}$; 2920, 1625, 1517, 1201; **M/Z** (ESI+); 178.12 (Found MH^+ ; 178.1225, $\text{C}_{11}\text{H}_{16}\text{NO}$ requires 178.1226).

7-trifluormethyl-2-methyl-5,6,7,8-tetrahydroquinolin-4(1H)-one (256).



The title compound was synthesised from a mixture of 7-trifluormethyl-2-methylquinolin-4(1H)-one & 5-trifluormethyl-2-methylquinolin-4(1H)-one (1.50 g, 6.61 mmol) according to general procedure **K**, and was isolated as a colourless solid (0.50 g, 2.14 mmol, 33%). **MP**; >250 °C; **HPLC**; 1.64 mins (84% reference area); **¹H NMR** (500 MHz, MeOD, 1:1) δ 5.99 (s, 1H, H-3), 2.73 – 2.60 (m, 2H, H-5 & 7), 2.53 (dd, $J = 16.3, 12.0$ Hz, 1H, H-5), 2.35 (s, 1H, H-8), 2.20 (ddd, $J = 17.7, 11.4, 5.9$ Hz, 1H, H-8), 2.11 (s, 3H, 2-Me), 2.09 – 2.01 (m, 1H, H-6), 1.42 (ddd, $J = 25.0, 12.1, 5.7$ Hz, 1H, H-6); **¹³C NMR** (101 MHz, DMSO) δ 177.8 (C-4), 146.2 (C_q), 141.3 (C_q), 121.1 (C_q), 113.0 (C_q), 37.4 (C-7), 25.6 (C-8), 21.2 (C-6), 20.8 (C-5), 18.9 (2-Me); CF_3 not observed $\nu_{\max}/\text{cm}^{-1}$; 2925, 1626, 1512, 1402, 1342, 1309, 1277, 1253, 1207; **M/Z** (ESI+); 232.10 (Found MH^+ ; 232.0953, $\text{C}_{11}\text{H}_{13}\text{F}_3\text{NO}$ requires 232.0949).

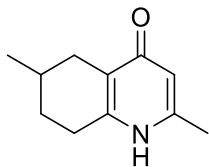
7-ethyl-2-methyl-5,6,7,8-tetrahydroquinolin-4(1H)-one (257).



The title compound was synthesised from 7-ethyl-2-methylquinolin-4(1H)-one (0.20 g, 1.06 mmol) according to general procedure **K**, and was isolated as a colourless solid (0.13 g, 0.68 mmol, 64%). **MP**; >258.4-259.2 °C; **¹H NMR**; (400 MHz, CDCl_3) δ 12.20 (s, 1H, NH), 6.09 (s, 1H, H-3), 2.88 – 2.66 (m, 2H, H-8b & 5b), 2.46 – 2.19 (m, 5H, 2-Me, H-8a & 5a), 1.95 (d, $J = 13.0$ Hz, 1H, H-6a), 1.63 (s, 1H, H-7a), 1.38 (td, $J = 13.9, 6.9$ Hz, 2H, CH_2CH_3), 1.33 – 1.22 (m, 1H, H-6b) 0.94 (t, $J = 7.4$, 3H, CH_2CH_3); **¹³C NMR** (100 MHz, CDCl_3) δ 178.9 (C-4), 146.9 (C_q), 145.8 (C_q), 122.4 (C_q), 113.0 (C_q), 34.9 (C-7), 33.2 (C-8), 28.5 (CH_2CH_3), 28.1 (C-6), 21.8 (C-5), 19.0

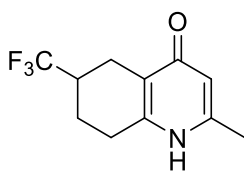
(2-Me), 11.3 (CH₂CH₃); $\nu_{\max}/\text{cm}^{-1}$; 2920, 1625, 1493, 1204; **M/Z** (ESI+); 192.14 (Found MH⁺; 192.1378 C₁₂H₁₈NO requires 192.1383).

2,6-Dimethyl-5,6,7,8-tetrahydroquinolin-4(1H)-one (258).



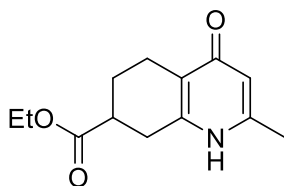
The title compound was synthesised from 2,6-dimethylquinolin-4(1H)-one (1.00 g, 5.78 mmol), according to general procedure **K**, and was isolated as a colourless solid (0.78 g, 4.30 mmol, 76%). **MP**; >250 °C; **HPLC**; 1.48 mins (100% reference area); δ **¹H NMR** (400 MHz, CDCl₃) δ 12.26 (s, 1H, NH), 6.09 (s, 1H, H-3), 2.88 – 2.64 (m, 3H, H-5a, 8a & 8b), 2.30 (s, 3H, 2-Me), 1.98 (dd, J = 16.9, 10.1 Hz, 1H, H-7b), 1.87 (d, J = 12.4 Hz, 1H, H-5b), 1.77 (m, 1H, H-6b), 1.39 (ddd, J = 23.9, 11.1, 6.0 Hz, 1H, H-7a), 1.08 (d, J = 6.5 Hz, 3H, Me-6a); **¹³C NMR** (101 MHz, CDCl₃) δ 178.9 (C-4), 146.3 (C_q), 145.3 (C_q), 122.4 (C_q), 112.9 (C_q), 30.2 (C-8), 29.9 (C-5), 28.4 (C-6), 27.2 (C-7), 21.6 (Me-6), 19.2 (2-Me); $\nu_{\max}/\text{cm}^{-1}$; 2918, 1624, 1525, 1365; **M/Z** (ESI+); 178.13 (Found MH⁺; 178.1280, C₁₁H₁₆NO requires 177.1154).

2-Methyl-6-(trifluoromethyl)-5,6,7,8-tetrahydroquinolin-4(1H)-one (259).



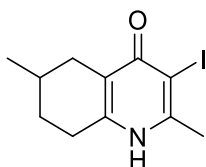
The title compound was synthesised from 2-methyl-6-(trifluoromethyl)quinolin-4(1H)-one (0.47 g, 2.0 mmol), according to general procedure **K**, and was isolated as a colourless solid (0.23 g, 0.99 mmol, 49%). **MP**; > 250 °C; **R_f**; 0.11 (10% MeOH:CDCl₃); **¹H NMR** (500 MHz, MeOD) δ 6.32 (s, 1H, H-3), 2.94 (dd, J = 16.7, 5.1 Hz, 1H, H-5a), 2.86 (dd, J = 8.4, 4.1 Hz, 2H, H-8a & b), 2.65 – 2.52 (m, 1H, H-6a), 2.41 (dd, J = 22.8, 11.5 Hz, 1H, H-7b), 2.36 (s, 3H, Me), 2.28 – 2.15 (m, 1H, H-5b), 1.75 (tt, J = 12.8, 9.1 Hz, 1H, H-7a); **¹³C NMR** (126 MHz, DMSO) δ 169.1 (C-4), 140.6 (C_q), 138.2 (C_q), 119.6 (q, J = 277 Hz, CF₃), 111.0 (C_q), 103.9 (C_q), 29.7 (q, J = 27.3 Hz, C-6), 17.2 (C-8), 12.5 (q, J = 2.8 Hz, C-5), 12.2 (q, J = 2.7 Hz, C-7), 9.4 (2-Me); $\nu_{\max}/\text{cm}^{-1}$; 2951, 1627, 1525, 1392, 1339, 1274, 1255, 1206; **M/Z** (ESI+); 232.10 (Found MH⁺; 232.0955, C₁₁H₁₃F₃NO requires 232.0949).

Ethyl-2-methyl-5,6,7,8-tetrahydroquinolin-4(1H)-one-7-carboxylate.



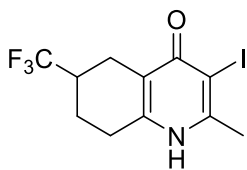
The title compound was synthesised from ethyl-2-methylquinolin-4(1H)-one-7-carboxylate (0.10 g, 0.43 mmol), according to general procedure **K**, and was isolated as a colourless solid (0.10 g, 0.40 mmol, 93%). **MP**; >250 °C; **HPLC**; 1.71 mins (81% reference area); **¹H NMR** (400 MHz, MeOD) δ 6.05 (s, 1H, H-3), 4.07 (qd, *J* = 7.1, 0.9 Hz, 2H, 7-CO₂CH₂CH₃), 2.88 – 2.64 (m, 3H, H-7,8), 2.49 (dt, *J* = 17.4, 5.4 Hz, 1H, H-5), 2.41 – 2.28 (m, 1H, H-5), 2.20 (s, 3H, 2-Me), 2.05 (dd, *J* = 9.5, 4.1 Hz, 1H, H-6), 1.87 – 1.58 (m, 1H, H-6), 1.16 (t, *J* = 7.1 Hz, 3H, 7-CO₂CH₂CH₃); **¹³C NMR** (101 MHz, MeOD) δ 179.2 (C-4), 174.3 (7-CO₂Et), 147.5 (C_q), 144.6 (C_q), 121.5 (C_q), 112.6 (C_q), 60.5 (7-CO₂CH₂CH₃), 38.2 (C-7), 28.2 (C-5), 24.4 (C-6), 20.2 (C-8), 17.4 (Me), 13.1 (7-CO₂CH₂CH₃); **v_{max}/cm⁻¹**; 2904, 1721, 1594, 1504, 1420, 1368, 1272, 1221; **M/Z** (ESI+); 236.13 (Found MH⁺; 236.1282 C₁₃H₁₇NO₃ requires 236.1281)

3-Iodo-2,6-dimethyl-5,6,7,8-tetrahydroquinolin-4(1H)-one (260)



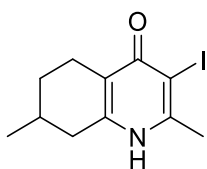
The title compound was synthesised from 2,6-dimethyl-5,6,7,8-tetrahydroquinolin-4(1H)-one (0.75 g, 4.24 mmol) according to general procedure **K**, and was isolated as colourless solid (0.74 g, 2.44 mmol, 58%). **MP**; >250 °C; **HPLC**: 1.58 mins (100% reference area); **¹H NMR** (500 MHz, MeOD) δ 2.36 (dd, *J* = 17.3, 4.8 Hz, H-5a), 2.25 (d, *J* = 4.8 Hz, 2H, H-8a & 8b), 2.15 (s, 3H, 2-Me), 1.57 (dd, *J* = 17.3, 10.4 Hz, 1H, H-7b), 1.51 (d, *J* = 10.9 Hz, 1H, H-5b), 1.36 (s, 1H, H-6b), 1.09 – 0.94 (m, 1H, H-7a), 0.69 (d, *J* = 6.6 Hz, 3H, 6-Me); **¹³C NMR** (126 MHz, MeOD) δ 175.7 (C-4), 148.0 (C_q), 144.2 (C_q), 135.4 (C-10) 119.1 (C-3), 30.4 (C-5), 29.1 (C-7), 27.8 (C-8), 25.6 (C-6), 24.0 (2-Me), 20.4 (6-Me); **v_{max}/cm⁻¹**; 2750, 1632, 1608, 1496; **M/Z** (ESI+); 304.02 (Found MH⁺; 304.0190, C₁₁H₁₅INO requires 304.0193).

3-Iodo-2-methyl-6-(trifluoromethyl)-5,6,7,8-tetrahydroquinolin-4(1H)-one (261).



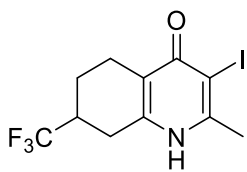
The title compound was synthesised from 2-methyl-6-(trifluoromethyl)-5,6,7,8-tetrahydroquinolin-4(1H)-one (0.23 g, 1.0 mmol) according to general procedure **K**, and was isolated as colourless solid (0.30 g, 0.84 mmol, 84%). **MP**; >250 °C; **HPLC**; 2.03 min (94% reference area); **¹H NMR** (400 MHz, DMSO) δ 11.58 (s, 1H, NH), 2.75 (d, *J* = 5.6 Hz, 1H, H-5a), 2.72 – 2.67 (m, 2H, H-8a & b), 2.62 (dd, *J* = 7.4, 5.8 Hz, 1H, 6a), 2.46 (s, 3H, Me), 2.31 (d, *J* = 22.7 Hz, 1H, H-7b), 2.15 (dd, *J* = 16.4, 11.1 Hz, 1H, H-5b), 2.07 (dd, *J* = 6.6, 5.4 Hz, 1H, H-7b), 1.68 – 1.51 (m, 1H, H-7a); **¹³C NMR** (101 MHz, DMSO) δ 173.74 (C-4), 148.27 (C_q), 143.32 (C_q), 131.20 (q, *J* = 269.3 Hz, CF₃), 115.43 (C-10), 92.91 (C-3), 37.48 (q, *J* = 25.9 Hz, C-6), 25.2 (C-8), 25.1 (Me), 22.17 (d, *J* = 1.5 Hz, C-5), 20.75 (d, *J* = 2.3 Hz, C-7); **v_{max}/cm⁻¹**; 2744, 1611, 1499, 1334, 1250; **M/Z** (ESI+); 357.99 (Found MH⁺; 357.9914, C₁₁H₁₂F₃INO requires 357.9910).

2,7-Dimethyl-3-iodo-5,6,7,8-tetrahydroquinolin-4(1H)-one (262).



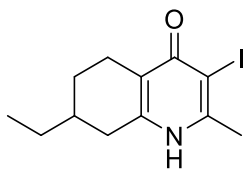
The title compound was synthesised from 2,7-dimethyl-5,6,7,8-tetrahydroquinolin-4(1H)-one (0.69 g, 3.95 mmol), according to general procedure **L**, and was isolated as a colourless solid (0.85 g, 2.82 mmol, 71%). **MP**; > 250 °C (decolouration observed at ~220 °C); **HPLC**; 1.67 mins (95% reference area) **¹H NMR** (400 MHz, MeOD) δ 13.63 (s, 1H, NH), 3.05 (dd, *J* = 18.3, 4.2 Hz, 1H, H-8), 3.00 – 2.90 (m, 1H, H-5), 2.84 (s, 3H, 2-Me), 2.75 – 2.63 (m, 1H, H-5), 2.54 (dd, *J* = 18.6, 9.8 Hz, 1H, H-8), 2.03 (m, 2H, H-6 & 7), 1.46 (ddd, *J* = 24.6, 10.9, 5.9 Hz, 1H, H-6), 1.15 (d, *J* = 6.5 Hz, 3H, 7-Me); **¹³C NMR** (101 MHz, CDCl₃/MeOD) δ 165.9 (C-4), 154.2 (C_q), 152.7 (C_q), 120.1 (C-10), 85.9 (C-3), 34.4 (C-8), 28.7 (C-6), 27.2 (C-7), 25.0 (2-Me), 22.1 (C-5), 20.6 (7-Me); **v_{max}/cm⁻¹**; 2862, 1606, 1495; **M/Z** (ESI+); 304.02 (Found MH⁺; 304.0192, C₁₁H₁₅INO requires 304.0193).

3-Iodo-7-trifluoromethyl-2-methyl-5,6,7,8-tetrahydroquinolin-4(1H)-one (263).



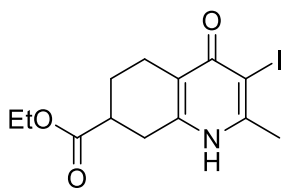
The title compound was synthesised from 7-trifluoromethyl-2-methylquinolin-4(1H)-one (0.48 g, 2.10 mmol) according to general procedure **K**, and was isolated as a colourless solid (0.69 g, 1.92 mmol, 91%). **MP**; >250 °C; **HPLC**; 1.95 mins (78% reference area); **¹H NMR** (500 MHz, MeOD) δ 2.85 (d, *J* = 16.9 Hz, 2H, H-5 & 8), 2.70 (dd, *J* = 18.2, 8.9 Hz, 1H, H-8), 2.62-2.56 (m, 1H, H-5), 2.56 (s, 1H, 2-Me), 2.40 (dd, *J* = 20.6, 8.9 Hz, 1H, H-7), 2.20 (d, *J* = 13.0 Hz, 1H, H-6), 1.59 (qd, *J* = 12.3, 5.7 Hz, 1H, H-6); **¹³C NMR** (101 MHz, DMSO) δ 173.7 (C-4), 148.2 (C_q), 141.0 (C_q), 117.7 (C-10), 93.1 (C-3), 37.3 (q, *J* = 27 Hz, C-7), 25.3 (C-8), 21.8 (Me), 21.1 (C-5 & 6) CF₃ not observed; **v_{max}/cm⁻¹**; 2646, 1640, 1608, 1475, 1395, 1344, 1311, 1277, 1253; **M/Z (ESI+)**; 357.99 (Found MH⁺; 357.9915, C₁₁H₁₂F₃INO requires 357.9910).

3-Iodo-7-ethyl-2-methyl-5,6,7,8-tetrahydroquinolin-4(1H)-one (264).



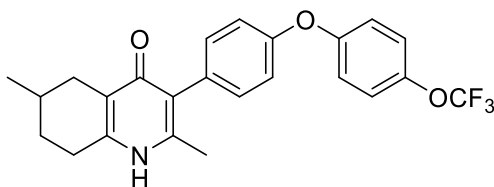
The title compound was synthesised from 7-ethyl-2-methyl-5,6,7,8-tetrahydroquinolin-4(1H)-one (0.12 g, 0.60 mmol) according to general procedure **M**, and was isolated as a colourless solid (0.19 g, 0.59 mmol, 99%). **MP**; 246.8-247.4 °C; **HPLC**; 1.96 mins (93% reference area); **¹H NMR** (400 MHz, MeOD) δ 2.62 (dd, *J* = 17.2, 4.4 Hz, 2H, H-5a & 8b), 2.47 (s, 3H, Me), 2.34 – 2.22 (m, 1H, H-5b), 2.18 (dd, *J* = 17.8, 9.6 Hz, 1H, H-8a), 1.92 – 1.81 (m, 1H, H-6a), 1.64 – 1.50 (m, 1H, H-7a), 1.34 (dtd, *J* = 14.1, 7.2, 2.2 Hz, 2H, CH₂CH₃), 1.21 (ddd, *J* = 24.1, 10.9, 5.6 Hz, 1H, H-6b), 0.91 (t, *J* = 7.4 Hz, 3H, CH₂CH₃); **¹³C NMR** (101 MHz, MeOD) δ 176.0 (C-4), 148.5 (C_q), 144.6 (C_q), 119.6 (C-10), 91.5 (C-3), 34.7 (C-7), 32.2 (C-8), 28.24 (CH₂CH₃), 27.7 (C-6), 24.4 (Me), 22.3 (C-5), 10.7 (CH₂CH₃); **v_{max}/cm⁻¹**; 2927, 1607, 1515, 1501; **M/Z (ESI+)**; 318.03 (Found MH⁺; 318.0261, C₁₂H₁₆INO requires 318.0349).

Ethyl-3-iodo-2-methyl-5,6,7,8-tetrahydroquinolin-4(1H)-one-7-carboxylate



The title compound was synthesised from ethyl-2-methyl-5,6,7,8-tetrahydroquinolin-4(1H)-one-7-carboxylate (80 mg, 0.34 mmol) according to general procedure **M**, and was isolated as a colourless solid (56 mg, 0.16 mmol, 46%). **MP**; 248-250 °C; **HPLC**; 1.70 mins (95% reference area); **¹H NMR** (400 MHz, MeOD) δ 4.15 (qd, *J* = 7.1, 1.7 Hz, 2H, , 7-CO₂CH₂CH₃), 2.91 – 2.72 (m, 3H, H-7 & 8), 2.66 (dt, *J* = 17.6, 5.0 Hz, 1H, H-5), 2.52 (s, 3H, Me), 2.51 – 2.40 (m, 1H, H-5), 2.15 (dd, *J* = 10.1, 4.3 Hz, 1H, H-6), 1.86 – 1.71 (m, 1H, H-6), 1.25 (t, *J* = 7.1 Hz, 3H, 7-CO₂CH₂CH₃); **¹³C NMR** (101 MHz, MeOD) δ 179.7 (7-CO₂Et), 178.5 (C-4), 152.7 (C_q), 146.7 (C_q), 122.7 (C-10), 95.9 (C-3), 64.9 (7-CO₂CH₂CH₃), 42.4 (C-7), 31.9 (C-5), 28.8 (C-6), 28.6 (Me), 25.6 (C-8), 17.7 (7-CO₂CH₂CH₃); **v_{max}/cm⁻¹**; 2914, 2187, 1721, 1608, 1490; 1383, 1336, 1290; **M/Z** (ESI+); 384.00 (Found MNa⁺; 384.0082, C₁₃H₁₇NO₃ requires 384.0067).

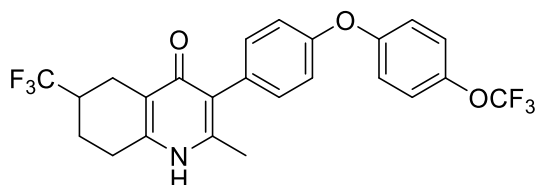
3(4-(4-trifluoromethoxyphenoxy)phenyl)-2,6-dimethyl-5,6,7,8-tetrahydroquinolin-4(1H)-one (265).



The title compound was synthesised from 3-iodo-2,6-dimethyl-5,6,7,8-tetrahydroquinolin-4(1H)-one (270 mg, 0.90 mmol) and 4-bromo(4-trifluoromethoxyphenoxy)phenyl (200 mg, 0.60 mmol) following general procedure **M**, and was isolated as a colourless solid (40 mg, 0.09 mmol, 15%). **MP**; >250 °C; **HPLC**; 3.03 (96% reference area); **¹H NMR** (500 MHz, MeOD)* δ 6.86 (d, *J* = 8.3 Hz, 4H, H-2',6',3'' & 5''), 6.79 – 6.64 (m, 4H, H-3',5',2'' & 6''), 2.43 (dd, *J* = 17.5, 4.9 Hz, 1H, H-5a), 2.37 (s, 2H, H-8a & b), 1.81 (s, 3H, 2-Me), 1.70 – 1.54 (m, 2H, H-7a & 5b), 1.45 (m, 1H, H-7b), 1.09 (dt, *J* = 20.7, 10.5 Hz, 1H, 6b), 0.76 (d, *J* = 6.6 Hz, 3H, Me-6); **¹³C NMR** (101 MHz, MeOD) δ 181.2 (C-4), 159.9 (C_q), 159.7 (C_q), 148.3 (C_q), 147.6 (C_q), 136.0 (C-2' & 6'), 135.0 (C_q), 129.3 (C_q), 126.7 (C_q), 126.4 (C-3'' & 5''),

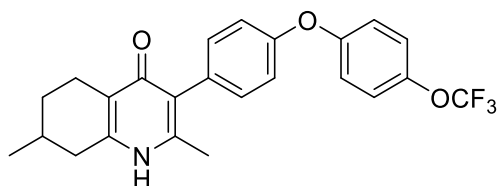
123.4 (C-3' & 5'), 122.7 (C-2'' & 6''), 34.1 (C-5), 33.6 (C-7), 32.3 (C-6), 30.6 (C-8), 25.2 (Me-6), 21.6 (2-Me); $\nu_{\max}/\text{cm}^{-1}$; 2928, 1620, 1499, 1459, 1239; **M/Z** (ESI+); 452.14 (Found MNa^+ ; 452.1446 $\text{C}_{24}\text{H}_{22}\text{F}_3\text{NO}_3\text{Na}$ requires 452.1444).

6-Ethyl-3-(4-(4-trifluoromethoxyphenoxy)phenyl)-2-methyl-5,6,7,8-tetrahydroquinolin-4(1H)-one (266).



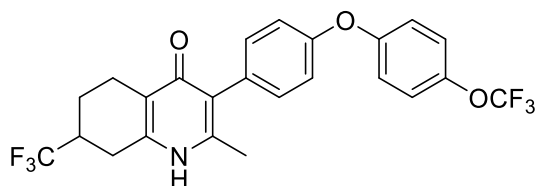
The title compound was synthesised from 3-iodo-2-methyl-6-(trifluoromethyl)-5,6,7,8-tetrahydroquinolin-4(1H)-one (300 mg, 0.84 mmol) and 4-bromo-(4-trifluoromethoxy)phenyl (185 mg, 0.56 mmol) following general procedure **M** and was isolated as a colourless solid. (20 mg, 0.04 mmol, 7%) **MP**; >250 °C; **HPLC**; 3.13 mins (100% reference area); **¹H NMR** (500 MHz, TFA) δ 7.39 (d, $J = 7.7$ Hz, 4H, H-2', 6', 3'' & 5''), 7.34 (d, $J = 7.1$ Hz, 2H, H-2'' & 6''), 7.24 (d, $J = 8.5$ Hz, 2H, H-3' & 5'), 3.32 (d, $J = 14.9$ Hz, 2H, H-8a & b), 3.21 (dd, $J = 13.8, 5.6$ Hz, 1H, H-5a), 2.89 (dd, $J = 18.0, 9.6$ Hz, 1H, H-6a), 2.73 (dd, $J = 15.3, 6.9$ Hz, 1H, H-5b), 2.57 (s, 3H, 2-Me), 2.52 (d, $J = 13.5$ Hz, 1H, H-7a), 2.07 (d, $J = 16.0$ Hz, 1H, H-7b); **¹³C NMR**; (126 MHz, MeOD)* δ 178.1 (C-4), 165.3 (C_q), 157.4 (C_q), 157.2 (C_q), 145.7 (C_q), 133.3 (C-2' & 6'), 132.1 (C_q), 127.9 (C_q), 123.7 (C-3'' & 5''), 121.3 (C_q), 120.8 (C-2'' & 6''), 120.1 (C-3' & 5'), 116.2 (C_q), 30.8 (C-6), 26.7 (C-5), 22.5 (C-8), 21.9 (C-7), 18.6 (2-Me); $\nu_{\max}/\text{cm}^{-1}$; 2946, 1631, 1497, 1339, 1239; **M/Z** (ESI+); 484.14 (Found MH^+ 484.1358, $\text{C}_{24}\text{H}_{20}\text{F}_6\text{NO}_3$ requires 484.1342).

3(4-(4-Trifluoromethoxyphenoxy)phenyl)-2,7-dimethyl-5,6,7,8-tetrahydroquinolin-4(1H)-one (267).



The title compound was synthesised from 3-iodo-2,7-dimethyl-5,6,7,8-tetrahydroquinolin-4(1H)-one (120 mg, 0.4 mmol) and 4-bromo(4-trifluoromethoxyphenoxy)phenyl (87 mg, 0.27 mmol) according to general procedure **M**, and was isolated as a colourless solid (30 mg, 0.07 mmol, 26%). **MP**; > 250 °C; **HPLC**; 3.04 mins (95% reference area); **¹H NMR** (400 MHz, DMSO) δ 10.90 (s, 1H, NH), 7.41 (d, J = 8.5 Hz, 2H, H-2' & 6'), 7.20 (d, J = 7.9 Hz, 2H, H-3'' & 5''), 7.14 (d, J = 8.5 Hz, 2H, H-3' & 5'), 7.03 (d, J = 7.9 Hz, 2H, H-2'' & 6''), 2.61 (m, 2H, H-5 & 8), 2.20 (dd, J = 16.4, 9.6 Hz, 2H, H 5 & 8), 2.08 (s, 3H, 2-Me), 1.81 (m, 2H, H-6 & 7), 1.24 (s, 1H, H-6), 1.04 (d, J = 5.9 Hz, 3H, 7-Me); **¹³C NMR** (101 MHz, DMSO) δ 176.0 (C-4), 156.4 (C_q), 154.9 (C_q), 144.0 (C_q), 143.2 (C_q), 142.7 (C_q), 133.0 (C-3'' & 5''), 132.7 (C_q), 124.1 (C_q), 123.4 (C-2' & 6'), 121.3 (C_q), 120.1 (C-3' & 5'), 118.7 (C-2'' & 6''), 34.8 (C-8), 30.5 (C-6), 28.1 (C-7), 22.2 (C-5), 21.6 (7-Me), 18.3 (2-Me); **$\nu_{\max}/\text{cm}^{-1}$** ; 2920, 2264, 1626, 1499, 1266; **M/Z** (ESI+); 452.14 (Found MNa⁺; 452.1449 C₂₄H₂₂F₃NO₃Na requires 452.1444).

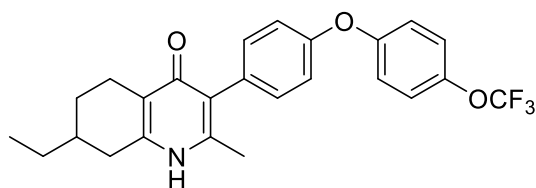
7-Trifluoromethyl-2-methyl-3(4-(4-trifluoromethoxyphenoxy)phenyl)-5,6,7,8-tetrahydroquinolin-4(1H)-one (268).



The title compound was synthesised from 7-trifluoromethyl-2-methylquinolin-4(1H)-one (360 mg, 0.99 mmol) and 4-bromo-(4-trifluoromethoxyphenoxy)phenyl (220 mg, 0.66 mmol) according to general procedure **N**, and was isolated as a colourless solid (95 mg, 0.20 mmol, 30%). **MP**; >250 °C; **HPLC**; 3.10 mins (100% reference area); **¹H NMR** (400 MHz, CDCl₃+TFA) δ 12.68 (s, 1H, NH), 7.36 – 7.20 (m, 6H, H-2', 6', 2'', 3'', 5'' & 6''), 7.17 (d, J = 8.8 Hz, 2H, H- 3' & 5'), 3.30 (dd, J = 18.1, 4.8 Hz, 1H, H-8), 3.15-3.00 (m, 2H, H-8 & 5), 2.82 – 2.62 (m, 2H, H-5 & 7), 2.45 (s, 3H, Me),

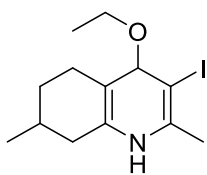
2.36 (d, $J = 10.9$ Hz, 1H, H-6), 1.85 (qd, $J = 11.6, 5.9$ Hz, 1H, H-6); $^{13}\text{C NMR}$ (101 MHz, CDCl_3) δ 165.0 (C-4), 160.1 (C_q), 153.4 (C_q), 151.5 (C_q), 148.7 (C_q), 146.0 (C_q), 131.4 (C-2' & 6'), 126.3 (q, $J = 279$ Hz, 7- CF_3), 123.9 (C_q), 123.0 (C-3'' & 5''), 121.4 (C-2'' & 6''), 120.9 (C_q), 120.4 (q, $J = 257$ Hz, OCF_3), 119.7 (C-3' & 5'), 37.2 (q, $J = \text{Hz}$, C-7), 26.0 (C-8), 20.3 (C-5), 19.8 (C-6), 18.1 (Me); $\nu_{\text{max}}/\text{cm}^{-1}$; 2940, 1614, 1497, 1242; **M/Z** (ESI+); 484.14 (Found MH^+ 484.1358, $\text{C}_{24}\text{H}_{20}\text{F}_6\text{NO}_3$ requires 484.1342).

7-Ethyl-2-methyl-3(4-(4-trifluoromethoxyphenoxy)phenyl)-5,6,7,8-tetrahydroquinolin-4(1H)-one (269).



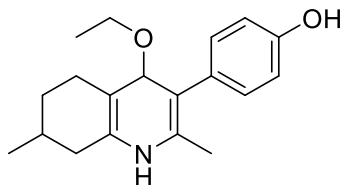
The title compound was synthesised from 3-Iodo-7-ethyl-2-methyl-5,6,7,8-tetrahydroquinolin-4(1H)-one (170 mg, 0.54 mmol) and 4-bromo(4-trifluoromethoxyphenoxy)phenyl (120 mg, 0.36 mmol) according to general procedure **M**, and was isolated as a colourless solid (17 mg, 0.04 mmol, 11%). **MP**; 218.0-220.0 °C; **HPLC**; 3.18 mins (76% reference area); $^1\text{H NMR}$ (500 MHz, MeOH)* δ 11.52 (s, 1H, NH), 7.16 (dd, $J = 15.3, 8.2$ Hz, 4H, H-2', 6', 3'' & 5''), 6.94 (dd, $J = 16.6, 8.3$ Hz, 4H, H-3', 5', 2'' & 6''), 2.78 (d, $J = 16.7$ Hz, 1H, H-5), 2.59 (d, $J = 12.4$ Hz, 1H, H-8), 2.39 (m, 1H, H-5), 2.13 (dd, $J = 16.9, 10.1$ Hz, 1H, H-8), 1.96 (s, 3H, Me), 1.91 (s, 1H, H-6), 1.59 (s (b), 1H, H-7), 1.36 (dt, $J = 14.9, 8.8$ Hz, 2H, 7- CH_2CH_3), 1.31 – 1.19 (m, 1H, H-6), 0.94 (t, $J = 7.2$ Hz, 3H, 7- CH_2CH_3); $^{13}\text{C NMR}$ (126 MHz, MeOD)* δ 176.8 (C-4), 155.8 (C_q), 155.5 (C_q), 144.7 (C_q), 144.6 (C_q), 132.2 (C-2' & 6'), 130.5 (C_q), 126.8 (C_q), 124.9 (C_q), 122.7 (C-3'' & 5''), 122.4 (C_q), 119.9 (C-2'' & 6''), 118.3 (C-3' & 5'), 34.8 (C-7), 33.0 (C-8), 28.5 (7- CH_2CH_3), 28.1 (C-6), 22.3 (C-5), 18.1 (2-Me), 11.4 (7- CH_2CH_3); $\nu_{\text{max}}/\text{cm}^{-1}$; 2922, 1619, 1464, 1241; **M/Z** (ESI+); 444.18 (Found MH^+ ; 444.1784 $\text{C}_{25}\text{H}_{25}\text{F}_3\text{NO}_3$ requires 444.1781).

4-Ethoxy-2,7-dimethyl-3-iodo-5,6,7,8-tetrahydroquinoline (270).



The title compound was synthesised from 2,7-dimethyl-3-iodo-5,6,7,8-tetrahydroquinolin-4(1H)-one (0.84 g, 2.77 mmol) according to general procedure **E**, and was isolated as an orange oil (0.78 g, 2.30 mmol, 83% reference area). **HPLC**; 2.06 mins (94% reference area); **¹H NMR** (400 MHz, CDCl₃) δ 4.05 – 3.91 (m, 2H, CH₃CH₂O), 3.02 – 2.88 (m, 2H, H-5 & 8), 2.73 (s, 3H, 2-Me), 2.69 – 2.57 (m, 1H, H-5), 2.44 (dd, J = 17.4, 10.4 Hz, 1H, H-8), 1.98 – 1.85 (m, 2H, H-6 & 7), 1.51 (t, J = 7.0 Hz, 3H, CH₃CH₂O), 1.40 – 1.27 (m, 1H, H-6), 1.10 (d, J = 6.5 Hz, 3H, 7-Me); **¹³C NMR** (101 MHz, CDCl₃) δ 163.9 (C_q), 159.0 (C_q), 158.2 (C_q), 123.9 (C-10), 90.9 (C-3), 68.4 (CH₃CH₂O), 40.5 (C-8), 30.4 (C-7), 29.3 (C-6), 29.0 (2-Me), 23.2 (C-5), 21.6 (7-Me), 15.6 (CH₃CH₂O); **v_{max}/cm⁻¹**; 2924, 1561, 1539, 1429, 1412, 1374, 1330; **M/Z (ESI)**; 354.03 (Found MNa⁺ 354.0319, C₁₃H₁₈INONa requires 354.0325).

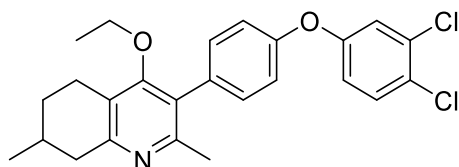
4-Ethoxy-2,7-dimethyl-3-(4-phenol)-5,6,7,8-tetrahydroquinoline (271).



The title compound was synthesised from 4-ethoxy-2,7-dimethyl-3-iodo-5,6,7,8-tetrahydroquinoline (760 mg, 2.30 mmol) according to general procedure **N**, and was isolated as a colourless powder (455 mg, 1.53 mmol, 67%). **MP**; 185.0-186.0 °C; **HPLC**; 2.20 mins (100% reference area); **¹H NMR** (400 MHz, CDCl₃) δ 7.03 (d, J = 8.5 Hz, 2H, H-2' & 6'), 6.84 (d, J = 8.5 Hz, 2H, H-3' & 5'), 3.50 – 3.33 (m, 2H, CH₃CH₂O), 2.96 (dd, J = 16.9, 4.6 Hz, 1H, H-8), 2.83 (ddd, J = 3.0, 4.9, 17.2 Hz, 1H, H-5), 2.58 – 2.49 (m, 1H, H-5), 2.44 (dd, J = 10.6, 17.5, H-8), 2.23 (s, 3H, 2-Me), 1.84 (dd, J = 11.2, 3.7 Hz, 2H, H-7 & 6a), 1.28 (ddd, J = 24.4, 11.3, 5.4 Hz, 1H, H-6b), 1.01 (d, J = 6.5 Hz, 3H, 7-Me), 0.95 (t, J = 7.0 Hz, 3H, CH₃CH₂O); **¹³C NMR** (101 MHz, CDCl₃) δ 162.5 (C_q), 156.5 (C_q), 155.9 (C_q), 155.2 (C_q), 131.2 (C-3' & 5'), 127.5 (C_q), 127.4 (C_q), 123.1 (C_q), 115.6 (C-3' & 5'), 68.1 (CH₃CH₂O), 40.3 (C-8), 30.6 (C-7), 29.0 (C-6), 22.7 (C-5), 22.5 (2-Me), 21.7 (7-Me), 15.6 (CH₃CH₂O); **v_{max}/cm⁻¹**; 2924, 1608, 1562, 1514, 1444, 1412,

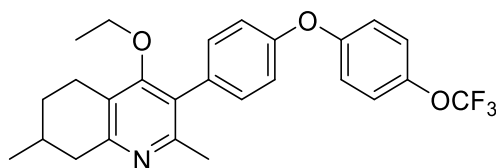
1327, 1267, 1239; **M/Z (ESI)**; 298.18 (Found MNa^+ 298.1822, $C_{19}H_{23}NO_2Na$ requires 298.1829).

4-Ethoxy-3-(4-(3,4-dichlorophenoxy)phenyl)-2,7-dimethyl-5,6,7,8-tetrahydroquinoline (272).



The title compound was synthesised from 4-ethoxy-2,7-dimethyl-3-(4-phenol)-5,6,7,8-tetrahydroquinoline (94 mg, 0.31 mmol) and 3,4-dichlorobenzene boronic acid (95 mg, 0.48 mmol) according to general procedure **F**, and was isolated as a colourless solid (47 mg, 0.11 mmol, 33%). **MP**; 78.0-78.4 °C; **HPLC**; 3.58 mins (96.% reference area); **¹H NMR** (400 MHz, $CDCl_3$) δ 7.33 (d, $J = 8.8$ Hz, 1H, H-5''), 7.20 (d, $J = 8.5$ Hz, 2H, H-2' & 6'), 7.04 (d, $J = 2.8$ Hz, 1H, H-6''), 6.99 (d, $J = 8.6$ Hz, 2H, H-3' & 5'), 6.83 (dd, $J = 8.8, 2.8$ Hz, 1H, H-2''), 3.53 – 3.31 (m, 2H, CH_3CH_2O), 2.94 (dd, $J = 17.3, 4.8$ Hz, 1H, H-8), 2.83 (ddd, $J = 17.3, 4.9, 3.1$ Hz, 1H, H-5), 2.53 (ddd, $J = 17.4, 11.4, 5.7$ Hz, 1H, H-5), 2.44 (dd, $J = 17.3, 10.4$ Hz, 1H, H-8), 2.25 (s, 3H, 2-Me), 1.85 (dd, $J = 6.2, 4.2$ Hz, 2H, H-6 & 7), 1.29 (qd, $J = 11.4, 5.3$ Hz, 1H, H-6), 1.03 (d, $J = 6.4$ Hz, 3H, 7-Me), 0.97 (t, $J = 7.0$ Hz, 3H, CH_3CH_2O); **¹³C NMR** (101 MHz, $CDCl_3$) δ 162.1 (C_q), 157.3 (C_q), 156.5 (C_q), 155.3 (C_q), 154.8 (C_q), 133.3 (C_q), 132.4 (C_q), 131.8 (C-2' & 6'), 131.1 (C-5''), 126.7 (C_q), 126.6 (C_q), 123.0 (C_q), 120.4 (C-6''), 119.1 (C-3' & 5'), 118.1 (C-2''), 68.2 (CH_3CH_2O), 41.0 (C-8), 30.6 (C-6), 29.1 (C-7), 23.1 (2-Me), 22.7 (C-5), 21.7 (7-Me), 15.6 (CH_3CH_2O); **ν_{max}/cm^{-1}** ; 2923, 1579, 1464, 1226; **M/Z (ESI)**; 442.13 (Found MH^+ 442.1347, $C_{25}H_{26}Cl_2NO_2$ requires 442.1335).

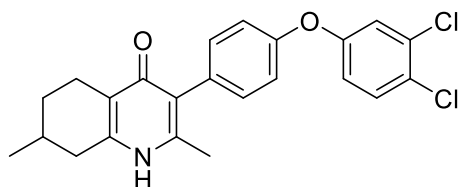
4-Ethoxy-3-(4-(4-(trifluoromethoxy)phenoxy)phenyl)-2,7-dimethyl-5,6,7,8-tetrahydroquinoline (273).



The title compound was synthesised from 4-ethoxy-2,7-dimethyl-3-(4-phenol)-5,6,7,8-tetrahydroquinoline (72 mg, 0.25 mmol) and 4-trifluoromethoxy boronic acid (79 mg, 0.38 mmol) according to

general procedure **F**, and was isolated as a colourless powder (82 mg, 0.18 mmol, 74%). **MP**; 117.8-118.3 °C; **HPLC**; 3.50 mins (97% reference area); **¹H NMR** (400 MHz, CDCl₃) δ 7.19 (d, *J* = 8.6 Hz, 2H, H-2' & 6'), 7.14 (d, *J* = 8.8 Hz, 2H, H-3'' & 5''), 7.00 (d, *J* = 8.6 Hz, 2H, H-3' & 5'), 6.98 (d, *J* = 8.8 Hz, 2H, H-2' & 6''), 3.54 – 3.35 (m, 2H, CH₃CH₂O), 2.93 (dd, *J* = 17.0, 5.2 Hz, 1H, H-8), 2.83 (ddd, *J* = 17.3, 5.2, 3.1 Hz, 1H, H-5), 2.53 (ddd, *J* = 17.4, 11.5, 5.8 Hz, 1H, H-5), 2.44 (dd, *J* = 17.4, 10.6 Hz, 1H, H-8), 2.24 (s, 3H, 2-Me), 1.92 – 1.80 (m, 2H, H-6 & 7), 1.37 – 1.22 (m, 1H, H-6), 1.04 (d, *J* = 6.5 Hz, 3H, 7-Me), 0.97 (t, *J* = 7.0 Hz, 3H, CH₃CH₂O); **¹³C NMR** (101 MHz, CDCl₃) δ 162.0 (C_q), 157.3 (C_q), 156.0 (C_q), 155.7 (C_q), 155.0 (C_q), 144.6 (C_q), 131.9 (C_q), 131.7 (C-2' & 6'), 126.7 (C_q), 122.9 (C_q), 122.7 (C-3'' & 5''), 119.7 (C-2'' & 6''), 118.8 (C-3' & 5'), 68.2 (CH₃CH₂O), 41.1 (C-8), 30.6 (C-6), 29.1 (C-7), 23.2 (2-Me), 22.7 (C-5), 21.7 (7-Me), 15.5 (CH₃CH₂O); **v_{max}/cm⁻¹**; 2933, 1555, 1500, 1429, 1222; **M/Z (ESI)**; 458.20 (Found MH⁺; 458.1956, C₂₆H₂₇F₃NO₃ requires 458.1938).

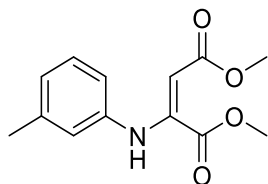
3-[4-(3,5-dichlorophenoxy)phenyl]-2,7-dimethyl-5,6,7,8-tetrahydro-1H-quinolin-4(1H)-one (274).



The title compound was synthesised from 4-Ethoxy-3-(4-(3,4-dichlorophenoxy)phenyl)-2,7-dimethyl-5,6,7,8-tetrahydroquinoline (40 mg, 0.09 mmol) according to general procedure **I** and was isolated as a colourless powder (13 mg, 0.03 mmol, 33%). **MP**; >250 °C; **HPLC**; 3.08 (96% reference area); **¹H NMR** (501 MHz, MeOD)* δ 7.32 (d, *J* = 8.8 Hz, 1H, H-5''), 7.14 (d, *J* = 8.5 Hz, 2H, H-2' & 6'), 7.05 (d, *J* = 2.7 Hz, 1H, H-6''), 6.97 (d, *J* = 8.5 Hz, 2H, H-3' & 5'), 6.84 (dd, *J* = 8.8, 2.7 Hz, 1H, H-2''), 2.68 – 2.55 (m, 2H, H-5 & 8), 2.31 (m, 1H, H-5), 2.20 (dd, *J* = 16.5, 11.0 Hz, 1H, H-8), 2.07 (s, 3H, 2-Me), 1.84 (d, *J* = 11.5 Hz, 2H, H-6 & 7), 1.25 (ddd, *J* = 24.4, 12.3, 6.7 Hz, 1H, H-6), 1.02 (d, *J* = 6.4 Hz, 3H, 7-Me); **¹³C NMR** (101 MHz, MeOD)* δ 177.5 (C-4), 156.8 (C_q), 155.0 (C_q), 144.4 (C_q), 143.7 (C_q), 133.0 (C_q), 132.2 (C-2' & 6'), 131.7 (C_q), 130.9 (C-5''), 125.4 (C_q), 122.7 (C_q), 120.1 (C-2''), 119.1 (C-3' & 5'), 117.9 (C-6''), 34.8 (C-8), 30.2 (C-6), 28.0 (C-

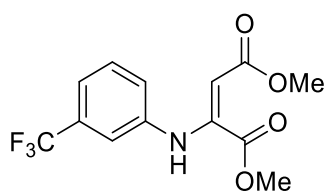
7), 21.7 (7-Me), 21.0 (C-5), 17.6 (2-Me); $\nu_{\max}/\text{cm}^{-1}$; 2926, 1504, 1465, 1293, 1263, 1227; **M/Z (ESI)**; 414.10 (Found MH⁺; 414.1024, C₂₃H₂₂Cl₂NO₂ requires 414.1022).

1,4-dimethyl-2-[(3-methylphenyl)amino]but-2-enedioate (275).



The title compound was synthesised from 3 methyl aniline (3.00 mL, 28.00 mmol) according to general procedure **O** and was isolated as a yellow/green oil (6.85 g, 27.51 mmol, 98%). **HPLC**; 3.41 mins (86% reference area); **¹H NMR** (400 MHz, CDCl₃) δ 9.64 (s, 1H, NH), 7.18 (t, J = 7.8 Hz, 1H, H-5), 6.93 (d, J = 7.6 Hz, 1H, H-4), 6.76 (s, 1H, H-2), 6.71 (d, J = 7.9 Hz, 1H, H-6), 5.38 (s, 1H, CH), 3.76 (s, 3H, OMe), 3.72 (s, 3H, OMe), 2.33 (s, 3H, 3-Me); **¹³C NMR** (101 MHz, CDCl₃) δ 169.9 (CO₂Me), 165.0 (CO₂Me), 148.2 (ArNHCR₂), 140.2 (C-1), 139.2 (C-3), 128.9 (C-5), 125.1 (C-4), 121.4 (C-2), 117.7 (C-6), 93.24 (CHR₂), 52.8 (OMe), 51.2 (OMe), 21.4 (Me); $\nu_{\max}/\text{cm}^{-1}$; 2952, 1736, 1669, 1587, 1491, 1434, 1275, 1250, 1208; **M/Z (ESI)**; 272.09 (Found MH⁺; 272.0892, C₁₃H₁₆NO₄ requires 272.0893).

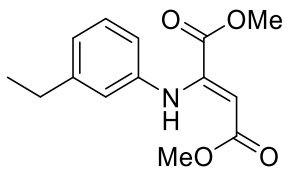
1,4-Dimethyl-2-[(3-trifluoromethylphenyl)amino]but-2-enedioate (276).



The title compound was synthesised from 3-trifluoromethylaniline (4.00 mL, 32.00 mmol) according to general procedure **O** and was isolated as yellow cuboid crystals (9.36 g, 30.89 mmol, 97%). **MP**; 51.8-53.6 °C; **HPLC**; 3.60 mins (82% reference area); **¹H NMR** (500 MHz, CDCl₃) δ 9.75 (s, 1H, NH), 7.42 (t, J = 7.9 Hz, 1H, H-5), 7.36 (d, J = 7.8 Hz, 1H, H-4), 7.14 (s, 1H, H-2), 7.08 (d, J = 8.0 Hz, 1H, H-6), 5.56 (s, 1H, Imine), 3.79 (s, 3H, CO₂Me), 3.76 (s, 3H, CO₂Me); **¹³C NMR** (126 MHz, CDCl₃) δ 169.7 (CO₂Me), 164.3 (CO₂Me), 146.9 (CNHR), 140.9 (C-1), 131.7 (q, J = 32.7 Hz, C-3), 129.7 (C-5), 123.5 (C-6), 120.5 (q, J = 3.9 Hz, C-4), 117.1 (q, J = 3.8 Hz, C-2), 95.9 (CR₂H), 52.9 (CO₂Me), 51.4 (CO₂Me); $\nu_{\max}/\text{cm}^{-1}$; 2957, 1727,

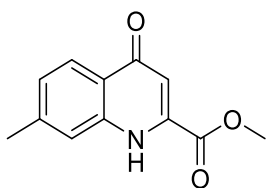
1669, 1609, 1438, 1330, 1271; **M/Z (ESI)**; 326.06 (Found MNa^+ 326.0607, $C_{13}H_{13}F_3NO_4$ requires 326.0611).

1,4-dimethyl-2-[(3-ethylphenyl)amino]but-2-enedioate (277)



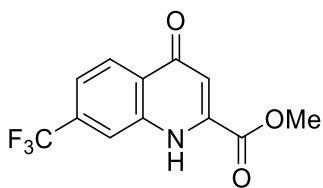
The title compound was synthesised from 3-ethyl aniline (3.90 mL, 32.00 mmol) according to general procedure **O** and was isolated as a yellow oil (7.20 g, 27.4 mmol, 84%). **HPLC**; 1.69 (68% reference area); **¹H NMR** (500 MHz, $CDCl_3$) δ 7.21 (t, $J = 7.8$ Hz, 1H, H-5), 6.96 (d, $J = 7.5$ Hz, 1H), 6.78 (s, 1H, H-2), 6.74 (dd, $J = 7.9, 2.1$ Hz, 1H), 5.39 (s, 1H, Alkene), 3.77 (s, 3H, OMe), 3.72 (s, 3H, OMe), 2.64 (q, $J = 7.6$ Hz, 2H, CH_3CH_2), 1.24 (t, $J = 7.6$ Hz, 3H, CH_3CH_2). **¹³C NMR** (126 MHz, $CDCl_3$) δ 169.9 (CO₂Me), 165.1 (CO₂Me), 148.2 (NHCR₂), 145.5 (C-1), 140.2 (C-3), 129.0 (C-5), 124.0 (C-4), 120.2 (C-2), 117.9 (C-6), 93.2 (CHR₂), 52.8 (OMe), 51.2 (OMe), 28.7 (CH₃CH₂Ar), 15.4 (CH₃CH₂Ar); **ν_{max}/cm^{-1}** ; 3283, 2953, 1737, 1670, 1586, 1434, 1209; **M/Z (ESI+)**; 286.10 (Found MNa^+ ; 286.1044 $C_{14}H_{17}NNaO_4$ requires 286.1050).

7-Methyl-2-(methoxycarboxylate)-quinolin-4(1H)-one (278)



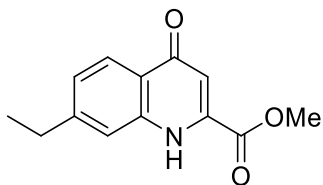
The title compound was synthesised from 1,4-dimethyl-2-[(3-methylphenyl)amino]but-2-enedioate (6.80 g, 27.3 mmol) according to general procedure **Q**, and was isolated as a colourless solid (386 mg, 1.78 mmol, 7%). **MP**; >250 °C; **HPLC**; 1.62 mins (98% reference area); **¹H NMR**; (400 MHz, MeOD) δ 8.02 (d, $J = 8.4$ Hz, 1H, H-5), 7.52 (s, 1H, H-8), 7.20 (dd, $J = 8.4, 1.2$ Hz, 1H, H-6), 6.80 (s, 1H, H-3), 3.93 (s, 3H, OMe), 2.41 (s, 3H, Me); **¹³C NMR** (101 MHz, MeOD) δ 179.9 (C-4), 162.3 (CO₂Me), 144.5 (C-7), 140.4 (C_q), 138.4 (C_q), 126.6 (C-5), 124.6 (C-8), 123.7 (C_q), 118.1 (C-6), 109.7 (C_q), 52.7 (OMe), 20.5 (Me); **ν_{max}/cm^{-1}** ; 2891, 1735, 1599, 1555, 1518, 1433, 1301, 1260, 1228; **M/Z (ESI)**; 218.08 (MH^+ found; 218.0808 $C_{12}H_{12}NO_3$ requires 218.0812).

7-Trifluoromethyl-2-(methoxycarboxylate)-quinolin-4(1H)-one (279).



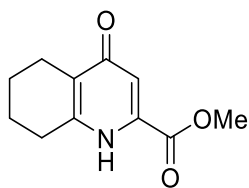
The title compound was synthesised from 1,4-dimethyl-2-[(3-trifluoromethylphenyl)amino]but-2-enedioate (9.00 g, 29.70 mmol) according to general procedure **Q** and was isolated as a colourless micro-crystal's (1.15 g, 4.24 mmol, 14%). **MP**; > 250 °C; **HPLC**; 2.25 mins (100% reference area); **¹H NMR** (500 MHz, DMSO) δ 12.35 (s, 1H, NH), 8.39 (s, 1H, H-8), 8.28 (d, J = 8.0 Hz, 1H, H-6), 7.66 (d, J = 9.7 Hz, 1H, H-5), 6.73 (s, 1H, H-3), 4.00 (s, 3H, CO₂Me); **¹³C NMR** (101 MHz, DMSO) δ 177.5 (C-4), 162.9 (C=O₂Me), 140.1 (C_q), 139.2 (C_q), 128.2 (C_q), 127.2 (C-6), 125.5 (C_q), 120.1 (C-5), 117.8 (C-8), 111.6, (C_q) 54.1 (CO₂Me); **$\nu_{\max}/\text{cm}^{-1}$** ; 3075, 2956, 1736, 1643, 1602, 1567, 1443, 1427, 1374, 1319, 1278, 1217; **M/Z (ESI)**; 294.03 (Found MNa⁺294.0348, C₁₂H₈F₃NO₃ requires 294.0348).

7-Ethyl-2-(methoxycarboxylate)-quinolin-4(1H)-one (280).



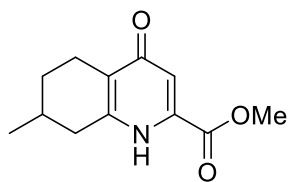
The title compound was synthesised from 1,4-dimethyl-2-[(ethylphenyl)amino]but-2-enedioate (7.20 g, 27.4 mmol) according to general procedure **Q**, and was isolated as a colourless solid (0.60 g, 2.59 mmol, 9.4%). **MP**; 173.8-174.6 °C; **HPLC**; 1.91 mins (97% reference area); **¹H NMR** (400 MHz, CDCl₃) δ 9.01 (s, 1H, NH), 8.18 (d, J = 8.7 Hz, 1H, H-5), 7.18 – 7.11 (m, 2H, H-6 & 8), 6.88 (s, 1H, H-3), 3.96 (s, 3H, OMe), 2.71 (q, J = 7.6 Hz, 2H, CH₂CH₃), 1.24 (t, J = 7.6 Hz, 3H, CH₂CH₃); **¹³C NMR** (101 MHz, CDCl₃) δ 179.5 (C-4), 163.6 (C=O₂Me), 150.4 (C-7), 139.3 (C_q), 135.9 (C_q), 126.3 (C-5), 125.4 (C-8), 124.7 (C_q), 116.2 (C-6), 111.7 (C_q), 53.8 (OMe), 29.0 (CH₂CH₃), 14.9 (CH₂CH₃); **$\nu_{\max}/\text{cm}^{-1}$** ; 3065, 2962, 1733, 1600, 1561, 1518, 1441, 1247 **M/Z (ESI+)**; 232.10 (Found MH⁺; 232.0967 C₁₃H₁₄NO₃ requires 232.0968).

2-(Methoxycarboxylate)-5,6,7,8-tetrahydro quinolin-4(1H)-one (282).



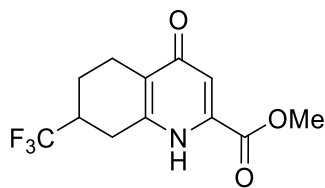
The title compound was synthesised from 2-(methoxycarboxylate)quinolin-4(1H)-one (0.50 g, 2.50 mmol) according to general procedure **N**, and was isolated as colourless solid (0.47 g, 2.40 mmol, 95% reference area). **MP**; 209.1-210.2 °C; **HPLC**; 1.39 mins (80% reference area); **¹H NMR** (500 MHz, CDCl₃) δ 8.89 (s, 1H, NH), 7.07 (s, 1H, H-3), 3.95 (s, 3H, OMe), 2.74 (t, *J* = 6.1 Hz, 2H), 2.56 (t, *J* = 6.2 Hz, 2H), 1.82 (dt, *J* = 8.0, 6.1 Hz, 1H, H-5), 1.79 – 1.69 (m, 1H, H-8); **¹³C NMR** (126 MHz, CDCl₃) δ 175.4 (C-4), 163.0 (CO₂Me), 147.6 (C_q), 135.5 (C_q), 127.4 (C_q), 115.4 (C_q), 53.7 (MeO), 27.8 (C-5), 22.1 (C-8), 21.6 (C-6), 21.3 (C-7); **v_{max}/cm⁻¹**; 2940, 1732, 1606, 1508, 1439, 1392, 1303, 1256, 1224; **M/Z** (ESI+); 208.10 (Found MH⁺; 208.0977, C₁₁H₁₄NO₃ requires 208.0974).

7-Methyl-2-(methoxycarboxylate)-5,6,7,8-tetrahydroquinolin-4(1H)-one (283).



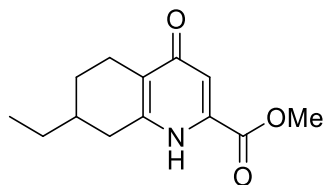
The title compound was synthesised from 7-methyl-2-(methoxycarboxylate)-quinolin-4(1H)-one (0.38 g, 1.73 mmol) according to general procedure **K** and was isolated as a colourless solid (0.37 g, 1.66 mmol, 96%). **MP**; 203.0-204.8 °C; **HPLC**; 1.45 (70% reference area); **¹H NMR**; (400 MHz, CDCl₃) δ 7.02 (s, 1H, NH), 7.02 (s, 1H, H-3), 3.99 (s, 3H, OMe), 2.86 – 2.73 (m, 1H, H-5), 2.68 (dd, *J* = 16.5, 4.5 Hz, 1H, H-8), 2.46 (ddd, *J* = 16.0, 11.9, 5.5 Hz, 1H, H-5), 2.35 (dd, *J* = 16.4, 10.3 Hz, 1H, H-8), 1.99-1.89 (m, 2H, H-7 & 6), 1.34 (tdd, *J* = 21.1, 12.0, 6.5 Hz, 1H, H-6), 1.11 (d, *J* = 6.5 Hz, 3H, Me); **¹³C NMR** (101 MHz, CDCl₃) δ 174.3 (C-4), 166.8 (CO₂Me), 163.4 (C_q), 144.8 (C_q), 127.2 (C_q), 116.2 (C_q), 53.5 (OMe), 36.0 (C-5), 30.0 (C-6), 28.1 (C-7), 21.9 (C-8), 21.2 (Me); **v_{max}/cm⁻¹**; 2924, 1731, 1605, 1511, 1254; **M/Z** (ESI); 222.11 (Found MH⁺; 222.1127, C₁₂H₁₆NO₃ requires 222.1125).

7-Trifluoromethyl-2-(methoxycarboxylate)-5,6,7,8-tetrahydroquinolin-4(1H)-one (284).



The title compound was synthesised from 7-trifluoromethyl-2-(methoxycarboxylate)-quinolin-4(1H)-one (0.54 g, 1.97 mmol) according to general procedure **K** and was isolated as a colourless solid (0.48 g, 1.75 mmol, 89%). **MP**; >250 °C ; **HPLC**; 1.61 mins (97%); **¹H NMR** (500 MHz, MeOD) δ 7.05 (s, 1H, H-3), 4.01 (s, 3H, OMe), 3.13 (dd, *J* = 17.3, 5.5 Hz, 1H, H-8), 2.97 – 2.82 (m, 2H, H-5 & 8), 2.74 (tdd, *J* = 12.3, 9.1, 3.3 Hz, 1H, H-7), 2.51 (ddd, *J* = 17.8, 9.4, 5.4 Hz, 1H, H-5), 2.32 – 2.19 (m, 1H, H-6), 1.68 (qd, *J* = 12.0, 5.5 Hz, 1H, H-6); **¹³C NMR**; (101 MHz, CDCl₃)⁺ δ 170.9 (C-4), 160.60 (C=O₂Me), 151.4 (C_q), 137.6 (C_q), 127.5 (C_q), 112.9 (C_q), 55.3 (OMe), 37.11 (q, *J* = 29.1 Hz, C-7), 26.6 (C-8), 20.5 (C-5), 19.5 (C-6); ***v*_{max}/cm⁻¹**; 2716, 1734, 1608, 1438, 1386, 1344, 1254, 1227; ***m/z* (ESI)**; 276.08 (Found MH⁺ 276.0840, C₁₂H₁₃F₃NO₃ requires 276.0842).

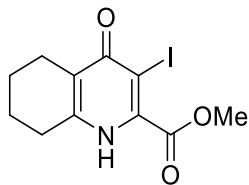
7-Ethyl-2-(methoxycarboxylate)-5,6,7,8-tetrahydroquinolin-4(1H)-one (285).



The title compound was synthesised from 7-ethyl-2-(methoxycarboxylate)-quinolin-4(1H)-one (0.60 g, 2.6 mmol) according to procedure **K**, and was isolated as a colourless solid (0.50 g, 2.12 mmol, 82%). **MP**; 126.4-128.0 °C; **HPLC** 1.75 min (92% reference area); **¹H NMR** (500 MHz, CDCl₃) δ 7.05 (s, 1H, H-3), 3.99 (s, 3H, OMe), 2.82 (ddd, *J* = 11.3, 6.7, 3.6 Hz, 1H, H-5), 2.75 (dd, *J* = 16.9, 4.8 Hz, 1H, H-8), 2.49 – 2.41 (m, 1H, H-5), 2.41-2.31 (m, 1H, H-8), 2.05 – 1.95 (m, 1H, H-6), 1.78 – 1.65 (m, 1H, H-7), 1.51 – 1.38 (m, 2H, CH₂CH₃), 1.38 – 1.26 (m, 1H, H-6), 1.01 (t, *J* = 7.4 Hz, 3H, CH₃CH₂); **¹³C NMR** (126 MHz, CDCl₃) δ 182.3 (CO₂Me), 174.3 (C-4), 163.5 (C_q), 127.5 (C_q), 116.1 (C_q), 90.6 (C_q), 53.6 (OMe), 35.0 (C-8), 34.5 (C-7), 28.6 (CH₃CH₂), 27.8 (C-6), 22.0 (C-5), 11.47 (7-CH₃CH₂); ***v*_{max}/cm⁻¹**; 2851,

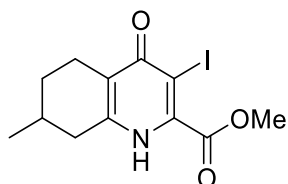
1733, 1607, 1511, 1437, 1259; **M/Z** (ESI+); 258.11 (Found MNa^+ ; 258.1099, $C_{13}H_{17}NNO_3$ requires 258.1101).

3-Iodo-2-(methoxycarboxylate)-5,6,7,8-tetrahydro quinolin-4(1H)-one (286)



The title compound was synthesised from 2-(methoxycarboxylate)-5,6,7,8-tetrahydro quinolin-4(1H)-one (0.45 g, 2.20 mmol) according to procedure **M** and was isolated as a colourless solid (0.61 g, 1.83 mmol, 84%). **HPLC**; 1.71 min (66% reference area); **MP**; 228.2 °C; **1H NMR** (400 MHz, DMSO) δ 11.93 (s, 1H, NH), 3.91 (s, 3H, OMe), 2.58 (s, 2H, H-5), 2.34 (t, 2H, H-8), 1.90 – 1.45 (m, 4H, H-6 & 7); **^{13}C NMR** (101 MHz, DMSO) δ 173.9 (C-4), 163.3 (CO_2Me), 145.3 (C_q), 141.7 (C_q), 121.3 (C-10), 89.8 (C-3), 53.8 (MeO), 26.4 (C-5), 23.1 (C-8), 21.9 (C-6), 21.6 (C-7); **ν_{max}/cm^{-1}** ; 2732, 1737, 1593, 1494, 1374, 1297, 1260, 1215; **M/Z** (ESI+); 333.99 (Found MH^+ ; 333.9935, $C_{11}H_{13}INO_3$ requires; 333.9935).

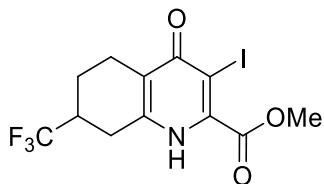
7-Methyl-3-iodo-2-(methoxycarboxylate)-5,6,7,8-tetrahydroquinolin-4(1H)-one (287).



The title compound was synthesised from 7-ethyl-2-(methoxycarboxylate)-5,6,7,8-tetrahydroquinolin-4(1H)-one (0.35 g, 1.58 mmol) according to general procedure **L** and was isolated as a yellow powder (0.30 g, 0.87 mmol, 55%). **MP**; 201.0-203.0 °C; **HPLC**; 1.96 mins (84% reference area); **1H NMR** (400 MHz, $CDCl_3$) δ 4.05 (s, 3H, OMe), 2.89 – 2.78 (m, 1H, H-5), 2.75 – 2.65 (m, 1H, H-8), 2.56 – 2.41 (m, 1H, H-8), 2.35 (dd, $J = 16.3, 9.8$ Hz, 1H, H-5), 1.95 (d, $J = 3.5$ Hz, 2H, H-6 & 7), 1.43 – 1.29 (m, 1H, H-6), 1.11 (d, $J = 6.5$ Hz, 3H, Me); **^{13}C NMR** (101 MHz, $CDCl_3$) δ 174.0 (C-4), 162.5 (CO_2Me), 143.7 (C_q), 129.6 (C_q), 122.0 (C-10), 94.2 (C-3), 53.5 (OMe), 35.8 (C-8), 30.0 (C-6), 28.1 (C-7), 22.9 (C-5), 21.1 (Me); **ν_{max}/cm^{-1}** ; 2929,

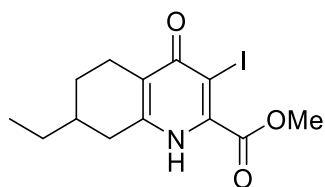
1745, 1505, 1329, 1228; **M/Z (ESI)**; 348.01 (Found MH⁺; 348.0090, C₁₂H₁₅INO₃ requires 348.0091).

7-Trifluoromethyl-3-iodo-2-(methoxycarboxylate)-5,6,7,8-tetrahydroquinolin-4(1H)-one (288).



The title compound was synthesised from 7-trifluoromethyl-2-(methoxycarboxylate)-5,6,7,8-tetrahydroquinolin-4(1H)-one (0.48 g, 1.72 mmol) according to general procedure **L** and was isolated as a colourless powder (0.44 g, 1.10 mmol, 64%). **MP**; 220.0-221.4 °C; **HPLC**; 2.21 mins (96% reference area); **¹H NMR** (500 MHz, MeOD) δ 4.03 (s, 3H, OMe), 3.02 (dd, *J* = 16.8, 4.0 Hz, 1H, H-8), 2.91 (d, *J* = 15.8 Hz, 1H, H-5), 2.86 – 2.80 (m, 1H, H-8), 2.75 (ddd, *J* = 14.1, 6.4, 2.5 Hz, 1H, H-7), 2.56 – 2.41 (m, 1H, H-5), 2.25 (d, *J* = 13.1 Hz, 1H, H-6), 1.68 (qd, *J* = 11.5, 5.3 Hz, 1H, H-6); **¹³C NMR** (126 MHz, MeOD) δ 177.4 (C-4), 163.7 (CO₂Me), 129.8 (C_q), 127.64 (C_q), 122.2 (C-10), 90.4 (C-3), 53.8 (MeO), 38.9 (q, *J* = 27.4 Hz, C-7), 26.7 (d, *J* = 3.8 Hz, H-8), 23.0 (C-5), 21.86 (d, *J* = 1.8 Hz, H-6); **v_{max}/cm⁻¹**; 2186, 1745, 1607, 1499, 1347, 1277, 1213; **M/Z (ESI)**; 423.96 (Found MNa⁺ 423.9625, C₁₂H₁₁F₃INO₃ requires 423.9628).

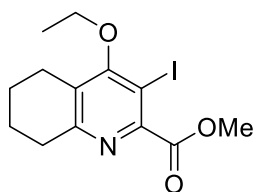
7-Ethyl-3-iodo-2-(methoxycarboxylate)-5,6,7,8-tetrahydroquinolin-4(1H)-one (288).



The title compound was synthesised from 7-ethyl-2-(methoxycarboxylate)-5,6,7,8-tetrahydroquinolin-4(1H)-one (0.50 g, 2.13 mmol) following general procedure **L** and was isolated as colourless solid (0.52 g, 1.43 mmol, 67%). **MP**; 177-179 °C; **HPLC**; 2.19 mins (82% reference area); **¹H NMR** (500 MHz, CDCl₃) δ 4.03 (s, 3H, OMe), 2.88 – 2.73 (m, 2H, H-8 & 5), 2.51-2.42 (m, 1H, H-5), 2.37 (dd, *J* = 16.6, 10.1 Hz, 1H, H-8), 2.01 (d, *J* = 13.7 Hz, 1H, H-6), 1.72 (s, 1H, H-7), 1.45 (tq, *J* = 13.8, 6.8 Hz, 3H,

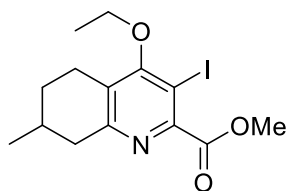
CH_2CH_3), 1.33 (dt, $J = 11.6, 6.2$ Hz, 1H, H-6), 1.00 (t, $J = 7.4$ Hz, 3H, CH_2CH_3); ^{13}C NMR (101 MHz, CDCl_3) δ 176.5 (C_q), 162.5 (C_q), 150.6 (C_q), 137.7 (C_q), 122.3 (C_q), 94.7 (C_q), 53.5 (OMe), 34.8 (C-7), 33.8 (C-6), 28.4 (CH_3CH_2 -7), 27.7 (C-6), 22.9 (C-5), 11.3 (CH_3CH_2 -7); $\nu_{\text{max}}/\text{cm}^{-1}$; 2854, 1742, 1523, 1500, 1228, 1208; **M/Z** (ESI+); 384.01 (Found MNa^+ ; 384.0063 $\text{C}_{13}\text{H}_{16}\text{INNaO}_3$ requires 384.0067).

4-Ethoxy-3-iodo-2-(methoxycarboxylate)-5,6,7,8-tetrahydroquinoline (292).



The title compound was synthesised from 3-iodo-2-(methoxycarboxylate)-5,6,7,8-tetrahydroquinolin-4(1H)-one (0.50 g, 1.51 mmol), according to general procedure **E** and was isolated as colourless crystals (0.45 g, 1.25 mmol, 83%). **MP**; 70.8-71.6 °C; **HPLC**; 3.31 mins (92% reference area); ^1H NMR (300 MHz, CDCl_3) δ 3.94 (q, $J = 7.0$ Hz, 2H, $\text{CH}_3\text{CH}_2\text{O}$), 3.90 (s, 3H, OMe), 2.84 (t, $J = 6.4$ Hz, 2H, H-5), 2.73 (t, $J = 6.2$ Hz, 2H, H-8), 1.87 – 1.64 (m, 4H, H-6 & 7), 1.43 (t, $J = 7.0$ Hz, 3H, $\text{CH}_3\text{CH}_2\text{O}$); ^{13}C NMR (101 MHz, CDCl_3) δ 166.8 (C-4), 164.7 (CO_2Me), 159.6 (C_q), 152.5 (C_q), 129.6 (C-10), 85.8 (C-3), 68.9 ($\text{CH}_3\text{CH}_2\text{O}$), 53.0 (MeO), 32.0 (C-8), 23.9 (C-5), 22.5 (C-7), 21.9 (C-6), 15.6 ($\text{CH}_3\text{CH}_2\text{O}$); $\nu_{\text{max}}/\text{cm}^{-1}$; 2935, 1737, 1539, 1427, 1370, 1330, 1297, 1201; **M/Z** (ESI+); 362.03 (Found MH^+ ; 362.0256, $\text{C}_{13}\text{H}_{17}\text{INO}_3$ requires 362.0248).

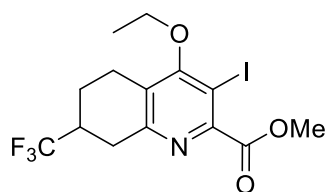
4-Ethoxy-7-methyl-3-iodo-2-(methoxycarboxylate)-5,6,7,8-tetrahydroquinoline (293).



The title compound was synthesised from 7-ethyl-3-iodo-2-(methoxycarboxylate)-5,6,7,8-tetrahydroquinolin-4(1H)-one (0.30 g, 0.86 mmol) according to general procedure **E**, and was isolated as an orange oil (0.25 g, 0.67 mmol, 77%). **MP**; 56.0-57.2 °C; **HPLC**; 3.63 mins (93% reference area); ^1H NMR (400 MHz, CDCl_3) δ 4.06 – 3.78 (m, 5H, OMe & $\text{CH}_3\text{CH}_2\text{O}$),

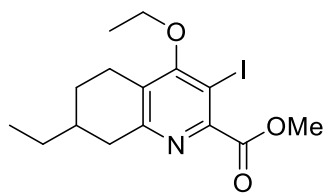
3.01 – 2.85 (m, 2H, H-5 & 8), 2.61 (ddd, $J = 17.3, 12.0, 5.6$ Hz, 1H, H-5), 2.48 – 2.32 (m, 1H, H-8), 1.85 (dd, $J = 7.1, 4.1$ Hz, 2H, H-6 & 7), 1.44 (t, $J = 7.02$ Hz, 3H, $\text{CH}_3\text{CH}_2\text{O}$), 1.28 (dtd, $J = 13.5, 11.2, 5.5$ Hz, 1H, H-6), 1.02 (d, $J = 6.4$ Hz, 3H, Me); $^{13}\text{C NMR}$ (101 MHz, CDCl_3) δ 166.9 (CO_2Me), 164.7 (C-4), 159.5 (C_q), 152.6 (C_q), 129.1 (C-10), 85.8 (C-3), 68.9 ($\text{CH}_3\text{CH}_2\text{O}$), 53.0 (OMe), 40.4 (C-8), 30.0 (C-6), 28.7 (C-7), 23.5 (C-5), 21.5 (Me), 15.6 ($\text{CH}_3\text{CH}_2\text{O}$); $\nu_{\text{max}}/\text{cm}^{-1}$; 2928, 1732, 1546, 1422, 1372, 1328, 1268, 1203; **M/Z (ESI)**; 376.04 (Found MH^+ ; 376.0407, $\text{C}_{14}\text{H}_{20}\text{INO}_3$ requires 376.0404).

4-Ethoxy-7-trifluoromethyl-3-iodo-2-(methoxycarboxylate)-5,6,7,8-tetrahydroquinoline (294).



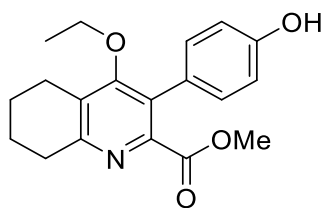
The title compound was synthesised from 7-trifluoromethyl-3-iodo-2-(methoxycarboxylate)-5,6,7,8-tetrahydroquinolin-4(1H)-one (0.52 g, 1.30 mmol) according to general procedure **E**, and was isolated as a colourless solid (0.41 g, 0.96 mmol, 74%). **MP**; 101.0-101.5 °C ; **HPLC**; 3.71 mins (72% reference area); $^1\text{H NMR}$ (400 MHz, CDCl_3) δ 4.15 – 3.90 (m, 2H, $\text{CH}_3\text{CH}_2\text{O}$), 4.01 (s, 3H, MeO) 3.34 – 3.20 (m, 1H, H-8), 3.18 – 3.07 (m, 1H, H-5), 2.97 (dd, $J = 17.6, 11.4$ Hz, 1H, H-8), 2.83 – 2.66 (m, 1H, H-5), 2.66 – 2.48 (m, 1H, H-7), 2.33 – 2.15 (m, 1H, H-6), 1.71 (ddd, $J = 25.1, 11.8, 5.4$ Hz, 1H, H-6), 1.54 (t, $J = 7.0$ Hz, 3H, $\text{CH}_3\text{CH}_2\text{O}$); $^{13}\text{C NMR}$ 101 MHz, CDCl_3) δ 166.6 (C-4), 164.9 (CO_2Me), 156.2 (C_q), 153.5 (C_q), 128.0 (C-10) 127.2 (q, $J = 278$ Hz, CF_3), 86.4 (C-3), 69.3 ($\text{CH}_3\text{CH}_2\text{O}$), 53.1 (OMe), 38.7 (q, $J = 28.1$ Hz, C-7), 30.8 (C-8), 22.6 (C-5), 21.1 (C-6), 15.6 ($\text{CH}_3\text{CH}_2\text{O}$); $\nu_{\text{max}}/\text{cm}^{-1}$; 2952, 1726, 1545, 1434, 1376, 1332, 1277, 1252, 1208; **M/Z (ESI)**; 451.99 (Found MNa^+ 451.9944, $\text{C}_{14}\text{H}_{15}\text{F}_3\text{INO}_3\text{Na}$ requires 451.9941).

4-Ethoxy-7-ethyl-3-iodo-2-(methoxycarboxylate)-5,6,7,8-tetrahydroquinoline
(295).



The title compound was synthesised from 7-ethyl-3-iodo-2-(methoxycarboxylate)-5,6,7,8-tetrahydroquinolin-4(1H)-one (0.51 g, 1.42 mmol) according to general procedure **E**, and was isolated as an orange oil (0.46 g, 1.18 mmol, 83%). **HPLC**; 1.91 mins (57%); **¹H NMR** (501 MHz, CDCl₃) δ 4.06 – 3.99 (m, 2H, CH₃CH₂O), 3.98 (s, 3H, MeO), 3.08 (dd, *J* = 16.9, 5.5 Hz, 1H, H-8), 3.03 – 2.96 (m, 1H, H-5), 2.67 (ddd, *J* = 18.0, 12.5, 5.7 Hz, 1H, H-5), 2.50 (dd, *J* = 17.4, 10.4 Hz, 1H, H8), 1.98 (ddd, *J* = 7.0, 5.9, 2.1 Hz, 1H, H-6), 1.75-1.65 (m, 1H, H-7), 1.51(t, *J* = 7.0 Hz, 3H, CH₃CH₂O), 1.43 (dt, *J* = 21.2, 6.9 Hz, 2H, CH₃CH₂), 1.36 – 1.31 (m, 1H, H-6), 0.99 (t, *J* = 7.4 Hz, 3H, CH₃CH₂); **¹³C NMR** (126 MHz, CDCl₃) δ 166.9 (C-4), 164.7 (CO₂Me), 159.6 (C_q), 152.6 (C_q), 129.4 (C-10), 85.8 (C-3), 68.9 (CH₃CH₂O), 53.0 (CO₂Me), 38.4 (C-8), 35.5 (C-7), 28.8 (CH₃CH₂), 27.9 (C-6), 23.6 (C-5), 15.6 (CH₃CH₂O), 11.3(CH₃CH₂); **v_{max}/cm⁻¹**; 2930, 1738, 1540, 1329, 1202; **M/Z** (ESI+); 412.04 (Found MNa⁺; 412.0375, C₁₅H₂₀INO₃Na requires 412.0386).

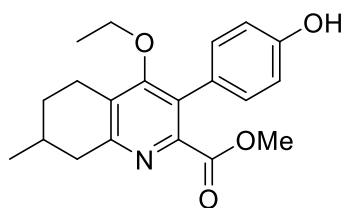
4-(4-Ethoxy--(methoxycarboxylate)-5,6,7,8-tetrahydroquinolin-3-yl)phenol
(296).



The title compound was synthesised from 4-ethoxy-3-iodo-2-(methoxycarboxylate)-5,6,7,8-tetrahydroquinoline (0.40 g, 1.11 mmol), according to general procedure **N**, and was isolated as a colourless solid (0.20 g, 0.61 mmol, 55%). **MP**; 188-190.2 °C; **HPLC**; 2.25 min (100% ref area); **¹H NMR** (500 MHz, CDCl₃) δ 7.11 (d, *J* = 8.6 Hz, 2H, H-2' & 6'), 6.77 (d, *J* = 8.6 Hz, 2H, H-3' & 5'), 3.60 (s, 3H, MeO), 3.43 (q, *J* = 7.0 Hz, 2H, CH₃CH₂O), 2.91 (t, *J* = 6.4 Hz, 2H, H-8), 2.71 (t, *J* = 6.3 Hz, 2H, H-5), 1.82 (m, 2H, H-7), 1.78 – 1.69 (m, 2H, H-6), 0.98 (t, *J* = 7.0 Hz, 3H, CH₃CH₂O); **¹³C NMR** (101 MHz, MeOD) δ 166.6 (CO₂Me), 164.1 (C_q), 157.6 (C_q), 156.8 (C_q),

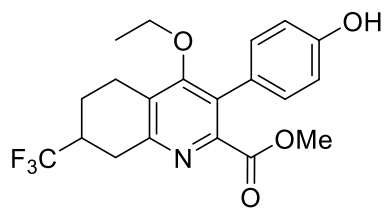
147.5 (C_q), 130.6 (C-2' & 6'), 128.9 (C_q), 127.1 (C_q), 124.0 (C_q), 114.8 (C-3' & 5'), 68.6 (CH₃CH₂O), 51.6 (MeO), 30.7 (C-8), 22.9 (C-5), 21.8 (C-7), 21.5 (C-6), 14.4 (CH₃CH₂O); **v_{max}/cm⁻¹**; 2957, 1727, 1612, 1576, 1518, 1431, 1370, 1328, 1306, 1277, 1235, 1207; **M/Z (ESI+)**; 328.16 (Found MH⁺; 328.1551, C₁₉H₂₂NO₄ requires; 328.1543).

4-Ethoxy-7-methyl-(methoxycarboxylate)-3-(4-phenol)-5,6,7,8-tetrahydroquinolineyl (297).



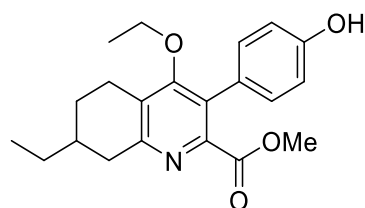
The title compound was synthesised from 4-ethoxy-7-ethyl-3-iodo-2-(methoxycarboxylate)-5,6,7,8-tetrahydroquinoline (0.25 g, 0.67 mmol) according to general procedure **N**, and was isolated as a colourless solid (0.08 g, 0.22 mmol, 33%). **MP**; 176.0-178.0; **HPLC**; 2.37 mins (95% reference area); **¹H NMR** (400 MHz, MeOD) δ 7.02 (d, *J* = 8.6 Hz, 2H, H-2' & 6'), 6.73 (d, *J* = 8.6 Hz, 2H, H-3' & 5'), 3.56 – 3.48 (m, 3H, OMe), 3.43 (ddd, *J* = 23.3, 11.6, 4.6 Hz, 2H, CH₃CH₂O), 2.89 (dt, *J* = 11.3, 4.6 Hz, 2H, H-5 & 8), 2.67 – 2.52 (m, 1H, H-5), 2.37 (dd, *J* = 17.4, 10.8 Hz, 1H, H-8), 1.91 – 1.77 (m, 2H, H-6 & 7), 1.29 (ddd, *J* = 24.9, 11.5, 5.6 Hz, 1H, H-6), 1.03 (d, *J* = 6.5 Hz, 3H, Me), 0.95 (t, *J* = 7.0 Hz, 3H, CH₃CH₂O); **¹³C NMR** (101 MHz, MeOD) δ 167.8 (CO₂Me), 162.8 (C-4), 157.4 (C_q), 157.3 (C_q), 149.1 (C_q), 130.5 (C-2' & 6'), 127.8 (C_q), 126.7 (C_q), 124.6 (C_q), 114.8 (C-3' & 5'), 68.1 (CH₃CH₂O), 51.3 (OMe), 39.9 (C-8), 29.9 (C-6), 28.7 (C-7), 22.6 (C-5), 20.5 (Me), 14.4 (CH₃CH₂O); **v_{max}/cm⁻¹**; 3381, 2924, 2511, 1698, 1610, 1425, 1330, 1270, 1213; **M/Z (ESI)**; 342.17 (Found MH⁺ 342.1703; C₂₀H₂₄NO₄ requires 342.1670).

4-Ethoxy-7-trifluoromethyl-3-(4-phenol)-2-(methoxycarboxylate)-5,6,7,8-tetrahydroquinoline (298).



The title compound was synthesised from 4-ethoxy-7-trifluoromethyl-3-iodo-2-(methoxycarboxylate)-5,6,7,8-tetrahydroquinoline (0.40 g, 0.93 mmol) according to general procedure **N**, and was isolated as a colourless solid (0.18 g, 0.46 mmol, 49%). **MP**; 212.0-214.0 °C; **HPLC**; 3.03 mins (93% reference area); **¹H NMR** (400 MHz, MeOD) δ 7.02 (d, J = 8.6 Hz, 2H, H-2' & 6'), 6.74 (d, J = 8.6 Hz, 2H, H-3' & 5'), 3.51 (s, 3H, OMe) 3.51 – 3.40 (m, 2H, OCH₂CH₃), 3.10 – 2.97 (m, 2H, H-5 & 8), 2.82 (dd, J = 16.8, 11.6 Hz, 1H, H-8), 2.73 – 2.56 (m, 2H, H-5 & 7), 2.22 – 2.08 (m, 1H, H-6), 1.61 (ddd, J = 24.8, 12.1, 5.4 Hz, 1H, H-6), 0.96 (t, J = 7.0 Hz, 3H, OCH₂CH₃); **¹³C NMR** (101 MHz, MeOD) δ 167.5 (C-4), 162.8 (CO₂Me), 157.4 (C_q), 154.2 (C_q), 149.8 (C_q), 130.5 (C-2' & 6'), 128.5 (C_q) 127.1 (C_q), 124.3 (C_q), 114.8 (C-3' & 5'), 68.4 (CH₃CH₂O), 51.4 (OMe), 38.4 (q, J = 27.6, C-7), 30.3 (C-8), 21.7 (C-5), 20.8 (C-6), 14.4 (CH₃CH₂O); **$\nu_{\max}/\text{cm}^{-1}$** ; 1737, 1578, 1520, 1428, 1333, 1271, 1206; **M/Z (ESI)**; 396.14 (Found MH⁺ 396.1416, C₂₀H₂₁F₃NO₄ requires 396.1417).

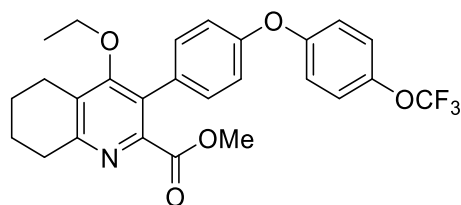
4-(4-Ethoxy-7-ethyl-(methoxycarboxylate)-5,6,7,8-tetrahydroquinolin-3-yl)phenol (299).



The title compound was synthesised following general procedure **N**, from 4-ethoxy-7-ethyl-3-iodo-2-(methoxycarboxylate)-5,6,7,8-tetrahydroquinoline (0.45 g, 1.15 mmol). The title compound was isolated as a viscous orange oil, which on further drying formed a colourless solid (0.20 g, 0.56 mmol, 49%). **MP**; 145.5-146.0 **HPLC**; 2.64 mins (80% reference area) **¹H NMR** (400 MHz, CDCl₃) δ 7.11 (d, J = 8.6 Hz, 2H, H-2' & 6'), 6.77 (d, J = 8.6 Hz, 2H, H-3' & 5'), 3.60 (s, 3H, OMe), 3.49 – 3.35 (m, 2H OCH₂CH₃), 3.06 (ddd, J = 17.5, 4.8, 1.0 Hz, 1H, H-8), 2.91 (ddd, J = 17.8, 5.2,

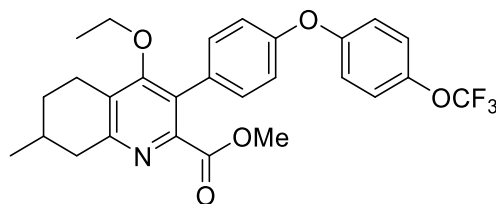
3.3 Hz, 1H, H-7), 2.63 – 2.40 (m, 1H, H-7), 2.49 (dd, $J = 10.7, 17.5$ Hz, 1H, H-8), 1.99 – 1.83 (m, 1H, H-6), 1.73 – 1.57 (m, 1H, H-7), 1.47 – 1.22 (m, 3H, 7-CH₂CH₃ & H-6), 0.97 (t, $J = 7.0$ Hz, 2H, OCH₂CH₃), 0.92 (t, $J = 7.4$ Hz, 3H, 7-CH₂CH₃); ¹³C NMR (101 MHz, CDCl₃) δ 166.6 (C-4'), 161.5 (CO₂Me), 157.1 (C_q), 154.6 (C_q), 147.5 (C_q), 129.7 (C-2' & 6'), 127.2 (C_q), 126.1 (C_q), 125.2 (C_q), 114.3 (C-3' & 5'), 67.4 (OCH₂CH₃), 51.4 (OMe), 37.7 (C-8), 34.6 (C-7), 27.8 (C-6), 22.0 (C-5), 14.5 (OCH₂CH₃), 10.387 (7-CH₂CH₃); $\nu_{\max}/\text{cm}^{-1}$: 2930, 1738, 1518, 1430, 1328, 1280, 1200; **M/Z** (ESI+); 378.17 (Found MNa⁺; 378.1673, C₂₁H₂₅NNaO₄ requires 378.1676).

4-Ethoxy-3(4-(4-trifluoromethoxyphenoxy)phenyl)-2-(methoxycarboxylate)-5,6,7,8-tetrahydroquinoline (300).



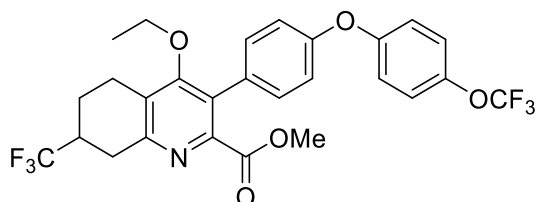
The title compound was synthesised from 4-(4-ethoxy--(methoxycarboxylate)-5,6,7,8-tetrahydroquinolin-3-yl)phenol (0.18 g, 0.55 mmol) according to general procedure **F** and was isolated as a viscous yellow oil (0.21 g, 0.43 mmol, 78%). **Rt** 2.46 min; ¹H NMR (500 MHz, CDCl₃) δ 7.32 (d, $J = 8.6$ Hz, 2H, H-2' & 6'), 7.22 (d, $J = 8.6$ Hz, 2H, H-3' & 5'), 7.05 (dd, $J = 8.8, 3.0$ Hz, 4H, H-2'', 3'', 5'' & 6''), 3.73 (s, 3H, OMe), 3.55 (q, $J = 7.0$ Hz, 2H, CH₃CH₂O), 3.05 (t, $J = 4.7$ Hz, 2H, H-8), 2.80 (t, $J = 6.2$ Hz, 2H, H-5), 1.99 – 1.88 (m, 2H, H-7), 1.88 – 1.79 (m, 2H, H-6), 1.09 (t, $J = 7.0$ Hz, 3H, CH₃CH₂O); ¹³C NMR (126 MHz, CDCl₃) δ 163.0 (CO₂Me), 161.9 (C-4), 160.5 (C_q), 155.5 (C_q), 144.7 (C_q), 143.4 (C_q), 142.8 (C_q), 131.2 (C-2' & 6'), 128.7 (C_q), 126.9 (C_q), 122.8 (C_q), 122.7 (C-3'' & 5''), 119.9 (C-2'' & 6''), 118.5 (C-3' & 5'), 68.6 (OCH₂CH₃), 52.5 (OMe), 32.5 (C-8), 23.4 (C-5), 22.6 (C-7), 22.1 (C-6), 15.5 (CH₃CH₂O); **LCMS**; MH⁺ 488.2 (100%).

4-Ethoxy-7-methyl-3(4-(4-trifluoromethoxyphenoxy)phenyl)-2-(methoxycarboxylate)-5,6,7,8-tetrahydroquinoline (301).



The title compound was synthesised from 7-ethyl-3-iodo-2-(methoxycarboxylate)-5,6,7,8-tetrahydroquinolin-4(1H)-one (70 mg, 0.21 mmol) according to general procedure **F**, and was isolated as a colourless solid (67 mg, 0.13 mmol, 62%). **MP**; 98.4-100.6 °C; **HPLC**; 4.10 mins (50% reference area); **¹H NMR**; (500 MHz, CDCl₃) δ 7.34 (d, *J* = 8.3 Hz, 2H, H-2' & 6'), 7.24 (d, *J* = 8.9 Hz, 2H, H-3'' & 5''), 7.17 – 7.04 (m, 4H, H-3', 5', 2'' & 6''), 3.73 (s, 3H, OMe), 3.65 – 3.48 (m, 2H, CH₃CH₂O), 3.12 (dd, *J* = 17.6, 4.8 Hz, 1H, H-8), 3.01 (d, *J* = 17.3 Hz, 1H, H-5), 2.82 – 2.66 (m, 1H, H-5), 2.60 (dd, *J* = 17.5, 10.2 Hz, 1H, H-8), 2.09 – 1.94 (m, 2H, H-6 & 7), 1.42 (ddd, *J* = 15.0, 10.8, 5.2 Hz, 1H, H-6), 1.15 (d, *J* = 6.4 Hz, 3H, 7-Me), 1.10 (t, *J* = 7.0 Hz, 3H, CH₃CH₂O); **¹³C NMR** (126 MHz, CDCl₃) δ 167.4 (C=O₂Me), 162.6 (C-4), 158.7 (C_q), 156.2 (C_q), 155.6 (C_q), 148.2 (C_q), 144.7 (C_q), 131.2 (C-2' & 6'), 129.9 (C_q), 128.1 (C_q), 126.6 (C_q), 122.7 (C-3'' & 5''), 119.9 (C-3' & 5'), 118.5 (C-2'' & 6''), 68.5 (CH₃CH₂O), 52.4 (CO₂Me), 41.0 (C-8), 30.2 (C-6), 28.9 (C-7), 23.0 (C-5), 21.5 (Me-7), 15.5 (CH₃CH₂O); **v_{max}/cm⁻¹**; 2948, 1731, 1578, 1547, 1497, 1427, 1329, 1267; **M/Z (ESI)**; 502.18, (Found MH⁺ 502.1835, C₂₇H₂₈F₃NO₅ requires 502.1836).

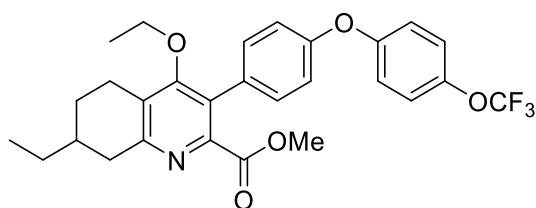
4-Ethoxy-7-trifluoromethyl-3(4-(4-trifluoromethoxyphenoxy)phenyl)-2-(methoxycarboxylate)-5,6,7,8-tetrahydroquinoline (302).



The title compound was synthesised from 4-ethoxy-7-trifluoromethyl-3-(4-phenol)-2-(methoxycarboxylate)-5,6,7,8-tetrahydroquinoline (160 mg, 0.04 mmol) according to general procedure **F**, and was isolated as a colourless powder (75 mg, 0.14 mmol, 34%). **RF**; 0.44 (EtOAc:Pet 10:1); **MP**; 106.4-107.6 °C; **HPLC** 3.19 mins (97% reference area);

¹H NMR (400 MHz, CDCl₃) δ 7.34 (d, *J* = 8.6 Hz, 2H, H-2' & 6'), 7.24 (d, *J* = 8.5 Hz, 2H, H-3'' & 5''), 7.11 – 7.03 (m, 4H, H-3', 5', 2'' & 6''), 3.74 (s, 3H, MeO), 3.64 – 3.45 (m, 2H, CH₃CH₂O), 3.31 (dd, *J* = 17.5, 4.0 Hz, 1H, H-8a), 3.15 (d, *J* = 15.5 Hz, 1H, H-5), 3.04 (dd, *J* = 17.3, 11.5 Hz, 1H, H-8b), 2.72 (ddd, *J* = 17.7, 12.0, 5.8 Hz, 1H, H-5), 2.66 – 2.53 (m, 1H, H-7), 2.29 (ddd, *J* = 7.9, 5.0, 2.2 Hz, 1H, H-6), 1.75 (ddd, *J* = 25.1, 12.1, 5.5 Hz, 1H, H-6), 1.10 (t, *J* = 7.0 Hz, 3H, CH₃CH₂O); **¹³C NMR** (101 MHz, CDCl₃) δ 167.0 (C-4), 162.5 (C=O₂Me), 156.7 (C_q), 155.3 (C_q), 155.2 (C_q), 149.3 (C_q), 144.8 (C_q), 131.1 (C-2' & 6'), 129.3 (C_q), 127.1 (C_q), 127.0 (C_q), 122.7 (C-3'' & 5''), 120.0 (C-2'' & 6''), 118.5 (C-3' & 5'), 68.8 (CH₃CH₂O), 52.5 (MeO), 38.91 (q, *J* = 27.7 Hz, C-7), 31.4 (C-8), 22.2 (C-5), 21.2 (C-6), 15.5 (CH₃CH₂O); **v_{max}/cm⁻¹**; 1734, 1498, 1331; **M/Z (ESI)**; 556.16 (Found MH⁺; 556.1559, C₂₇H₂₄F₆NO₅ requires 556.1553).

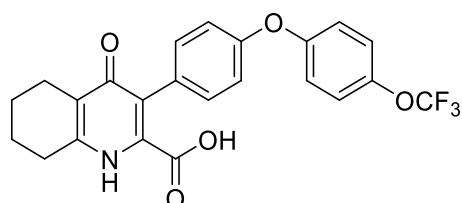
4-Ethoxy-7-ethyl-3-(4-(4-trifluoromethoxyphenoxy)phenyl)-2-(methoxycarboxylate)-5,6,7,8-tetrahydroquinoline (303).



The title compound was synthesised from 4-(4-ethoxy-7-ethyl-(methoxycarboxylate)-5,6,7,8-tetrahydroquinolin-3-yl)phenol (180 mg, 0.51 mmol) according to general procedure **F**, and was isolated as a colourless solid (134 mg, 0.26 mmol, 50%); **MP**; 93.0-94.0 °C; **HPLC**; 2.51 (92% reference area); **¹H NMR** (500 MHz, CDCl₃) δ 7.35 (d, *J* = 8.5 Hz, 2H, H-2' & 6'), 7.24 (d, *J* = 8.9 Hz, 2H, H-3'' & 5''), 7.09-7.06 (m, 4H, H-3', 5', 2'' & 6''), 3.74 (s, 3H, MeO), 3.63 – 3.46 (m, 2H, CH₃CH₂O), 3.18 (dd, *J* = 17.4, 4.3 Hz, 1H, H-8), 3.07 – 2.94 (m, 1H, H-5), 2.68 (ddd, *J* = 18.0, 11.7, 5.9 Hz, 1H, H-5), 2.60 (dd, *J* = 17.5, 10.6 Hz, 1H, H-6), 2.04 (ddd, *J* = 6.8, 5.1, 2.3 Hz, 1H, H-7), 1.82 – 1.68 (m, 1H, H-6), 1.55 – 1.44 (m, 2H, CH₃CH₂), 1.43 – 1.36 (m, 1H, H-7), 1.10 (t, *J* = 7.0 Hz, 3H, CH₃CH₂O), 1.04 (t, *J* = 7.4 Hz, 3H, CH₃CH₂); **¹³C NMR** (126 MHz, CDCl₃) δ 167.3 (C=O₂Me), 162.4 (C-4), 158.7 (C_q), 156.4 (C_q), 155.5 (C_q), 148.3 (C_q), 144.69 (q, *J* = 1.8 Hz, C-4''), 131.1 (C-2' & 6'), 129.9 (C_q), 128.4 (C_q), 127.0 (C_q), 122.7 (C-3'' & 5''), 119.8 (C-2'' & 6''), 118.5 (C-3' & 5'), 68.5 (CH₃CH₂O), 52.4 (MeO), 39.0 (C-8), 35.7

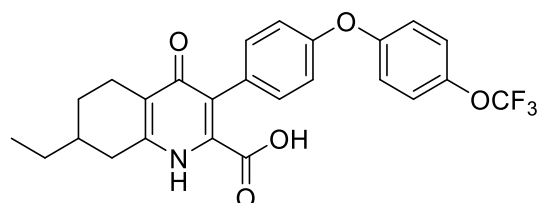
(C-7), 28.9 (CH₃CH₂), 28.1 (C-6), 23.1 (C-5), 15.5 (CH₃CH₂O), 11.4 (CH₃CH₂); $\nu_{\max}/\text{cm}^{-1}$; 2942, 1732, 1578, 1497, 1427, 1330, 1266; **M/Z (ESI)**; 516.20 (Found MH⁺; 516.1988, C₂₈H₂₉F₃NO₅ requires 516.1992).

3(4-(4-Trifluoromethoxyphenoxy)phenyl)-2-(carboxylate)-5,6,7,8-tetrahydroquinolin-4(1H)-one (304).



The title compound was synthesised following general procedure **B** from 4-ethoxy-3(4-(4-trifluoromethoxyphenoxy)phenyl)-2-(methoxycarboxylate)-5,6,7,8-tetrahydroquinoline (200 mg, 0.42 mmol) and was isolated as a colourless solid (80 mg, 0.18 mmol, 43%). **HPLC**; 2.76 min (100% reference area); **MP**; 210 °C; **HPLC**; 2.76 mins (100% reference area); **¹H NMR** (400 MHz, DMSO) δ 7.41 (d, J = 8.8 Hz, 2H, H-2' & 6'), 7.21 (d, J = 8.3 Hz, 2H, H-2'' & 6''), 7.12 (d, J = 8.8 Hz, 2H, H-3' & 5'), 7.01 (d, J = 8.3 Hz, 2H, H-3'' & 5''), 2.64 (t, J = 5.6 Hz, 2H, H-5), 2.35 (t, J = 5.6 Hz, 2H, H-8), 1.94 – 1.33 (m, 4H, H-6 & 7); **¹³C NMR** (101 MHz, DMSO) δ 165.4 (C-4), 165.3 (C=O₂H), 156.4 (C_q), 155.4 (C_q), 144.0 (C_q), 132.3 (C-2'' & 6''), 131.6 (C_q), 124.5 (C_q), 124.3 (C_q), 123.4 (C-2' & 6'), 121.9 (C_q), 120.1 (C-3' & 5'), 119.3 (C_q), 118.4 (C-3'' & 5''), 26.9 (C-5) 22.6 (C-8), 22.0 (C-6), 21.8 (C-7); $\nu_{\max}/\text{cm}^{-1}$; 1704, 1594, 1495, 1273; **M/Z (ESI+)**; 446.12 (Found MH⁺; 446.1207, C₂₃H₁₉F₃NO₅ requires 446.1210).

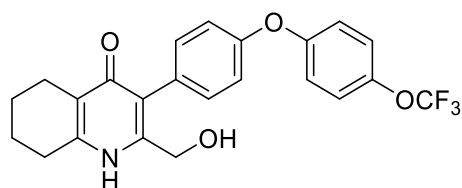
7-Ethyl-3(4-(4-trifluoromethoxyphenoxy)phenyl)-2-(carboxylate)-5,6,7,8-tetrahydroquinolin-4(1H)-one (305).



The title compound was synthesised from 4-ethoxy-7-ethyl-3-(4-(4-trifluoromethoxyphenoxy)phenyl)-2-(methoxycarboxylate)-5,6,7,8-tetrahydroquinoline (50 mg, 0.11 mmol) according to general procedure **I**, and was isolated as a colourless powder (49 mg, 0.10 mmol, 100%); **MP**; 206.0-207.4 °C; **HPLC**; 3.03 mins (95%

reference area); **¹H NMR** (501 MHz, MeOD)* δ 7.17 (d, *J* = 8.4 Hz, 2H, H-2' & 6'), 7.11 (d, *J* = 8.7 Hz, 2H, H-3'' & 5''), 6.98 (d, *J* = 8.7 Hz, 2H, H-2'' & 6''), 6.96 (d, *J* = 8.4, 2H, H-3' & 5'), 2.89 (dd, *J* = 16.9, 4.7 Hz, 1H, H-8), 2.76 (d, *J* = 18.2 Hz, 1H, H-5), 2.50 – 2.33 (m, 2H, H-5 & 8), 2.01-1.94 (m, 1H, H-6), 1.72-1.63 (m, 1H, H-7), 1.40 (p, *J* = 7.7 Hz, 2H, 7-CH₂CH₃), 1.35 – 1.27 (m, 1H, H-6), 0.94 (t, *J* = 7.4 Hz, 3H, 7-CH₂CH₃); **¹³C NMR** (126 MHz, MeOD)* δ 172.9 (C=O), 156.7 (C_q), 155.6 (C_q), 147.8 (C_q), 144.5 (C_q), 131.5 (C-2' & 6'), 127.9 (C_q), 125.1 (C_q), 122.5 (C-3'' & 5''), 119.6 (C-2'' & 6''), 118.6 (C-3' & 5'), 34.3 (C-5), 33.3 (C-7), 28.2 (7-CH₂CH₃), 27.2 (C-6), 22.0 (C-8), 11.1 (7-CH₂CH₃); **v_{max}/cm⁻¹**; 2926, 1595, 1496; **M/Z** (ESI+); 474.15 (Found MH⁺; 474.1522 C₂₅H₂₃F₃NO₅ requires 474.1523).

3(4-(4-Trifluoromethoxyphenoxy)phenyl)-2-(methylhydroxy)-5,6,7,8-tetrahydroquinolin-4(1H)-one (306).

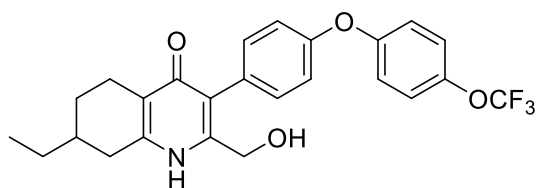


3(4-(4-trifluoromethoxyphenoxy)phenyl)-2-

(carboxylate)-5,6,7,8-tetrahydroquinolin-4(1H)-one (80 mg, 0.17 mmol) was dissolved in methanol (5.00 mL) with the addition of HCl (1.00 mL, conc.) heated to 80 °C for 24 hours. The reaction mixture was diluted with water (10.00 mL) and the organics extracted with EtOAc (3 × 10.00 mL) before being dried and concentrated *in vacuo*. The crude material was then dissolved in dry THF under inert atmosphere and cooled to 0 °C. Diisobutylaluminium hydride was then added slowly with stirring. After two hours the reaction pH was lowered to 3 by addition of HCl_(aq) (2.00 M). Dilution of the solution with water caused precipitation. The title compound was isolated as via filtration as a pale-yellow solid (38 mg, 0.09 mmol, 55%). **MP**; 215 °C; **HPLC**; 2.72 mins (95% reference area); **¹H NMR** (400 MHz, DMSO) δ 11.06 (s, 1H, NH), 7.41 (d, *J* = 8.8 Hz, 2H, H-2' & 6'), 7.25 (d, *J* = 8.6 Hz, 2H, H-3'' & 5''), 7.15 (d, *J* = 9.1 Hz, 2H, H-3' & 5'), 7.05 (d, *J* = 8.6 Hz, 2H, H-2'' & 6''), 5.53 (s, 1H, OH), 4.25 (s, 2H, CH₂OH), 2.67 (t, *J* = 5.6 Hz, 2H, H-5), 2.35 (t, *J* = 6.2 Hz, 2H, H-8), 1.82 – 1.56 (m, 4H, H-6 & 7); **¹³C NMR** (101 MHz, DMSO) δ 166.2 (C-4), 156.3 (C_q), 155.4 (C_q), 144.1 (C_q), 132.9 (C-3'' & 5''), 132.0 (C_q), 131.0 (C_q),

123.5 (C-2' & 6'), 122.7 (C_q), 120.2 (C-3' & 5'), 120.0 (C_q), 119.3 (C_q), 118.7 (C-2'' & 6''), 58.9 (CH₂OH), 26.9 (C-5), 22.5 (C-8), 22.2 (C-7), 21.9 (C-6); **v_{max}/cm⁻¹**; 2930, 1630, 1538, 1495, 1234; **M/Z (ESI+)**; 432.14 (Found MH⁺; 432.1445, C₂₃H₂₁F₃NO₄ requires 432.1423).

7-Ethyl-3(4-(4-trifluoromethoxyphenoxy)phenyl)-2-(methylhydroxy)-5,6,7,8-tetrahydroquinolin-4(1H)-one (307)

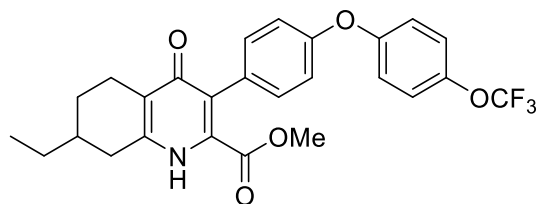


7-ethyl-3(4-(4-

trifluoromethoxyphenoxy)phenyl)-2-(methoxycarboxylate)-5,6,7,8-

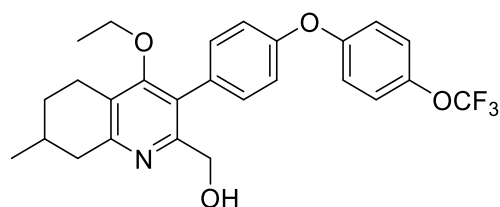
tetrahydroquinolin-4(1H)-one (30 mg, 0.06 mmol) and sodium borohydride (10 mg, 0.24 mmol) were charged into an oven dried flask flushed with N₂. THF (2.00 mL) and MeOH (1.00 mL) was added at 0 °C and reaction stirred. Partial conversion observed after 1 hour, but no further progress. Additional sodium borohydride (10 mg, 0.24 mmol) was added and reaction left over night. Reaction was neutralised with HCl (2.00 M) and organics extracted with ethyl acetate (3 × 10.00 mL). Organics were combined and concentrated before purification by column chromatography (CHCl₃:MeOH) The title compound was isolated as colourless flakes (8 mg, 0.02 mmol, 28%); **MP**; >250 °C; **HPLC**; 3.02 mins (100% reference area); **¹H NMR** (400 MHz, MeOD) δ 7.18 (d, *J* = 9.1 Hz, 2H, H-2' & 6'), 7.14 (d, *J* = 8.6 Hz, 2H, H-3'' & 5''), 7.01 (d, *J* = 9.1 Hz, 2H, H-3' & 5'), 6.97 (d, *J* = 8.6 Hz, 2H, H-2'' & 6''), 4.28 (s, 4H, CH₂OH), 2.79 (dd, *J* = 17.2, 4.8 Hz, 1H, H-8), 2.70 – 2.57 (m, 1H, H-5), 2.30 (dd, *J* = 16.5, 10.3 Hz, 2H, H-8 & 5), 1.91 (m, 1H, H-6), 1.60 (s(b), 1H, H-7), 1.37 (p, *J* = Hz 2H, CH₂CH₃), 1.31 – 1.14 (m, 1H, H-6), 0.94 (t, *J* = 7.4 Hz, 3H, CH₂CH₃); **¹³C NMR** (101 MHz, MeOD) δ 177.3 (C-4), 156.4 (C_q), 156.1 (C_q), 146.1 (C_q), 145.1 (C_q), 132.0 (C-3'' & 5''), 129.8 (C_q), 123.6 (C_q), 123.3 (C_q), 122.4 (C-2' & 6'), 119.4 (C-3' & 5'), 118.7 (C-2'' & 6''), 58.4 (CH₂OH), 34.9 (C-7), 32.7 (C-8), 28.2 (7-CH₂CH₃), 27.6 (C-6), 21.7 (C-5), 10.3 (7-CH₂CH₃); **v_{max}/cm⁻¹**; 2929, 1618, 1498, 1246; **M/Z (ESI)**; 460.17 (Found MH⁺; 460.1729, C₂₅H₂₆F₃NO₄ requires; 460.1730).

7-Ethyl-3(4-(4-trifluoromethoxyphenoxy)phenyl)-2-(methoxycarboxylate)-5,6,7,8-tetrahydroquinolin-4(1H)-one



7-Ethyl-3(4-(4-trifluoromethoxyphenoxy)phenyl)-2-(carboxylate)-5,6,7,8-tetrahydroquinolin-4(1H)-one (50 mg, 0.10 mmol) was dissolved in methanol and conc. Sulphuric acid (0.05 mL) added slowly. The reaction was heated to 80 °C and stirred. The reaction was monitored by LCMS and on completion neutralised with sodium hydroxide, organics were then extracted with ethyl acetate (3 × 5.00 mL), washed with water and brine, before drying over MgSO₄. After concentrating *in vacuo* the title compound was isolated as a white solid (30 mg, 0.06 mmol, 61%), due to limited quantities the compound was progressed without further analysis.

4-Ethoxy-7-methyl-3(4-(4-trifluoromethoxyphenoxy)phenyl)-2-(methylhydroxy)-5,6,7,8-tetrahydroquinoline (308).

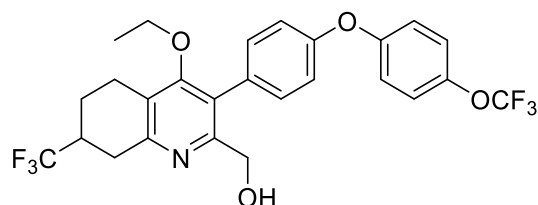


4-Ethoxy-7-methyl-3(4-(4-

trifluoromethoxyphenoxy)phenyl)-2-(methoxycarboxylate)-5,6,7,8-tetrahydroquinoline (62 mg, 0.12 mmol) and sodium borohydride (20 mg, 0.48 mmol) were charged into a nitrogen flushed flask, a mixture of THF : Methanol (3.00 mL, 2:1) was added and the reaction stirred at 0 °C for 30 minutes before slowly being allowed to warm to room temperature. Reaction mixture was concentrated *in vacuo* and purified by column chromatography to afford the title compound as a colourless solid (42 mg, 0.09 mmol, 74%). **MP**; 90.0-91.0 °C ; **HPLC**; 3.35 mins (91% reference area); **¹H NMR** (500 MHz, CDCl₃) δ 7.21-7.12 (m, 4H, H-2', 6', 3'' & 5''), 6.99 (d, *J* = 8.2 Hz, 4H, 3',5', 2'' & 6''), 4.72 (s, 1H, OH), 4.32 (s, 2H, CH₂OH), 3.48 (qd, *J* = 14.5, 6.6 Hz, 2H, CH₃CH₂O), 2.96 (d, *J* = 17.4 Hz, 1H, H-8), 2.86 (d, *J* = 16.5 Hz, 1H, H-5), 2.63 – 2.50 (m, 1H, H-5), 2.46 (dd, *J* = 17.6, 10.5 Hz, 1H, H-8), 1.88 (s_(b), 2H, H-6

& 7), 1.37 – 1.26 (m, 1H, H-6), 1.06 (d, $J = 5.8$ Hz, 3H, Me), 1.00 (t, $J = 6.7$ Hz, 3H, $\text{CH}_3\text{CH}_2\text{O}$); ^{13}C NMR; (126 MHz, CDCl_3) δ 162.2 (C_q), 156.6, (C_q), 156.6 (C_q), 155.4 (C_q), 154.4 (C_q), 149.2 (C_q), 144.8 (C_q), 131.4 (C-2' & 6'), 129.2 (C_q), 124.1 (C_q), 122.7 (C-3'' & 5''), 119.9 (C-2'' & 6''), 118.8 (C-3' & 5'), 68.5 ($\text{CH}_3\text{CH}_2\text{O}$), 61.7 (CH_2OH), 40.8 (C-8), 30.6 (C-7), 29.0 (C-6), 22.8 (C-5), 21.6 (Me), 15.6 ($\text{CH}_3\text{CH}_2\text{O}$); $\nu_{\text{max}}/\text{cm}^{-1}$; 2930, 1581, 1501, 1433, 1383, 1333, 1220; **M/Z (ESI)**; 474.19 (Found MH^+ 474.1891, $\text{C}_{26}\text{H}_{27}\text{F}_3\text{NO}_4$ requires 474.1886)

4-Ethoxy-7-trifluoromethyl-3(4-(4-trifluoromethoxyphenoxy)phenyl)-2-(methoxyhydroxy)-5,6,7,8-tetrahydroquinoline (309).

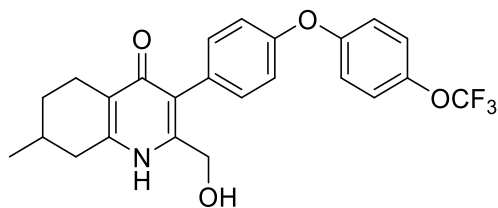


4-Ethoxy-7-trifluoromethyl-3(4-(4-

trifluoromethoxyphenoxy)phenyl)-2-(methoxycarboxylate)-5,6,7,8-

tetrahydroquinoline (70 mg, 0.13 mmol) and sodium borohydride (20 mg, 0.50 mmol) were charged into an oven dried flask flushed with N_2 . THF (2.00 mL) and MeOH (1.00 mL) was added at 0 °C and reaction stirred for 42 hours. Reaction was neutralised with HCl (2.00 M) and organics extracted with ethyl acetate (3 × 10.00 mL), dried over MgSO_4 and concentrated to give the product as a colourless solid (45 mg, 0.09 mmol, 66%). **HPLC**; 3.37 mins (89% reference area); ^1H NMR (400 MHz, CDCl_3) δ 7.16 (d, $J = 8.7$ Hz, 4H, H-2', 6', 3'' & 5''), 7.00 (dd, $J = 8.8, 1.4$ Hz, 4H, H-3', 5', 2'' & 6''), 4.57 (s, 1H, OH), 4.33 (s, 2H, 2- CH_2OH), 3.59 – 3.38 (m, 2H, $\text{CH}_3\text{CH}_2\text{O}$), 3.15 (dd, $J = 17.7, 4.7$ Hz, 1H, H-8), 3.00 (d, $J = 17.9$ Hz, 1H, H-5), 2.92 (dd, $J = 17.3, 11.7$ Hz, 1H, H-8), 2.66 – 2.42 (m, 2H, H-5 & 7), 2.24 – 2.11 (m, 1H, H-6), 1.64 (ddd, $J = 25.1, 12.2, 5.5$ Hz, 1H, H-6), 1.01 (t, $J = 7.0$ Hz, 3H, $\text{CH}_3\text{CH}_2\text{O}$); ^{13}C NMR (101 MHz, CDCl_3) δ 162.12 (C_q), 156.8 (C_q), 155.5 (C_q), 155.2 (C_q), 153.2 (C_q), 131.3 (C-2' & 6'), 128.7 (C_q), 124.4 (C_q), 123.2 (C_q), 122.7 (C-3'' & 5''), 120.1 (C-2'' & 6''), 118.8 (C-3' & 5''), 68.7 ($\text{CH}_3\text{CH}_2\text{O}$), 61.7 (CH_2OH), 39.0 (q, $J = 27.7$ Hz, C-7), 31.1 (C-8), 22.0 (C-5), 21.5 (C-6), 15.6 ($\text{CH}_3\text{CH}_2\text{O}$); $\nu_{\text{max}}/\text{cm}^{-1}$; 2933, 1579, 1498, 1435, 1389, 1343, 1239; **M/Z (ESI)**; 528.16 (Found MH^+ 528.1611, $\text{C}_{26}\text{H}_{24}\text{F}_6\text{NO}_4$ requires 528.1604).

7-Methyl-3(4-(4-trifluoromethoxyphenoxy)phenyl)-2-(methylhydroxy)-5,6,7,8-tetrahydroquinolin-4(1H)-one (310).



4-ethoxy-7-methyl-3(4-(4-

trifluoromethoxyphenoxy)phenyl)-2-(methylhydroxy)-5,6,7,8-

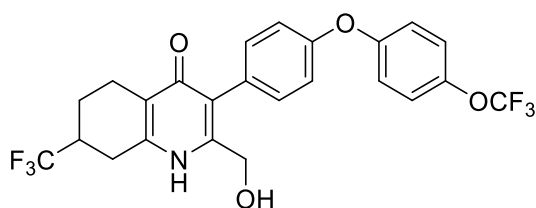
tetrahydroquinoline (40 mg, 0.08 mmol) was dissolved in acetic acid (1.00 mL) and hydrogen bromide (40% aq, 0.50 mL) and heated to reflux for 18 hours.

The reaction was then cooled and neutralised with sodium hydroxide causing a precipitate to form. The precipitate was isolated by filtration and re-dissolved

in a mixture of DMSO (2.00 mL) and sodium hydroxide (aq) (2.00 mL, 2.00 M) and heated to 140 °C for 12 hours before cooling and neutralising with HCl

(2.00 M) causing precipitation. The title compound was isolated by filtration as a colourless solid (12 mg, 0.03 mmol, 32%). **MP**; 230-232 °C; **HPLC**; 2.85 min (85% reference area); **¹H NMR** (400 MHz, Acetone) δ 7.35 (d, *J* = 8.8 Hz, 2H, H-3'' & 5''), 7.27 (d, *J* = 8.4 Hz, 2H, H-2' & 6'), 7.12 (d, *J* = 8.8 Hz, 2H, H-2'' & 6''), 7.01 (d, *J* = 8.4 Hz, 2H, H-3' & 5'), 4.40 (s, 2H, CH₂OH), 2.75 (d, *J* = 4.4 Hz, 1H, H-8), 2.68 (d, *J* = 15.5 Hz, 1H, H-5), 2.30 (dt, *J* = 12.5, 7.5 Hz, 2H, H-8 & 5), 1.93 – 1.82 (m, 2H, H-7 & 6), 1.25-1.35 (m, 1H, H-6), 1.08 (d, *J* = 6.5 Hz, 3H, Me); **¹³C NMR**; (101 MHz, Acetone) δ 179.0 (C-4), 157.3 (C_q), 156.4 (2 × C_q), 145.1 (C_q), 133.3 (C-2' & 6'), 131.9 (C_q), 123.7 (C-3'' & 5''), 123.1 (C_q), 120.8 (C_q), 120.6 (C-2'' & 6''), 119.2 (C-3' & 5'), 59.6 (CH₂OH), 35.8 (C-8), 31.3 (C-6 & 7), 23.0 (C-5), 21.7 (Me): **M/Z (ESI)**; 446.16 (Found MH⁺ 446.1586, C₂₄H₂₃F₃NO₄ requires 446.1573).

7-Trifluoromethyl-3(4-(4-trifluoromethoxyphenoxy)phenyl)-2-(methylhydroxy)-5,6,7,8-tetrahydroquinolin-4(1H)-one (311).



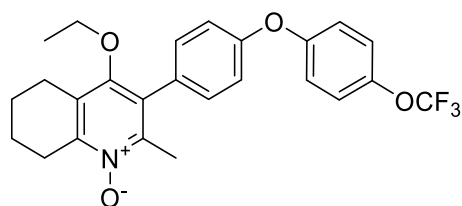
4-Ethoxy-7-trifluoromethyl-3(4-(4-

trifluoromethoxyphenoxy)phenyl)-2-(methylhydroxy)-5,6,7,8-

tetrahydroquinoline (40 mg, 0.08 mmol) was dissolved in acetic acid (1.00 mL)

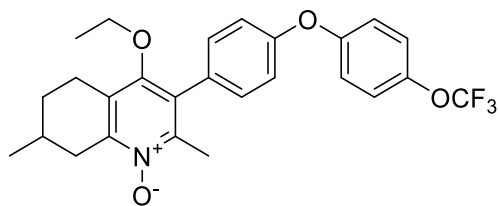
and hydrogen bromide (40% aq, 0.50 mL) and heated to reflux for 18 hours. The reaction was then cooled and neutralised with sodium hydroxide causing a precipitate to form. The precipitate was isolated by filtration and re-dissolved in a mixture of DMSO (2.00 mL) and sodium hydroxide (aq) (2.00 mL, 2.00 M) and heated to 140 °C for 12 hours before cooling and neutralising with HCl (2.00 M) causing precipitation. The title compound was isolated, by filtration, as a colourless solid (7 mg, 0.01 mmol, 18%). **MP**; >250 °C; **HPLC**; 2.94 mins (98% reference area); **¹H NMR** (501 MHz, MeOD) δ 7.17 (d, J = 8.4 Hz, 2H, H-2' & 6'), 7.13 (d, J = 8.7 Hz, 2H, H-3'' & 5''), 7.01 (d, J = 9.2 Hz, 2H, H-3' & 5'), 6.97 (d, J = 8.7 Hz, 2H, H-2'' & 6''), 4.29 (s, J = 15.1 Hz, 2H, CH₂OH), 2.97 (dd, J = 16.9, 4.9 Hz, 1H, H-5), 2.85 – 2.68 (m, 2H, H-8 & 5), 2.61 (dd, J = 14.8, 11.6 Hz, 1H, H-7), 2.35 (ddd, J = 17.3, 11.7, 5.7 Hz, 1H, H-5), 2.21 – 2.09 (m, 1H, H-5), 1.56 (qd, J = 12.1, 5.6 Hz, 1H, H-6); **¹³C NMR** (126 MHz, MeOD) δ 178.4 (C-4), 157.6 (C_q), 157.6 (C_q), 148.1 (C_q), 145.7 (C_q), 143.6 (C_q), 133.3 (C-2' & 6'), 130.8 (C_q), 125.1 (C_q), 123.7 (C-3'' & 5''), 122.9 (C-2'' & 6''), 120.7 (C_q), 120.0 (C-3'' & 5''), 59.7 (CH₂OH), 39.2 (q, J = 27.7 Hz, H-7), 26.9 (C-8), 22.2 (C-5), 22.1 (C-6); **v_{max}/cm⁻¹**; 1619, 1493, 1232; **M/Z (ESI)**; 500.13 (Found MH⁺ 500.1286, C₂₄H₁₉F₆NO₄ requires 500.1291).

N-Oxy-4-ethoxy-3-(4-(4-(trifluoromethoxy)phenoxy)phenyl)-2-methyl-5,6,7,8-tetrahydroquinoline (312).



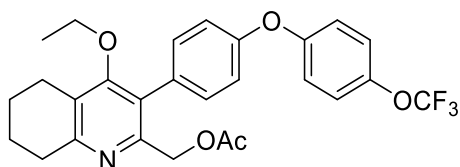
The title compound was synthesised from 4-ethoxy-3-(4-(4-trifluoromethoxyphenoxy)phenyl)-2-methyl-5,6,7,8-tetrahydroquinoline (200 mg, 0.45 mmol) according to general procedure **Q**. However trituration did not result in precipitation and it was decided to progress the material without further purification as the crude oil (ethyl acetate and mcpba identified in NMR).

N-Oxy-4-ethoxy-3-(4-(4-(trifluoromethoxy)phenoxy)phenyl)-2,7-dimethyl-5,6,7,8-tetrahydroquinoline (313).



The title compound was synthesised from 4-Ethoxy-3-(4-(4-(trifluoromethoxy)phenoxy)phenyl)-2,7-dimethyl-5,6,7,8-tetrahydroquinoline (200 mg, 0.44 mmol) according to general procedure **Q** and was isolated as a colourless solid (100 mg, 0.21 mmol, 48%). **MP**; 104.7-105.5 °C ; **HPLC** 3.86 mins (93% reference area); **¹H NMR** (400 MHz, CDCl₃) δ 7.26 – 7.18 (m, 4H, H-2',6', 3'' & 5''), 7.07 (dd, *J* = 8.8, 6.6 Hz, 4H, H-2'',6'', 3' & 5'), 3.59 – 3.40 (m, 2H, OCH₂CH₃), 3.32 (dd, *J* = 19.2, 5.7 Hz, 1H, H-8), 3.00 – 2.90 (dt, *J* = 17.2, 4.0 Hz 1H, H-5), 2.60 (ddd, *J* = 17.2, 12.2, 5.3 Hz, 1H, H-5), 2.43 (dd, *J* = 19.2, 10.2 Hz, 1H, H-8), 2.37 (s, 3H, 2-Me), 1.90 (dd, *J* = 8.8, 5.4 Hz, 2H, H-6 & 7), 1.31 (ddd, *J* = 16.8, 12.3, 5.0 Hz, 1H, H-6), 1.17 (d, *J* = 6.5 Hz, 3H, 7-Me), 1.03 (t, *J* = 7.0 Hz, 3H, OCH₂CH₃); **¹³C NMR** (101 MHz, CDCl₃) δ 156.7 (C_q), 155.3 (C_q), 152.5 (C_q), 148.7 (C_q), 146.6 (C_q), 144.8 (C_q), 131.6 (C-2' & 6'), 129.8 (C_q), 129.2 (C_q), 126.5 (C_q), 122.7 (C-3'' & 5''), 120.0 (C-2'' & 6''), 118.7 (C-3' & 5'), 68.8 (OCH₂CH₃), 33.8 (C-8), 29.6 (C-6), 28.2 (C-7), 23.1 (C-5), 21.7 (7-Me), 16.2 (2-Me), 15.4 (OCH₂CH₃); **v_{max}/cm⁻¹**; 2939, 1495, 1331, 1299, 1217; **M/Z (ESI)**; 474.19 (Found MH⁺ 474.1889 C₂₆H₂₇F₃NO₄ requires 474.1887).

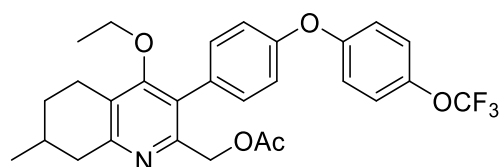
4-Ethoxy-3-(4-(4-(trifluoromethoxy)phenoxy)phenyl)-2-methylhydroxyacetate-5,6,7,8-tetrahydroquinoline (314).



The title compound was synthesised from *N*-Oxy-4-ethoxy-3-(4-(4-(trifluoromethoxy)phenoxy)phenyl)-2-methyl-5,6,7,8-tetrahydroquinoline (250 mg, 0.54 mmol) according to general procedure **T** and was isolated with mcpba contamination as an orange oil (148 mg, 0.30 mmol, 55%). **HPLC**; 3.35 mins (56% reference area); **¹H NMR**; (400 MHz, CDCl₃) δ 7.21(d, *J* = 8.6 Hz, 2H, H-2' & 6'), 7.15 (d, *J* = 8.9 Hz, 2H, H-3'' &

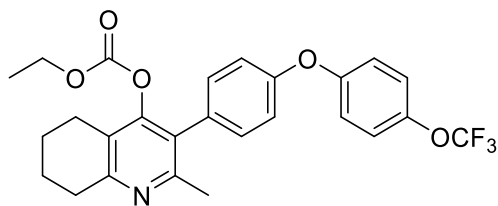
5''), 7.03 – 6.95 (m, 4H, H-3', 5', 2'' & 6''), 4.87 (s, 2H, 2-CH₂OAc), 3.46 (q, J = 6.9 Hz, 2H, OCH₂CH₃), 2.91 (t, J = 6.3 Hz, 2H, H-8), 2.69 (t, J = 6.2 Hz, 2H, H-5), 1.95 (s, 3H), 1.86 – 1.70 (m, 4H, H-6 & 7), 0.98 (t, J = 7.0 Hz, 3H, OCH₂CH₃); **¹³C NMR**; (101 MHz, CDCl₃) δ 170.5 (CH₂O₂CMe), 162.3 (C_q), 158.4 (C_q), 156.5 (C_q), 155.5 (C_q'), 151.2 (C_q), 144.7 (C_q), 131.5 (C-2' & 6'), 130.0 (C_q), 127.8 (C_q), 125.5 (C_q), 122.7 (C-3'' & 5''), 119.9 (C-2'' & 6''), 118.6 (C-3' & 5'), 68.4 (OCH₂CH₃), 65.9 (2-CH₂OAc), 41.1 (C-5), 30.4 (C-8), 29.0 (C-6), 23.0 (C-7), 21.7 (O₂CMe), 20.9 (Me-2), 15.6 (OCH₂CH₃). **v_{max}/cm⁻¹**; 2938, 1738, 1578, 1497, 1434, 1370, 1330, 1233; **M/Z (ESI)**; 502.18 (Found MH+ 502.1838 C₂₇H₂₈F₃NO₅ requires 502.1836)

4-Ethoxy-3-(4-(4-(trifluoromethoxy)phenoxy)phenyl)-2-methylhydroxyacetate
7-methyl-5,6,7,8-tetrahydroquinoline (315)



The title compound was synthesised from *N*-Oxy-4-ethoxy-3-(4-(4-(trifluoromethoxy)phenoxy)phenyl)-2,7-dimethyl-5,6,7,8-tetrahydroquinoline (100 mg, 0.21 mmol) according to general procedure **T**, and was isolated as a colourless amorphous solid (85 mg, 0.17 mmol, 79%). **HPLC**; 3.36 mins (83% reference area); **¹H NMR** (400 MHz, CDCl₃) δ 7.30 (d, J = 8.6 Hz, 2H, H-2' & 6'), 7.23 (d, J = 8.7 Hz, 2H, H-3'' & 5''), 7.07 (m, 4H, H-3', 5', 2'' & 6''), 4.95 (s, 2H, 2-CH₂OAc), 3.64 – 3.45 (m, 2H, OCH₂CH₃), 3.07 (dd, J = 16.9, 5.0 Hz, 1H, H-8), 2.97 (ddd, J = 17.6, 5.1, 2.7 Hz, 1H, H-5), 2.71 – 2.61 (m, 1H, H-5), 2.57 (dd, J = 17.6, 10.6 Hz, 1H, H-8), 2.04 (s, 3H, O₂CMe), 2.00 – 1.88 (m, 2H, H-6 & 7), 1.39 (qd, J = 11.4, 5.5 Hz, 1H, H-6), 1.13 (d, J = 6.4 Hz, 3H, 7-Me), 1.07 (t, J = 7.0 Hz, 3H, OCH₂CH₃); **¹³C NMR** (101 MHz, CDCl₃) δ 170.5 (O₂CMe), 162.3 (C-4), 158.4 (C-4'), 156.5 (C-1''), 155.5 (C-2), 151.2 (C-9), 144.7 (C-4''), 131.6 (C-2' & 6'), 130.0 (C-1'), 127.8 (C-3), 125.5 (C-10), 122.7 (C-3'' & 5''), 119.9 (C-2'' & 6''), 118.6 (C-3' & 5'), 68.4 (OCH₂CH₃), 65.9 (CH₂OAc), 41.1 (C-8), 30.4 (C-6), 29.0 (C-7), 23.0 (C-5), 21.7 (7-Me), 20.9 (O₂CMe), 15.5 (OCH₂CH₃); **v_{max}/cm⁻¹**; 2929, 1740, 1578, 1554, 1498, 1434, 1372, 1332, 1270; **M/Z (ESI)**; 516.20 (Found MH+ 516.1990, C₂₈H₂₉F₃NO₅ requires 516.1992) (major peak 474 loss of acetate)

4-Ethoxycarbonate-2-methyl-3-(4-(4-(trifluoromethoxy)phenoxy)phenyl)-5,6,7,8-tetrahydro quinoline (318).



2-Methyl-3-(4-(4-

(trifluoromethoxy)phenoxy)phenyl)-5,6,7,8-tetrahydroquinolin-4(1H)-one (100 mg, 0.24 mmol) and sodium hydride (9 mg, 60% dispersion, 0.25 mmol) were charged into a nitrogen flushed flask. THF (anhydrous, 2.00 mL) was added and reaction stirred at 60 °C until solids had dissolved. Ethyl chloroformate (20 μ L, 0.24 mmol) was then added and the reaction stirred for 1 hour. The reaction mixture was concentrated *in vacuo* and the residue purified by column chromatography. The title compound was isolated as a clear oil that, on extensive drying, formed a colourless solid (20mg, 0.04 mmol, 17%). **HPLC**; 2.95 mins (74% reference area); **¹H NMR** (400 MHz, CDCl₃) δ 7.13 (d_{ap}, J = 8.4 Hz, 2H, H-2', 6', 3'' & 5''), 6.97 (dd_{ap}, J = 8.9, 2.7 Hz, 2H, H- 2'', 6'', 3' & 5'), 4.04 (q, J = 7.1 Hz, 2H, CH₃CH₂O), 2.88 (t, J = 6.3 Hz, 2H, H-7), 2.56 (t, J = 6.1 Hz, 2H, H-6), 2.26 (s, 3H, Me), 1.88 – 1.79 (m, 2H, H-8), 1.75 (dd, J = 10.6, 4.9 Hz, 2H, H-5), 1.11 (t, J = 7.1 Hz, 3H, CH₃CH₂O); **¹³C NMR** (101 MHz, CDCl₃) δ 158.1 (C-4), 156.5 (C-1''), 155.5 (C-4'), 155.2 (C-2), 153.9 (C-9), 151.9 (EtOCO), 144.7 (C-4''), 131.2 (C-2' & 6), 129.9 (C-1'), 126.8 (C-3), 122.7 (C-10, 3'' & 5''), 119.9 (C-2'' & 6''), 118.8 (C-3' & 5'), 65.0 (CH₃CH₂O), 32.5 (C-7), 23.1 (Me), 22.7 (C-6), 22.5(C-8), 22.0 (C-5), 14.01 (CH₃CH₂O); **ν_{\max} /cm⁻¹**; 2936, 1759, 1596, 1498, 1436, 1220; **M/Z (ESI)**; 488.17 (Found 488.1675, MH⁺ requires C₂₇H₂₄F₃NO₅ 488.1679).

Molecular Modelling/Chemogenomics.

X-ray structures of the cytochrome *bc*₁ complex are available from the Protein DataBank. A homology model of the *T. gondii* cytochrome *bc*₁ complex was generated using the Phyre webserver. Molecular modelling and docking was performed on high performance Linux clusters at the University of Leeds, using specialist software: Maestro & Glide (Schrodinger).

List of References

- 1 J. P. Dubey, The History of *Toxoplasma gondii* The First 100 Years, *J. Eukaryot. Microbiol.*, 2008, **55**, 467–475.
- 2 C. A. K. Despommier, Dickinson D. Gwadz, Robert W. Hotez, Peter J. Knirsch, *Parasitic Diseases*, Apple Tree Productions, 5th edn., 2006.
- 3 F. Robert-Gangneux and M.-L. Dardé, Epidemiology of and diagnostic strategies for toxoplasmosis., *Clin. Microbiol. Rev.*, 2012, **25**, 264–96.
- 4 W. J. S. Jr, A. T. Smith and B. R. Joyce, Understanding mechanisms and the role of differentiation in pathogenesis of *Toxoplasma gondii* - A Review, *NIH Public Access*, 2010, **104**, 155–161.
- 5 G. K. U. niv Kaya, An overview of classification of the phylum Apicomplexa., *Kafkas Univ Vet Fak Derg*, 2001, **7**, 223–228.
- 6 J. P. Dubey, D. S. Lindsay and C. A. Speer, Structures of *Toxoplasma gondii* tachyzoites, bradyzoites, and sporozoites and biology and development of tissue cysts., *Clin. Microbiol. Rev.*, 1998, **11**, 267–99.
- 7 K. Mai, P. A. Sharman, R. A. Walker, M. Katrib, D. de Souza, M. J. McConville, M. G. Wallach, S. I. Belli, D. J. P. Ferguson and N. C. Smith, Oocyst wall formation and composition in coccidian parasites, *Mem. Inst. Oswaldo Cruz*, 2009, **104**, 281–289.
- 8 A. M. Tenter, A. R. Heckeroth and L. M. Weiss, *Toxoplasma gondii*: from animals to humans, *Int. J. Parasitol.*, 2000, **30**, 1217–1258.
- 9 L. Jacobs, J. S. Remington, M. L. Melton, S. The and N. Feb, The Resistance of the Encysted Form of *Toxoplasma gondii*, *J. Parasitol.*, 1957, **46**, 11–21.
- 10 J. P. Dubey, Advances in the life cycle of *Toxoplasma gondii*, *Int. J. Parasitol.*, 1998, **28**, 1019–1024.
- 11 D. J. P. Ferguson, *Toxoplasma gondii* and sex: essential or optional extra?, *Trends Parasitol.*, 2002, **18**, 355–359.
- 12 G. Pappas, N. Roussos and M. E. Falagas, Toxoplasmosis snapshots: global status of *Toxoplasma gondii* seroprevalence and implications for pregnancy and congenital toxoplasmosis. *Int. J. Parasitol.*, 2009, **39**, 1385–94.
- 13 J. P. Dubey, History of the discovery of the life cycle of *Toxoplasma*

- gondii*, *Int. J. Parasitol.*, 2009, **39**, 877–882.
- 14 E. Gilot-fromont, M. Lélou, M. Dardé, C. Richomme, D. Aubert, E. Afonso, A. Mercier, C. Gotteland and I. Villena, The Life Cycle of *Toxoplasma gondii* in the Natural Environment, 2012, 3–36.
- 15 D. K. Howe and L. D. Sibley, *Toxoplasma gondii* comprises three clonal lineages: correlation of parasite genotype with human disease., *J. Infect. Dis.*, 1995, **172**, 1561–6.
- 16 J. P. J. Saeij, J. P. Boyle and J. C. Boothroyd, Differences among the three major strains of *Toxoplasma gondii* and their specific interactions with the infected host, *Trends Parasitol.*, 2005, **21**, 476–481.
- 17 J. L. Jones, M. E. Parise and A. E. Fiore, Neglected parasitic infections in the United States: toxoplasmosis., *Am. J. Trop. Med. Hyg.*, 2014, **90**, 794–9.
- 18 J. P. Dubey, *Toxoplasmosis of Animals and Humans*, CRC press, Second., 2010.
- 19 S. E. Siegel, M. N. Lunde, A. H. Gelderman, R. H. Halterman, J. A. Brown, A. S. Levine and R. G. Graw, Transmission of Toxoplasmosis by Leukocyte Transfusion, *Blood*, 1971, **37**.
- 20 P. S. Mead, L. Slutsker, V. Dietz, L. F. McCaig, J. S. Bresee, C. Shapiro, P. M. Griffin and R. V. Tauxe, Food-related illness and death in the United States, *Emerg. Infect. Dis.*, 1999, **5**, 607–625.
- 21 V. Vaillant, H. de Valk, E. Baron, T. Ancelle, P. Colin, M.-C. Delmas, B. Dufour, R. Pouillot, Y. Le Strat, P. Weinbreck, E. Jouglu and J. C. Desenclos, Foodborne infections in France., *Foodborne Pathog. Dis.*, 2005, **2**, 221–232.
- 22 J. Montoya and O. Liesenfeld, Toxoplasmosis, *Lancet*, 2004, **363**, 1965–1976.
- 23 P. Ryan, S. F. Hurley, A. M. Johnson, M. Salzberg, M. W. Lee, J. B. North, J. J. McNeil and A. J. McMichael, Tumours of the brain and presence of antibodies to *Toxoplasma gondii*., *Int. J. Epidemiol.*, 1993, **22**, 412–419.
- 24 G. Desmonts and J. Couvreur, Congenital Toxoplasmosis, *N. Engl. J. Med.*, 1974, **290**, 1110–1116.
- 25 J. G. Montoya and J. S. Remington, Toxoplasmic chorioretinitis in the

- setting of acute acquired toxoplasmosis., *Clin. Infect. Dis.*, 1996, **23**, 277–282.
- 26 E. Delair, D. Monnet, S. Grabar, J. Dupouy-Camet, H. Yera and A. P. Brézin, Respective Roles of Acquired and Congenital Infections in Presumed Ocular Toxoplasmosis, *Am. J. Ophthalmol.*, 2008, **146**, 851–855.
- 27 S. Zhu, Psychosis may be associated with toxoplasmosis., *Med. Hypotheses*, 2009, **73**, 799–801.
- 28 A. Minto and F. J. Roberts, The psychiatric complications of toxoplasmosis, *Lancet*, 1959, **273**, 1180–1182.
- 29 N. Kar and B. Misra, Toxoplasma seropositivity and depression: a case report., *BMC Psychiatry*, 2004, **4**, 1.
- 30 R. E. Holliman, Toxoplasmosis, behaviour and personality, *J. Infect.*, 1997, **35**, 105–110.
- 31 J. Shanmugam, K. Naseema, C. Sarada and D. Rout, Toxoplasma gondii IgM antibody prevalence study in patients suffering from neurological disorders, *Indian J Pathol Microbiol*, 1995, **38**, 423–426.
- 32 J. Lindová, M. Novotná, J. Havlíček, E. Jozífková, A. Skallová, P. Kolbeková, Z. Hodný, P. Kodym and J. Flegr, Gender differences in behavioural changes induced by latent toxoplasmosis., *Int. J. Parasitol.*, 2006, **36**, 1485–92.
- 33 T. B. Cook, L. A. Brenner, C. R. Cloninger, P. Langenberg, A. Igbide, I. Giegling, A. M. Hartmann, B. Konte, M. Friedl, L. Brundin, M. W. Groer, A. Can, D. Rujescu and T. T. Postolache, ‘Latent’ infection with Toxoplasma gondii: Association with trait aggression and impulsivity in healthy adults., *J. Psychiatr. Res.*, 2014.
- 34 R. Gratzl, G. Sodeck, P. Platzner, W. Jäger, J. Graf, A. Pollak and T. Thalhammer, Treatment of toxoplasmosis in pregnancy: Concentrations of spiramycin and neospiramycin in maternal serum and amniotic fluid, *Eur. J. Clin. Microbiol. Infect. Dis.*, 2002, **21**, 12–16.
- 35 E. Schoondermark-van de Ven, T. Vree, W. Melchers, W. Camps and J. Galama, In vitro effects of sulfadiazine and its metabolites alone and in combination with pyrimethamine on Toxoplasma gondii, *Antimicrob. Agents Chemother.*, 1995, **39**, 763–765.

- 36 F. Sordet, Y. Aumjaud, H. Fessi and F. Derouin, Assessment of the activity of atovaquone-loaded nanocapsules in the treatment of acute and chronic murine toxoplasmosis., *Parasite*, 1998, **5**, 223–229.
- 37 I. M. Rollo, The mode of action of sulphonamides, proguanil and pyrimethamine on plasmodium gallinaceum, *Br. J. Pharmacol. Chemother.*, 1955, **10**, 208–214.
- 38 R. M. Richards, R. B. Taylor and Z. Y. Zhu, Mechanism for synergism between sulphonamides and trimethoprim clarified., *J. Pharm. Pharmacol.*, 1996, **48**, 981–984.
- 39 M. L. Black, Sequential blockage as a theoretical basis for drug synergism., *J. Med. Chem.*, 1963, **6**, 145–53.
- 40 W. Sirawaraporn and Y. Yuthavong, Potentiating effect of pyrimethamine and sulfadoxine against dihydrofolate reductase from pyrimethamine-sensitive and pyrimethamine-resistant *Plasmodium chabaudi.*, *Antimicrob. Agents Chemother.*, 1986, **29**, 899–905.
- 41 T. Tenson, M. Lovmar and M. Ehrenberg, The Mechanism of Action of Macrolides, Lincosamides and Streptogramin B Reveals the Nascent Peptide Exit Path in the Ribosome, *J. Mol. Biol.*, 2003, **330**, 1005–1014.
- 42 W.-H. R. Garin JP, Pellerat J, Maillard, Theoretical bases of the prevention by spiramycin of congenital toxoplasmosis in pregnant women, *Press. Med*, 1968, **76**, 2266.
- 43 D. C. McFadden, S. Tomavo, E. A. Berry and J. C. Boothroyd, Characterization of cytochrome b from *Toxoplasma gondii* and Qo domain mutations as a mechanism of atovaquone-resistance, *Mol. Biochem. Parasitol.*, 2000, **108**, 1–12.
- 44 A. L. Baggish and D. R. Hill, Antiparasitic agent atovaquone., *Antimicrob. Agents Chemother.*, 2002, **46**, 1163–73.
- 45 V. Barton, N. Fisher, G. A. Biagini, S. A. Ward and P. M. O'Neill, Inhibiting *Plasmodium* cytochrome bc1: a complex issue., *Curr. Opin. Chem. Biol.*, 2010, **14**, 440–6.
- 46 F. G. Araujo, J. Huskinson-Mark, W. E. Gutteridge and J. S. Remington, In vitro and in vivo activities of the hydroxynaphthoquinone 566C80 against the cyst form of *Toxoplasma gondii.*, *Antimicrob. Agents Chemother.*, 1992, **36**, 326–30.

- 47 A. Trauner, C. M. Sassetti and E. J. Rubin, Genetic Strategies for Identifying New Drug Targets., *Microbiol. Spectr.*, 2014, **2**, 1–16.
- 48 M. E. Bunnage, Getting pharmaceutical R&D back on target, *Nat. Chem. Biol.*, 2011, **7**, 335–339.
- 49 F. Calderón, D. Barros, J. M. Bueno, J. M. Coterón, E. Fernández, F. J. Gamo, J. L. Lavandera, M. L. León, S. J. F. Macdonald, A. Mallo, P. Manzano, E. Porras, J. M. Fiandor and J. Castro, An Invitation to Open Innovation in Malaria Drug Discovery: 47 Quality Starting Points from the TCAMS., *ACS Med. Chem. Lett.*, 2011, **2**, 741–6.
- 50 L. L. Ling, T. Schneider, A. J. Peoples, A. L. Spoering, I. Engels, B. P. Conlon, A. Mueller, T. F. Schäberle, D. E. Hughes, S. Epstein, M. Jones, L. Lazarides, V. A. Steadman, D. R. Cohen, C. R. Felix, K. A. Fetterman, W. P. Millett, A. G. Nitti, A. M. Zullo, C. Chen and K. Lewis, A new antibiotic kills pathogens without detectable resistance., *Nature*, 2015, **517**, 455–459.
- 51 J. Weigelt, Structural genomics—Impact on biomedicine and drug discovery, *Exp. Cell Res.*, 2010, **316**, 1332–1338.
- 52 O. Gileadi, S. Knapp, W. H. Lee, B. D. Marsden, S. Müller, F. H. Niesen, K. L. Kavanagh, L. J. Ball, F. von Delft, D. A. Doyle, U. C. T. Oppermann and M. Sundström, The scientific impact of the Structural Genomics Consortium: a protein family and ligand-centered approach to medically-relevant human proteins, *J. Struct. Funct. Genomics*, 2007, **8**, 107–119.
- 53 A. Karawajczyk, F. Giordanetto, J. Benningshof, D. Hamza, T. Kalliokoski, K. Pouwer, R. Morgentin, A. Nelson, G. Müller, A. Piechot and D. Tzalis, Expansion of chemical space for collaborative lead generation and drug discovery: the European Lead Factory Perspective, *Drug Discov. Today*, 2015, **20**, 1310–1316.
- 54 N. Roberts, J. Martin, D. Kinchington, A. Broadhurst, J. Craig, I. Duncan, S. Galpin, B. Handa, J. Kay and A. Krohn, Rational design of peptide-based HIV proteinase inhibitors, *Science*, 1990, **248**, 358–361.
- 55 J. Erickson, D. Neidhart, J. VanDrie, D. Kempf, X. Wang, D. Norbeck, J. Plattner, J. Rittenhouse, M. Turon, N. Wideburg *et. al*, Design, activity, and 2.8 Å crystal structure of a C2 symmetric inhibitor

- complexed to HIV-1 protease, *Science*, 1990, **249**, 527–533.
- 56 Y. Li, C. Kang, Y. Li and C. Kang, Solution NMR Spectroscopy in Target-Based Drug Discovery, *Molecules*, 2017, **22**, 1399.
- 57 R. E. Hubbard, in *Structure-Based Drug Discovery*, ed. R. E. Hubbard, Royal Society of Chemistry, Cambridge, 2006, pp. 32–53.
- 58 K. Ampornpanai, R. M. Johnson, P. M. O'Neill, C. W. G. Fishwick, A. H. Jamson, S. Rawson, S. P. Muench, S. S. Hasnain and S. V. Antonyuk, X-ray and cryo-EM structures of inhibitor-bound cytochrome *bc₁* complexes for structure-based drug discovery, *IUCrJ*, 2018, **5**, 200–210.
- 59 V. J. Gillet, W. Newell, P. Mata, G. Myatt, S. Sike, Z. Zsoldos and A. P. Johnson, SPROUT: recent developments in the de novo design of molecules., *J. Chem. Inf. Comput. Sci.*, 1994, **34**, 207–17.
- 60 J. A. Grant, M. A. Gallardo and B. T. Pickup, A fast method of molecular shape comparison: A simple application of a Gaussian description of molecular shape, *J. Comput. Chem.*, 1996, **17**, 1653–1666.
- 61 Z. Zsoldos, D. Reid, A. Simon, S. B. Sadjad and A. P. Johnson, eHiTS: A new fast, exhaustive flexible ligand docking system, *J. Mol. Graph. Model.*, 2007, **26**, 198–212.
- 62 D. A. Morrison, Evolution of the Apicomplexa: where are we now?, *Trends Parasitol.*, 2009, **25**, 375–82.
- 63 L. Lim and G. I. McFadden, The evolution, metabolism and functions of the apicoplast., *Philos. Trans. R. Soc. Lond. B. Biol. Sci.*, 2010, **365**, 749–63.
- 64 M. Mather, K. Henry and A. Vaidya, Mitochondrial Drug Targets in Apicomplexan Parasites, *Curr. Drug Targets*, 2007, **8**, 49–60.
- 65 D. L. Vander Jagt, L. A. Hunsaker, N. M. Campos and B. R. Baack, d-Lactate production in erythrocytes infected with *Plasmodium falciparum*, *Mol. Biochem. Parasitol.*, 1990, **42**, 277–284.
- 66 W. Gutteridge, Conversion of dihydroorotate to orotate in parasitic protozoa, *Biochim. Biophys. Acta - Gen. Subj.*, 1979, **582**, 390–401.
- 67 P. M. Pelphrey, V. M. Popov, T. M. Joska, J. M. Beierlein, E. S. D. Bolstad, Y. A. Fillingham, D. L. Wright and A. C. Anderson, Highly efficient ligands for dihydrofolate reductase from *Cryptosporidium*

- hominis and *Toxoplasma gondii* inspired by structural analysis, *J. Med. Chem.*, 2007, **50**, 940–950.
- 68 M. E. Welsch, J. Zhou, Y. Gao, Y. Yan, G. Porter, G. Agnihotri, Y. Li, H. Lu, Z. Chen and S. B. Thomas, Discovery of Potent and Selective Leads against *Toxoplasma gondii* Dihydrofolate Reductase via Structure-Based Design, *ACS Med. Chem. Lett.*, 2016, **7**, 1124–1129.
- 69 H. Alday and J. Doggett, Drugs in development for toxoplasmosis: advances, challenges, and current status, *Drug Des. Devel. Ther.*, 2017, **11**, 273–293.
- 70 M. M. McFarland, S. J. Zach, X. Wang, L.-P. Potluri, A. J. Neville, J. L. Vennerstrom and P. H. Davis, A Review of Experimental Compounds Demonstrating Anti-*Toxoplasma* Activity., *Antimicrob. Agents Chemother.*, 2016.
- 71 C. J. Canfield, W. K. Milhous, A. L. Ager, R. N. Rossan, T. R. Sweeney, N. J. Lewis and D. P. Jacobus, PS-15: A potent, orally active antimalarial from a new class of folic acid antagonists, *Am. J. Trop. Med. Hyg.*, 1993, **49**, 121–126.
- 72 M. E. Fichera and D. S. Roos, A plastid organelle as a drug target in apicomplexan parasites., *Nature*, 1997, **390**, 407–9.
- 73 Y. Lee, J. Y. Choi, H. Fu, C. Harvey, S. Ravindran, W. R. Roush, J. C. Boothroyd and C. Khosla, Chemistry and biology of macrolide antiparasitic agents, *J. Med. Chem.*, 2011, **54**, 2792–2804.
- 74 S. P. Muench, J. Stec, Y. Zhou, G. A. Afanador, M. J. McPhillie, M. R. Hickman, P. J. Lee, S. E. Leed, J. M. Auschwitz, S. T. Prigge, D. W. Rice and R. McLeod, Development of a triclosan scaffold which allows for adaptations on both the A- and B-ring for transport peptides, *Bioorganic Med. Chem. Lett.*, 2013, **23**, 3551–3555.
- 75 K. Drlica and X. Zhao, DNA gyrase, topoisomerase IV, and the 4-quinolones., *Microbiol. Mol. Biol. Rev.*, 1997, **61**, 377–392.
- 76 A. A. Khan, F. G. Araujo, K. E. Brighty, T. D. Gootz and J. S. Remington, Anti-*Toxoplasma gondii* activities and structure-activity relationships of novel fluoroquinolones related to trovafloxacin, *Antimicrob. Agents Chemother.*, 1999, **43**, 1783–1787.
- 77 F. Dubar, R. Wintjens, É. S. Martins-Duarte, R. C. Vommaro, W. de

- Souza, D. Dive, C. Pierrot, B. Pradines, A. Wohlkonig, J. Khalife and C. Biot, Ester prodrugs of ciprofloxacin as DNA-gyrase inhibitors: synthesis, antiparasitic evaluation and docking studies, *Medchemcomm*, 2011, **2**, 430.
- 78 S. Lourido, J. Shuman, C. Zhang, K. M. Shokat, R. Hui and L. D. Sibley, Calcium-dependent protein kinase 1 is an essential regulator of exocytosis in *Toxoplasma*., *Nature*, 2010, **465**, 359–62.
- 79 E. T. Larson, K. K. Ojo, R. C. Murphy, S. M. Johnson, Z. Zhang, J. E. Kim, D. J. Leibly, A. M. W. Fox, M. C. Reid, E. J. Dale, B. G. K. Perera, J. Kim, S. N. Hewitt, W. G. J. Hol, C. L. M. J. Verlinde, E. Fan, W. C. Van Voorhis, D. J. Maly and E. A. Merritt, Multiple determinants for selective inhibition of apicomplexan calcium-dependent protein kinase CDPK1, *J. Med. Chem.*, 2012, **55**, 2803–2810.
- 80 M. B. Harbut, B. a Patel, B. K. S. Yeung, C. W. McNamara, a T. Bright, J. Ballard, F. Supek, T. E. Golde, E. a Winzeler, T. T. Diagona and D. C. Greenbaum, Targeting the ERAD pathway via inhibition of signal peptide peptidase for antiparasitic therapeutic design., *Proc. Natl. Acad. Sci. U. S. A.*, 2012, **109**, 21486–91.
- 81 S. N. Mageed, F. Cunningham, A. W. Hung, H. L. Silvestre, S. Wen, T. L. Blundell, C. Abell and G. a McConkey, Pantothenic acid biosynthesis in the parasite *Toxoplasma gondii*: a target for chemotherapy., *Antimicrob. Agents Chemother.*, 2014.
- 82 D. Maubon, A. Bougdour, Y.-S. Wong, M.-P. Brenier-Pinchart, A. Curt, M.-A. Hakimi and H. Pelloux, Activity of the histone deacetylase inhibitor FR235222 on *Toxoplasma gondii*: inhibition of stage conversion of the parasite cyst form and study of new derivative compounds., *Antimicrob. Agents Chemother.*, 2010, **54**, 4843–50.
- 83 T. L. Schultz, C. P. Hencken, L. E. Woodard, G. H. Posner, R. H. Yolken, L. Jones-Brando and V. B. Carruthers, A thiazole derivative of artemisinin moderately reduces *Toxoplasma gondii* cyst burden in infected mice., *J. Parasitol.*, 2014, **100**, 516–21.
- 84 A. Fomovska, R. D. Wood, E. Mui, J. P. Dubey, L. R. Ferreira, M. R. Hickman, P. J. Lee, S. E. Leed, J. M. Auschwitz, W. J. Welsh, C. Sommerville, S. Woods, C. Roberts and R. McLeod, Salicylanilide

- inhibitors of *Toxoplasma gondii*, *J. Med. Chem.*, 2012, **55**, 8375–8391.
- 85 R. P. Tenório, C. S. Carvalho, C. S. Pessanha, J. G. De Lima, A. R. De Faria, A. J. Alves, E. J. T. De Melo and A. J. S. Góes, Synthesis of thiosemicarbazone and 4-thiazolidinone derivatives and their in vitro anti-*Toxoplasma gondii* activity, *Bioorganic Med. Chem. Lett.*, 2005, **15**, 2575–2578.
- 86 B. Krivogorsky, P. Grundt, R. Yolken and L. Jones-Brando, Inhibition of *Toxoplasma gondii* by indirubin and tryptanthrin analogs, *Antimicrob. Agents Chemother.*, 2008, **52**, 4466–4469.
- 87 S. Mitchell, A. Zajac, D. WL and D. Lindsay, Efficacy of ponazuril in vitro and in preventing and treating *Toxoplasma gondii* infections in mice., *J. Par*, 2004, **90**, 639–642.
- 88 J. S. Doggett, A. Nilsen, I. Forquer, K. W. Wegmann, L. Jones-Brando, R. H. Yolken, C. Bordón, S. a Charman, K. Katneni, T. Schultz, J. N. Burrows, D. J. Hinrichs, B. Meunier, V. B. Carruthers and M. K. Riscoe, Endochin-like quinolones are highly efficacious against acute and latent experimental toxoplasmosis., *Proc. Natl. Acad. Sci. U. S. A.*, 2012, **109**, 15936–41.
- 89 G. A. Biagini, N. Fisher, A. E. Shone, M. A. Mubarak, A. Srivastava, A. Hill, T. Antoine, A. J. Warman, J. Davies, C. Pidathala, R. K. Amewu, S. C. Leung, R. Sharma, P. Gibbons, D. W. Hong, B. Pacorel, A. S. Lawrenson, S. Charoensutthivarakul, L. Taylor, O. Berger, A. Mbekeani, P. A. Stocks, G. L. Nixon, J. Chadwick, J. Hemingway, M. J. Delves, R. E. Sinden, A.-M. Zeeman, C. H. M. Kocken, N. G. Berry, P. M. O'Neill and S. A. Ward, Generation of quinolone antimalarials targeting the *Plasmodium falciparum* mitochondrial respiratory chain for the treatment and prophylaxis of malaria., *Proc. Natl. Acad. Sci. U. S. A.*, 2012, **109**, 8298–303.
- 90 M. McPhillie, Y. Zhou, K. El Bissati, J. Dubey, H. Lorenzi, M. Capper, A. K. Lukens, M. Hickman, S. Muench, S. K. Verma, C. R. Weber, K. Wheeler, J. Gordon, J. Sanders, H. Moulton, K. Wang, T.-K. Kim, Y. He, T. Santos, S. Woods, P. Lee, D. Donkin, E. Kim, L. Fraczek, J. Lykins, F. Esaa, F. Alibana-Clouser, S. Dovgin, L. Weiss, G. Brasseur, D. Wirth, M. Kent, L. Hood, B. Meunier, C. W. Roberts, S. S. Hasnain, S. V

- Antonyuk, C. Fishwick and R. McLeod, New paradigms for understanding and step changes in treating active and chronic, persistent apicomplexan infections., *Sci. Rep.*, 2016, **6**, 29179.
- 91 F. Barna, K. Debache, C. A. Vock, T. Kuster and A. Hemphill, In Vitro effects of novel ruthenium complexes in *Neospora caninum* and *Toxoplasma gondii* tachyzoites, *Antimicrob. Agents Chemother.*, 2013, **57**, 5747–5754.
- 92 C. Hunte, H. Palsdottir and B. L. Trumpower, Protonmotive pathways and mechanisms in the cytochrome bc₁ complex, *FEBS Lett.*, 2003, **545**, 39–46.
- 93 Z. Zhang, L. Huang, V. M. Shulmeister, Y. I. Chi, K. K. Kim, L. W. Hung, A. R. Crofts, E. A. Berry and S. H. Kim, Electron transfer by domain movement in cytochrome bc₁., *Nature*, 1998, **392**, 677–84.
- 94 H. Palsdottir, C. G. Lojero, B. L. Trumpower and C. Hunte, Structure of the yeast cytochrome bc₁ complex with a hydroxyquinone anion Q_o site inhibitor bound., *J. Biol. Chem.*, 2003, **278**, 31303–11.
- 95 M. W. Mather, E. Darrouzet, M. Valkova-Valchanova, J. W. Cooley, M. T. McIntosh, F. Daldal and A. B. Vaidya, Uncovering the molecular mode of action of the antimalarial drug atovaquone using a bacterial system, *J. Biol. Chem.*, 2005, **280**, 27458–27465.
- 96 R. E. Sharp, A. Palmitessa, B. R. Gibney, J. L. White, C. C. Moser, F. Daldal and P. L. Dutton, Ubiquinone binding capacity of the *Rhodobacter capsulatus* cytochrome bc₁ complex: Effect of diphenylamine, a weak binding Q_o site inhibitor, *Biochemistry*, 1999, **38**, 3440–3446.
- 97 I. K. Srivastava, J. M. Morrissey, E. Darrouzet, F. Daldal and A. B. Vaidya, Resistance mutations reveal the atovaquone-binding domain of cytochrome b in malaria parasites, *Mol. Microbiol.*, 1999, **33**, 704–711.
- 98 M. J. Capper, P. M. O'Neill, N. Fisher, R. W. Strange, D. Moss, S. a. Ward, N. G. Berry, A. S. Lawrenson, S. S. Hasnain, G. a. Biagini and S. V. Antonyuk, Antimalarial 4(1H)-pyridones bind to the Q_i site of cytochrome bc₁, *Proc. Natl. Acad. Sci.*, 2015, **4**, 201416611.
- 99 A. M. Stickles, M. Justino de Almeida, J. M. Morrissey, K. a. Sheridan, I. P. Forquer, A. Nilsen, R. W. Winter, J. N. Burrows, D. a. Fidock, A. B.

- Vaidya and M. K. Riscoe, Subtle changes in endochin-like quinolone (ELQ) structure alter site of inhibition within the cytochrome bc₁ complex of Plasmodium falciparum, *Antimicrob. Agents Chemother.*, 2015, **59**, AAC.04149-14.
- 100 M. J. Gordon, J. A., Fishwick, C. W. G., McPhillie, New Opportunities in the Structure-based Design of Anti-Protozoan Agents, *Curr Top Med Chem*, 2017.
- 101 A. Nilsen, G. P. Miley, I. P. Forquer, M. W. Mather, K. Katneni, Y. Li, S. Pou, A. M. Pershing, A. M. Stickles, E. Ryan, J. X. Kelly, J. S. Doggett, K. L. White, D. J. Hinrichs, R. W. Winter, S. a Charman, L. N. Zakharov, I. Bathurst, J. N. Burrows, A. B. Vaidya and M. K. Riscoe, Discovery, synthesis, and optimization of antimalarial 4(1H)-quinolone-3-diarylethers., *J. Med. Chem.*, 2014, **57**, 3818–34.
- 102 WO2012167237 A2, 2012.
- 103 WO2010065905 A2, 2009.
- 104 US20120010237 A1, 2011.
- 105 J. M. Bueno, E. Herreros, I. Angulo-Barturen, S. Ferrer, J. M. Fiandor, F. J. Gamo, D. Gargallo-Viola and G. Derimanov, Exploration of 4(1H)-pyridones as a novel family of potent antimalarial inhibitors of the plasmodial cytochrome bc₁., *Future Med. Chem.*, 2012, **4**, 2311–23.
- 106 C. L. Yeates, J. F. Batchelor, E. C. Capon, N. J. Cheesman, M. Fry, A. T. Hudson, M. Pudney, H. Trimming, J. Woolven, J. M. Bueno, J. Chicharro, E. Fernández, J. M. Fiandor, D. Gargallo-Viola, F. Gómez de las Heras, E. Herreros and M. L. León, Synthesis and structure-activity relationships of 4-pyridones as potential antimalarials., *J. Med. Chem.*, 2008, **51**, 2845–52.
- 107 Y. Zhang, W. A. Guiguemde, M. Sigal, F. Zhu, M. C. Connelly, S. Nwaka and R. K. Guy, Synthesis and structure-activity relationships of antimalarial 4-oxo-3-carboxyl quinolones., *Bioorg. Med. Chem.*, 2010, **18**, 2756–66.
- 108 R. W. Winter, J. X. Kelly, M. J. Smilkstein, R. Dodean, G. C. Bagby, R. K. Rathbun, J. I. Levin, D. Hinrichs and M. K. Riscoe, Evaluation and lead optimization of anti-malarial acridones., *Exp. Parasitol.*, 2006, **114**, 47–56.

- 109 R. M. Beteck, F. J. Smit, R. K. Haynes and D. D. N'Da, Recent progress in the development of anti-malarial quinolones., *Malar. J.*, 2014, **13**, 339.
- 110 R. Winter, J. X. Kelly, M. J. Smilkstein, D. Hinrichs, D. R. Koop and M. K. Riscoe, Optimization of endochin-like quinolones for antimalarial activity., *Exp. Parasitol.*, 2011, **127**, 545–51.
- 111 L. A. Kelley, S. Mezulis, C. M. Yates, M. N. Wass and M. J. E. Sternberg, The Phyre2 web portal for protein modeling, prediction and analysis, *Nat. Protoc.*, 2015, **10**, 845–858.
- 112 C. A. Lipinski, *Drug Discov. Today Technol.*, 2004, 1, 337–341.
- 113 F. Lovering, J. Bikker and C. Humblet, Escape from flatland: Increasing saturation as an approach to improving clinical success, *J. Med. Chem.*, 2009, **52**, 6752–6756.
- 114 Z. Rankovic, CNS Physicochemical Property Space Shaped by a Diverse Set of Molecules with Experimentally Determined Exposure in the Mouse Brain, *J. Med. Chem.*, 2017, **60**, 5943–5954.
- 115 R. H. Bradbury, C. P. Allott, M. Dennis, J. A. Girdwood, P. W. Kenny, J. S. Major, A. A. Oldham, A. H. Ratcliffe, J. E. Rivett, D. A. Roberts and P. J. Robins, New Nonpeptide Angiotensin, *J. Med. Chem.*, 1993, **36**, 1245–1254.
- 116 R. H. Bradbury, C. P. Allott, M. Dennis, J. A. Girdwood, P. W. Kenny, J. S. Major, A. A. Oldham, A. H. Ratcliffe and J. E. Rivett, New nonpeptide angiotensin II receptor antagonists. 3. Synthesis, biological properties, and structure-activity relationships of 2-alkyl-4-(biphenylmethoxy)pyridine derivatives, *J. Med. Chem.*, 1993, **36**, 1245–1254.
- 117 A. Sobczak and W. Z. Antkowiak, Synthesis of 2,3-Disubstituted 4-Pyridone From a β -Aminocarboxylate Derivative and Acetoacetate, *Synth. Commun.*, 2005, **35**, 2993–3001.
- 118 D. A. Evans, J. L. Katz and T. R. West, Synthesis of diaryl ethers through the copper-promoted arylation of phenols with arylboronic acids. An expedient synthesis of thyroxine, *Tetrahedron Lett.*, 1998, **39**, 2937–2940.
- 119 A. Harder and A. Haberkorn, Possible mode of action of toltrazuril: studies on two *Eimeria* species and mammalian and *Ascaris suum*

- enzymes., *Parasitol. Res.*, 1989, **76**, 8–12.
- 120 J. Jöckel, B. Wendt and M. Löffler, Structural and Functional Comparison of Agents Interfering with Dihydroorotate, Succinate and NADH Oxidation of Rat Liver Mitochondria.
- 121 M. Conrad and L. Limpach, Synthesen von Chinolinderivaten mittelst Acetessigester., *Berichte Der Dtsch. Chem. Gesellschaft*, 1887, **20**, 944–948.
- 122 A. Giroux, Y. Han and P. Prasit, One pot biaryl synthesis via in situ boronate formation, *Tetrahedron Lett.*, 1997, **38**, 3841–3844.
- 123 E. Kerns, L. Di and G. Carter, In Vitro Solubility Assays in Drug Discovery, *Curr. Drug Metab.*, 2008, **9**, 879–885.
- 124 R. Censi, P. Di Martino, R. Censi and P. Di Martino, Polymorph Impact on the Bioavailability and Stability of Poorly Soluble Drugs, *Molecules*, 2015, **20**, 18759–18776.
- 125 S. R. B. and H. M. W., *The Organic Chemistry of Drug Design and Drug Action*, Elsevier Inc., Third., 2014.
- 126 Richard A. Friesner, Robert B. Murphy, Matthew P. Repasky, Leah L. Frye, Jeremy R. Greenwood, Thomas A. Halgren, and Paul C. Sanschagrín and D. T. Mainz†, Extra Precision Glide: Docking and Scoring Incorporating a Model of Hydrophobic Enclosure for Protein–Ligand Complexes, 2006.
- 127 W. Lindstrom, G. M. Morris, C. Weber and R. Huey, Using AutoDock for Virtual Screening, *October*, 2005, 1–36.
- 128 H. Yang, J. Li, G. Du and L. Liu, Microbial Production and Molecular Engineering of Industrial Enzymes: Challenges and Strategies, *Biotechnol. Microb. Enzym.*, 2017, 151–165.
- 129 A. K. Lukens, R. W. Heidebrecht Jr, C. Mulrooney, J. A. Beaudoin, E. Comer, J. R. Duvall, M. E. Fitzgerald, D. Masi, K. Galinsky, C. A. Scherer, M. Palmer, B. Munoz, M. Foley, S. L. Schreiber, R. C. Wiegand and D. F. Wirth, Diversity-Oriented Synthesis Probe Targets Plasmodium falciparum Cytochrome b Ubiquinone Reduction Site and Synergizes With Oxidation Site Inhibitors, 2012, 14–18.
- 130 J. X. Qiao and P. Y. S. Lam, *Synthesis.*, 2011, 829–856.
- 131 X. Jin, T. L. Luong, N. Reese, H. Gaona, V. Collazo-Velez, C. Vuong,

- B. Potter, J. C. Sousa, R. Olmeda, Q. Li, L. Xie, J. Zhang, P. Zhang, G. Reichard, V. Melendez, S. R. Marcisin and B. S. Pybus, Comparison of MDCK-MDR1 and Caco-2 cell based permeability assays for anti-malarial drug screening and drug investigations, *J. Pharmacol. Toxicol. Methods*, 2014, **70**, 188–194.
- 132 Q. Wang, J. D. Rager, K. Weinstein, P. S. Kardos, G. L. Dobson, J. Li and I. J. Hidalgo, Evaluation of the MDR-MDCK cell line as a permeability screen for the blood-brain barrier, *Int. J. Pharm.*, 2005, **288**, 349–359.
- 133 L. D. Marroquin, J. Hynes, J. A. Dykens, J. D. Jamieson and Y. Will, Circumventing the Crabtree Effect: Replacing Media Glucose with Galactose Increases Susceptibility of HepG2 Cells to Mitochondrial Toxicants, *Toxicol. Sci.*, 2007, **97**, 539–547.
- 134 A. A. Boteva and O. P. Krasnykh, The methods of synthesis, modification, and biological activity of 4-quinolones (review), *Chem. Heterocycl. Compd.*, 2009, **45**, 757–785.
- 135 V. Abet, F. Filace, J. Recio, J. Alvarez-Builla and C. Burgos, Prodrug approach: An overview of recent cases, *Eur. J. Med. Chem.*, 2017, **127**, 810–827.
- 136 Y. Hamada, Recent progress in prodrug design strategies based on generally applicable modifications, *Bioorganic Med. Chem. Lett.*, 2017, **27**, 1627–1632.
- 137 J. Rautio, H. Kumpulainen, T. Heimbach, R. Oliyai, D. Oh, T. Järvinen and J. Savolainen, Prodrugs: Design and clinical applications, *Nat. Rev. Drug Discov.*, 2008, **7**, 255–270.
- 138 R. B. McComb, G. N. J. Bowers and S. Posen, in *Alkaline Phosphatase*, 1979, vol. Suppl 116, pp. 633–2322.
- 139 T. Heimbach, D. M. Oh, L. Y. Li, N. Rodríguez-Hornedo, G. Garcia and D. Fleisher, Enzyme-mediated precipitation of parent drugs from their phosphate prodrugs, *Int. J. Pharm.*, 2003, **261**, 81–92.
- 140 V. J. Stella and K. W. Nti-Addae, Prodrug strategies to overcome poor water solubility, *Adv. Drug Deliv. Rev.*, 2007, **59**, 677–694.
- 141 G. P. Miley, S. Pou, R. Winter, A. Nilsen, Y. Li, J. X. Kelly, A. M. Stickles, M. W. Mather, I. P. Forquer, A. M. Pershing, K. White, D. Shackelford,

- J. Saunders, G. Chen, L. M. Ting, K. Kim, L. N. Zakharov, C. Donini, J. N. Burrows, A. B. Vaidya, S. A. Charman and M. K. Riscoe, ELQ-300 prodrugs for enhanced delivery and single-dose cure of malaria, *Antimicrob. Agents Chemother.*, 2015, **59**, 5555–5560.
- 142 A. Nilsen, A. N. LaCrue, K. L. White, I. P. Forquer, R. M. Cross, J. Marfurt, M. W. Mather, M. J. Delves, D. M. Shackleford, F. E. Saenz, J. M. Morrissey, J. Steuten, T. Mutka, Y. Li, G. Wirjanata, E. Ryan, S. Duffy, J. X. Kelly, B. F. Sebayang, A.-M. Zeeman, R. Noviyanti, R. E. Sinden, C. H. M. Kocken, R. N. Price, V. M. Avery, I. Angulo-Barturen, M. B. Jiménez-Díaz, S. Ferrer, E. Herreros, L. M. Sanz, F.-J. Gamo, I. Bathurst, J. N. Burrows, P. Siegl, R. K. Guy, R. W. Winter, A. B. Vaidya, S. a Charman, D. E. Kyle, R. Manetsch and M. K. Riscoe, Quinolone-3-diarylethers: a new class of antimalarial drug., *Sci. Transl. Med.*, 2013, **5**, 177ra37.
- 143 WO 2010094738 A1, 2010.
- 144 Schrödinger LLC, 2014.
- 145 R. M. Cross, J. R. Maignan, T. S. Mutka, L. Luong, J. Sargent, D. E. Kyle and R. Manetsch, Optimization of 1,2,3,4-Tetrahydroacridin-9(10H)ones as Antimalarials Utilizing Structure À Activity and Structure À Property Relationships, 2011, **9**, 4399–4426.
- 146 W. Werner, Methylierung und hydrierung von 2-alkyl-chinolon-4, *Tetrahedron*, 1969, **25**, 255–261.
- 147 US4242121 A1, 1980.
- 148 I. Granoth, A. Kalir, Z. Pelah and E. D. Bergmann, Debrominative Phosphorylation, *Isr. J. Chem.*, 1970, **8**, 613–620.
- 149 Ivanova, No Title, *Zhurnal Org. Khimii*, 1968, **4**, 1836–1773.
- 150 F. Fontaine, A. Héquet, A.-S. Voisin-Chiret, A. Bouillon, A. Lesnard, T. Cresteil, C. Jolivald and S. Rault, Boronic species as promising inhibitors of the Staphylococcus aureus NorA efflux pump: Study of 6-substituted pyridine-3-boronic acid derivatives., *Eur. J. Med. Chem.*, 2015, **95**, 185–98.
- 151 A. Fomovska, Q. Huang, K. El Bissati, E. J. Mui, W. H. Witola, G. Cheng, Y. Zhou, C. Sommerville, C. W. Roberts, S. Bettis, S. T. Prigge, G. A. Afanador, M. R. Hickman, P. J. Lee, S. E. Leed, J. M. Auschwitz, M.

- Pieroni, J. Stec, S. P. Muench, D. W. Rice, A. P. Kozikowski and R. McLeod, Novel N-Benzoyl-2-Hydroxybenzamide Disrupts Unique Parasite Secretory Pathway, *Antimicrob. Agents Chemother.*, 2012, **56**, 2666–2682.
- 152 M.-J. Gubbels, C. Li and B. Striepen, High-Throughput Growth Assay for *Toxoplasma gondii* Using Yellow Fluorescent Protein, *Antimicrob. Agents Chemother.*, 2003, **47**, 309–316.
- 153 A. J. Warman, T. S. Rito, N. E. Fisher, D. M. Moss, N. G. Berry, P. M. O'Neill, S. A. Ward and G. A. Biagini, Antitubercular pharmacodynamics of phenothiazines, *J. Antimicrob. Chemother.*, 2013, **68**, 869–880.

Appendix

The following are the experimental details of experiments performed by collaborators as indicated in the body of the text. Experimental details are reproduced as provided.

***In Vitro* Challenge Assay for Toxoplasma Tachyzoites**

Experimental procedure (provided by Rima McLeod, University of Chicago): Protocol adapted from Fomovska, et. al. ^{84,151}. Human foreskin fibroblasts (HFF) were cultured on a flat, clear-bottomed, black 96-well plate to 90% to 100% confluence. IMDM (1x, [+] glutamine, [+] 25 mM HEPES, [+] Phenol red, 10% FBS [Gibco, Denmark]) was removed from each well and replaced with IMDM-C(1x, [+] glutamine, [+] 25 mM HEPES, [-] Phenol red, 10% FBS)[Gibco, Denmark]). Type I RH parasites expressing Yellow Fluorescent Protein (RH-YFP) were lysed from host cells by double passage through a 27-gauge needle. Parasites were counted and diluted to 32,000/mL in IMDM-C. Fibroblast cultures were infected with 3200 tachyzoites of the Type I RH strain expressing Yellow Fluorescent Protein (RH-YFP) and returned to incubator at 37° C for 1-2 hours to allow for infection¹⁵². Various concentrations of the compounds were made using IMDM-C, and 20 µl were added to each designated well, with triplicates for each condition. Controls included pyrimethamine/sulfadiazine (current standard of treatment), 0.1% DMSO only, fibroblast only, and an untreated YFP gradient with 2-fold dilutions of the parasite. Cells were incubated at 37° C for 72 hours. Plates were read using a fluorimeter (Synergy H4 Hybrid Reader, BioTek) to ascertain the amount of yellow fluorescent protein, in relative fluorescence units (RFU), as a measure of parasite burden after treatment. Data was collected using Gen5 software. IC₅₀ was calculated by graphical analysis in Excel.

An initial screening assay of 10 µM, 1µM, 100 nM, and 10 nM was performed. Compounds were not considered effective or pursued for further analysis if there were no signs of inhibition of tachyzoites at 1µM. If compounds did appear to be effective at 1 µM, another experiment was conducted to assess effect at 1 µM, 500 nM, 250 nM, 125 nM, 62.5 nM, and 31.25 nM.

Cytotoxicity Assay run with above: Toxicity assays were conducted using WST-1 cell proliferation reagent (Roche) as described in Fomovska, et. al. (18,19). HFF were grown on a flat, clear-bottomed, black 96-well plate. Confluent HFF were treated with inhibitory compounds at concentrations of 10 μ M and 50 μ M. Compounds were diluted in IMDM-C, and 20 μ l were added to each designated well, with triplicates for each condition. A gradient of 2-fold-decreasing concentrations of DMSO from 10% to 0% in clear IMDM-C was used as a control. The plate was incubated for 72 hours at 37° C. 10 μ l of WST-1 reagent (Roche) were added to each well and the cells were incubated for 30 to 60 minutes. Absorbance was read using a fluorimeter at 420 nm. A higher degree of colour change (and absorbance) indicated mitochondrial activity and cell viability.

In vitro Challenge Assay for Bradyzoites

Experimental procedure (provided by Rima McLeod, University of Chicago): HFF cells were grown in IMDM (1x, [+] glutamine, [+] 25 mM HEPES, [+] Phenol red, 10% FBS, [Gibco, Denmark]) on removable, sterile glass disks in the bottom of a clear, flat-bottomed 24-well plate. Cultures were infected with 3×10^4 parasites (EGS strain) per well, in 0.5 mL media and plate was returned to incubator at 37° C overnight. The following day, the media was removed and clear IMDM and compounds were added to making various concentrations of the drug, to a total volume of 0.5 mL. 2 wells were filled with media only, as a control. Plates were returned to the 37° C incubator for 72 hours and checked once every 24 hours. If tachyzoites were visible in the control before 72 hours, the cells were fixed and stained. Cells were fixed using 4% paraformaldehyde and stained with Fluorescein-labelled Dolichos Biflorus Agglutinin, DAPI, and BAG1. Disks were removed and mounted onto glass slides and visualized using microscopy (Nikon TI7). Slides were scanned using a CRi Panoramic Scan Whole Slide Scanner and viewed using Panoramic Viewer Software. Effects of the compounds were quantified by counting cysts in the controls and treated cells. Cysts and persisting organisms were counted in a representative field of view and then multiplied by a factor determined by the total area of the disk in order to estimate the number of cysts and organisms in each condition.

X-ray crystallography studies

Experimental procedure (provided by Svetlana Antonyuk, University of Liverpool): Cytochrome *bc₁* was purified as described. Crude bovine mitochondria were isolated from fresh cow heart and solubilised in DDM. The solution was clarified by ultracentrifugation at 200,000 g for 1 hour at 4 °C and the supernatant applied to a DEAE CL-6B sepharose column ca. 50 ml pre-equilibrated in 50 mM KPi (pH 7.5), 250 mM NaCl, 3 mM NaN₃, 0.1 g/L DDM, washed with two CV and eluted along a gradient from 250 mM to 500 mM NaCl. Cyt. *bc₁* containing fractions were pooled and concentrated before loading on a Sepharose S300 column ca. 120 ml equilibrated with 20 mM KMOPS (pH 7.2), 100 mM NaCl, 0.5 mM EDTA, 0.1 g/L DDM at 0.5 ml/min. 10 mM β-mercaptoethanol stock in DMSO was added to the eluted protein in a two-fold molar excess and allowed to incubate at 4 °C for 1 hour. Increasing amounts of PEG4000 were then added to precipitate cyt. *bc₁* and separate remaining contaminants. The cyt. *bc₁* was then resuspended before buffer exchange into a final buffer (25 mM KPi (pH 7.5), 3 mM NaN₃, 0.015% DDM) and concentrated to 40 mg/ml. 1.6% HECAMEG was added to the protein solution prior to crystals growing by the hanging drop vapour diffusion method against a reservoir of 50 mM KPi (pH 6.8), 100 mM NaCl, 3 mM NaN₃, 9% PEG4000, 0.16% HECMAEG. Crystals were flash frozen in 23% glycerol in reservoir solution as a cryoprotectant. Multiple wedges of data were collected at 100K from different points on the same crystal at I24 Diamond Light Source using 0.9686 Å X-rays with a Pilatus3 6M detector. Datasets were processed in iMosflm and combined using BlendS89 to produce a complete merged dataset. Refinement was carried out with RefmacS91 using ProSMARTS90 to generate secondary structure restraints to assist in the low-resolution refinement. The ligand **57** was produced using JLigandS92 and modelled in the Q_i site of cyt. *bc₁* using CootS93. Cycles of alternating Refmac5 and manual modelling resulted in a completed model. Data collection and refinement statistics are summarised in Table 1. For 3715 residues 95.2% are Ramachandran favoured, 4.6% allowed and 0.3% outliers.

Solubility assay

Experimental procedure (provided by ChemPartner Ltd):

1. Add 10 μL test compound in 990 μL PBS (pH 7.4) or FaSSIF (pH 6.5)
2. Sample tubes are shaken for 1 hour (1000 rpm) at room temperature.
3. Samples are centrifuged (10 min - 12000 rpm) to precipitate un-dissolved particles.
4. Supernatants are collected for LCMSMS or LC-UV analysis.

Components (MW)	FaSSIF
Na Taurocholate (537.68)	3 mM (1.61 g)
Lecithin (768)	0.2 mM (0.132 g)
NaOH (40)	34.8 mM (1.392 g)
NaCl (58.5)	68.62 mM (4.01 g)
Maleic Acid (116.07)	19.12 mM (2.22 g)
Deionized Water	QS to 1 L
pH	6.5

Microsomal stability assays

Experimental procedure (provided by ChemPartner Ltd):

1. Buffer A: 1.0 L of 0.1 M monobasic Potassium Phosphate buffer containing 1.0 mM EDTA. Buffer B: 1.0 L of 0.1 M Dibasic Potassium Phosphate buffer containing 1.0 mM EDTA. Buffer C: 0.1 M Potassium Phosphate buffer, 1.0 mM EDTA, pH 7.4 by titrating 700 mL of buffer B with buffer A while monitoring with the pH meter.
2. Reference compounds (Ketanserin) and test compounds spiking solution, 500 μM spiking solution: add 10 μL of 10 mM DMSO stock solution into 190 μL ACN. 1.5 μM spiking solution in microsomes (0.75 mg/mL): add 1.5 μL of 500 μM spiking solution and 18.75 μL of 20 mg/mL liver microsomes into 479.75 μL of Buffer C on ice.
3. Prepare NADPH stock solution (6 mM) by dissolving NADPH into buffer C.
4. Dispense 30 μL of 1.5 μM spiking solution containing 0.75 mg/mL microsomes solution to the assay plates designated for different time points (0-, 5-, 15-, 30-, 45-min) on ice.
5. For 0-min, add 135 μL of ACN containing IS to the wells of 0-min plate and then add 15 μL of NADPH stock solution (6 mM).
6. Pre-incubate all other plates at 37 $^{\circ}\text{C}$ for 5 minutes.

7. Add 15 μL of NADPH stock solution (6 mM) to the plates to start the reaction and timing.
8. At 5-min, 15-min, 30-min, and 45-min, add 135 μL of ACN containing IS to the wells of corresponding plates, respectively, to stop the reaction.
9. After quenching, shake the plates at the vibrator (IKA, MTS 2/4) for 10 min (600 rpm/min) and then centrifuge at 5594 g for 15 min (Thermo Multifuge \times 3R).
10. Transfer 50 μL of the supernatant from each well into a 96-well sample plate containing 50 μL of ultra-pure water (Millipore, ZMQS50F01) for LC/MS analysis.

Protein Binding assay

Experimental procedure (provided by ChemPartner Ltd):

1. Spiking Solutions of Test and Reference Compounds

1.1 Solution A (0.5 mM): Add 10 μL of 10mM stock solution into 190 μL of DMSO.

1.2 Solution B (0.02 mM): Add 8 μL of Solution A into 192 μL of 0.05 M sodium phosphate buffer. The final DMSO concentration in Solution B is 4%.

2. Preparation of Test and Reference Compounds in plasma

2.1 Preload a 96-well plate with 380 μL aliquots of plasma in the wells designated for plasma and buffer, respectively.

2.2 Spike 20 μL of Solution B (0.02 mM of test and reference compounds) into the pre-loaded plasma in the 96-well plate. The final test concentration is 1 μM containing 0.2% DMSO.

3. Dialysis Sample Loading

3.1 Preparing plasma against buffer system (duplicate):

Apply aliquots of 100 μL of blank dialysis buffer to the receiver side of dialysis chambers. Then apply aliquots of 100 μL of the plasma spiked with test and reference compounds to the donor side of the dialysis chambers.

(always add the blank buffer to the receiver first, clearly mark the buffer and plasma chamber holes to avoid cross contamination).

3.2. Preparing T0 plasma samples for initial concentrations (duplicate):

3.2.1 Aliquot 25 μL of the plasma spiked with test and reference compounds into a 96-well sample preparation plate as T0 plasma samples

3.2.2 Mix the aliquots with same volume of blank buffer (50:50, v/v).

3.2.3 Quench the samples with 200 μ L of acetonitrile containing internal standard (IS).

3.3 Cover the dialysis block with a plastic lid and place the entire apparatus in a shaker (60 rpm) for 5 hours at 37°C.

3.4 Preparing dialyzed samples after 5-hour incubation:

3.4.1 Aliquot 25 μ L from both the donor sides and receiver sides of the dialysis apparatus into new sample preparation plates and mix the aliquots with same volume of opposite matrixes (blank buffer to plasma and vice versa).

3.4.2 Quench the samples with 200 μ L acetonitrile containing internal standard (IS). Vortex all the samples (from 0h and 5h) at 600 rpm for 10 min followed by centrifugation at 5594 g for 15 minutes (Thermo Multifuge \times 3R).

3.4.3 Transfer 50 μ L of the supernatants to a new 96-well plate and mix the samples with 50 μ L of Milli-Q water. Cover the sample plate and store it in a freezer (-20 °C) until LC/MS/MS analysis.

MDCK MDR1 Permeability

Experimental procedure (provided by ChemPartner Ltd):

1. Prewarm HBSS Buffer in 37°C water bath.
2. Take compounds from -20°C, sonicate for a few minutes (no less than 1 minute)
3. Solution preparation

Donor solution buffer: For A-to-B direction: HBSS buffer with 0.3% DMSO and 5 μ M LY: add 150 μ L DMSO and 50 μ L LY (5mM) into 50 ml HBSS buffer (pH7.4). HBSS buffer with 0.1% DMSO and 5 μ M LY: add 50 μ L DMSO and 50 μ L LY (5mM) into 50 mL HBSS buffer (pH7.4). For B-to-A direction: HBSS buffer with 0.3% DMSO: add 150 μ L DMSO into 50 ml HBSS buffer (pH7.4). HBSS buffer with 0.1% DMSO: add 50 μ L DMSO into 50 ml HBSS buffer (pH7.4). Receiver solution buffer: For A-to-B direction: Prepare HBSS buffer with 0.4% DMSO: add 200 μ L DMSO into 50 ml HBSS buffer (pH7.4). For B-to-A direction: Prepare HBSS buffer with 0.4% DMSO and 5uM LY: add 200 μ L DMSO and 50 μ L LY (5mM) into 50 ml HBSS buffer (pH7.4).

CYP inhibition assay

Experimental procedure: (provided by ChemPartner Ltd)

1. Preheat 0.1 M potassium phosphate buffer (K-buffer), pH 7.4:

100 mM K-Buffer: mix 9.5 mL Stock A into 40.5 mL Stock B, bring total volume to 500 mL with Milli-Q water, titrate the buffer with KOH or H₃PO₄ to pH 7.4.

Stock A (1 M monobasic potassium phosphate): 136.5 g of monobasic potassium phosphate in 1 L of Milli-Q water;

Stock B (1 M dibasic potassium phosphate): 174.2 g of dibasic potassium phosphate in 1 L of Milli-Q water.

2. Prepare serial dilution for test compound and reference inhibitors (400 ×) in a 96-well plate:

2.1 Transfer 8 μL of 10 mM test compounds to 12 μL of ACN.

2.2 Prepare inhibitor spiking solution for CYP1A2, CYP2C9 and CYP2D6 in cocktail: 12 μL of 1 mM α-Naphthoflavone + 10 μL of 40 mM Sulfaphenazole + 10 μL of 10 mM Quinidine + 8 μL of DMSO

2.3 Prepare individual inhibitor spiking solution for CYP3A4 and CYP2C19: 8 μL of DMSO stock to 12 μL of ACN.

2.4 Perform 1:3 serial dilutions in DMSO: ACN mixture (v/v: 40:60).

3. Prepare 4 × NADPH cofactor (66.7 mg NADPH in 10 mL 0.1 M K-buffer, pH7.4)

4. Prepare 4 × substrate (2 mL for each isoform) as indicated in the table below (add HLM where required on ice).

5. Prepare 0.2 mg/mL HLM solution (10 μL of 20 mg/mL to 990 μL of 0.1 M K-buffer) on ice.

6. Add 400 μL of 0.2 mg/mL HLM to the assay wells and then add 2 μL of 400 × test compound set (serially diluted, see step 2.1) into the designated wells (see table 1) on ice.

7. Add 200 μL of 0.2 mg/mL HLM to the assay wells and then add 1 μL of serially diluted reference inhibitor solution (see step 2.2 and 2.3) into the designated wells (see table 1) on ice.

8. Add following solutions (in duplicate) in a 96-well assay plate on ice:

8.1 Add 30 μL of 2 × test compound and reference compound in 0.2 mg/mL HLM solution (see step 6 and 7);

8.2 Add 15 μL of 4× substrate solution (see step 4).

9. Pre-incubate the 96-well assay plate and NADPH solution at 37°C for 5 minutes.

10. Add 15 μL of pre-warmed 8 mM NADPH solution to into the assay plates to initiate the reaction. (See step 3)
11. Incubate the assay plate at 37 °C. 5 min for 3A4, 10 min for 1A2, 2C9 and 2D6, and 45 min for 2C19.
12. Stop the reaction by adding 120 μL of ACN containing IS (see IS preparation in Table 2).
13. After quenching, shake the plates at the vibrator (IKA, MTS 2/4) for 10 min (600 rpm/min) and then centrifuge at 3220 g for 15 min.
14. Transfer 50 μL of the supernatant from each well into a 96-well sample plate containing 50 μL of ultra-pure water (Millipore, ZMQS50F01) for LC/MS analysis.

hERG inhibition assay

Experimental procedure: (provided by ChemPartner Ltd)

1. Cell culture and cell requirements 2.1.1. A CHO cell line stably transfected with hERG cDNA and expressing hERG channels was used for the study. Cells were maintained in petri dishes or flasks at 37 °C in a humidified incubator with 5% CO₂ and cultured in medium (from Invitrogen) containing:

- Ham's F12
- 10% (v/v) heat inactivated FBS
- 100 $\mu\text{g}/\text{ml}$ Hygromycin B
- 100 $\mu\text{g}/\text{ml}$ Geneticin

2. Cells were allowed to grow and reach a confluence rate at about 80-90% in the above condition. Before the experiment, the cells were treated with Detachin (from Genlantis) for 3-5 min. at 37 °C followed by gentle pipette tituration 15-20 times at room temperature with culture media, then the cells were re-suspended in serum-free culture medium containing CHO-S-SFM II medium (from Invitrogen) buffered with HEPES (25 mM). The cells used in QPatch study must meet following criteria: under microscopy examination, the majority of cells in suspension should be single and isolated; their viability should be greater than 95%, with only a few debris and cell clumps (which may clog the holes in QPlate during whole-cell clamp recording); cell density should be ranged within $3-8 \times 10^6$ cells/ml in the final suspension before applying to the QPatch stir chamber. Cells in such condition can be used for recording only for four hours after harvesting.

T.gondii *In Vivo* mouse assay

Experimental procedure (provided by Rima McLeod, University of Chicago)

IVIS: Mice were infected intraperitoneally with 20X10³ *Toxoplasma gondii* (Pru strain expressing luciferase) tachyzoites. Treatment commenced 2 hours later with **169** (5mg/kg) which was dissolved in DMSO and administered intraperitoneally in a total volume of 0.05ml. Mice were imaged every second day starting on day 4 post infection using an IVIS Spectrum (Caliper Life Sciences) for a 1 minute exposures, with medium binning, 20 minutes post injection with 150 mg/kg of D-luciferin potassium salt solution.

Brain cysts: Mice were infected intraperitoneally with 20x 10³ *Toxoplasma gondii* tachyzoites. Treatment commenced 2 hours later with **169** (5mg/kg) which was dissolved in DMSO and administered intraperitoneally in a total volume of 0.05ml. After 30 days, treatment with **169** was begun each day for 14 days intraperitoneally. In experiments when tafenoquine was administered alone or with **169** in some groups 3mg/kg tafenoquine was administered once on day -1. Cysts in brain were quantitated days after discontinuing the **169**.

***P.berghei* causal prophylaxis *in vivo* model**

Experimental procedure (provided by Mark Hickman, Walter Reed Army Institute of Research): *P. berghei* sporozoites were obtained from laboratory-reared female *Anopheles stephensi* mosquitoes which were maintained at 18 degrees C for 17-22 days after feeding on a luciferase expressing *P. berghei* infected Swiss CD1ICR Using a dissecting microscope, the salivary glands were extracted from malaria-infected mosquitoes and sporozoites were obtained. Briefly, mosquitoes were separated into head/thorax and abdomen. Thoraxes and heads were triturated with a mortar and pestle and suspended in medium RPMI 1640 containing 1% C57BL/6 mouse serum (Rockland Co, Gilbertsville, PA, USA). 50–80 heads with glands total were placed into a 0.5 ml Osaki tube on top of glass wool with enough dissection media to cover the heads. Until all mosquitoes had been dissected, the Osaki tube was kept on ice. Sporozoites that were isolated from the same batch of mosquitoes were inoculated into C57BL/6, 2D knock-out and 2D knock-out/2D6 knock-in C57BL/6 mice on the same day to control for biological variability in sporozoite preparations. On day 0, each mouse was inoculated intravenously in the tail

vein with approximately 10,000 sporozoites suspended in 0.1 ml volume. They were stained with a vital dye containing fluorescein diacetate (50 mg/ml in acetone) and ethidium bromide (20 µg/ml in phosphate buffered saline; Sigma Chemical Co, St. Louis, MO, USA) and counted in a hemocytometer to ensure that inoculated sporozoites were viable following the isolation procedure. Viability of the sporozoites ranged from 90 to 100%.

Animals: The mice used in these experiments were albino C57BL/6 female mice which were housed in accordance with the current Guide for the Care and Use of Laboratory Animals (1996) under an IACUC approved protocol. All animals were quarantined for 7 days upon arrival, and the animals were fed standard rodent maintenance food throughout the study.

Test compound and administration; Animals were dosed with experimental compound **169** based on body weight. The suspension solution of orally administered drugs were conducted in 0.5% (w/v) hydroxyethyl cellulose and 0.2% Tween 80 in distilled water. To insure the size of the compounds in the dosing solution were under 50 µM, the suspension was homogenized using a homogenizer (PRO Scientific Inc, Monroe, CT, USA) with a 10 mm open-slotted generator running at 20,000-22,000 rpm for 5 min in an ice bath. **169** was administered on 3 consecutive days (-1, 0, +1) relative to sporozoite infection or a single dose on day 0. Drug suspensions were administered to mice using by oral gavage using an 18-gauge intragastric feeder for the 3-day dosing regimen, **169** was administered at 0.625 mg/kg and for the single dose regimen administered on day 0, compounds were administered at 2.5 mg/kg.

In vivo imaging: All of the *in vivo* bioluminescent imaging methods utilized have been described previously [6]. Briefly TQ and NPC-1161B were administered orally on days -1, 0 and 1 with respect to sporozoite inoculation. All inoculated mice were imaged using the Xenogen IVIS-200 Spectrum (Caliper Life Sciences, Hopkinton, MA, USA) IVIS instrument at 24, 48 and 72 hours post-sporozoite infection. The bioluminescent imaging experiments were conducted by IP injection of the luciferase substrate, D-Luciferin potassium salt, (Xenogen, California and Goldbio, St Louis, MO, USA), into mice at a concentration of 200 mg/kg 15 min before bioluminescent images were obtained. Three minutes after luciferin administration the mice were anesthetized using isoflurane, and the mice were positioned ventral side up

on a 37 degree C platform with continual anaesthesia provided through nose cone delivery of isoflurane. All bioluminescent images were obtained using 5 minute exposures with f-stop = 1 and large binning setting. Photon emission from specific regions was quantified using Living Image® 3.0 software (Perkin Elmer),

Additionally, blood stage parasitaemia was assessed 3 days after imaging was completed by treating small quantities of blood obtained from tail bleeds with the fluorescent dye Yoyo-1 measured by using a flow cytometry system

Hep G2 toxicity studies

Experimental procedure (provided by Giancarlo A. Biagini & Dr Richard S. Priestley, Liverpool School of Tropical Medicine):

Mammalian mitochondrial toxicities were determined as described in Warman *et al.*¹⁵³ In brief, Hep G2 cells cultured in either glucose media (DMEM containing 25 mM D-glucose and 1 mM sodium pyruvate and supplemented with 5 mM HEPES, 10% FBS and 500 µg/mL pen-strep) or galactose media (DMEM supplemented with 1 mM D-galactose, 2 mM L-glutamine, 5 mM HEPES, 10% FBS, 1 mM sodium pyruvate and 500 µg/mL pen-strep), were added to 96-well plates (100 µL, 1 x 10⁴ cells/well) and incubated for 24 h at 37°C. After incubation, various concentration of test compounds, rotenone or tamoxifen (100 µM – 1 nM) were added to a final volume of 200 µL/well, and incubated for another 24 h at 37°C. The plates were subsequently incubated in the presence of 1 mg/mL MTT for 2 hr at 37 °C. After incubation, the media was removed and DMSO added (100 µL/well). The plates were shaken for 5 min before well absorbance at 560 nm was measured using a Varioskan plate reader (ThermoScientific).